COORDINATION DYNAMICS OF WALKING

by

KATY LYNN WORSTER

B.S., University of Colorado, 2005

A thesis submitted to the

Faculty of the Graduate School of the

University of Colorado in partial fulfillment

of the requirements for the degree of

Doctor of Philosophy

Bioengineering

2015

UMI Number: 3702117

UMI

Dissertation Publishing

UMI 3702117

ProQuest

ProQuest LLC.
789 East Eisenhower
Parkway
P.O. Box 1346

This thesis for the Doctor of Philosophy degree by Katy Lynn Worster

has been approved for the

Department of Bioengineering

by

James J. Carollo, Advisor

Kendall Hunter, Chair

Joanne Valvano

Zhaoxing Pan

Richard Weir

April 20, 2015

Worster, Katy Lynn (Ph.D., Bioengineering)

Coordination Dynamics of Walking

Thesis directed by Associate Professor James J. Carollo

ABSTRACT

Although coordination has been identified as a fundamental element necessary for the successful achievement of walking, this aspect of gait has yet to be embraced into instrumented gait analysis, perhaps in part due to the lack of a normative reference and unfamiliarity of mathematical methods that are best suited to capture this essential behavior. Therefore, this work focused on expanding clinical gait analysis techniques by validating nonlinear methods that describe the influence of neurological control on the musculoskeletal system. This body of work investigated the coordination dynamics during gait in both prospective and retrospective subjects free of gait pathology, subjects with spastic cerebral palsy, and subjects with a lower limb amputation using motion capture and mathematical models to help elucidate the complexities of gait and enhance therapeutic interventions. This investigation quantified coordination strategies employed by an unimpaired subject when presented with various walking conditions and challenges mimicking various inhibitions associated with performing the task of swing limb advancement. Two novel indices of coordination dynamics were created to provide a concise metric and ease their inclusion into future research applications. The first normative reference dataset of these coordination measures was created from a large cohort of unimpaired subjects. While there is presently not a gold standard method for quantifying coordination during gait, the exciting correlations between the proposed measures and select clinical performance tasks indicate the coordination measures quantify essential inter-segmental coordination dynamics of walking. The theoretical pendular software model created shows swing limb advancement is not a purely passive motion, but instead an actively controlled motion. Comparisons between the various cohorts revealed the proposed measures of coordination are more suitable for characterizing motor control strategies contributing to a gait pattern, quantify organization of individual segments, identify mechanisms of change, and reveal the loci of impairment(s). The proposed measures of coordination dynamics are capable of distinguishing between different gait pathologies and patterns associated with altered limb advancement during the swing period of gait. Results from this multidisciplinary work have the strong potential to directly impact the clinical treatment of persons with aberrant coordination dynamics during gait.

The form and content of this abstract are approved. I recommend its publication.

Approved: James J. Carollo

ACKNOWLEDGMENT

DEDICATION

This dissertation is dedicated to my mom and dad, for their endless love, support, and encouragement.

TABLE OF CONTENTS

Chapter

LIST OF TABLES

LIST OF FIGURES

1 Introduction

1.1 Problem Statement

Instrumented gait analysis (IGA) is often employed to quantitatively describe the pathological gait pattern of an individual whose walking is negatively affected by neuromuscular impairments. Over the years, IGA measures have served a vital role in both clinical and research applications by providing a means to quantitatively and objectively identify factors contributing to a pathological gait pattern, provide supporting evidence for clinical interventions, and assist in assessment of treatment outcomes. Due to the methods for constructing conventional IGA measures and the nature of the actions or relationships they quantify (e.g. joint angles, joint kinetics, temporal-spatial), these measures describe the motion of limbs or joints but are unable to characterize the underlying dynamics of the motion. Together these underlying dynamics form a constitutive element of bipedalism, coordination. For this body of work, coordination is defined as the organization of the timing and position of individual segments and segment pairs in the cyclical task of gait. The vital role of coordination in maintaining a normative gait pattern becomes apparent in the gait patterns of individuals with neurological pathologies. Aberrant coordination is a hallmark behavior of neurological pathologies and in cases of impaired selective motor control often contributes to the inability to successfully achieve swing limb advancement. Swing limb advancement is a critical task of bipedalism because it advances the leg, affects footfall for the next cycle, and requires the appropriate coordination and control of body segments. The coordinated behavior of leg segments in gait is the result of a complex dynamical system that requires organized neurological control of the musculoskeletal system. Due to the complexity of this resultant motor behavior, dynamic systems theory based measures provide more suitable methods than conventional IGA measures for characterizing selective motor control strategies contributing to a gait pattern because they quantify organization of individual segments, identify mechanisms of change, and loci of impairment. Since the fundamental organization of the leg segments during gait is linked to gait pathology and guides the rationale for interventions, this dissertation proposes the incorporation of measures of coordination dynamics into IGA will open new avenues for understanding the complexity of fundamental element of gait and allow clinicians the means to more effectively and efficiently treat patients with neuromuscular gait impairments. The purpose of this dissertation is to expand clinical IGA techniques with measures of inter-segmental coordination by validating nonlinear methods that describe the resultant motor behavior, coordination dynamics, of the leg segments during the critical task of swing limb

advancement in gait.

1.2 Rationale

Coordination is an essential, though often elusive, aspect of movement that has long been recognized as an important factor of motion [1,2,4,5]. However, the ability to employ a method that effectively captures coordination and presents the behavior in a concise manner has often been just as elusive as the concept of coordination. The application of angle-angle diagrams was a step in the right direction since these measures describe the relationship between two joints as a low dimensional descriptor [3]. Similar to conventional IGA measures, angle-angle diagrams are constructed from a skeletal hierarchy and therefore these joint based measures prove unsuitable tools for delving deeper into the behavior of individual segments or pairing of segments. This need for quantitative descriptors of coordination was identified in the development of motor control theory and the mathematical field of dynamical systems theory was proposed as a solution [4,5,6]. With considerable advancements in motion capture equipment and computers, the marriage between movement analysis and dynamic systems theory was later revisited by Stergiou et al. (2004) who demonstrated dynamic systems theory based measures can be easily derived from segment marker trajectories of motion capture data. These efforts support the theoretical construct that dynamic systems theory can effectively characterize coordination dynamics and the practicality of applying dynamic systems theory measures to the positional data of IGA in order to generate such measures. If these measures of coordination are to be adopted in clinical or research IGA applications, then it must be demonstrated that these measures provide valuable insights into an aberrant gait pattern that is otherwise unobtainable with existing, traditional IGA measures. Therefore, these nonlinear methods were applied to the motion capture data of subjects with a normal gait pattern and two subject groups with different causes for impaired swing limb advancement (SLA): cerebral palsy and lower limb amputation. Since the fundamental organization of the leg segments during gait is linked to gait pathology and guides the rationale for interventions, this dissertation evaluated coordination dynamics, in the context of a compound pendulum, for three cohorts and provides a new framework for swing period coordination dynamics. The cyclical motion of the legs during gait is often compared to the motion of various types of pendulums. While this pendular motion of the legs has been modeled as a limit cycle in dynamic systems theory, this motion analogy has also been a cornerstone for assumptions used in software and hardware modeling of human gait, especially in robotics, passive dynamic walkers, and clinical IGA. Although a few studies have investigated the

validity of these pendular analogies between normal human gait and theoretical pendulum models, the majority focus on the stance period inverted pendulum model of a normal gait pattern, used conventional descriptors of gait, and typically adjusted the small sample of human based gait data to fit a theoretical model. Therefore, these nonlinear methods were applied to describe the swing period coordination dynamics of two linkages in a mathematical model of double compound pendulum and compared to the thigh-shank coordination dynamics generated from the IGA data of human subjects.

1.3 Research Objectives

The research objectives of this dissertation were divided into four aims. The first aim of this dissertation was to construct a normative reference for coordination measures that characterizes normal gait. This normative reference not only provided a control for the two populations with impaired swing limb advancement studied in this work but also offers a framework for coordination dynamics of the leg segments in the normal gait cycle. Since there is not a gold standard coordination measure during the task of gait, the second aim of this dissertation compares the proposed model of coordination dynamics for the three different subject populations to performance measures from select tasks that characterize certain aspects of coordination. This aim relates the proposed measures of coordination to the impaired swing limb advancement condition and offers a means to map coordination findings from the proposed model to these gait pathologies. The third aim assessed the passive pendular of the leg during swing limb advancement by using coordination dynamics measures to compare various theoretical pendula dynamics to the coordination dynamics of subjects with normal and atypical gait patterns. Finally, the fourth aim generates these coordination measures for two subject groups with different causes for impaired swing limb advancement in order to demonstrate the clinical value and utility of these measures. Coordination of the legs during walking requires the elegant organization of the neuromuscular system's many elements and appropriate consolidation of the system's redundant degrees of freedom while considering task and environmental constraints. Coordination of the leg segments during gait is adversely affected in individuals with selective motor control impairments resulting from neuromuscular pathology. Elucidating the coordination of this complex biological system requires an analysis methodology of motion capture data capable of isolating an individual segment's contribution to the system's behavior and identifying the timing and sequencing of adjacent and non-adjacent segment pairs. Phase portraits (PP) and continuous relative phase diagrams (CRPD) are dynamic systems theory derived nonlinear methods

that quantify the pendular like motion of the legs and respective segments during the continuous, cyclical task of gait. It is proposed the lack of a unifying, refined methodology, normative reference, and clinically meaningful demonstrations of the practical benefits and important motor control insights offered by these nonlinear measures have stalled their incorporation into IGA. Therefore, the proposed model of coordination dynamics during walking describes a straightforward methodology for generating descriptors of coordination dynamics based on dynamical systems theory. The first aim of this work was to generate a reference dataset of coordination measures in the sagittal plane coordination for the pelvis, thigh, shank, and foot segments and segment pairings (pelvis-thigh, thigh-shank, shank-foot, thigh-foot) from a large group of individuals free of gait pathology.

Aim 1. Demonstrate the proposed measures of coordination dynamics characterize a normal gait pattern and construct a normative reference from a large cohort of individuals free of gait pathology.

There is currently not a standard method for quantifying coordination dynamics during the cyclical task of gait in clinical populations demonstrating gait pathology. Since there is not an established reference to compare the proposed measures of coordination dynamics, these coordination dynamics measures will be compared to three clinical analogues. While none of these analogues individually encompass the global behavior of inter-segmental coordination, each analogue describes a constitutive element of coordination and therefore will be used to create description of the population. First, performance measures from the Selective Control Assessment of the Lower Extremity (SCALE) will be employed to assess each prospective subject's voluntary selective motor control ability. Although the SCALE exam has been validated for subjects with cerebral palsy, it will be administered to all prospective subjects because selective motor control is essential to successfully execute limb advancement during swing period. Secondly, all prospective subjects will also perform lower extremity tasks from the International Cooperative Ataxia Rating Scale (ICARS) and Scale for the Assessment and Rating of Ataxia (SARA) exams, which have been validated for individuals with cerebellar ataxia. Each prospective subject will perform gait related ICARS/SARA tasks because this characterizes an individual's execution of a motor plan and simultaneous ability to make corrections, both of which are essential to the execution of the feed-forward motor task of advancing the swing limb. Lastly, each prospective subject will perform a lower extremity version of the speed-accuracy test to provide a measure of the subject's information processing abilities during swing. This allows for characterization of each subject's ability to process and integrate proprioceptive and cognitive information used by the movement control system to successfully advance the limb during swing period.

4

Characterizing an individual or population with select constitutive elements of coordination from these clinical exams provides insight into features of the movement control system. While there is not a gold standard measure of inter-segmental coordination, the construct validity of coordination described by these individual components of motor control should be related to the global behavior quantified by the proposed measures of coordination dynamics.

Aim 2. Explore the relationship between the proposed measures of coordination dynamics and select clinical performance measures that characterize aspects of coordination.

Hypothesis 2A. Impairments in the speed and accuracy of voluntary reciprocal movements, as tested in a timed, spatially constrained lower extremity tapping task, will be significantly correlated with task specific coordination deficits characterizing selective motor control.

Hypothesis 2B. The degree of selective motor control impairments, as tested by the Selective Control Assessment of the Lower Extremity (SCALE), will be significantly correlated with task specific coordination deficits.

Hypothesis 2C. Cerebellar based impairments in spatial accuracy of movement and dynamic balance, tested by lower extremity tasks from the International Cooperative Ataxia Rating Scale (ICARS) and Scale for the Assessment and Rating of Ataxia (SARA), are significantly correlated with task specific coordination deficits.

Modeling human movement not only eliminates the complex and intrinsic variables associated with human based data but also this allows for experimentation of conditions, such as those outlined by the hypotheses of this aim, that cannot be tested on human subjects due to the practicality of such experiments. Furthermore an accurate model of swing limb advancement provides a means for determining an optimal solution to the task of walking and a more accurate framework for clinical interventions. The motion of the legs during the stance and swing phases of walking has been likened to the motion of inverted and compound pendula, respectively. This analogy is grounded in the fact that walking appears to be highly optimized with respect to the mechanics of the motion and importance of the conservation of energy driven by evolutionary adoption and refinement of bipedal gait. The vast majority of swing period gait models alter the initial conditions of the model in order to produce a motion that is similar that of the human legs. While these models may achieve their goal of replicating a motion that is similar to that of a human's swing leg, a human is not able to alter inertial properties of their legs. Since inertial properties and initial conditions of most existing swing limb models are altered, it becomes nearly impossible to distinguish which aspects

of the resulting motion are due to motor control strategies and those of the model's alterations. Although the provided pendulum model is more simplistic than other swing period pendulum models, this pendulum model retains the initial conditions and inertial properties, derived from data of human subjects, and is therefore more aptly suited for comparing the swing period motion to that of actual human subjects. While the vast majority of patients with neurological movement disorders primarily struggle with advancing the limb in swing, this critical portion of the gait cycle is rarely addressed in clinical interventions, in part due to the lack of mathematical models and clinically useful techniques for identifying the locus of deviation from the optimal motion. The hypotheses of Aim 3 determine the optimal, ideal pendulum for each subject population during swing period using nonlinear measures of coordination dynamics.

Aim 3. Assess the construct validity that the sagittal plane motion of the thigh and shank during swing period of gait is analogous to the motion of a compound pendulum using measures of coordination dynamics.

Hypothesis 3A. A subject with a lower limb amputation will have coordination dynamics measures with the smallest residual when compared to a passive double pendulum.

Hypothesis 3B. A subject with cerebral palsy will have coordination dynamics measures with the smallest residual when compared to an over-damped double pendulum.

Hypothesis 3C. A subject free of gait pathology will have coordination dynamics measures with the smallest residual when compared to a critically damped double pendulum.

The fourth aim of this body of work focuses on identifying abnormal swing period coordination dynamics in populations who struggle with this crucial task. Although impaired selective motor control, resulting in aberrant coordination dynamics, is the hallmark of neurological pathologies, conventional measures of gait fail to capture this essential element. Without the ability to quantify coordination dynamics, current rehabilitation therapies will remain inadequate and the ability to accurately assess the relative effectiveness between therapeutic interventions remains elusive. Traditionally, data from instrumented gait analysis is used to provide linear measures of gait critical for the proper selection of clinical interventions targeted at reducing aberrant motions. Our initial investigations using nonlinear measures support the theoretical significance of detecting coordination in gait, reveal distinct patterns of movement associated with various pathological gaits, and offer a framework for insight into faulty coordination dynamics that is not available in traditional gait measures. The coordinated coupling and uncoupling of leg segments can be described using nonlin-

ear measures derived from principles of dynamical systems theory. Using the construct of repetitive pendular motion, these dynamic systems theory based nonlinear measures tease out the effects of coordination dynamics by quantifying changes in the underlying organization of leg segments, unveil the mechanism of change, and loci of impairment in the gait cycle; all of which are not available with conventional gait measures. Since the fundamental organization of the leg segments during gait is linked to gait pathology and guides the rationale for clinical interventions, it is essential prior to clinical adoption of these measures to demonstrate that the proposed nonlinear measures of coordination dynamics are able to distinguish between the gait patterns of populations with different physiological reasons for impaired swing limb advancement.

Aim 4. Demonstrate the proposed measures of coordination dynamics can distinguish between different gait pathologies and patterns associated with altered limb advancement during the swing period of gait.

Hypothesis 4A. There is a statistically significant difference ($p \leq 0.05$) between select measures from the mean phase portraits and relative phase diagrams for normal, stiff knee, crouch, and mechanically altered gait patterns.

1.4 Organization of Dissertation Chapters

This chapter provides an introduction to the research project and an overview of the objectives of this investigation. Chapter 2 presents background information relevant to the three main subjects encompassed by this research: coordination, pendular dynamics, and instrumented gait analysis. Chapter 3 provides a description of the proposed model for coordination dynamics of the swing period of gait. Chapter 4 describes the experimental and analytical methodology of this body of work. Chapter 5 presents the results from the experiments detailed in the previous chapter and as a result of implementing the model and data analysis procedures. Chapter 6 contains a discussion and interpretation of these results with respect to the aims and hypotheses from chapter 1. Lastly, chapter 7 summarizes the project and offers suggestions for future directions and improvements to the proposed model of coordination dynamics.

2   Background and Previous Work

Bipedal locomotion is a learned motor behavior that, in the absence of pathology, appears to be a simple motion, but is in fact the emergent behavior of a complex, dynamical system. Characteristics of an adult walking pattern are the result of years of experimenting with various control strategies of the locomotor system in diverse environments and constraints, which is why these patterns are typically not achieved until ages 7 to 9 years [8]. To establish a general relationship between elements of the neuromusculoskeletal system, this chapter begins with a brief overview of the physiology of locomotion in regards to the neurological control of the musculoskeletal system during gait. Assisting in clinical assessment and treatment of individuals with an abnormal gait pattern and contributing to the general understanding of gait are the two main motivations behind gait analysis. Within instrumented gait analysis, there is a diverse and broad spectrum of equipment and measurements used to characterize a gait pattern. Therefore an overview of the two main theories of locomotion and role of instrumented gait analysis in research and clinical applications are presented, with a special focus on two subject groups with impaired swing limb advancement. This is followed by descriptions of common descriptors of gait derived from instrumented gait analysis data and performance measures that characterize certain aspects of coordination. Finally, this chapter concludes with a description of previous investigations that support the use of dynamic systems theory based measures to characterize the coordination dynamics of various gait patterns.

2.1   Physiology of Locomotion

Bipedal walking is a fundamental human behavior, takes years to develop, and is a critical aspect of life because an individual's independence, interactions with the environment, health, and quality of life are markedly compromised when gait or mobility are impaired. Successful execution of bipedal gait requires sufficient strength, balance, postural stability, endurance, and coordination. From a systems perspective, coordinated movement patterns arise from self-organizing subsystems in relation to both internal and external constraints and are the result of dynamic interactions between these subsystems. The control of gait requires the integration of peripheral sensory information and appropriate execution and modulation of a motor plan through descending supraspinal pathways. Therefore, coordination is a constitutive element of gait that relies upon different aspects of the musculoskeletal and nervous systems. The physiology of these locomotion systems significantly affects an individual's ability to efficiently perform the task of gait and adapt to various task and

environmental constraints experienced during independent ambulation. An understanding of the physiology of these systems and the corresponding neurological control is crucial for appreciating bipedal walking and the important contribution of instrumented gait analysis in rehabilitation of various movement disorders.

2.1.1 Neurologic Control of Musculoskeletal System

Although neural activation of skeletal muscle precedes skeletal muscle activation, a brief overview of the musculoskeletal system is provided to set the stage for a more in depth discussion of control of the locomotor system. Using tendons, cartilage, muscles, bones and connective tissue the musculoskeletal system provides support, protection, stability, and the production of forces and moments about joints necessary for movement of the body and performance daily living activities. The nervous system controls skeletal muscle with action potentials, which are rapid and uniform electrical signals that propagate through the excitable membranes of nerve cells to the skeletal muscle. The excitation-contraction coupling is a sequence of microscopic events by which an action potential from a neuron is converted into a mechanical response in a muscle fiber. The striated appearance of skeletal muscle when viewed with a microscope is due to the repeating series of sarcomeres, which are the basic unit of this tissue. Sarcomeres are comprised of thick and thin filaments and the interaction of these contractile proteins is the mechanism within a muscle fiber responsible for the generation of force. Although muscles may change length during contraction, the overlapping myosin and actin filaments of sarcomeres slide past each other by the cyclical formation and releasing of cross-bridges (e.g. sliding-filament mechanism). The number of cross-bridges formed between overlapping contractile proteins and length of the sarcomere are two mechanical properties of skeletal muscle that influence the amount of force (tension) a muscle is capable of generating [9]. Along with this length-tension relationship, the maximum force production of skeletal muscle is also influenced by the load-velocity, which is the sigmoidal relationship between the velocity of changes in muscle length muscle and force production capability, and the force-time relationship, which describes the delay in force development in the muscle-tendon unit from the start of the motor action potential to the peak muscle tension [9].

Skeletal muscles are often referred to as the body's motors because they convert chemical energy into mechanical work. The mechanical work (e.g. force) generated by muscles is transmitted to the bones via tendons and produces the joint moments necessary for walking. Skeletal muscle is attached to bone by tendons, which are mostly composed of the structural protein collagen. In addition to being the structural connection between muscle and bone, the relatively compliant physiology of

tendons allows this tissue to positively contribute to the overall function of the muscle-tendon unit [9]. Specifically, the magnitude of muscle-tendon deformation that occurs during muscle contraction is dependent upon the tendon's compliance and directly affects the muscle's length-tension and force-velocity relationships. Along with anatomical and structural properties of the muscle-tendon unit, the nervous system provides continuous resistance (e.g. muscle tone) in order to prevent full relaxation of skeletal muscles and ensure they are ready to respond quickly and smoothly to excitation. In conjunction with sensory information, the locomotor system also integrates the motor plan and current orientation of segments with this underlying muscle tone during the execution of the intended motion.

As the sarcomere of skeletal muscle is the functional unit of force generation, the motor unit is the functional unit of movement. A motor unit consists of one α-motorneuron and the extrafusal muscle fibers it innervates. The central nervous system controls muscle force production by regulating the activity of motor units within a muscle. The amount of force exerted by a muscle depends upon how many of its motor units are activated (e.g. motor unit recruitment) and the rate at which the motor neurons discharge action potentials (e.g. rate coding) [11]. By altering the activation frequency or number of activated motor units, the nervous system is able to elegantly orchestrate the biomechanical interactions between muscles, tendons, and bones and thus efficiently control the degrees of freedom in the system to produce the desired motion.

Correct determination of the joint positions and movements during a motion are fundamental functions of the locomotor system. Sensory organs within the skeletal muscle detect peripheral sensory information about a joint's position and velocity and changes in muscle length and tension. This sensory information is relayed from these sensors to the central nervous system via corticospinal tracts and is integrated into the voluntary motor scheme. The skeletal muscle spindle and golgi tendon are sensory organs responsible for monitoring skeletal muscle tone. The muscle spindle is an intrafusal muscle fiber that occurs in varying numbers for each skeletal muscle. They are particularly numerous in skeletal muscles that require fine control, such as the intrinsic muscles of the hand. Muscle spindles are attached to the connective tissue septae and are aligned in parallel with the skeletal muscle fibers. This physiological alignment is important because during contraction of the muscle fibers the spindles are kept taut as the muscle fibers contract and thus allow these sensory elements to detect changes in muscle fiber length.

Voluntary contraction of a muscle requires the activation of several motor units, which are recruited in order of increasing size [12]. Studies investigating patterns of muscle activation recruited during postural control and balance tasks have led to the proposal that the central nervous system

simplifies the enormous control demands through the use of muscle synergies [13,14]. Synergies are flexible, emergent properties of a system that are the functional coupling of groups of muscles, which act together as a unit in order to coordinate redundant elements and reduce the system's degrees of freedom [1]. The ability to adapt these synergies is essential to meet any changing task and environmental constraints while executing a movement. The coordinated organization of muscles and joints resulting in a synergy is considered the functional unit of motor behavior. The precise timing and order of muscle activity and positional relationship of segments therefore provide the definition of a coordinated movement. From this perspective, coordination is clearly an essential element of bipedal walking, which requires the ordered timing and sequence of several functional synergies (e.g. extension, flexion) amongst the limbs.

The outline provided below elaborates upon the general scheme for voluntary motor responses. This scheme describes the supplemental motor areas and associated areas in the brain and lists the main steps involved in the creation, execution, and modification of a voluntary movement plan. Further elaboration of this general scheme's steps is also presented with an emphasis on the motor task of gait.

1. Sensory inputs about the body and environment come into the individual's conscious attention.

2. The somatosensory cortex uses these sensory inputs (e.g. somatosensory, visual, vestibular) to create a sensory map.

3. From this sensory map, a movement plan is developed (parietal lobes, supplementary cortex, premotor cortex).

4. The movement plan is sent to the premotor cortex, where muscle groups necessary for the execution of the plan are specified.

5. The updated plan is then sent to the cerebellum and basal ganglia for further modifications and refinement.

6. The cerebellum and basal ganglia send the refined movement plan to the motor cortex and brain stem.

7. Descending pathways from the motor cortex and brainstem activate spinal cord networks and spinal motor neurons then activate the pre-selected muscles.

8. Spinal reflex pathways compensate for unexpected environmental variables and activate more or fewer motor neurons accordingly.

9. Sensory consequences and changes are evaluated by the cerebellum, which compares the actual movement with the intended movement plan and revises the movement plan to correct for any errors.

The cerebellum, motor cortex, and basal ganglia are considered the three important brain areas that contribute to coordination of a movement such as walking. Although the cerebellum does not play a primary role in either sensory or motor function, lesions of the cerebellum result in impaired motor output. Similar to the cerebellum, lesions of the basal ganglia do not result in loss of motor or sensory function but do however significantly impair motor control and the resulting movement. Since voluntary movement is produced through the corticospinal tracts, upper motor neuron lesions (e.g. motor cortex) results in loss of motor control and negatively affects the individual's ability to perform voluntary movements (e.g. walking). Upper motor neurons are neurons that connect the brain to the spinal cord and lower motor neurons connect the spinal cord to skeletal muscles. Disruptions in sensory information, such as that needed to maintain muscle length or tension, contribute to the aberrant coordination characteristic of the underlying motor disorder. To appreciate the role of essential subsystems involved in the general scheme for voluntary movement presented above, a brief discussion of these structures and their contribution follows.

Muscle Spindle. The complete feedback mechanism of the muscle spindle is also known as the fusimotor system [15]. The fusimotor system continually modulates the α-motorneurons innervating the extrafusal muscle fibers and plays an important role in the peripheral sensory feedback mechanisms (e.g. stretch reflex) used by the central nervous system for motor control and motor learning. When Ia afferent receptors are excited, a monosynaptic response at the spinal level excite the agonist muscle and a polysynaptic, long-loop response will excite agonist muscles and dampen (inhibit) antagonist muscles [15,16]. The muscle spindle is located in the belly of skeletal muscles and consists of intrafusal fibers and sensory neuron endings that wrap around the central regions of the intrafusal fibers. Muscle spindles are innervated with sensory and motor neurons that support the detection of the absolute, static muscle length and dynamic changes in muscle length [16]. The extrafusal skeletal muscle fibers are innervated by α-motorneurons, which send afferent action potentials to the central nervous systems and receive input from upper motor neurons via the corticospinal pathway, thus contributing to the initiation of muscle contraction. Muscle spindles are also innervated by β-motorneurons, which relay both changes in muscle length and the rate of changes in muscle length to the central nervous system. Additionally, γ-motorneurons innervate intrafusal muscle fibers and are responsible for maintaining appropriate tension in muscles spindles. Without the co-activation

of α and γ-motorneurons, the muscle fibers would lose tension during muscle contraction causing the muscle spindles to loosen as the muscle contracts. Since γ-motorneurons set the tension of the spindle cell, these neurons are thought to control and regulate the sensitivity of the spindle receptors in response to stretching of the muscle fibers.

Golgi Tendon Organ. The golgi tendon organs are encapsulated organs attached in series to the collagenous fibers of tendons at the point of muscle insertions and also exist in the fascial coverings of muscles [11,17]. Golgi tendon organs provide afferent information about the forces (i.e. tension) between a muscle and its tendon [16,18]. Afferent neurons coming from the golgi tendon organs to the spinal cord are stimulated by muscle tension and selectively inhibit the α-motorneurons of the agonist muscles while facilitating those of the antagonist muscles. Since golgi tendon organs are not innervated by efferent neurons, they are not subject to control from the central nervous system. However, these sensory organs do contribute to the information used by the somatosensory cortex to create and update a sensory map of the body prior to and during a movement. Activation of the golgi tendon organ reflex inhibits the muscle in which it lives and excites the antagonist muscle, which in the past has led researchers to hypothesize this reflex acts as a protection mechanism against muscle forces that could lead to injury of the muscle-tendon unit. In the stance period of gait, golgi tendon organs of extensor muscles in the legs are active and inhibit flexor muscles until the forces on the stance leg are removed during swing. More recent research into the function of golgi tendon organs has led to a new hypothesis that these sensory organs modulate muscle output when the muscle begins to become fatigued.

Dorsal Column-Medial Lemniscal Pathway. The dorsal column-medial lemniscal pathway sends mostly proprioceptive information regarding muscles, tendons, and joints to the somatosensory cortex, which integrates this information and creates and updates the sensory map [18]. Proprioceptors in the legs have a separate pathway to the brainstem via the lateral column where it joins the dorsal column. Higher brain centers can selectively modulate the information coming from this pathway.

Somatosensory Cortex. The somatosensory cortex receives sensory information from joint receptors, muscle spindles, and cutaneous receptors (e.g. mechanoreceptors, nocireceptors, thermoreceptors) [18]. This cortex uses cross-modality processing of the sensory inputs to provide information about movement in a given body area and is transposed upon an existing map of the entire body. This analysis is the beginning of the spatial processing that is essential to spatially coordinating movements of the body and its interaction with the surrounding environment.

Cerebellum. Although the cerebellum does not primarily participate in the sensory or motor function of movement, it is considered one of three central nervous system structures integral to

movement because it receives afferent information from almost every sensory system, refines the motor plan, and regulates motor output by correcting for errors [16,18]. For example, sensory information from the four spinocerebellar tracts relay information from the spinal cord about the arms, neck, trunk, and legs and helps the cerebellum determine if a desired movement matches the motor plan. Additionally, sensory information via the spino-olivo-cerebellar tract is used in the process of motor learning. As a function of its neural circuitry, the cerebellum it acts as a comparator that compensates for errors in a movement by comparing intention (e.g. motor plan) with performance and is therefore a regulator of motor output. In conjunction with peripheral sensory input, the cerebellum receives information from other brain structures about the programming and execution of movements. A copy of the information sent from the moor cortex to the spinal cord is also sent to the cerebellum and is known as an efference copy or corollary discharge. Sensory feedback, reafference, is received by one of the three deep nuclei (fastigial nucleus, interposed nucleus, dentate nucleus) of the cerebellum before continuing on to the cortex.

Basal Ganglia. There are four distinct circuits in the basal ganglia that run parallel to each other. The skeletomotor circuit, which consists of both a direct and an indirect circuit, is perhaps the most well-known of these since it is associated with movement disorders as a result of basal ganglia dysfunction. This circuit receives input from many areas of the cortex. These signals are relayed through the various nuclei (e.g. putamen, caudate nucleus, globus pallidus, subthalamic nucleus, and substantia nigra) of the basal ganglia and then continue on to the thalamus before being sent back to cortex. The direct pathway of the skeletomotor circuit receives sensory input, often associated with pre-movement activities, and responds to stimuli that have motivational significance. The direct pathway increases cortical activity, while the indirect pathway decreases cortical activity. In normal resting state, the two pathways are in balance with a slight edge to indirect pathway [19]. Therefore the skeletomotor circuit (comprised of the premotor cortex, supplementary motor cortex, primary motor cortex, thalamus, basal ganglia) contributes to both the preparation and execution of movement. The basal ganglia are more involved in internally generated movements while the cerebellum is involved in visually triggered and guided movements.

Motor Cortex. There are several different processing areas in the motor cortex involved with voluntary movement. All of these areas interact with information from the somatosensory cortex, basal ganglia, and cerebellum and contribute to the development and execution of a movement plan. It is hypothesized that a motor map, often referred to as a motor homunculus, is located in this cortex and is similar to the sensory map and its homunculus. The corticospinal tract, output of the primary motor cortex, contributes to the pyramidal tract that makes excitatory monosynaptic

14

connections to α-motorneurons, which contract muscles, and polysynaptic connections to gamma motor neurons, which control muscle spindle length [16]. This tract also consists of neurons from the supplementary cortex (controls movements initiated internally), dorsal and ventral premotor areas (controls movements activated by external stimuli), and the somatosensory cortex [16]. It has been proposed that the supplementary area also participates in the assembly of the central motor program or forms a motor subroutine [16].

Thalamus. Nearly all sensory information, except the olfactory system, from the body passes through the thalamus. Located between the cerebral cortex and the midbrain, the thalamus selectively relays sensory information and motor signals to the cerebral cortex and activates motor regions of the frontal lobe [16,18]. The thalamus sends proprioceptive information to the primary somatosensory cortex and thus contributes to the development and maintenance of the sensory map.

The Muscle Stretch Reflex. The excitation of the Ia afferent neurons in muscle spindles results in one of two responses: stretch reflex or long-loop (e.g. transcortical) reflex. The stretch reflex loop is a negative feedback mechanism designed to maintain muscle length and is significantly affected by the inherent compliance of the muscle-tendon unit [20]. The stretch reflex is initiated by a mechanical lengthening of muscle fibers causes the simultaneous activation of terminal fibers in the β-motorneurons of the muscle spindle. The amplitude of the sensory receptor's action potential is proportional to the intensity of the muscle lengthening and if it is sufficiently large will elicit an action potential that propagates along the β-motorneurons to the central nervous system. When the α-motorneurons are excited, the skeletal muscle innervated by these neurons and synergistic recruited muscles are also excited and contract. Additionally, the β-motorneurons excite Ia inhibitory interneurons, which in turn inhibit α-motorneurons of the antagonistic muscles.

Although the stretch reflex is not consciously controlled during voluntary movement, it can significantly influence a person's ability to successfully execute a motor plan. When the excitatory input from muscle spindles is inhibited or removed, the supraspinal drive to alpha motor neurons must increase to produce sufficient force to generate the desired voluntary movement, thus causing an increase in perceived effort, which can lead to fatigue [15]. Individuals with spastic cerebral palsy (neuromuscular movement disorders) often have excessive spasticity. Spasticity, elicited by velocity dependent changes in muscle length, is broadly defined by the Support Program for Assembly of a Database for Spasticity as "disordered sensory-motor control resulting from an upper motor neuron lesion" [22]. This lack of inhibition, which is normally transmitted along the corticospinal tract, causes a disruption of the negative feedback loop that exists between muscle spindles and α-motorneurons. Removal or inhibition of this negative feedback results in excessive and abnormal

15

muscle activation [20].

Central Pattern Generators. In 1914, Graham Brown's theory proposed that even in the absence of muscle reflexes, rhythmic motor patterns (e.g. those seen in locomotion) could be produced by special neural networks (e.g. central pattern generators) [17]. It is hypothesized that central pattern generators at the spinal level, are an organization of intrinsic oscillatory networks that are activated and modulated by central nervous system structures and afferent sensory input [18]. However, this schema relies upon a mysterious "black box" or general homunculus to supply the details of coordination of oscillatory movements and leaves a rather unsatisfactory model for further development and understanding of this control. Alternatively, the dynamic systems approach (e.g. dynamic pattern generation) proposes that there is not a supreme controller but instead movement production is the result of an integration of central nervous system structures, external stimuli, internal sensory information, and environmental factors. Even though both theories offer different advantages and disadvantages, coordination and control of that coordination must coexist in order to account for active central generation of oscillatory movements, such as gait, and control or modifications of coordination to accommodate internal and environmental factors.

2.2   Modeling Locomotion

As evident by the Edwin Smith Surgical Papyrus Ancient Egyptian medical text (ca. 1500 BCE) and Aristotle's reflections (384-322 BCE), humans have been interest in the physiological elements required to produce movement and studied the motion of walking for millennia [23,24]. Baker's article presenting a timeline and account of gait analysis prior to the invention of computers provides a thorough history of this discipline [24]. The work of Inman and Eberhart during the mid twentieth century is often considered to mark the beginning of modern gait analysis because it laid the groundwork for the invaluable contributions by Perry, Sutherland, and Gage whose efforts demonstrated the clinical utility for assessing walking disorders with instrumented gait analysis [25,26,27,28,29]. Inman identified two basic functional requisites of gait that are necessary for any form of bipedalism, regardless of the degree of impairment: 1) continuing ground reaction forces that support the body and 2) periodic forward movement of each foot from one position of support to the next [30]. Interestingly, these two fundamental characteristics of bipedal walking hold true for any form of bipedalism regardless of the severity or cause of movement disability (e.g. neuromuscular disease, musculoskeletal alteration). Expanding upon Inman's two functional requisites of gait, Perry divided the gait cycle into the following three functional subdivisions or "tasks": weight acceptance, single

limb support, and swing limb advancement [26]. It is worth noting that Winter also independently identified these three functional tasks [31]. Additionally, Perry identified patterns from observational gait analysis, electromyography, and kinetics from a cohort of subjects free of gait pathology to further elaborate upon these gait tasks and create the framework (temporal events) for the phases of the gait cycle and the critical events present within these phases (Figure 2.2.1). This framework outlines the fundamental aspects of an unimpaired gait pattern and forms the present working definition of a normal gait cycle, which temporally unifies many of the conventional measures of gait.

The Gait Cycle

Periods	Stance Period					Swing Period		
Tasks	Weight Acceptance		Single Limb Support		Swing Limb Advancement			
Phases	Initial Contact (0%)	Loading Response (0-10%)	Mid Stance (10-30%)	Terminal Stance (30-50%)	Pre Swing (50-60%)	Initial Swing (60-75%)	Mid Swing (75%-87%)	Terminal Swing (87-100%)
Temporal Events	Initial Contact	B: Initial Contact E: Opposite Foot-off	B: Opposite Foot-Off E: Heel-off (body leads foot)	B: Heel-off (body leads foot) E: Opposite initial contact	B: Opposite initial contact E: Foot-off	B: Foot-off E: Feet adjacent (knee extends)	B: Feet adjacent (knee extends) E: Tibia Vertical	B: Tibia vertical E: Initial contact
Critical Events	• Heel first initial contact	• Hip stability • Controlled knee flexion for shock absorption • Controlled ankle PF	• Controlled tibial advancement	• Controlled ankle DF with heel rise • Trailing limb posture	• Passive knee flexion to 40° • Rapid ankle PF	• Max knee flexion (>60°)	• Max hip flexion (30°) • DF to neutral	• Knee extension to neutral

Figure 2.2.1: Periods, task, phases, and important temporal and critical events of the unimpaired gait cycle [26,32].

Although several differences between a normal and pathological gait patterns can be detected with observational gait analysis, instrumented gait analysis uses various instrumentation and measurements to detect and quantify these differences. By tracking and recording the motion of segments during the task of gait, the ability to measure and analyze aspects of human movement, that are otherwise observationally undetectable, creates the means to enhance the general understanding of walking and advance rehabilitative techniques for correcting atypical gait patterns. The utilization of instrumented gait analysis can be divided into two different yet often overlapping applications: clinical and research. Clinical gait analysis generates measures that identify factors contributing to a pathological gait pattern, provides supporting evidence for clinical interventions, and assists in the assessment of treatment outcomes. Quantitative measures derived from instrumented gait

analysis support clinical decision making by providing objective, reproducible descriptors of gait pathology that can be stratified by severity and characterize overall gait performance. Over the last few decades, techniques and instrumentation for instrumented gait analysis have evolved significantly to the point where it is considered by many to be an integral component of rehabilitation planning and assessment of treatment outcome for individuals with an aberrant gait pattern [33].

Since there is a diverse spectrum of research that instrumented gait analysis comprises of a diverse and broad spectrum, only a select few applications that are relevant to this body of work are mentioned. Treadmill gait training is an appealing rehabilitation modality for patients with a neuromuscular impairment because it offers a means for task-specific gait training, repetition, manually and robotically guided assistance, systematically controlled progression of walking speed, and the option for partial body weight support. Although numerous studies have examined potential differences between overground (OG) and treadmill (TM) walking in order to assess the validity of this OG walking analogue, the findings from these studies are often inconclusive and conflicting. A challenge in the development of prosthetic limb control for individuals with a lower limb amputation is simulating control and feedback from both the efferent and afferent pathways of the nervous system. Several passive mechanically passive and electronically controlled prostheses are designed to mimic the kinematics and kinetics of intact, healthy individuals. Additionally, using this baseline of a normative gait pattern, several research studies use instrumented gait analysis techniques to assess changes in existing prosthetics, refinement of control algorithms, compare different prosthetics, and evaluate new prosthetic designs [34,35,36]. Research using instrumented gait analysis measures has also been beneficial in the field of robotic assisted gait training, especially for treadmill training with active orthoses [37,38,39]. Normative gait patterns and standard deviations from instrumented gait analyses provide the baseline reference control algorithms and safety limits for robotic orthoses and exoskeletons. Research studies often use conventional measures of instrumented gait analysis in their experimental protocol to tests these control algorithms, assess the effects of changes in device design, and efficacy of such rehabilitation devices in targeted patients.

Three-dimensional tracking of passive and active markers, placed on specific anatomical landmarks, provides locations of segments as an individual walks in the motion capture environment. This positional data of segments can be used to define each complete gait cycle, which then provides the temporal framework that allows conventional measures of gait to be described on the same time scale. Segment positions are used to calculate temporal-spatial descriptors of gait, which are used to detect asymmetries and characterize overall functional performance. When segments are tracked with markers, the positional data of these markers can be used to create coordinate systems for each

corresponding segment. Kinematic curves, quantifying changes in joint angles with respect to time, are angles constructed from the axes of two adjacent segments and separated into the three planes of motion. A more in depth explanation of temporal-spatial and kinematic variables is provided later in this chapter. In addition to these conventional instruments gait analysis measures, kinetics and dynamic electromyography are considered traditional gait measures. Triaxial force platforms measure the magnitude and direction of ground reaction force of the stance limb. The skeletal hierarchy used for constructing kinematics is also used, in a process known as inverse dynamics, to estimate the forces, moments, and powers at each joint in the kinematic chain. These kinetic variables offer insights into power generation/absorption by the musculotendon complexes as they act on a joint and provide insights into the relationships between the angular motion of joints (kinematics) and the muscle forces that generate joint moments. As previously mentioned, skeletal muscles are the motors of the body and the recruitment and firing rate of motor units by the nervous system. An electromyogram is the cumulative myoelectric activity of several motor unit action potentials, which can be recorded with either surface or percutaneous electrodes and amplifiers [23]. Since different combinations of muscle activity during gait produces lower limb kinematic patterns, dynamic electromyography is often incorporated into instrumented gait analysis because it provides a recording of the phasic muscle activity of monoarticular and biarticular muscles used in walking. Temporally normalizing kinematics, kinetics, and electromyographic data to the gait cycle aids in the interpretation of this data by providing a common time scale based on foot strikes and allows for intra-subject and inter-subject comparisons. A more in depth explanation of the select conventional measures of gait utilized in this investigation is provided in a subsequent section. This brief overview of common equipment and measurements used in instrumented gait analysis is by no means exhaustive. Fortunately, there are numerous texts on these areas that provide more extensive coverage of the various types of equipment used to capture human movement and the measurements derived from the data record by various instrumentation [23,29,31,32,40].

Interpreting the vast amount of data recorded during an instrumented gait analysis and relating this information to the multiple physiological interactions contributing to a gait pattern in a clinically meaningful way can be challenging. As evident in Perry's divisions of the gait cycle, there are several complex motor behaviors whose timing and organization are essential for completing the task of gait. In particular, the task of swing limb advancement is a crucial function performed during single limb stance and requires sufficient balance, strength, and coordination to successfully execute. Therefore, the following section expounds upon this portion of the gait cycle in the context of a gait pattern free of pathology. Establishing this framework for swing limb advancement provides a useful

reference for the various mathematical models of gait used to emulate this motion and the model developed in this dissertation. Lastly, this reference of the functional requirements and physiological interactions necessary for successfully completing this gait task assists in understanding how different physiological impairments in the neuromusculoskeletal system can negatively affect the inability to perform this task efficiently.

2.2.1 Task of Swing Limb Advancement

The task of swing limb advancement begins with the occurrence of opposite foot strike of the contralateral leg, coincides with the beginning of the pre-swing period of the gait cycle, and involves four of the eight phases of gait. Swing limb advancement incorporates the swing period of gait and is completed when the foot of the swinging limb makes contact, ideally heel first initial contact, with the walking surface. In a normal gait pattern, the main functional objectives during the task of swing limb advancement are: proper positioning of the limb for swing (pre-swing phase), uncoupling of the thigh-foot extension synergy at foot off, sufficient clearance above the ground by the foot (initial and mid-swing), forward advancement of the limb (initial and mid-swing), and proper placement of the leg in anticipation of heel first initial contact and loading response (terminal swing).

Swing limb advancement requires the precise timing and elegant organization of the leg segments and is the resulting behavior of a complex, dynamical system as evident by the following subtle, yet essential coordination mechanisms. During pre-swing, the lateral weight transfer from the stance limb to the contralateral limb, at opposite foot on, is required for the necessary changes in posture, provides a brief second instance of double limb support, and unloads the advancing limb in preparation for rapid advancement during swing phase at the instant of foot off. At foot off, the simultaneous uncoupling of ankle plantarflexion and hip extension is essential if the swinging limb is to efficiently capitalize upon the ballistic forward propulsion provided by the ankle plantarflexion moment, which along with hip flexion will ensure sufficient limb clearance and advancement from its trailing limb posture. Achieving sufficient knee flexion for uninhibited foot clearance and leg swing is an important function of the leg during swing limb advancement. Adequate knee flexion, sufficient forward limb momentum from rapid hip flexion, and activation of the biceps femoris muscle to reach maximum knee flexion are three mechanisms, whose precise timing and magnitude must be accomplished in order to lift the foot enough for unobstructed ground clearance and limb advancement [26]. In addition to identifying these critical functions in initial swing, Dr. Perry presented the paradoxical relationship between the knee and ankle joints while lifting the foot. Passive knee extension is not only critical for foot clearance, but also in order to efficiently utilize the compound

pendular dynamics of the legs whose forward momentum will advance the limb in preparation for the impending foot strike. Once the foot is located ahead of the hip joint center, the pendular motion of the leg segments and momentum from hip flexion contributes to completion of swing limb advancement (e.g. passive knee extension) [26]. Finally, during the last few percentages of the gait cycle the segments are precisely oriented for the impending foot strike and subsequent loading response. Active dorsiflexion from the anterior tibialis positions the ankle neutrally for a heel first initial contact. Simultaneously, preparation for weight acceptance is achieved by contraction of the hamstring muscles, which decelerates the shank and creates slight flexion at the knee (preventing hyperextension of the joint at foot strike).

Poor anticipatory planning and impaired execution of a motor program during swing limb advancement is exhibited in individuals with neurological impairments, which also contributes to an increased risk of falling [16]. Anticipatory planning and execution of a motor plan are essential for successfully achieving swing limb advancement and preparation of the leg segments for heel first initial contact. Bipedal gait, especially during single limb support, is considered an inherently unstable motion. The ability to anticipate these oscillations in stability and make appropriate corrections is essential for the prevention of falling and adaptation to any changes in task and environmental factors [41]. The anticipation of footfall and the time constraint of swing period affect the temporal organization of the leg segments during the execution of swing limb advancement. There is an increasing interest in understanding anticipatory motor control because this offers insights into the elaborate coordination strategies required in the task of swing limb advancement. A method that quantifies coordination dynamics, which are the resulting behavior of appropriate anticipatory planning and unimpeded execution of the motor plan, is essential for understanding the sequential organization of leg segments. The model of coordination dynamics presented in this body of work was used to understand the dynamical mechanisms underlying this task by identifying the exact timing during the gait cycle when segments are contributing to an aberrant coordination behavior and specify the segments responsible for impairing advancement of the swinging limb. The methodology presented offers a means for quantifying the timing and sequencing of muscle synergies, providing clinicians with insights into how the nervous system is controlling the various limb segments in order to produce the purposeful and coordinated movement of swing limb advancement. Characterizing this essential task of gait will enhance current instrumented gait analysis methods and understanding of gait patterns affected by neurological impairments resulting in the inappropriate timing and interactions between segments.

2.2.2 Modeling Swing Limb Advancement as a Pendulum

A mathematical model of a system provides a means for describing the system in a quantitative form, from which a hypothesis about the system and its behavior can be extensively tested. A major aim of modeling gait is to identify and characterize the behavior of normal and pathological gait through the use of appropriate computational tools. The cyclical motion of the legs during gait is often compared to the motion of various types of pendulums, in particular to a single or double pendulum. This analogy has been a cornerstone for assumptions used in software and hardware modeling of human gait, especially in the robotics, passive dynamic walker, and clinical gait analysis disciplines. Surprisingly, there have been only a small number of studies investigating the validity of these pendular analogies between normal human gait and theoretical pendulum models. Furthermore the few experiments investigating the relationship between the theoretical analogy and actual human movement have focused primarily on the stance period of normal gait and only compared this relationship using conventional descriptors of gait (i.e. temporal-spatial measures, kinematics, kinetics, and energetics). The human gait data from this study was compared to an ideal, optimized theoretical pendulum model in order to assess the validity of this analogy and to determine the corresponding ideal theoretical dynamics for a compound pendulum. Therefore the experiments and analysis of Aim 3 used conventional measures of gait and nonlinear measures to describe the coordination dynamics of various theoretical pendulum software models and compare the theoretical pendular dynamics to those of subjects with normal and atypical gait patterns.

For six decades, two prevailing theories of walking have been used to mechanistically describe this task: Inman's six determinants of gait (kinematic) and the pendulum analogy (kinetic). In 1966, Elftman reported that energy expenditure is minimized at certain walking frequencies42. This experimental finding was expounded upon by Inman, who presented six kinematic determinants of gait that he proposed were employed to decrease energy expenditure by minimizing the excursion of the center of gravity in both the vertical and horizontal directions. These determinants are based upon the premise that deviations in the trajectory of the center of gravity are energetically costly, which is supported by studies theorizing one evolutionary advantage for humans was bipedal walking requires lower energetic cost than quadrupedal walking [43,44,45]. The hypothesis that bipedal walking is energy efficient is further supported by studies showing the swinging limb constitutes the major energy demand during walking [46,47,48] and therefore necessitates the optimization of the mechanical motion in order to minimize energy costs and be evolutionarily advantageous. The six determinants are: 1) pelvic rotation, 2) pelvic tilt, 3) knee flexion in early stance, 4)

ankle mechanism in stance, 5) foot mechanism leading into foot off, and 6) lateral displacement of the body/pelvis30. These determinants of gait were meant to provide an initial framework for deconstructing the kinematic motions observed in normal and pathological gait patterns and begin to establish a mechanistic approach to understanding fundamental elements required for a normal gait pattern; contrary to the common misconception that these were intended to be taken literally [49]. When viewed retrospectively, it becomes clear how Inman's initial approach to understanding kinematic descriptors of gait eventually developed into today's gait cycle divisions, critical and temporal events, and tasks, which are used to describe the walking pattern of humans, passive dynamic walkers, and various pendula.

In a similar motivation to provide a theory that accounts for how energetic costs during bipedal walking are efficiently minimized, pendular theories were proposed [50,51] and used to generate the initial mathematical models for passive dynamic walkers [51,52,53], which significantly contributed to the logic and design of many of today's lower extremity robotics, prosthetics, and exoskeletons. As illustrated in the figure below, two pendular systems are likened to the motion of the legs during walking: an inverted pendulum (stance leg) and a compound pendulum (swing leg).

Inverted Penduluar Motion of Stance Period

Compound Pendular Motion of Swing Period

Direction of Walking ⟶

Direction of Walking ⟶
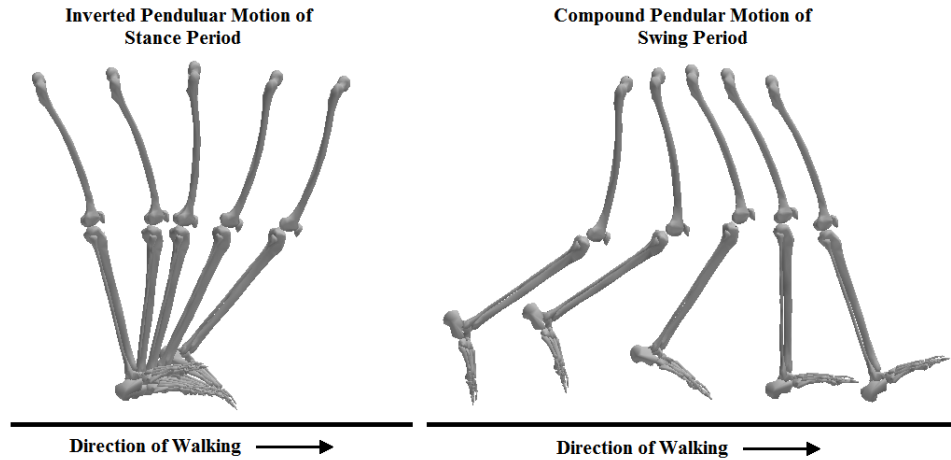
Figure 2.2.2: Motion of the lower limb segments progressing through the gait cycle illustrating the similarity of an inverted pendulum (left) and compound pendulum (right).

Unlike Inman's approach, pendular models tackle the goal of reducing energetic costs during walking from a dynamics and energetics perspective. Proponents of the pendulum theory over Inman's determinants of gait often note studies showing that when people are instructed to consciously reduce the vertical displacement of their center of mass, that more metabolic energy is expended compared to when the individuals are instructed to walk with their usual gait pattern [54,55,56]. While inverted pendular models of the stance leg's motion may have kinetic and gravitational po-

tential energies with similar center of mass trajectories as that in human gait, pendulum model theory of the swing (and stance) period of gait do not require any energy expenditure. This poses a disconnect between pendular analogies and the actual motion of walking because numerous human gait studies have used electromyography data to prove there is muscle activity during this period of gait and energy consumption [26,57,58]. Dynamic walking models have been generated to enhance the simple passive pendular models of gait and offer a means to model different control strategies (e.g. muscle activation), notoriously difficult modeling of the transition from stance to swing, and focuses on the types of work performed on the model as opposed to the energy expenditure [56]. While none of these theories about walking satisfactorily models the actual performance of this task by humans, even simple models can constructively contribute to the study of walking. For example, the simple compound pendulum model of swing period limb dynamics created in this body of work is justified because the intent of this model was to demonstrate how dynamic systems theory based measures, which is rooted in the pendular motion of a limit cycle oscillator, can be used to describe and compare the coordination between any two moving bodies, whether they are leg segments or pendulum linkages.

Mathematical models are necessary tools for structuring the current body of knowledge and can transform existing theories of motion control into testable hypotheses. If models and theory are one half of advancing our understanding of gait, then experimentation is the other side of the coin because it is the primary mechanism for adding new information to an existing body of knowledge. If the purpose of studying human walking with simplified pendular models is to help advance the understanding the gait patterns expressed by various populations, then it is important to keep these differences in mind and appreciate what changes can be made to the model that are also physiologically possible to execute as a person walks. This approach to studying gait with a pendular mathematical model was a fundamental consideration for the design of experiments and experimental methodologies for Aim 3. Specifically, the defining properties and initial conditions of the simple compound pendulum mathematical model were calculated from tri-planar motion capture data of human subjects who underwent an instrumented gait analysis. Furthermore, the various permutations of the pendulum model's constitutive behavior were compared to the instrumented gait analysis data from different cohorts of subjects with varying degrees in the ability to perform swing limb advancement.

2.2.3 Gait Patterns with Impaired Swing Limb Advancement

Successful and efficient execution of swing leg advancement requires the elegant coordination and control of body segments, dynamic balance control, and integration of sensory and environmental information. Since this task requires the precise organization and intricate interaction of many structures within the body, it can easily be inhibited by a number of biomechanical and neurological impairments. Unsuccessfully performing swing limb advancement not only hinders a person's ability to achieve critical gait events, but also results in such inefficiencies as decreased walking speed, altered step width and length, and variable balance (e.g. increased risk of falling). In order for the proposed model of coordination dynamics to be incorporated into the instrumented gait analysis measurement repertoire, these measures must demonstrate that they are useful for any form of bipedalism regardless of the severity or cause of movement disability (Aim 4). Therefore, two different populations with aberrant swing limb advancement were studied. First, the gait pattern of subjects with cerebral palsy were studied to because they provide examples of how neuromuscular impairments can lead to impaired swing limb advancement. Second, the gait patterns of subjects with a lower limb amputation were studied their difficulty with the task of swing limb advancement stems from the inability to control their limb below the level of amputation due to loss of neuromusculoskeletal elements as opposed to an inappropriate execution of a movement plan.

2.2.3.1 Spastic Cerebral Palsy

Cerebral palsy is a movement disorder resulting from a static, non-homogeneous encephalopathy that occurs in the brain of a preterm or term infant. Approximately 3 per 1000 live births have cerebral palsy, making this condition the most common pediatric movement disorder [59]. Although cerebral palsy is not a progressive disease, as individuals with cerebral palsy grow older they are reporting pervasive health issues and secondary impairments such as diminishing independent ambulation, musculoskeletal pain, chronic fatigue, and signs of premature aging [60]. These life-altering impairments cost the nation upwards of $11 billion in medical expenses each year and there is growing evidence that lack of coordination brought on by neuromuscular disease is linked to these impairments. This suggests there is a profound and often overlooked need for improving existing rehabilitation strategies in an effort to reduce long-term health problems in this population.

The subjects with spastic cerebral palsy studied in this dissertation were classified with the following categories: a) Physiology (e.g. spastic) b) Anatomical location of the injury resulting in either or unilateral (e.g. hemiplegic) or bilateral (e.g. diplegic) involvement c) Gait pattern (e.g.

stiff knee, crouch) Spastic, ataxic, and athetoid (or dyskinetic) are the three main classifications of cerebral palsy and are based upon the types of motor impairment and affected areas of the brain61. Spastic cerebral palsy, henceforth referred interchangeably with cerebral palsy, occurs in 70% of all cases, making it the most common type [62]. The vast majority of individuals with cerebral palsy have either hemiplegia (22% of preterm births, 44% of term births) or diplegia (66% of preterm births, 29% of term births), with the remaining having quadriplegia (7% of preterm births, 10% of term births) [61]. Since this body of work examined the gait pattern of individuals with either one or both legs affected by impaired selective motor control, the classification of diplegia also includes individuals with quadriplegia.

Impaired selective motor control is a classic characteristic of spastic cerebral palsy that is defined as a negative motor sign due to the insufficient control of muscle activity. Motor signs that lead to an increase in the frequency or magnitude of muscle contraction or movement patterns are defined as positive motor signs [63]. Tremor and hypertonia are examples of positive motor signs. Negative motor signs are notoriously more difficult to quantify, especially since both positive and negative motor signs are often present in a motor disorder and are thought to be connected rather than independent. For example, the diplegic gait pattern of a child with spastic cerebral palsy may be due to the inability to generate sufficient voluntary muscle force about a joint (positive motor sign) as well as an inability to isolate the activation of specific muscles (negative motor sign). Reduced selective motor control is defined as the inability to selectively activate specific muscle synergies to generate a movement pattern, which in the case of gait leads to an undesirable response in certain phases of the gait cycle, lack of flexibility to adapt to changes in task and environmental demands, and an overall aberrant gait pattern.

Various neural imaging modalities have shed further light onto the physiological characteristics leading to the negative and positive motor signs present in individuals with cerebral palsy. Brain scans of children with spastic cerebral palsy have revealed the most common location of damage was to the corticospinal tracts in the periventricular white matter [64]. Damage to the corticospinal tracts hinders an individual's ability to control force production, speed, timing, and movement patterns, thus resulting in impairment of such voluntary movements as walking. Correlations between injury to the corticospinal tracts and motor disability in individuals with spastic cerebral palsy have been found in over one-third of those with hemiplegia and quadriplegia [64,65].

Increased muscle excitation due to spasticity resulting in pathological co-contraction of muscles is a hallmark characteristic of cerebral palsy that contribute to overall functional motor deficits. In gait, these motor deficits interfere with the successful execution of a movement pattern and are

particularly evident during the task of swing limb advancement. Lance (1980) defined spasticity as "... a motor disorder characterized by a velocity-dependent increase in tonic stretch reflexes, with exaggerated tendon jerks resulting from hyper-excitability of the stretch reflex...". When spasticity is the primary impairment contributing to an aberrant gait pattern, excessive activity of a spastic muscle occurs at times in the gait cycle when the muscle is being lengthened. For example, the quadriceps muscles are lengthened in early stance during weight acceptance and at foot off as the knee flexes. Spasticity in the rectus femoris muscle prevents passive knee flexion in pre-swing and forces the individual to adopt compensatory movements in order to advance the swing limb. Spasticity in the hamstring muscles inhibits sufficient knee extension during terminal swing which is necessary for preparation of initial contact and corresponds to the one time in the gait cycle when this muscle is lengthened.

Although the primary lesion leading to spasticity is located in the central nervous system, numerous studies have demonstrated that the structure of skeletal muscle in patients with spasticity is dramatically altered and abnormal [10,67]. Furthermore, abnormal bone growth as the result of atypical forces and loads generated from muscle spasticity and the exaggerated of the stretch reflex contribute to this movement disorder. Co-contraction of muscles about joints (e.g. simultaneous flexion of the hip, knee, and ankle joints) is also associated with spastic gait patterns. Leonard et al. (1991) found that compared to children without cerebral palsy, children with cerebral palsy retained pathologic co-contraction about joints and were unable to dissociate certain synergies due to spasticity [68]. Secondary impairments of upper motor lesions, such as changes in skeletal muscle mechanical properties and inappropriate activation of muscles as a result of spasticity, illustrate many factors can contribute to an aberrant gait pattern associated with cerebral palsy and reveal the complexities in how a gait pattern is uniquely affected in each individual. Even though the gait pattern of an individual with cerebral palsy is unique due to the location of the upper motor neuron lesion, there are general characteristics and combinations of movement patterns identified with measures of instrumented gait analysis that have been categorized into pathological gait patterns. In particular, as a consequence of spasticity, co-contractures, and aberrant muscle excitation two of the most common abnormal gait patterns associated with cerebral palsy occur in the plane of progression (sagittal) about the knee joint: stiff knee gait and crouch gait [69].

Stiff Knee Gait Pattern. A stiff knee gait pattern can be present in either hemiplegic or diplegic patients and is one of the most common gait patterns associated with cerebral palsy [112]. The stiff knee gait pattern is associated with excessive knee extension throughout the swing period of gait, especially during initial swing and mid-swing phases. Contracture about the knee is caused

by an inability to cease excitation of the rectus femoris muscle during swing limb advancement and therefore causes a delay in both the timing (after 72% of the gait cycle) and magnitude of maximum knee flexion (less than 45°) [69]. Inability to dissociate this extension synergy at foot off delays initiation of limb advancement, interferes with foot clearance, disrupts the smooth stance to swing transition and resulting compound pendular motion of the segments in swing, and forces the individual to adopt inefficient compensatory movements using the contralateral (stance) limb in order to avoid tripping and achieve forward movement of the swinging limb [26,70,113].

Crouch Gait Pattern. A crouch gait pattern displays excessive hip, knee, and ankle flexion throughout the gait cycle. These excessive joint angle positions can be the result of the contractures, spasticity, lever arm dysfunction, and bone deformities either individually or in any combination [32,71,72]. Contractures of the hamstring and iliopsoas muscles manifests as an inability to generate sufficient hip extension and inadequate knee extension in terminal swing. Spasticity in the hamstring muscles results in excessive knee flexion and prevents the desired knee extension in preparation for a heel first initial contact. In conjunction with insufficient hip extension, excessive ankle dorsiflexion as a result of weak triceps surae muscles is often present and contributes to a decreased ability to generate sufficient ankle moments and powers at foot off for advancement of the swing limb [69]. Weak quadriceps muscles are also often present in a crouch gait pattern and as a consequence further contribute to excessive knee flexion throughout the gait cycle. These altered joint angle patterns and weakness of certain muscles manifest in the temporal-spatial variables as decreased stride length and decreased walking speed. A crouch gait pattern can be present in patients with either hemiplegia or quadriplegia, but is more commonly associated with diplegia. Depending upon the location of an individual's upper motor neuron lesion, a stiff knee gait pattern may also be present with a crouch gait pattern.

2.2.3.2   Lower Limb Amputation

In 2005, it was estimated that 1.6 million Americans were living with the loss of a limb, 65% of which had a lower extremity amputation, and by the year 2050 this total population of individuals with an amputation is expected to reach 3.6 million [73]. Among these Americans living with the loss of a limb, the main reasons for amputation are dysvascular disease (54%), trauma (45%), and cancer (less than 2%)73. The large health care costs associated with a lower limb amputation, in part due to concomitant illnesses [74], secondary disabilities resulting from amputation (e.g. pain, degenerative arthritis, osteoporosis, re-amputation) [75,76], and decreased quality of life and mobility [77,78] renders this population with significant ambulatory impairments and thus is an ideal beneficiary

of insights gained from instrumented gait analysis. There are several reasons for an amputation, but since the purpose of this work is to investigate the neurological control of the residual limb by an intact and unimpaired nervous system, only acquired amputations to treat trauma, congenital limb deficiencies, and management of tumors were considered. In conjunction with a prosthetic's mechanical quality and properties, the level of amputation significantly contributes to the overall altered gait pattern. Longitudinal lower limb deficiencies refer to the reduction or absence of a bone within the long axis of the leg, as illustrated in the figure below [79].
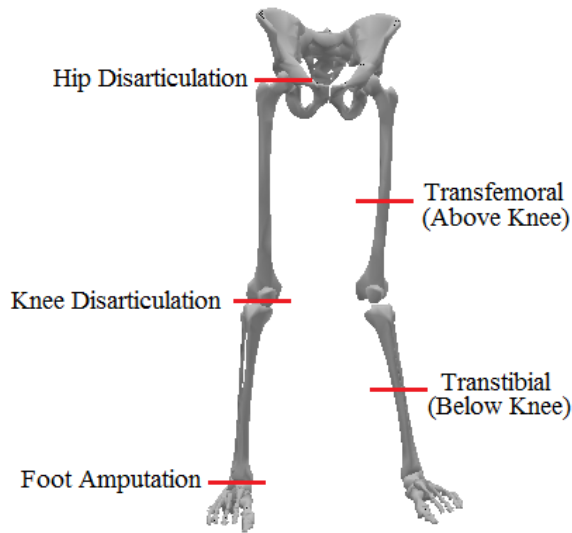
Figure 2.2.3: Diagram of longitudinal levels of amputation for the lower extremity.

In response to the large number of surviving World War II veterans returning home with lower limb amputations, Inman and Eberhart use instrumented gait analysis to enhance the understanding of normal and lower limb amputation gait patterns and improve prosthesis design with knowledge gained from their studies [30,80,81]. Since then, many studies have used kinematics, kinetics, electromyography, and temporal-spatial measures to evaluate the functional effects of various prosthetics and level of amputation on the individual's gait pattern [78]. A general consensus exists that there are significant differences in the gait of individuals with an amputation compared to healthy individuals free of gait pathology or limb amputation. Prinsen et al. (2011) performed a systematic review of IGA studies investigating individuals with a lower limb amputation and found that individuals with either a transtibial or transfemoral amputation used similar compensatory strategies at the hip to compensate for insufficient power generation at the ankle during foot off and for limb advancement in swing [82]. Also, the timing and duration of critical gait events has been found in numerous studies to be delayed and significantly elongated when compared to normal gait [78]. Since

a major goal of prosthetic intervention is to provide the patient with the most efficient gait possible and emulate an unimpaired gait pattern as closely as possible, the use of instrumented gait analysis measures to identify asymmetries and deviations has provided valuable insights and quantitative data for improving rehabilitation programs and informing prosthetic design.

After an amputation, the locomotor system is challenged to relearn the task of walking without the afferent sensory motor input below the level of amputation and adapt to the altered mechanical properties of the prosthetic. During the initial phase of rehabilitation, the individual with an amputation compensates for the neuromusculoskeletal changes by adopting various gait compensations that place a great reliance upon the intact limb. To facilitate limb clearance and advancement during swing period, the prosthetic leg is typically made slightly shorter than the non-amputated leg. In conjunction with an increase in time spent on the intact limb and shift of load bearing responsibility increasing on the intact limb [80], this intentional leg length discrepancy may also contribute to increased forces on the intact limb and explain the prevalence of osteoarthrosis that occurs in the non-amputated limb [75]. In general individuals with a lower limb amputation spend more time in stance on the intact limb [83,84,85], load the intact limb more while decreasing loads on the prosthetic limb [85,86,87], and have higher forces on the intact limb which combined have been shown to lead to increased degenerative joint disease, pain, and decreased mobility [75,88,89]. Numerous studies have reported the metabolic energy cost during walking for an individual with an amputation is significantly greater than energy expenditure of healthy individuals without an amputation [58,90,91,92,93]. Although metabolic energy expenditure is highly dependent upon an individual's physical condition, the general trend of an increased metabolic cost of walking has been shown to significantly increase with higher levels of amputation and for bilateral amputations [58]. Changes in walking speed has been correlated to increasing levels of amputation and is therefore commonly used to describe an individual's overall ability to efficiently perform the task of gait [82]. Unlike metabolic cost, walking speed is easily calculated from three dimensional segment trajectories, which are captured and used to describe other conventional instrumented gait analysis measures, and does not require additional equipment. Walking speed and asymmetries in temporal-spatial and kinematic variables have become the standard means used to assess the gait pattern of an individual with an amputation, especially in gait rehabilitation [94].

The majority of studies examining the gait of individuals with a LLA assume the leg acts like a passive compound pendulum. Even studies investigating mechanically passive and electronically controlled prosthetics focus their investigation on the task of weight acceptance and swing initiation (e.g. pre-swing). The majority of prosthetics used by individuals with a LLA are passive, mechanical

devices that try to emulate a normal gait pattern. Improvements in material quality and insights from IGA have helped to advance and refine the designs of such mechanical mechanisms, however because they are passive these devices are still unable to completely account for smooth weight acceptance, adequate power generation for foot off, and adapt to different walking conditions (e.g. speed). To address the effects of lost neurological control of a joint below or at the level of amputation and provide a gait pattern more analogous to that of an individual free of gait pathology, electronically controlled prosthetics were designed. For example, the microprocessor of the C-Leg® is able to identify the initiation of swing phase and minimize knee resistances in order to assist in the initiation of swing phase knee flexion for individuals with a transfemoral amputation [95]. Active control of this prosthetic's otherwise passive pendular motion has been shown to shift kinematic curves and temporal-spatial measures closer toward normal kinematic curves of non-amputated legs [35,78]. However, several gait abnormalities persisted with both electronically controlled and mechanically passive devices with a fixed ankle angle during swing [84]. Measures of coordination dynamics may reveal additional insights into a patient's control of the affected limb that could be used to provide real-time adjustments to the electronic algorithms controlling the prosthetic joint so as to more closely emulate a normal gait pattern.

Limb amputation leads to major change in biomechanical and neurophysiological relationships that also influence the physiological quality of the residual limb and contribute to the individual's overall walking ability. Several research studies have found that a major reorganization of both afferent and efferent projections occurs in such patients and that this neurological reorganization contributes to the changes in motor patterns seen in persons with lower limb amputations [96]. These theoretical models suggest the motor control system can re-organize after the reduction or removal of biomechanical constraints and result in a change in coordination. Compensation for loss of proprioceptive cues, which normally help signal the initiation and terminal of certain gait events, and altered inertial properties can be achieved in individuals with a LLA who are free of neuromuscular pathology. Describing movement at the level of coordination in this population has the potential to enhance the efficacy of a patient's rehabilitation by providing insights into how the nervous system is adapting to and controlling the altered biomechanical properties of the residual limb and prosthetic. Therefore it was anticipated that subjects with a lower limb amputation would adopt distinctly different coordination patterns, depending upon the level of amputation, than the other two populations studied and that these alternative SLA strategies are be detectable with the coordination dynamics measures utilized in this investigation. As the level of amputation increases, these measures of coordination dynamics were also expected to follow similar trends as

the conventional measures of gait and show greater deviations from an unimpaired gait pattern.

Individuals with a lower limb amputation and an unimpaired nervous system constitute the third population studied in this body of work. Similar to individuals with cerebral palsy, individuals with a lower limb amputation have an aberrant swing leg motion and altered swing limb advancement. However, unlike the aberrant neurological control characteristic of individuals with cerebral palsy, swing limb advancement is altered in an individual with a lower limb amputation due to the inability to control joints at or below the level of amputation as a result of the physical removal of essential locomotor system elements. Gait rehabilitation strives toward helping the patient achieve a symmetrical gait pattern by focuses on reducing coordination impairments. Conventional instrumented gait analysis measures (e.g. temporal-spatial, kinematic) are often used to help identify asymmetries and track changes during and after therapeutic interventions. However, since an amputated leg has inherently different functional abilities (e.g. insufficient ankle power generation at foot off) and has different physiological capabilities compared to the intact limb (e.g. loss of ankle plantarflexor muscles) then it seems unfair to hold these two limbs (intact and amputated) to the same functional performance criteria. Perhaps by including measures of coordination dynamics, insights into the relationships between the control strategies of the intact and amputated limbs can help rehabilitation interventions (e.g. behavior of muscle synergies at specific instances in gait cycle) by facilitating/enabling maximum possible adaptability of each limb. When considering a person's ability to re-organize coordination strategies and the biomechanical design of a prosthesis, it becomes clear the success of a patient's rehabilitation, ideal prosthetic behavior, and adoption of optimized coordination patterns necessitates a measure for coordination dynamics. Therefore, the gait patterns of individuals with a lower limb amputation were studied and have been classified into two general categories: transtibial (below knee) and transfemoral (above knee).

Transtibial Amputation Gait Pattern. Transtibial amputations are the most common lower extremity amputations and account for 55% of all individuals with loss of a lower limb [97]. The gait task of weight acceptance and pre-swing period limb advancement are significantly impacted by the loss of the ankle joint and foot. The gastrocnemius-soleus complex is the major muscle group responsible for generating the plantarflexion moment at foot off and combined with the hip flexors provides the ballistic power to propel the swinging limb forward. However, for individuals with a transtibial amputation the hip flexors become the dominant motor to provide sufficient power generation for swing limb advancement. Several IGA studies have been conducted to characterize the gait pattern associated with a transtibial amputation, many of which have reported the following characteristics: decreased walking speed compared to unimpaired gait [78,90], knee flexion contractures greater than

10° [98], delayed and insufficient peak knee flexion [37,78], increased energy expenditure [90], persistent ankle dorsiflexion due to prosthetic ankle joint's inability to plantarflex [90], and a correlation between decreased walking speed and reduced muscle strength [100]. A classic example of early stance deviations in subjects with a transtibial amputation is a reduced and delayed knee flexion curve with prolonged heel support and delayed forefoot contact. Ensuring appropriate knee flexion in an individual with a transtibial amputation is notoriously one of the most challenging aspects of the dynamic alignment process. Electromyography activation patterns of subjects with a transtibial amputation were observed to be different than those in subjects with an intact limb [101], suggesting an explanation to the underlying cause of an attenuated and delayed stance peak knee flexion lies in the subject's motor control strategies or coordination. When a lower limb amputation removes the gastrocnemius-soleus muscle complex, the hip flexor muscles not only become the source of swing limb advancement but also place an increase in energy expenditure [78,90]. Presently, the majority of efforts to reduce energy cost of prosthetic gait have focused on improving stance period events and power generation at foot off [78]. It is proposed that efforts to improve swing limb advancement mechanics, which are a precursor to initial contact and weight acceptance, may contribute to improving the orientation of segments/prosthetic at initial contact and the task of weight acceptance. Insights into limb-prosthetic compensatory coordination dynamics of the amputated limb during swing limb advancement may help elucidate motor control strategies adopted by an individual with a LLA that could help assist in rehabilitation techniques and electronically controlled prosthetics.

Transfemoral Amputation Gait Pattern. In addition to losing neurological control at the ankle, a transfemoral amputation removes neurological control at the knee as well leaving the hip as the lowest intact joint to control the distal prosthetic linkages. The increased demand on the hip muscles, limitations of prosthetic feet, and reliance on compensatory movements in the intact limb, trunk, and pelvis makes walking with a transfemoral amputation even more challenging than walking with a transtibial amputation. As previously mentioned, walking speed has been shown to be a good indicator of walking ability and thus has been shown to have good correlations with gait disability [26,58,90,102]. Therefore, it is perhaps of no great surprise that individuals with a transfemoral amputation have been reported to have a slower walking speed, slower cadence, and shorter stride length compared to individuals free of gait impairment and individuals with a transtibial amputation [78]. Whatever weight acceptance peak remained in the sagittal knee kinematic curve of an individual with a transtibial amputation, is now none existent in the knee kinematic curve of an individual with a transfemoral amputation because knee flexion in stance is used to avoid collapsing of the prosthetic limb. The sagittal hip kinematic curve of an individual with a transfemoral amputation loses the

smooth, rounded transitions between different tasks in the gait cycle and becomes more abrupt, thus causing this gait descriptor to be significantly different from that of an individual without an amputation. A decreased amount of the amputated limb's hip range of motion compared to the ipsilateral intact limb has also been reported [78]. Compared to an individual without an amputation and lower levels of an amputation, increased muscle activity magnitude and duration in the residual limb, increased and asymmetric tri-planar displacement of the trunk and pelvis, and increased energy expenditure are seen in individuals with a transfemoral amputation [78].

2.2.4   Conventional Measures of Instrumented Gait Analysis

Conventional measures derived from instrumented gait analysis data typically describe the orientation of joints, timing of muscle excitation, ground reaction forces produced at joints by contractions of skeletal muscles, and overall gait performance in regards to the duration of walking and distance covered. A brief overview of the conventional measures calculated in this body of work follows.

2.2.4.1   Temporal-Spatial Variables

Temporally normalizing the gait cycle (GC) allows for intra-subject and inter-subject comparison of gait cycles. Using Perry's divisions of the gait cycle, the duration of periods, phases, tasks, and instances of single and double limb support are examples of temporal descriptors of a gait cycle. Asymmetries in one or both sides of an individual's gait pattern can be detected by unequal durations of these gait cycle divisions. Since the gait cycle is temporally normalized, the divisions of the gait cycle (e.g. periods, tasks, phases, etc.) can be mapped onto a unit circle, making these asymmetries easily detectable, as shown in the following figure[114].
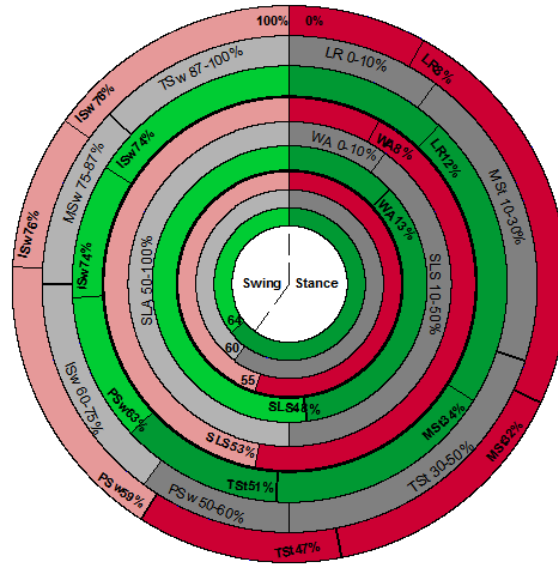
Figure 2.2.4: Divisions of the gait cycle depicted on a unit circle, read clockwise, for a fictitious subject's left (red) and right (green) gait cycles with reference to a normative control (grey) using the values displayed in Figure 2.2.1.

Typically, one gait cycle is defined as the time interval between two successive foot strikes of the same leg. The distance traversed by that leg can be used to calculate spatial descriptors. Step length, stride length, and base of support are variables used to describe the spatial relationships of the placement of the feet on the walking surface and are depicted in the following figure [40].
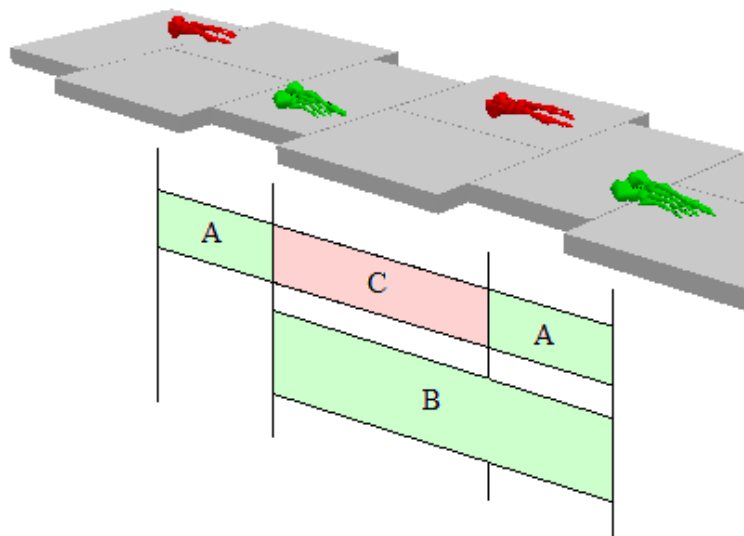
Figure 2.2.5: Isometric view depicting variables used to describe spatial relationships between the feet (typically using the centroid location of the heel marker) and their placement on the ground (grey rectangles). A = right step length, B = right stride length, C = left step length.

Walking speed is defined as the time required to travel a certain distance, often measured as the first foot strike and last foot strike in a trial, and is therefore a temporal and spatial descriptor commonly used as an overall gait performance measure [40]. Stride width, also known as walking base and base of support, is often used as a descriptor of an individual's dynamic balance and coordination. Balance (e.g. postural control) is commonly defined as the ability to maintain the body's projected center of mass (e.g. center of gravity) within the base of support [16]. However, when walking the body continually oscillates between states of balance (double limb support) and imbalance as the forward progression of body segments cause the center of mass to fall outside of the base of support. Advancement of the swinging limb and sufficient forward and lateral placement of the foot with respect to the center of mass prevents falling and allows for the system to regain stability. Increase widening and variability of the base of support have been associated with various neuromuscular disorders [16]. Additionally, tandem walking or heel-to-toe walking is a common variation of gait that is difficult to perform when an individual has poor balance and/or impaired coordination. Decreases in spatial measures such as step length and stride length, which characterize the forward progression during a gait cycle, can be attributed to spasticity (cerebral palsy) and adoption of compensatory motions to account for biomechanical limitations in the contralateral limb (lower limb amputation).

2.2.4.2 Kinematics

Three dimensional tracking of motion capture markers placed on specific anatomical locations of segments can be used to construct an anatomical coordinate system for the segment being tracked. These anatomical coordinate systems can then be expressed with respect to each other and the motion capture environment's global coordinate system. Kinematic curves are created from a parent-child segment relationship, in which the child segment's coordinate system is expressed with respect to the parent segment's local coordinate system. Kinematic curves are generated by transforming one segment's coordinate system into another and calculated from the angle formed between two axes of these coordinate systems. For example, the knee flexion/extension kinematic curve is the angle formed in the sagittal plane between the shank's long axis and the thigh's long axis. Kinematic curves are typically based upon a skeletal hierarchy (distal segment with respect to adjacent, ipsilateral proximal segment) and provide a means for describing changes in joint angles throughout a gait cycle. The magnitude and timing of kinematic curve features, such as extrema, are often used to characterize how an individual's gait pattern diverges from a normal reference. Additionally, deviations from the normal range of kinematic curves can be indicative of gait pathology (e.g. cerebral

palsy) and functional limitations causing an aberrant gait pattern (e.g. lower limb amputation).

In an effort to provide clinicians with a multivariate that could be used to describe an individual's overall gait pathology, a gait deviation index (GDI) was created help consolidate the vast amount of multidimensional data from an instrumented gait analysis [103]. The GDI is constructed from nine of the twelve kinematic curves using techniques of principle component analysis. Application of the GDI is continuing to grow in instrumented gait analysis as a measure of how close a subject's joint angles are to a normative reference. By scaling the kinematic differences between a large normative reference, a GDI score can be calculated for an individual and thus provide a means for quantifying and stratifying the severity gait pathology and comparison of multiple gait patterns caused by different pathologies. Another benefit of the GDI calculation methodology is that it can be constructed from variables with different units. One disadvantage to this particular technique is that the feature analysis steps used to construct the normative reference features must originate from a large dataset of normative gait data. If this method is to reliably calculated and constructed from different gait measures (e.g. kinetics) or for movement tasks (e.g. running) then similarly large reference dataset are required.

2.2.5 Conventional Measures of Coordination

Depending upon the context, coordination can have several different definitions and is comprised of numerous elements such as information processing, balance, selective motor control, postural control, muscle synergies, attention, and memory. Presently, a gold standard for quantifying coordination during the task of gait does not exist because coordination is an inherently abstract concept that can not be directly measured like strength or endurance and is a complex sensorimotor process involving several systems. Several of the conventional measures of coordination that are relevant to this body of work are presented below.

2.2.5.1 Performance Measures

Clinical performance measures offer insights into specific aspects of coordination while performing isolated motions or tasks. Numerous functional scales have been created to provide a standardized means of detecting and scoring the presence and severity of aberrant coordination and are used in various clinical assessments. The following performance measures were used to characterize the different subject populations studied and specifically address the hypotheses of Aim 2.

<u>Assessment of Selective Motor Control</u>. As previously discussed, impaired selective motor control contributing to functional motor deficits is characteristic of the gait pattern of individuals with

spastic cerebral palsy. Fowler et al. (2009) created and validated a clinical method for assessing selective voluntary motor control of specific motions of the hip, knee, ankle, subtalar, and toe joints [104]. The assessment rates the individual's ability to move each joint independently at the same speed and directions as the corresponding demonstrated motion. The assessment also accounts for involuntary movements are other joints while performing the isolated selective voluntary movement. With the exception of hip flexion, all of the tasks are performed while the individual is seated. This assessment has been validated for individuals with cerebral palsy and found to correlate with inter-joint measures of coordination during gait that were generated from phase portraits and continuous relative phase diagrams based in a local coordinate system [105]. While the presence of additional impairments affecting functional mobility such as balance, spasticity, weakness, and skeletal deformity may also contribute to a person's SCALE score, this clinical performance measure was chosen for characterizing selective voluntary motor control because of the assessment's simplicity, short administration time, and minimal required training. Lastly, this particular set of selected voluntary lower extremity tasks is perhaps the best set of performance measures that relates to the coordination construct in the task of gait. Therefore, comparisons of prospective subject's SCALE scores and their coordination dynamics while walking are expected to reflect similar trends in motor control deficits relating to impaired selective motor control. This set of performance measures were used to characterize the degree of selective motor control impairments in the prospective subjects (Aim 2, Hypothesis 2B).

Assessment of Cerebellar Influence in Gait. The International Cooperative Ataxia Rating Scale (ICARS) and Scale for the Assessment and Rating of Ataxia (SARA) are semi-quantitative assessments for various activities of daily living, gait, posture, speech, and oculomotor skills that can all be impaired in patients with cerebellar disease [106,107]. These standardized clinical rating systems were originally designed to provide a standardized rating system for cerebellar disease. Although these two assessments have predominantly been applied to subjects with spinocerebellar disease (e.g. ataxia), Tison et al. (2002) studied the ICARS assessment for varying levels of severity of cerebellar signs in patients with multiple system atrophy and parkinson's disease, which are both neurodegenerative diseases [108]. Although neither of the two atypical gait populations in this study have a neurodegenerative disease, the lower extremity tasks from the ICARS and SARA assessments offer a means of characterizing the coordination of an individual while performing these gait related and lower extremity tasks. Even though neither of these two populations (e.g. cerebral palsy, lower limb amputation) have cerebellar degeneration, they do have an altered ability to smoothly and effectively perform voluntary movement. These assessments of overall coordination can therefore

be used as a reference for assessing overall gait performance ability and offer another means for characterizing coordination. Therefore, motion capture data of prospective subjects in this study was collected during the following ICARS/SARA based tasks: over-ground walking at a self-selected speed, tandem waking at a self-selected speed, and walking at a self-selected speed with 90° turns to the left and right. Additionally, each subject's ability to perform the voluntary movement of sliding the heel down the opposing limb's shin in as straight of a line as possible was recorded with high definition video. In an effort to provide greater fidelity to these measures, additional quantitative measures were calculated from the motion capture data as the subjects performed these walking tasks and are provided in detail with the study's other methods in Chapter 4.

Speed-Accuracy Tradeoff. From the Bernstein perspective, the central nervous system's organization of individual variables into a larger group (e.g. synergy) during a movement decreases the degrees of freedom in the system and allows for simpler control strategies, which in the case of bipedal gait result in complex oscillatory patterns [1,2,4,5]. A resultant motor behavior is the culmination of factors from environment, task constraints, and individual's ability to process this information and then execute the motor plan with consideration to all these elements [109]. The ability to identify internal and external stimuli relevant to execution of the motor plan, selection of the appropriate response, and prepare for the executing of the modified the motor program are the main steps of information processing [110]. Information processing is one aspect of coordinated movement because it contributes to how an individual plans and controls for a movement, especially in response to changes in one or more of the environmental, task, or personal constraints. In 1954, Fitts performed a series of upper extremity experiments that exemplifies the influence of information processing in a motion by systematically changing one task constraint at a time, elucidating the subject's decision making process and resulting relationship between speed and accuracy [111]. Considering the movement limitations (e.g. endurance, strength, etc.) of this study's subjects with gait pathology, it was not feasible to perform a full lower extremity replication of the numerous variations and iterations in Fitts' original experiments. Therefore, a variation of Fitts' experiment was designed to explore the relationship between the measures of coordination dynamics and the accuracy of moving the leg in a repetitive, reciprocal mimicking the motion of swing limb advancement in gait during a fixed time. Additionally, the comparisons between an individual's selected speed of the limb during this task and the swing period of gait were also compared. While the affects of information processing during gait are not the focus of this work, this experiment for prospective subjects provides another means for characterizing the impairments in the speed and accuracy of voluntary reciprocal movements (Aim 2, Hypothesis 2A).

2.3 Investigations Prior to Pre-doctoral Work

Prior to the commencement of and in tandem with this pre-doctoral work, the following three investigations into the utility and clinical significance of these coordination dynamics measures were conducted. All of these investigations support the overall significance of the dissertation work, especially in regards to Aims 1 and 4.

These previous investigations provided the opportunity to refine the methodology for calculating these measures of coordination dynamics, apply these measures to different pathological gait patterns, and demonstrate benefits for incorporating these measures into the instrumented gait analysis repertoire. Additionally, findings from these prior investigations provide sufficient evidence to justify this pre-doctoral investigation into the value and ability of these nonlinear measures to describe the coordination dynamics employed in different gait patterns and the motion of swing limb advancement through mathematical and physical experiments. The next chapter discusses the rationale for why the dynamic systems theory perspective is ideally suited for characterizing the coordination dynamics in the cyclical task of gait, especially in regards to swing limb advancement. An explanation of the two dynamic systems theory based measures that were used to quantify coordination dynamics of both retrospective and prospective subjects during swing limb advancement (Aims 1, 2, 4) and the pendular motion of the mathematical model of a double compound pendulum developed (Aim 3). A justification and rationale for implementing these nonlinear measures is provided and compared to other measures of coordination derived from instrumented gait analysis data.

Changes in Coordination and Functional Outcomes After Rectus Femoris Transfer Procedure in Children with Spastic Cerebral Palsy. The purpose of this ongoing retrospective study is to determine if functional gait outcomes after the rectus femoris transfer procedure are associated with improvements in inter-segmental coordination in children with spastic cerebral palsy. Preliminary findings from this study have revealed there are significant changes in inter-segmental coordination for these children and re-organization of motor control strategies after the removal of the biomechanical constraint (e.g. inappropriate firing of the rectus femoris muscle). Findings from this investigation were reported in a podium presentation and conference paper at the 2010 joint conference for the Gait and Clinical Movement Analysis Society (GCMAS) and European Society for Movement Analysis in Adults and Children (ESMAC. Posters and conference papers of reference subject findings were presented at the GCMAS 2011 conference and the 2013 Coleman Institute Conference for Cognitive Disabilities.

Use of Nonlinear and Conventional Gait Analysis Methods to Model Gait Abnormalities Associated

with Spastic Cerebral Palsy. The purpose of this retrospective study was to determine if inter-segmental coordination measures about the knee joint are significantly correlated to conventional gait performance measures and if these coordination measures can be used to help determine if a subject has one of the four gait abnormalities considered in this study. The four pathological gait patterns examined in this study were 1) stiff knee, 2) crouch, 3) recurvatum, and 4) jump knee. Our results indicated inter-segmental coordination measures are significantly correlated to conventional gait measures and provide specific and unique movement patterns that are characteristic of movement abnormalities associated with the four pathological knee centered gait patterns. Additionally, novel insights into the coordination dynamics of walking with one of the abnormal gait patterns were gained from using nonlinear measures. These insights are not revealed with conventional instrumented gait analysis measures. Findings from this investigation were disseminated as a podium presentation at the North American Society for the Psychology of Sport and Physical Activity (NASPSPA) 2010 conference and published as a conference paper in the 2010 Journal of Sport and Exercise Psychology.

Inter-segmental Coordination and Ankle-Foot Orthoses during Gait in Children with Spastic Cerebral Palsy. The purposes of this on-going retrospective descriptive study are to: 1) characterize the lower extremity inter-segmental coordination during over-ground walking of children with spastic cerebral palsy who exhibit an equinus gait pattern; 2) examine changes in inter-segmental coordination associated with use of an ankle-foot orthosis; and 3) examine relationships between changes in inter-segmental coordination and changes in select kinematic and functional gait parameters associated with the use of an ankle-foot orthosis. The initial findings from this study support the hypothesis that by providing an intervention at distal segments, coordination dynamics are improved for more proximal segments that are not directly impacted by the intervention and therefore, demonstrates this intervention (e.g. ankle-foot orthosis) affects a subject's coordination dynamics.

These previous investigations provided the opportunity to refine the methodology for calculating these measures of coordination dynamics, applied these measures of coordination to different pathological gait patterns, and demonstrated some of the benefits for incorporating these measures into the instrumented gait analysis repertoire. Additionally, findings from these previous investigations provide sufficient evidence to justify this pre-doctoral investigation into the value and ability of these nonlinear measures to describe the coordination dynamics employed in different gait patterns and the motion of swing limb advancement through mathematical and physical experiments. The next chapter discusses the rationale for why the dynamic systems theory perspective is ideally suited for characterizing the coordination dynamics of the leg segments during the cyclical of walking, espe-

cially in regards to the gait task of swing limb advancement. An explanation of the two dynamic systems theory based measures that were used to quantify coordination dynamics of this investigation's prospective and retrospective subjects during swing limb advancement (Aims 1, 2, 4) and the pendular motion of the mathematical model of a compound pendulum developed (Aim 3). A justification and rationale for implementing these nonlinear measures is provided and compared to other measures of coordination derived from instrumented gait analysis data.

3   A Model for the Coordination Dynamics of Walking

This chapter begins with a brief overview of dynamic systems theory and how coordination dynamics of walking can be quantified by two nonlinear measures derived from this field of mathematics. Further discussion of these coordination measures and their specific application to gait details how they complement conventional gait analysis methods by providing coordination dynamics insights that are not ascertained from traditional instrumented gait analysis measures. A review of alternative models and measures of coordination dynamics, also derived from instrumented gait analysis data, is presented. Lastly, assumptions and limitations for the proposed model of coordination dynamics and a rationale for the chosen methodology is discussed.

3.1   Dynamic Systems Theory Approach to Coordination

Dynamics systems theory is a field of mathematics that models the behavior of a system throughout the course of time [4,5,7]. A dynamical system is a complex system comprised of many constitutive elements defined by a set of variables, who's physical behavior (e.g. state) can be described with mathematics as it changes state (e.g. behavior) in time. Analytical methods derived from dynamical systems theory provides tools that can be used to analyze movement patterns that emerge from a system's self-organization. As Chapter 2 discussed, human movement is a network of co-dependent subsystems working together toward a functional outcome. These synergistic organization of a movement pattern is based upon many factors: morphological (e.g. muscle-tendon properties), biomechanical (e.g. Newtonian laws of physics), environmental (e.g. walking surface and incline), and task constraints (e.g. different walking speeds, treadmill, obstacle avoidance) [7,109]. As presented in the previous chapter, being able to interpret, combine, and determine which instrumented gait analysis measures capture the state of the neuromuscular system is quite a challenging task. Fortunately, tools derived from dynamic systems theory are low dimensional descriptors that consolidate the complex, multifactorial variables of a system and can be used to create simpler models of an otherwise complex physiological behavior.

Instrumented gait analysis (IGA) quantitatively describes the pathological gait pattern of an individual whose walking is negatively affected by neuromuscular impairments. Traditional IGA measures identify factors contributing to a pathological gait pattern, provide supporting evidence for clinical interventions, and assist in assessment of treatment outcomes. Due to the methods for constructing conventional IGA measures and nature of the actions or relationships they quantify

(e.g. joint angles, joint kinetics, temporal-spatial), these measures describe the motion of limbs or joint but are unable to characterize the underlying dynamics of the motion. The coordinated behavior of leg segments in gait is the result of a complex dynamical system that requires organized neurological control of the musculoskeletal system. The phase portrait (PP) and continuous relative phase diagram (CRPD) from dynamic systems theory (DST) use the same motion capture data as IGA measures, but are inherently designed to describe the organization of limb segments resulting in a gait pattern. These DST based measures are more suitable for characterizing selective motor control strategies contributing to a gait pattern, quantify organization of individual segments, identify mechanisms of change, and loci of impairment. Since the fundamental organization of the leg segments during gait is linked to gait pathology and guides the rationale for interventions, it is proposed that adding PPs and CRPDs to IGA will open new avenues for understanding the complexity of coordination and allow clinicians the means to more effectively and efficiently treat patients with neuromuscular gait impairments. A fundamental objective of this body of work was to provide a context for the utility of these measures as a complement to conventional IGA measures and present a normative dataset that can be used in research or the clinic.

A brief discussion of the construction of common IGA measures and understanding of the variables they describe is essential for recognizing why these measures are unsuitable for quantifying coordination. Conventional IGA uses three-dimensional data to create kinematic, kinetic, and temporal-spatial descriptors to analyze the recorded movement. Kinematic curves are created from a parent-child segment relationship, in which the child segment's motion is expressed with respect to the parent segment's local coordinate system. Therefore kinematic curves describe the changes in joint angles using a local coordinate system and kinetic measures are based upon this skeletal hierarchy. Electromyographic data provide information about timing and duration of muscle activity, but are usually not quantitatively paired with other IGA data. While these conventional measures are essential for understanding certain aspects of gait, due to the high dimensional nature of coordination, the ability to effectively describe the complexity and number of variables of this behavior is lost using typical IGA measures. These customary techniques cannot isolate an individual segment's contribution to the motion or locate the timing and sequencing of a segment or segment pairs. Therefore, it is proposed that conventional IGA measures do not provide the appropriate perspective and level of analysis necessary to understand the underlying motor control mechanisms responsible for generating the resulting gait pattern. Furthermore, coordination strategies between segments often consist of non-adjacent segment relationships in addition to the interplay between adjacent segments4. These nonlinear methods are inherently conducive to pairing any combination

of segments and are ideal for investigating inter-segmental coordination dynamics of non-adjacent segments. This dissertation also contends that by maintaining the segments in a global coordinate system, the DST tools presented in this dissertation are more akin to the perspective in which clinicians observe and evaluate an individual's characteristic gait pattern.

To appreciate the ideal pairing between DST and coordination from a motor control perspective, a definition of coordination and review of previous pivotal investigations that contributed to the application of DST in IGA is presented. Coordination of the legs during walking requires the elegant organization of the neuromuscular system's many elements and appropriate consolidation of the system's redundant degrees of freedom while considering task and environmental constraints [1]. This constitutive element of bipedalism has long been recognized as an important factor of motion, especially in cases when coordination of the leg segments during gait is adversely affected in individuals with selective motor control impairments resulting from neuromuscular pathology. However, the ability to employ a method that effectively captures coordination and presents the behavior in a concise manner has often been as elusive as the concept of coordination. The application of angle-angle diagrams was an important precursor because these measures describe the relationship between two joints as a low dimensional descriptor [3,115]. Similar to conventional IGA measures, angle-angle diagrams are constructed from a skeletal hierarchy and therefore these joint based measures prove unsuitable tools for delving deeper into the behavior of individual segments or non-adjacent segments. The need for quantitative descriptors of coordination was identified in the development of motor control theory and the mathematical field of DST was proposed as a solution4. Clark et al. (1993) applied DST based measures to motion capture data of infants during their first year of independent walking, demonstrating the elegant pairing of DST concepts to the dynamical system of gait [116]. With considerable advancements in motion capture systems and computational performance, the marriage between movement analysis and DST was later revisited by Stergiou et al. (2004) who demonstrated DST based measures can be easily calculated from segment marker trajectories recorded from motion capture data [7]. DST principles have been absorbed into current motor control practice and re-introduction of these techniques applied to motion capture data has offered a means to bridge these theoretical constructs with practical applications in IGA. It is proposed the lack of a unifying methodology, normative reference, and clinically meaningful demonstrations of the practical benefits and important motor control insights offered by these nonlinear measures have slowed their incorporation into IGA. In an effort to continue advancing the application of DST techniques to locomotion, this dissertation presents a refined methodology for two DST measures applied to motion capture data from a large cohort of individuals without gait pathology.

A conceptual framework for how PPs and CRPDs quantify the complex behavior of coordination is established using an overview of the relationships between DST principles and aspects of conventional motor control theory. The behavior of coordination can be characterized by the timing and position of an individual segment and pairs of segments throughout the cyclical task of gait. Since the cyclical oscillations of the leg segments during gait are analogous to the motion of various pendula, this motion can be modeled as a limit cycle in phase space. As a limit cycle, the trajectory of a leg segment can be represented in a PP, providing a suitable vehicle for examining the motion of an individual segment. For IGA, this moves the level of analysis from kinematic space to state space of the limit cycle oscillator.

From the Bernstein perspective, the organization of individual variables into a larger group is defined as a synergy [4]. Employing synergies during a movement essentially decreases the degrees of freedom in the system, thus allowing for simpler control strategies [2]. Synergies are the central nervous system's partial solution to the degrees of freedom problem and in the case of gait, generate complex and oscillatory patterns [5]. The CRPD provides important clues into the organizational strategies governing the constitutive oscillators (e.g. segment pairs) and conversely, the PPs describe properties of individual oscillators (e.g. segment) affecting the coordinated behavior of this dynamic system. Phase portraits provide clinically meaningful insights about how an individual segment's oscillations contribute to the overall motion of the limb. The relative phase angle is a collective variable that concisely captures both spatial and temporal patterns between two segments. The CRPD presents this low dimensional metric throughout the gait cycle and describes the coupling and uncoupling of segments' oscillations. Consolidation of the dynamic system's numerous variables into the relative phase angle allows for inferences to be made about the underlying control processes. When temporally normalized to the gait cycle, these measures offer concise, easily calculated, and clinically meaningful descriptors of individual segment and inter-segmental behavior as a result of selective motor control.

Investigations into intra-limb coordination of gait have been conducted by a few researchers in the past using variety of methods, ranging from the earlier application of angle-angle diagrams to more recent DST based methods [117,118]. These studies have contributed to an increasing awareness in the gait community about the importance of expanding traditional means of characterizing gait and served as initial steps in understanding coordination in certain atypical gait patterns. The majority of studies reported small sample sizes and as is often the case in studies of subjects with cerebral palsy or stroke, the unaffected limb served as a comparison to the affected limb's motion [119]. While comparisons between a subject's affected and unaffected leg shed insights into the compensatory

strategies employed by the individual, because of the asymmetry of such gait patterns the use of an unaffected limb is not a true analogue to a normative reference.

This body of work demonstrates how PPs and CRPDs complement conventional IGA measures and by describing movement at the level of coordination, how these DST based measures explain the mechanisms underlying temporal-spatial and kinematic differences observed in typical and atypical gait patterns. The following sections provide an explanation of the two dynamic systems theory based measures that are used in this model and an explanation of the insights and value for describing gait with each of these measures.

3.1.1 Phase Portrait

As discussed in Chapter 2, the motion of the leg segments during gait results from the elegant organization of the intricate muscle synergies and has been compared to the dynamics of a compound pendulum's linkages. This coordinated coupling and uncoupling of leg segments can be modeled using principles of dynamical systems theory [6,7] and is a reflection of a person's voluntary motor control. This analogy of the leg's motion in this context proves useful and appropriate because in dynamics systems theory, the state of the system is influenced by changes in energy (e.g. kinetic, potential) that occurs within the system during each orbit (e.g. gait cycle). Using this theoretical construct, the oscillatory, cyclical motion of a pendulum can be described as a limit cycle. A limit cycle is the two-dimensional trajectory of an oscillatory system's variables, which are represented as a periodic orbit in phase space. Phase space describes all possible states (e.g. behaviors) of a dynamical system and portrays how these states evolve in time [4,5,7]. The limit cycle trajectory of a simple, frictionless pendulum in phase space would be an elliptical whose closed path completely describes the relationship between position and velocity as a function of time. In the application of gait, a phase portrait can be constructed to describe the relationship between the angular displacement and angular velocity of a segment throughout each gait cycle (e.g. limit cycle). As shown in the following phase portrait, read in a clockwise direction, is simply a set of trajectories (e.g. limit cycles) in phase space and can contain any number of limit cycles (Figure 3.1.1).
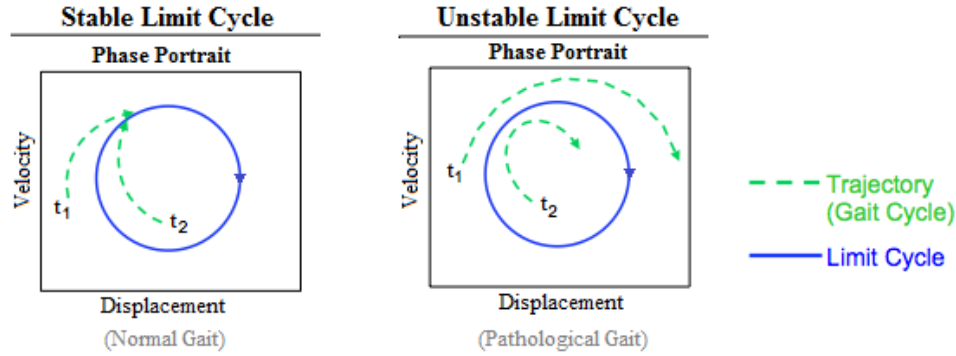
Figure 3.1.1: Diagram of an ideal, closed orbit limit cycle (blue) with different trajectories (green) of a theoretical dynamical system. A stable limit cycle is analogous to a normal gait pattern because it returns to a preferred state even after perturbations or changes in initial conditions. An unstable limit cycle is analogous to an irregular pathological gait pattern because the subject is unable to return to the same state after perturbation or from one gait cycle to the next.

The application of this theory has been tested for the task of gait in previous investigations. Several investigations using phase portraits and instrumented gait analysis have demonstrated that phase portraits capture a system's state and its stability when an individual's gait is perturbed [120,121]. Additionally, Clark and Phillips (1993) demonstrated that preferred lower extremity movements can be mapped onto a phase portrait as a limit cycle oscillator and have different shapes and characteristics for different gait pathologies116. Furthermore, numerous other investigations have revealed that changes in the phase portrait's trajectory shape are correlated to new movement behaviors, either pathological or typical [117,119,122]. Since the shape of phase portraits for lower extremity segments provides visual evidence validating that the behavior of segments during gait can be described as limit cycle oscillators, the different trajectory features and deviations from an ellipse or circle are indicative of the active modulation and changes of the segment by the nervous system. These changes in phase portrait trajectory capture the different energy exchanges (e.g. acceleration, deceleration) of a segment throughout the gait cycle [123]. Phase portrait curve features (e.g. zero crossings, extrema) can be identified and used to quantitatively describe differences in phase portrait trajectories and thus motor behaviors for the same individual or different subjects. Therefore, phase portraits can provide clinically meaningful insights about how an individual segment's oscillations contribute to the overall motion of the limb.
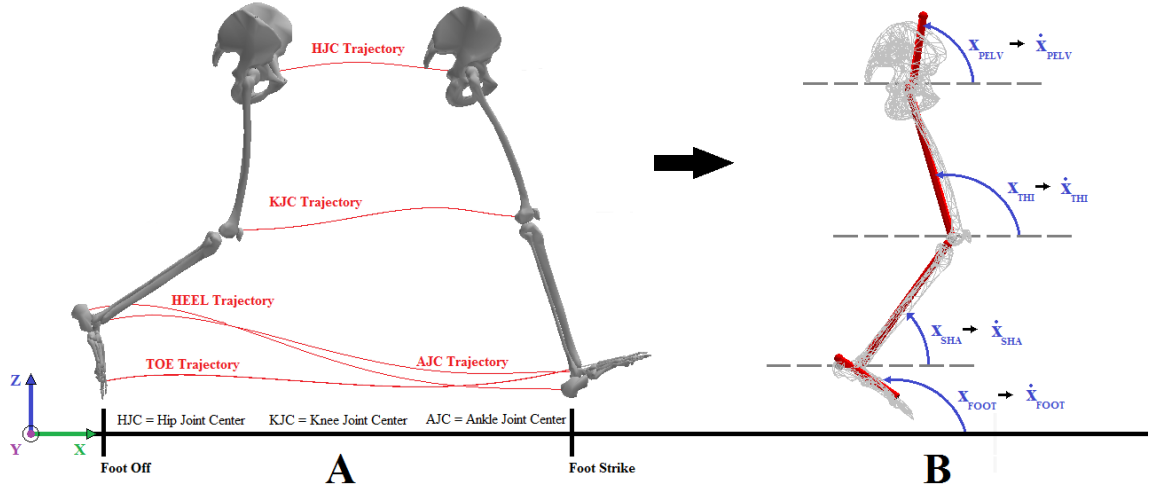
Figure 3.1.2: Phase portrait construction from tri-planar marker data.
Tri-planar marker based trajectories and segment coordinate systems (A) from instrumented gait analysis provide angular displacement and angular velocity (B), with respect to the horizontal, and are used to construct phase portraits.

At this time, the proposed model of coordination dynamics uses the angular displacement and angular velocity from a segment's marker trajectory to generate the corresponding segment's phase portrait. However, phase portraits could be constructed from other system variables such as angular acceleration and provide different insights into the system. For reasons that will be further elaborated in a following section of this chapter, the angular displacement and angular velocity was resampled and normalized to each valid gait cycle in the motion capture trial. Although this model allows for flexibility in selecting a segment's defining markers, joint centers calculated from the conventional lower body marker set [124] were used because they were already calculated for the standard instrumented gait analysis methods. Additionally, while this model is easily adjustable to different coordinate system definitions, the sagittal plane for both motion capture environments was defined by the floor (horizontal) and perpendicular to the floor (vertical) and therefore maintained as this work's defining global sagittal plane axes.

3.1.2 Continuous Relative Phase Diagram

The proposed model of coordination dynamics uses PPs to characterize the individual behaviors of a segment with respect to the global coordinate system. For sagittal plane PPs, the global reference is the same as the level walking surface (e.g. over-ground, treadmill). The phase angle is calculated from a segment's PP, is a low-dimensional parameter that consolidates a segment's spatio-temporal oscillatory behavior, and represents the progression of the limit cycle's trajectory

49

throughout the gait cycle. The unaltered arctangent function was used to calculate the phase angle of a segment for each percent of the gait cycle. The phase angle is defined as the angle between the phase portrait's horizontal and the vector formed from the phase portrait origin (0, 0) to the coordinates of the phase portrait trajectory for each percent gait cycle (Figure 3.1.3).
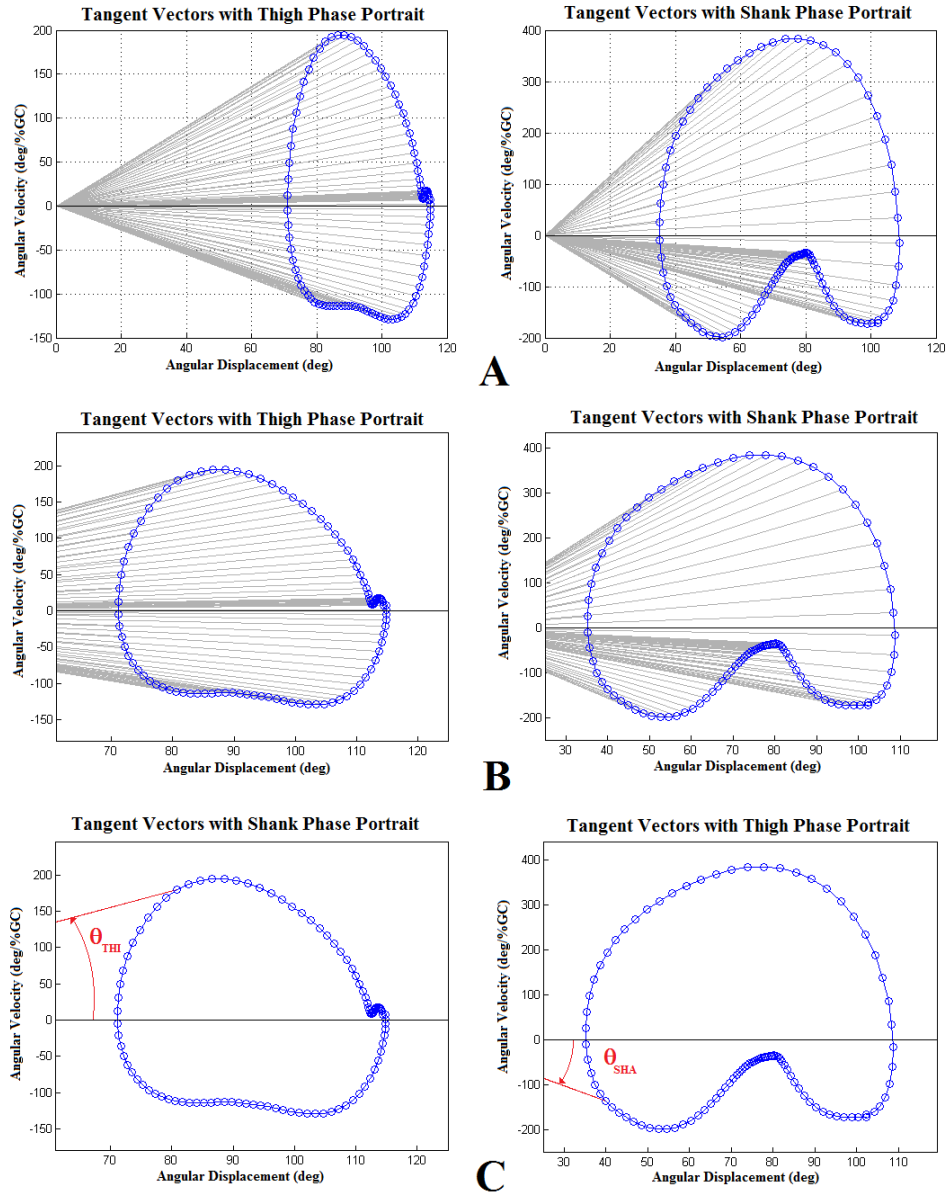
Figure 3.1.3: Diagram of how a segment's phase angle is calculated with respect to the horizontal of the phase portrait, for one complete gait cycle from a normal reference subject's thigh (left column) and shank (right column). Vectors from the origin (0,0) to the phase portrait coordinates for each percent gait cycle (A). Zoomed-in view of the vectors and phase portrait trajectory (B). Phase angle for one percent gait cycle on the thigh and shank (C).

Phase portraits for the pelvis, thigh, shank, and foot were generated and the following equation

50

was used to calculate the corresponding phase angles (ϑ_{seg}) for each segment [7].

Algorithm 3.1 Phase Angle

$$\theta(\%GC)_{seg} = \tan^{-1}\left(\frac{x(\%GC)}{\dot{x}(\%GC)}\right)$$

For each segment pairing (i.e. pelvis-thigh, thigh-shank, shank-foot, thigh-foot), the phase angles from any two segments' PPs were used to calculate the pair's relative phase angles (φ) for each instance in time (e.g. each percent gait cycle). This model of coordination dynamics calculates the relative phase using the following equation and generates CRPDs by plotting the relative phase angles with respect to each percent gait cycle [7].

Algorithm 3.2 Relative Phase Angle

$$\phi(\%GC) = \theta(\%GC)_{Distal} - \theta(\%GC)_{Proximal}$$

The relative phase angle is a low-dimensional descriptor because it encompasses the angular displacements and angular velocities from two segments and is a function of time. Therefore, the magnitude and timing of the relative phase angle provides a simple scalar value quantifying the multifactorial elements of inter-segmental coordination (e.g. temporal and spatial organization) between any two segments. In addition to overall spatio-temporal patterns of CRPDs, characteristics of CRPDs shape can be quantified by calculating such curve features as zero-crossings, extrema, slopes, and inflection points. These curve features provide information about certain coordination events and the segmental relationships. An extremum on a CRPD indicates the instance when the relationship between the two constitutive segments is the most out-of-phase (e.g. instance of reversal). Since DST assumes that the motions of segments approximate a sinusoid, then it can be assumed that when the relative phase angle equals 0° the segments are in-phase with each other [4-7,132]. This CRPD zero-crossing indicates the instant when the two segments' phase angles are changing at the same rate with respect to each other. Similarly, when the relative phase angle equals 180° the oscillating segments are out-of-phase with each other [4-7,132]. Both of these CRPD features refer to the segments' phase portrait trajectories and the relationship in phase space, not Euclidean space. Inflection points on a CRPD indicate the instant when the phase angles of the two segments begin changing their relationship to each other. For example, an inflection point on a thigh-shank CRPD could indicate the instant when the thigh's phase angle begins changing more or has larger values than the shank's phase angle. The slope of a CRPD gives insights into how the rate of the segment's phase angles are moving with respect to each other. For example, a negative slope indicates the proximal segment is changing its phase angle (e.g. angular displacement and angular

velocity) at a faster rate than the distal segment and thus has a greater influence on the calculation of the relative phase angle. The inverse is true for a positive slope on a CRPD. Lastly, the temporal normalization of the relative phase angle to the to gait cycle also allows for intra-subject and inter-subject comparisons. By maintaining this common temporal scale with conventional measures of instrumented gait analysis, curve features from other measures and critical and temporal gait events can be mapped onto these measures of coordination dynamics.

The ability to quantitatively investigate coordination dynamics between any two segments is an inherent advantage of CRPDs. The CRPD's low dimensional relative phase angle captures the relative coupling and uncoupling between segments, thus capturing an individual's ability to differentiate joint movements out of flexion or extension (e.g. voluntary motor control). CRPDs quantitatively describe functional synergies in gait and provide an excellent means for making inferences about selective motor control, a primary impairment in individuals with neurological diagnoses. Throughout the evolution of each gait cycle, a CRPD captures the transition from one pattern to another (e.g. stance to swing). One goal of using IGA in rehabilitation is to identify impaired coordination using conventional IGA measures (e.g. temporal-spatial variables, kinematics) and reduce those coordination impairments by improving intra and inter-limb coordination. CRPDs concisely describe the organizational strategies (e.g. symmetries, synergies) of two leg segments and offer insights into how the nervous system is imposing functional constraints on the limbs. The organizational changes between two segments, through the use of synergies, that account for functional actions can be identified using common curve features such as extrema, zero-crossings, and inflection points. Since the CRPD encapsulates both temporal and spatial symmetries and dynamics of the legs during gait, the degree to which two segments move in and out of various synergies is easily quantified by the percent gait cycle and magnitude of the relative phase angle. Previous investigations mentioned in Chapter 2 have demonstrated this CRPD functionality by modeling the gait of children with spastic cerebral palsy exhibiting a stiff knee gait pattern before and after a rectus femoris transfer (Valvano et. al, 2010). In the previous investigations mentioned in Chapter 2, beneficial insights from PPs and CRPDs have also provided the means to explore temporal constraints associated with the dynamics of footfall and non-adjacent segments during swing limb advancement.

3.2   Model Assumptions & Limitations

Even though walking is typically described and characterized by the gait cycle and subsequent subdivisions, this motor task is considered a continuous task as opposed to a discrete one. A

continuous task is defined as a coordinated movement that does not have an arbitrary start and end and can depend upon the context of the movement. Given this definition, walking and running are two examples of a continuous task. In the example of gait, the previous gait cycles influence the subsequent ones as well as the events within a gait cycle, which are influential precursors to the remaining phases within that gait cycle. Discrete tasks (e.g. hop, jump, or reach to grasp) are coordinated movements that have definitive start and end points [110]. Dynamic systems theory assumes that stable movement patterns emerge from a dynamic system and the variability a system contains reflects changes in states and embodies the system's search for stability. Opponents of DST view variability in a system's motor control to be a linear decline in efficiency as opposed to the impetus for a nonlinear change to a different movement pattern reflecting the system's process of self-organization [110,135]. Furthermore, some have argued that since the proposed measures of coordination (e.g. PPs, CRPDs) are grounded in the assumption that segments move as limit cycle oscillators, these measures of coordination may not be appropriate for discrete tasks and that other motor control paradigms (e.g. generalized motor programs) are more suitable for discrete tasks [110]. Fortunately, this body of work bypasses this issue because it examines the continuous, oscillatory task of gait, which supports the application of the DST paradigm.

Since this model's measures are derived from tri-planar marker trajectories, the measures are unable to identify the contribution of specific muscles in a movement, which some may argue is a more direct measure of the neurological activity, and thus motor control employed during gait. Advantages and disadvantages of this position and alternative methodology are addressed in the following section. Given the provided definition of coordination, which is considered an emergent spatiotemporal motor behavior culminating from numerous interactions within the neuromusculoskeletal system as opposed to a single physiological element (e.g. heart rate, muscle force production, action potential) that can be measured directly, the exploration of behavioral measures (e.g. PPs, CRPDs) maintains their relevance and applicability.

Lastly, in spite of efforts taken to limit the influence of human error in experiments, it is not possible to completely eliminate such errors. Further details of efforts taken to reduce any contributions from human error and validate various calculations and analyses are provided in Chapter 4. Although there have been significant improvements and advancements in motion capture instrumentation (e.g. cameras), there are inherent errors and assumptions with instrumented gait analysis, such as marker placement, motion artifact, and motion capture model assumptions (e.g. joint center estimation), which are currently unavoidable. As with other conventional gait analysis measures, the PPs and CRPDs used in this model are not immune to these assumptions and potential errors.

3.3   Alternative Perspectives to Modeling Coordination in Gait

Just as there are different theories and models of human gait (Chapter 2), there are also numerous definitions of coordination, even within the context of gait, and models for characterizing each theory. Every model has its unique set of limitations and is subject to change as research reveals new information and technological advances expand measurement capabilities. It is not the intent of this body of work to declare one theory or model is the definitive means for characterizing coordination in gait, because it is the author's belief that models and corresponding measures should be selected based upon the driving questions that will be answered by these descriptors. In the context of coordination dynamics derived from instrumented gait analysis data, model and measurement selection should be made with consideration to the corresponding level of motion capture data analysis that best characterizes these factors (e.g. definition of coordination) and goals for describing movement performance. To set the stage for the following section of this chapter on the proposed model's methodological rationale, the following subsections provide a brief overview of other coordination models.

3.3.1   Central Pattern Generators & Motor Plan Theories

The neurophysiological construct of central pattern generators (CPG) and the motor program are two theories of motor behavior in animals that despite their dominance fail to provide a satisfactory explanation of movement. Thelen proposed that the main reason these two theories are insufficient is because they approach motor control as a computer controlling an electronic device and therefore view the execution of a motor plan as being generated only from neural commands [5]. However, it is apparent from even the general overview of the locomotor system presented in Chapter 2 that movement is the orchestration of a complex system comprised of intrinsic elements (e.g. neuromusculoskeletal system, segment mass, energy exchange, etc.) and extrinsic factors (e.g. walking surface, task constraints, etc.). When motor control is viewed as a constant fixed (e.g. CPGs) and predetermined patterns (motor program), several shortcomings arise from these theories because they are unable to explain how a person is able to walk in different directions, avoid obstacles, the variability in normal and pathological movements, and adapt to changes in environmental or task conditions and constraints [5,110]. Dynamic systems theory provides a more satisfactory explanation to these shortcomings because it is based upon dynamic patterns, which are not fixed to a hierarchy, that characterize changes in a system's behavior over time as it searches for a stable state.

3.3.2   Using Electromyography to Quantify Coordination

It has been proposed that muscle synergies are motor control strategy that simplifies the redundant degrees of freedom in the body and allows for the low-dimensional organization of the locomotor system, which is necessary to produce efficient movements [1,13,14]. Several studies have therefore used dynamic electromyography (EMG) data to identify patterns of muscle synergies used during different walking conditions and by different populations [125,126,127]. Models of coordination proposed using muscle synergies are grounded in the length-tension and force-velocity relationships of skeletal muscle. These studies propose that muscle recruitment for different synergy patterns is variable and modulated by the nervous system as a function of the muscle's length [125]. Furthermore, these muscle-force relationships are often employed in musculoskeletal computer simulations [128], which can be used to estimate functional impacts of different muscle synergies based upon kinematic, kinetic, and EMG data [127]. Although EMG data collected during instrumented gait analysis comprises of both the amplitude and timing of muscle activity, the relationship between muscle force production and EMG amplitude while performing a dynamic movement like gait is not a reliable, linear relationship. As mentioned in Chapter 2, there is an optimal length at which a muscle can produce the maximum force (e.g. length-tension relationship) and optimal speed for force generation (e.g. force-velocity relationship). These relationships are generated from muscle forces during a static position and therefore break down during a dynamic motion because of the properties of the sliding filament mechanism discussed in Chapter 2 [23]. Use of dynamic EMG data is further confounded by the noise inherent to this data (often requiring considerable filtering) and changes in the muscle's relationship to the electrode as it contracts [23]. Using tri-planar marker based trajectories to generate measures of coordination dynamics avoids these issues and simplifies the data collection and analysis process. However, marker based descriptors of coordination dynamics are not able to identify the contribution of individual muscles. There is great potential for future collaboration between and combination of measures from these two models of motor control.

3.4   Rationale for Model's Methodology

As previously mentioned, the dynamic systems perspective of gait separates itself from conventional dualistic approaches of movement (e.g. structure vs. function, brain vs. behavior) and instead embraces variability as an essential element describing a system's state and spatiotemporal changes, considers pattern changes occurring in different time scales, and considers the unique expression of movement for each individual instead of generalizations based solely on demographics (e.g. gender,

age, etc.). The task of gait is uniquely expressed in each individual, with variability from gait cycle to gait cycle [130]. Therefore using dynamic systems theory to develop a model of the coordination dynamics of walking is an ideal pairing because this theory of movement embraces the individualistic variability of gait, the emergent behavior resulting from the various aspects and interactions of the locomotor system, environmental and task factors [109], and whose measures (e.g. PP, CRPD) are rooted in these principles and thus ideally suited to describe the coordination dynamics of gait.

One advantage to the proposed methods for generating PPs and CRPDs is that these are derived from three-dimensional marker trajectories placed on segments during a motion capture session. Clinical instrumented gait analysis typically uses standardized, well-documented marker sets to define segments [124]. By using marker trajectories, the need for additional instrumentation (e.g. electromyography) and the associated costs, placement time, and analyses are removed. As previously stated, by temporally normalizing the PPs and CRPDs to the gait cycle, intra-subject and inter-subject comparisons using these measures of coordination can be made, just as is standard practice for conventional instrumented gait analysis measures. By maintaining these similarities to conventional gait analysis measures' marker locations, processing methods for motion capture data, and temporal scale, this proposed model of coordination dynamics requires minimal work to adopt into instrumented gait analysis practice.

Although other investigations into coordination dynamics using DST based measures have been conducted, the manner in which these measures have previously been generated varies and essential details about PPs calculations are often missing. If comparisons between studies using coordination dynamics are to be unified, as it is for conventional IGA measures, it is imperative to establish a standardized method of generating these DST measures. To address this discontinuity in the literature and justify this model's methodology, the following rationale discusses the normalization of these measures, selection of an arctangent function, and practicality of coordinate system transformations. Marker trajectories and derived nonlinear measures were kept in global coordinates instead of local coordinate systems used in the traditional skeletal hierarchy of joint based variables (e.g. kinematics) for the following reasons.

First, maintaining global coordinates allows for a truly individual segment behavior description. When measures are transformed into a joint based coordinate system the variable loses the ability to distinguish which segment of a joint is causing a change in the measure or identify the amount each of the segments contributes to the phase angle or relative phase angles. Numerous studies have reported CRPD calculations with various different techniques and quite often use joint angles in the calculation of phase relationships [105,132,133,134]. It is proposed the use of joint angles in the

calculation of phase relationships is an inappropriate methodology because it does not evaluate the coordinative relationships between the segments of interest. The fault of this strategy is revealed in the phase comparison of two joint angles. An example of using the hip-knee angle relationship to generate a CRPD is presented to demonstrate the flaw with a joint angle methodology. The hip angle is generated from the pelvis and thigh segments, where the thigh is transformed into the local coordinate system of the pelvis. Similarly, the knee angle is traditionally constructed from a skeletal hierarchy where the shank is described with respect to the thigh's local coordinate system. For the calculation of the relative phase angle, each of the phase angles that are calculated then contain a similar body segment, the thigh. Therefore when calculating the CRPD from the hip-knee angle relationship, the thigh segment is used twice in the calculation of the relative phase angle. Calculating the relative phase in this way does not lend authority to the interpretation used and directly inhibits the validity of describing motions during movement. The classic paradigm presented by Kelso where segmental angles are used provides further justification for this methodology4. When two fingers move in the same direction and with the same velocity they are in-phase with each other and are out-of-phase for the converse. This segmental motion is analogous to a simple pendulum and as previously discussed, PPs are rooted in this oscillatory pendular motion. The trademark paper by Clark and Phillips (1993) [116] provided an eloquent guide for the development and analysis of segment-segment angles and presented correct interpretation of these measures using the framework of the dynamical systems theory as initially laid out by Kelso [4], Kugler [131], Turvey [6], and later by Thelen [5], and utilized by Stergiou [7,130] and others [129]. Calculating variables in the segment angle manner provides meaningful and interpretable results that can be used to describe phase relationships properly.

Second, retaining global coordinates allows for identification of a segment's coordination events and eliminates gratuitous coordinate system transformations when quantifying non-adjacent segment coordination patterns. The clinical value of this methodological flexibility becomes especially apparent during swing limb advancement. The knee is passively flexing during the initial phases of swing as a result of active hip and ankle moment generation. Therefore the ability to study the relationships between non-adjacent segments, such as the thigh and foot, provides valuable insights into the uncoupling and coupling of various segment combinations. Third, maintaining measures in the global coordinate system allow for a more direct comparison to the motion viewed by clinicians during observational gait analysis. Additionally, the arctangent function used was not normalized but kept in the original quadrants, range, and domain, thus adhering to this trigonometric function's original definition. After performing PP calculations with Matlab's alternative arctangent functions,

it was found that noise is induced into the phase angle calculation when using alternative arctangent functions that force the domain of the outputs into different or additional quadrants (Appendix D). Not only is the normalization of the arctangent unnecessary and an extraneous calculation but the induced noise from such alterations is undesirable when considering the result of these efforts only presents the phase angles about the origin of the PP's coordinate system and increases the difficulty in discerning induced noise from physiologically significant variations in these curves. This decision to not apply additional normalization techniques to the phase angles is further supported in the paper by Kurz (2002) [129].

This chapter provided an overview of two dynamic systems theory based measures and their ability to simplify and quantitatively describe the complex coordination dynamics required during walking. The model of the coordination dynamics during swing limb advancement presented in this dissertation provides a quantitative means to uncover and understand the organizational strategies employed to solve one of the fundamental aspect of movement science: Bernstein's degrees of freedom problem. The next chapter will present the various mathematical pendulum models, experiments for prospective subjects, and accompanying analyses of prospective and retrospective subject data that will be used to test the dissertation's hypotheses.

4 Experimental Methodology

4.1 Purpose of Experiments

It has been verified that kinematic curves are a valid means for quantifying the angle created by two adjacent segments because each segment forms a vector and the angle between the two vectors can be calculated using basic geometry. To date, there is not a gold standard method for quantifying a individual's coordination dynamics while performing the cyclical task of gait. Since there is not an established reference to compare the proposed measures (e.g. PP, CRPD) of coordination, these nonlinear measures will be compared to the best available analogues: performance measures from a selective motor control exam, instrumented gait analysis data, performance measures of speed-accuracy during a cyclical leg motion, walking tasks that challenge a subject's dynamic balance, and a mathematical model of a pendulum whose initial conditions and parameters are based upon instrumented gait analysis measures from human subjects. The following sections of this chapter describe the experimental methodology, analysis techniques, and how each experiment's data will be used to test the hypotheses and aims of this dissertation.

The purpose of the experiments detailed in this chapter is to collect experimental evidence for testing of the hypotheses associated with each aim. While Aim 1 does not have any hypotheses, the collection and analysis of experimental data for a large cohort free of gait pathology was used to establish a normative reference, which provides the necessary foundation for the other aims and hypotheses. Aim 2's hypotheses examine the relationship between functional descriptors of other aspects of coordination and the proposed measures of coordination dynamics and serve as means to characterize the subjects. The hypotheses for Aim 3 use a software based mathematical model of a double pendulum to model the motion of the thigh and shank during swing period and thus test the construct validity of the long held analogy that these leg segments mimic the motion of a passive compound pendulum. Lastly, the hypothesis of Aim 4 was designed with the clinical utility of these measures in mind by determining if the measures of coordination could be used to distinguish between different gait patterns and thus demonstrate another valuable clinical application of these gait measures.

4.2 Subjects

This study consists of gait data from subjects with an unimpaired gait pattern and subjects with an atypical gait pattern resulting from either cerebral palsy (e.g. stiff knee or crouch gait pattern)

or a lower limb amputation (e.g. transtibial or transfemoral). Retrospective subject motion capture data was accessed from the Center for Gait and Movement Analysis (CGMA) subject databases and consists of unimpaired subjects, subjects with spastic cerebral palsy, and subjects with a lower limb amputation. Prospective subject data was collected by the experimenter for this study and consists of motion capture data for subjects free of gait pathology and subjects diagnosed with spastic cerebral palsy. Approval to conduct this research was granted by the Colorado Multiple Institutional Review Board. Consent for all prospective subjects and assent for participants under 14 years of age was obtained in the privacy of the CGMA laboratory's clinical exam room. A Health Insurance Portability and Accountability Act (HIPAA) waiver was granted to review all retrospective subjects, meeting the study's inclusion criteria, whose instrumented gait analysis data is stored on the server at CGMA. Prospective subjects were recruited from Denver, Colorado and surrounding areas.

Prospective participants were first screened with the script provided in Appendix A and an initial visit at CGMA was scheduled for the interested participants that satisfied this initial screening. At the participant's visit, the study was explained to the individual and if after meeting the inclusion criteria and if the participant agreed to be enrolled in the study, the consent (assent when applicable) forms were completed. The prospective subject then was assigned a study number for de-identification of all motion capture data (Table 4.1).

For the study's retrospective subjects, all personal health information (PHI) was obtained, stored, and accessed from the secure database server of clinical gait analyses performed at the CGMA, which is only accessible to CGMA staff. Only the principal investigator and co-investigators had access to a subject's PHI prior to de-identification. In order to identify retrospective subjects for this study, a retrospective subject's medical records were reviewed so as to obtain a subject's name, medical records number (MRN), diagnosis, age, and anthropometrics. Any patient found to be ineligible was not considered in this study and no single patient exceptions were permitted. A retrospective subject's motion capture data (e.g. marker data, kinematic graphs, and video) was then examined to verify the diagnoses (e.g. stiff knee gait, crouch gait pattern) and walking ability (e.g. unassisted) of the subject, as documented in the subject's medical records and IGA clinical report. After confirming the motion capture trials met the study's inclusion criteria, then the subject was then entered into the study.

Once it had been deemed that a subject satisfied the study's inclusion criteria, all of the subject's motion capture data was immediately relabeled and de-identified with the subject's study number. To protect subject privacy, each subject was assigned a number and a letter designation associated with the corresponding group, as shown in the table below.

Table 4.2.1: Study's prospective and retrospective subject designations

Prospective Population	Letter	Numbering
Unimpaired	N	1000-1019
Lower Limb Amputation	B	1000-1019
Cerebral Palsy	C	1000-1019

Retrospective Population	Letter	Numbering
Unimpaired	N	1020-1300
Lower Limb Amputation	B	1020-1300
Cerebral Palsy	C	1020-1300

4.2.1 Unimpaired Subjects

Male and female subjects free of gait pathology between the ages of 7 and 100 years of age were eligible for participating in this study as part of the reference cohort. All unimpaired subjects whose data met the inclusion criteria for this study from the CGMA normative motion capture database were incorporated into this study as retrospective reference subjects. Additionally, prospectively captured data from 20 unimpaired subjects who satisfied the following inclusion and exclusion criteria. Prospective subjects were recruited from the Denver Colorado area. No exceptions to these criteria were made for any of reference subjects.

Unimpaired Subject Inclusion Criteria:

- Males and females between the ages of 7 and 100 years of age.

- Ability to walk, unassisted continuously for 3 minutes.

- If under the age of 18, parent consent and subject assent.

- Cumulative time for over-ground walking trials must be at least 3 minutes

Unimpaired Subject Exclusion Criteria:

- Orthopaedic surgery at a hip, knee, or ankle within the last 2 years.

- An acute traumatic injury to a lower extremity affecting the subject's gait.

- Leg length discrepancy greater than 2 cm.

- Diagnosis of a neuromuscular or cardiovascular impairment that affects gait.

- Medications or medical devices that affect gait.

- Pain in the hip, knee, and/or ankle joints.

4.2.2   Subjects with Cerebral Palsy

The subjects in this investigation consist of both prospectively captured motion capture data and retrospective motion capture data from the CGMA database. All gait data from subjects with cerebral palsy, who satisfied the following criteria, in the CGMA subject motion capture database were incorporated into this study as retrospective subjects with spastic cerebral palsy (CP). Subjects with spastic cerebral palsy who were between the ages of 7 and 100 years of age were eligible for participating in this study as part of the atypical gait group. All retrospective subjects with cerebral palsy satisfied the following inclusion and exclusion criteria. Any potential subjects who do not satisfy these criteria were not incorporated into the study; no exceptions were made.

Subject with Spastic Cerebral Palsy Inclusion Criteria:

- Males and females between the ages of 7 and 100 years of age.

- Retrospective gait data must contain a complete lower body marker set and valid kinetic data.

- Only gait data trials of the subject walking unassisted will be used.

- Diagnosis of spastic cerebral palsy.

- Exhibits either stiff knee gait pattern, characterized by insufficient and delayed peak knee flexion during swing (less than 45°), or crouch gait pattern, characterized by excessive hip flexion and knee flexion (greater than 30° throughout stance) [69].

Subject with Spastic Cerebral Palsy Exclusion Criteria:

- Orthopaedic surgery at a hip, knee, or ankle within the last 2 years.

- Leg length discrepancy greater than 2 cm.

- Medications or medical devices that affect gait.

- Subject used assistance during walking (e.g. orthoses, walkers, crutches, canes, etc.)

- Pain in the hip, knee, and/or ankle joints.

4.2.3   Subjects with a Lower Limb Amputation

All gait data from subjects with a lower limb amputation, who satisfied the following criteria, in the CGMA subject motion capture database were incorporated into this study. Subjects with a lower limb amputation who were between the ages of 7 and 100 years of age were eligible for

participating in this study as part of the atypical gait group. All prospective and retrospective lower limb amputation subjects in this study met the following inclusion and exclusion criteria. Any potential subjects who do not satisfy these criteria were not be incorporated into the study; no exceptions were made.

Subject with Lower Limb Amputation Inclusion Criteria:

- Males and females between the ages of 7 and 100 years of age.

- Ability to walk continuously and unassisted for 3 minutes.

- If under the age of 18, parent consent and subject assent.

- Has been using the prosthetic limb for at least 6 months for independent ambulation prior to gait analysis at CGMA.

- Below knee or above knee amputation.

Subject with Lower Limb Amputation Exclusion Criteria:

- Orthopaedic surgery at a hip, knee, or ankle within the last 2 years.

- Diagnosis of a neuromuscular or cardiovascular impairment that affects gait.

- Medications that affect gait.

- Has been using the prosthetic limb for less than 6 months for independent ambulation prior to gait analysis at CGMA.

4.3   Equipment

The equipment described in this section of the chapter pertains to two motion capture data collection environments: an over-ground environment and a treadmill environment. The material in this section applies to both motion capture environments. Following the conventional gait model [136], passive retro-reflective markers were placed on lower extremity bony landmarks and locations of all subjects by clinicians and staff experienced in IGA. Marker trajectories were recorded using Vicon MX motion capture system, whose details for the two motion capture environments are provided in the following sections. Additionally, ground reaction forces and dynamic, surface electromyography data were collected simultaneously from most retrospective subjects but were not used in this analysis. After manually identifying foot floor contact events, filling any marker trajectory gaps, applying a Woltring filter with mean square error of 17 to all marker trajectories, and

applying the Vicon Plug-in-Gait model for each subject's trials in the Vicon Nexus software, the most representative trial for each subject was selected from the five trials captured for each subject using a custom Matlab program. Using the kinematics and temporal-spatial measures from the gait cycles of each trial from a subject, the program calculated the variance ratio for each trial. The subject's representative trial had the lowest variance ratio and was used for all analyses. The custom Matlab programs, described in section 4.3.3 Software, extracted and used the necessary information from each c3d file to calculate the study's kinematic, temporal-spatial, and nonlinear variables.

Both CGMA motion capture environments are routinely checked to ensure the cameras provide the same level of accuracy in detection and marker centroid calculations. Due to this continual practice of quality assurance, there is high confidence in the validity of comparing motion capture data from these two environments.

4.3.1   Over-ground Motion Capture Environment

The main motion capture environment at the CGMA laboratory utilizes thirteen infrared cameras of the Vicon MX-40 motion capture system to record the three dimensional position of passive retro-reflective markers. Marker trajectories were recorded by the Vicon system at 120Hz. All prospective subjects traversed a 362 cm walkway in this motion capture environment, with additional room at each of the walkway for gait initiation and termination. Two high definition video cameras recorded the sagittal and coronal plane video of each prospective and retrospective subject. To preserve a prospective subject's privacy and confidentiality, all bi-planar video only recorded the subject from the shoulders down, thereby automatically de-identifying all video upon collection.

Retrospective subject data from the older motion capture environment was also incorporated into the study. The older motion capture environment used eight CCD analog cameras of the Vicon Pulnix TM-6710 motion capture system to record the three dimensional position of passive retro-reflective markers. All marker trajectories were recorded by the Vicon system at 120 Hz. The same motion capture marker sets and motion capture data analysis (e.g. filtering, models) were used for both over-ground motion capture environments.

4.3.2   Treadmill Motion Capture Environment

The treadmill capture environment at the CGMA laboratory utilizes a split belt instrumented Bertec treadmill, Medtronic body weight support system, and eight infrared Vicon MX-40 motion capture camera system to record the three dimensional position of passive retro-reflective markers. Marker trajectories were recorded by the Vicon system at 120 Hz. Two standard definition video

cameras recorded the sagittal and coronal plane video while each prospective subject walked on the treadmill. To preserve a prospective subject's privacy and confidentiality, all bi-planar video only recorded the subject from the shoulders down, thereby automatically de-identifying all video upon collection. In the treadmill motion capture environment, there was additional equipment used to modify the swing limb advancement and impose range of motion limitations for the unimpaired prospective subjects in order to mimic the biomechanical limitations seen in subjects with cerebral palsy. Further explanations about this additional treadmill room equipment are provided in the following sub-sections.

4.3.2.1 Body Weight Support System

As a safety precaution during all treadmill walking trials, every prospective subject wore wearing a safety harness that was attached to a body weight support system (BWSS). In the event the subject began to fall, the BWSS would engage and catch the person before hitting the ground and prevent any fall related injuries. To reduce discomfort and provide an optimal fit, the harness was selected to match the size of each subject. To help reduce BWSS related variables that could alter their gait pattern, none of the prospective subjects held the handrails during the TM trials.

4.3.2.2 Swing Limb Assist Device

The leg swing extension assistive device (LSEAD) is a non-invasive piece of rehabilitation equipment that was attached to the subject's shoes during treadmill walking (Figure 4.3.1). The LSEAD device assists swing limb advancement by using a linear spring and pulley system to pull the subject's leg forward (when facing the device) during swing and thereby provide an assistive force. The device was also used when the subjects walked in the opposite direction, thus providing resistance to swing limb advancement.
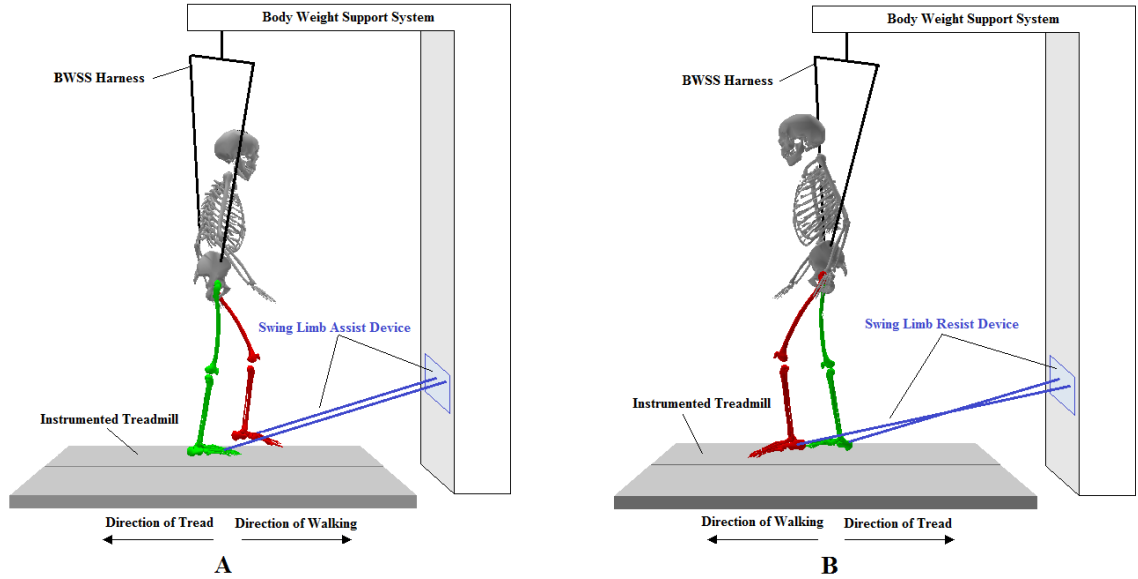
Figure 4.3.1: Leg swing extension assistive device providing swing limb assistance (A) and resistance (B) when a prospective subject walks on the treadmill with the bodyweight support system.

4.3.2.3 Restricting Range of Motion

Two different braces were used to simulate the restricted range of knee and ankle joint motion commonly seen in individuals with stiff knee and crouch gait patterns. The braces were only applied to the dominant leg of the prospective unimpaired subjects.

Knee Brace. A locking knee brace with wraparound thigh and shank attachment points was used to restrict the range of motion for the prospective subjects free of gait pathology as they walked on the treadmill. The knee angle dial and locking pins were used to position and fix the knee brace into a fully extended position (180° extension) and a flexed position (60° flexion). To simulate the stiff knee gait (full extension) and crouch gait (flexion) patterns and study how subjects adapted to these fixed knee positions, the knee brace was worn on the subject's dominant leg. The brace was fit to each subject using the generic sizes of small, medium, and large. Since the lateral knee, thigh, and shank motion capture markers were moved to put the brace on the subject's leg, a new static trial was taken for the knee brace condition. By constraining movement at a joint, such as the knee, in individuals free of gait pathology, the resulting changes in coordination due to limiting the degrees of freedom at the knee were studied.

Ankle Brace. An ankle brace, which fixed the ankle in a neutral position, was used to restrict ankle dorsiflexion and plantarflexion during walking in subjects free of gait pathology. The brace was fit to each subject using the generic sizes of small, medium, and large. Since the lateral shank,

ankle, and foot markers motion capture markers were moved to put the brace on the subject's leg, a new static trial was taken for the ankle brace condition. Solid ankle-foot orthoses are commonly prescribed by clinicians to address excessive plantarflexion due to spasticity in the muscles of the leg's posterior compartment. Other studies have shown that constraining joint motion at the ankle has a significant impact on the timing and sequencing of muscle activation. Therefore by providing restriction at the ankle joint, it was expected that subjects free of gait pathology would adopt a different walking strategy by changing the coordination of more proximal segments.

4.3.3 Software

All motion capture data files and initial motion capture file processing was performed using the Vicon LifeSciences Software Suite. After manually identifying foot floor contact events, applying a Woltring filter with mean square error of 17 to all marker trajectories, and applying the Vicon Plug-in-Gait model for each subject's trials in the Vicon Nexus 1.8.5 software, the most representative trial for each subject was selected from the five trials captured for each subject using a custom Matlab program. Using the kinematics and temporal-spatial measures from the gait cycles of each trial from a subject, this Matlab program calculated the variance ratio for each trial. A subject's representative trial had the lowest variance ratio. A flowchart of the custom Matlab code's algorithm for selecting a subject's representative trial is located in Appendix E. Only the right leg segments from each unimpaired subject's representative trial contributed to dataset and only affected legs in the other subject populations were used to create those respective datasets.

A custom BodyBuilder program was written to create the virtual target boundaries for the speed-accuracy task (prospective subjects only) and used to validate the virtual target boundaries generated by custom Matlab program (CERBERUS), which analyzed this motion capture task. Numerous custom Matlab programs were written to calculate the variables for the various aims and their hypotheses. Table 4.2 provides a list of the main custom Matlab programs, their corresponding aims, and primary purpose.

Table 4.3.1: List of custom Matlab programs used for data analysis.

Program	Aim	Purpose
DIONYSOS	Aim 1, 4	Generate PPs and CPRDs from c3d file(s) or pendulum model
GAMS	Aim 1, 4	Generate conventional IGA measures
PEGASUS	Aim 3	Compound pendulum model
CERBERUS	Aim 2	Analyzes speed-accuracy, tandem walking, and 90° turning tasks
CDI	Aim 1, 4	Generates coordination dynamics index from c3d file
CPS	Aim 1, 4	Generates coordination performance score from c3d file
SAP	Ai 1, 2, 3, 4	Calculates descriptive statistics and correlation matrix

As detailed more in the following sections, statistical analyses were performed in Microsoft Excel, JMP, Minitab, SAS, or Matlab and all descriptive statistical analyses were performed in at least two different software programs to reduce the occurrence of errors and serve as an internal validation of calculations.

4.4 Experimental Protocols

The following experimental protocols are described for two clinical populations: unimpaired subjects and subjects with an atypical gait pattern (e.g. cerebral palsy or lower limb amputation). There are two separate datasets for these subjects, one consisting of only prospective subjects and a second consisting of only retrospective subjects. The prospective subject dataset is distinguished from the retrospective subject dataset by a battery of clinical measures and donning of shoes to enable multiple task variations for both the over-ground and treadmill motion capture environments. The following experimental protocol mainly focuses on the prospective experimental procedures.

Prior to any motion capture experiments, the anthropometrics of each prospective subject was measured and recorded with a tape measure, calipers, and scale. These anthropometric values were entered into the motion capture computers and used to create a unique skeletal coordinate system for each subject. This virtual skeletal coordinate system was used by conventional and nonlinear methods to calculate various measures of gait. Table 4.3 provides a list of the anthropometrics that were measured from each prospective subject.

Table 4.4.1: Anthropometrics measured from each subject, where * indicates prospective subject measurements.

Anthropometrics
Height (cm)
Body mass (kg)
Left & right leg length (cm)
Left & right knee width (cm)
Left & right ankle width (cm)
Left & right elbow width (cm)*
Left & right wrist thickness (cm)*
Left & right hand thickness (cm)*

For all prospectively captured data, each subject wore a full body marker set and his or her own shoes (Figure 4.4.1, Figure 4.4.2). All retrospective subjects wore a lower body marker set, which is identical to the full body marker sets shown below but does not include the head, torso, or arm markers.
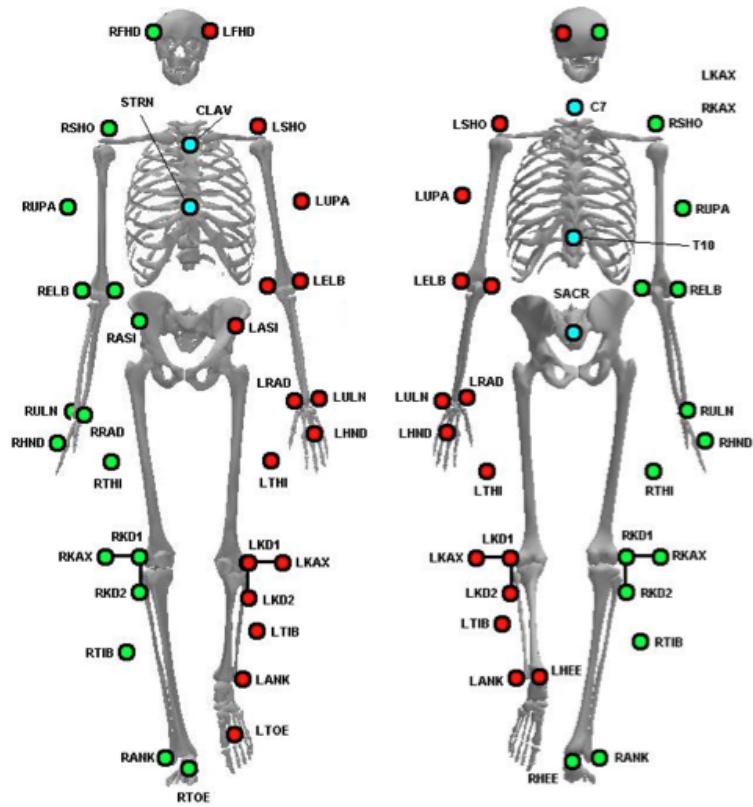
Figure 4.4.1: Anterior (left) and posterior (right) views of full body static marker set.
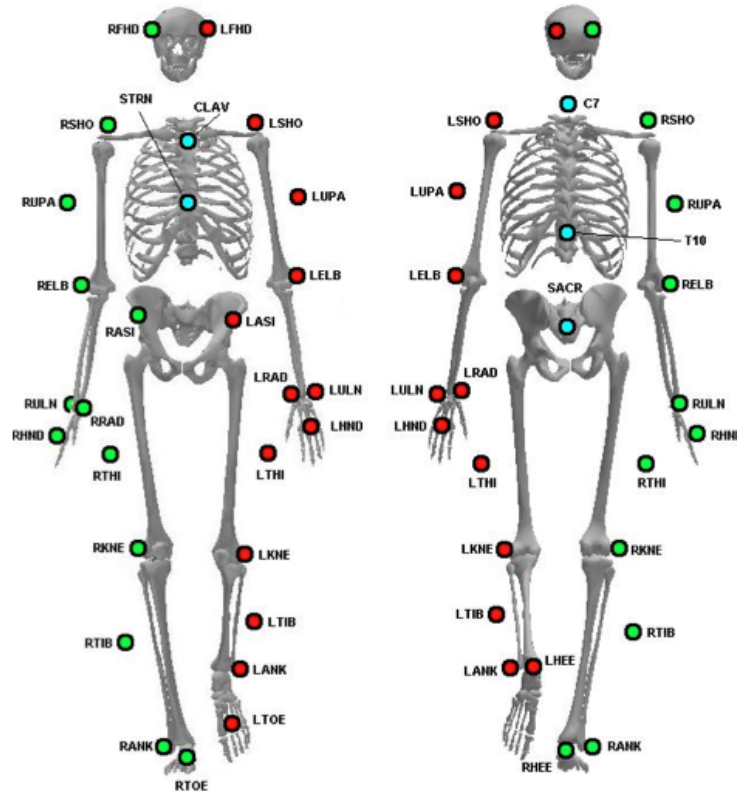
Figure 4.4.2: Anterior (left) and posterior (right) views of the full body dynamic marker set.

All retrospective subjects with unimpaired gait or cerebral palsy were barefoot during over-ground walking. Retrospective and prospective subjects with a lower limb amputation wore shoes on both the prosthetic and intact limb during all motion capture trials.

4.4.1 Unimpaired Prospective Subject Experimental Protocol

The following table (Table 4.4) outlines the order of experiments, data capture procedure for each unimpaired prospective subject, and corresponding instrumentation associated with each experiment/task. Prior to placing markers on a prospective subject, the investigator measured each subject's anthropometric data (Table 4.3).

Table 4.4.2: Overview of the location and instrumentation used for experiments for the unimpaired prospective subjects.

Location	Task	Instrumentation
Clinical Exam Room	Anthropometric Data	Calipers, tape measure, scale
OG MoCap	1. Walk at Vss 2. Speed-Accuracy Task 3. Modified ICARS Tasks	1-3. Full body marker set Biplanar HD Video
TM MoCap	4. Level walking at Vss 5. Speed Tasks 6. Assistive Task 7. Resistive Task 8. Knee/Ankle Range of Motion Tasks 9. SCALE & ICARS Tasks	4-9. Full body marker set Biplanar HD Video

4.4.1.1 Prospective Unimpaired Subject: Over-ground Walking Task

To establish each subject's baseline gait for over-ground walking, each subject walked in the main motion capture laboratory (over-ground) while wearing a full body marker set (Figure 4.3). Each subject will walk at a self-selected walking speed (Vss) on the level over-ground surface until at least 3 minutes of gait data has been collected. The motion capture software (Vicon LifeSciences Suite) will be used to provide the mean walking speed and mean step length for each subject.

4.4.1.2 Prospective Unimpaired Subject: Speed-Accuracy Task

Each prospective subject performed a lower extremity speed-accuracy task to characterize any impairment in a subject's accuracy of voluntary reciprocal movements. This task is a modified version of the upper extremity speed-accuracy task that adapts this clinical task for the anterior-posterior swinging motion of the lower leg, similar to the swing period motion during the gait cycle [14,15]. Square foot targets were size for each subject, using the distance between the subject's first and fifth metatarsal head. These anatomical boney locations were identified by palpation and the distance was measured with calipers while the subject wore the same shoes in which all motion capture data was conducted. Three sets of foot targets were created: 100% of the subject's shoe/foot width, 80% of the shoe/foot width, and 120% of the shoe/foot width. For consistency and in consideration of the bi-planar video cameras, one foot target was placed with a 10cm offset from either force plate number 6 or force plate number 3 of the main lab's ten force plate array, depending on the subject's dominant leg (Figure 4.4). The mean step length was calculated from the first three over-ground walking tasks and used as the distance between the leading edge of each foot target and provided the location of the second foot target. Foot targets were secured to the floor using tape and a clear protective coating. Prior to starting each trial, the target location was

doubled checked by this investigator to ensure no movement had occurred as a result of the previous trial.

For this task, the subject stood on one leg while on the force plate array in the over-ground motion capture environment. The subject then used the swing limb to alternate tapping of the foot between the forward target (located on a force plate) and backward target (located on a different force plate) as quickly as possible while maintaining accuracy of tapping the foot on each target. Subjects were instructed to position themselves in order to see each target prior to a foot tap and so as to reduce the influence of obscured vision, which could hinder the subject's accuracy. Subjects performed the task with the smallest target first and then all subsequent targets were positioned over the previous smaller target so only the current target was visible. The targets were placed in a plastic protective sheet, which was taped securely to the floor, in order to reduce wear on the target and ensure placement of each target was consistent.
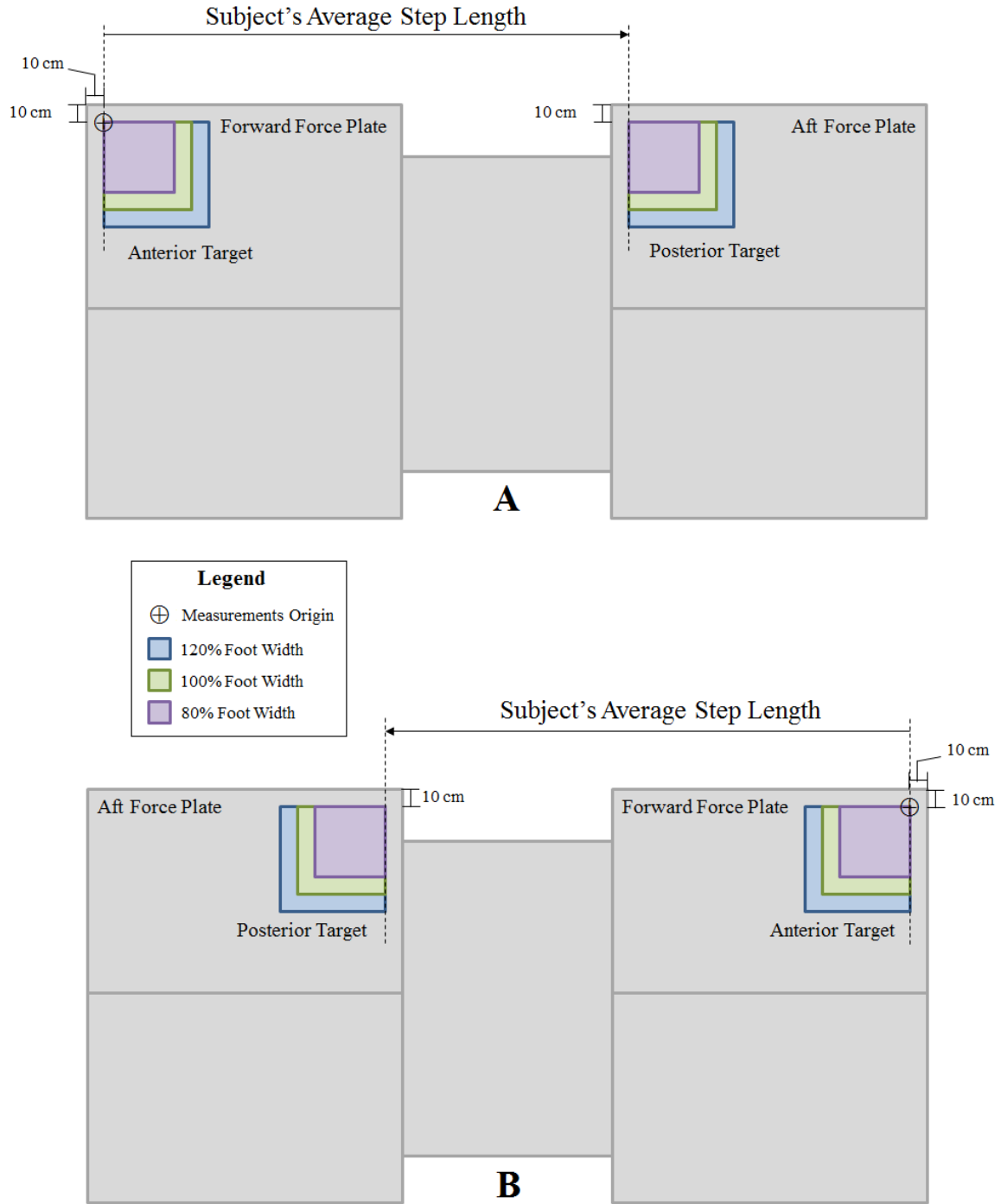
Figure 4.4.3: Speed-Accuracy task target setup and sizing. A) Target setup for a right leg, B) target setup for a left leg.

For safety and subject stability, all subjects used both hands to hold onto a fixed support bar while performing the task. The following figure provides a schematic of the speed-accuracy task to be performed by each prospective unimpaired subject.
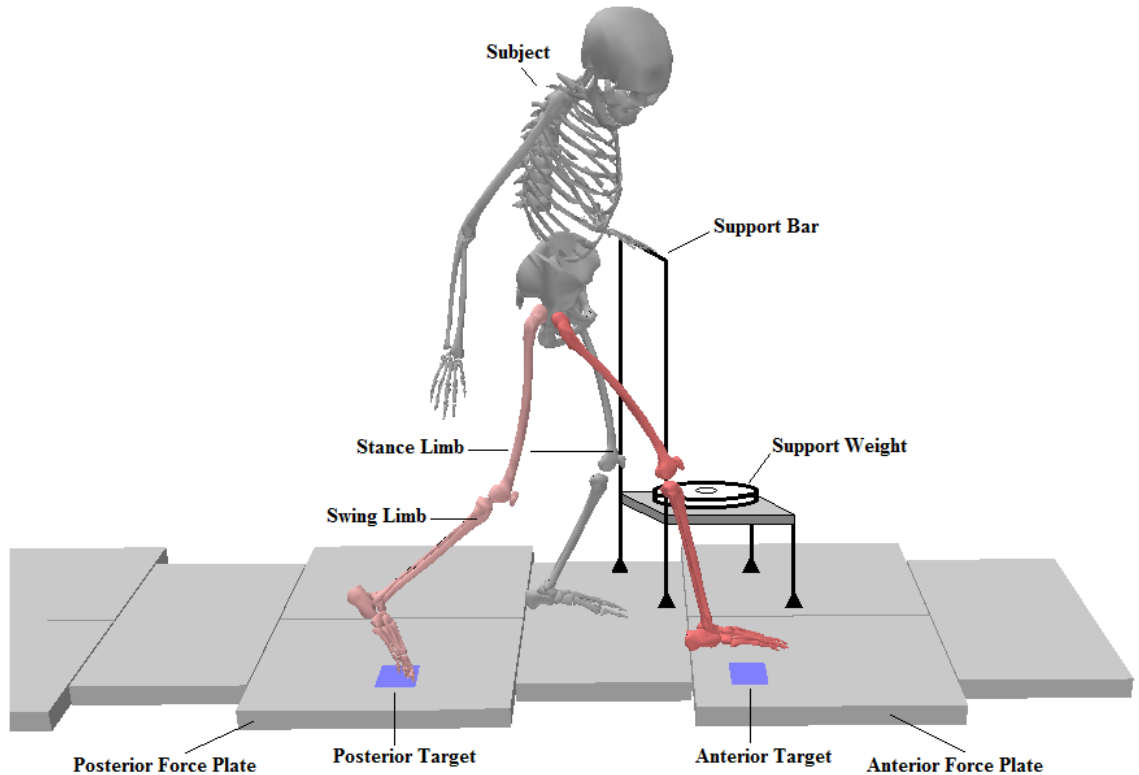
Figure 4.4.4: Functional diagram of the lower extremity speed-accuracy task.

The duration of each trial was fixed to 30 seconds. This temporal constraint was selected with consideration to the potential limited endurance of subjects with an atypical gait pattern and was loosely based upon the Fitts' experimental paradigm [110]. The purpose of this experiment is to characterize any prospective subject's speed and accuracy impairments during the reciprocal leg movements and explore the relationship between this experiment's outcomes and the measures of coordination dynamics. To provide enough samples for statistical comparison of these different task conditions, each subject performed this task three times for each set of foot targets, totaling 9 trials.

4.4.1.3   Prospective Unimpaired Subject: Modified ICARS/SARA Tasks

Prospective subjects performed select walking tasks from the International Cooperative Ataxia Rating Scale (ICARS) and Scale for the Assessment and Rating of Ataxia (SARA) exams. In the main motion capture environment, all prospective unimpaired subjects performed the tandem walking and 90° turning tasks. For the tandem walking task, each subject was instructed to walk while touching the advance foot's heel to the lagging foot's toe (Figure 4.4.5). Subjects were allowed

to freely position their arms for balance during this task. Each subject performed this task four times on the same walkway as the over-ground walking tasks.

Direction of Walking
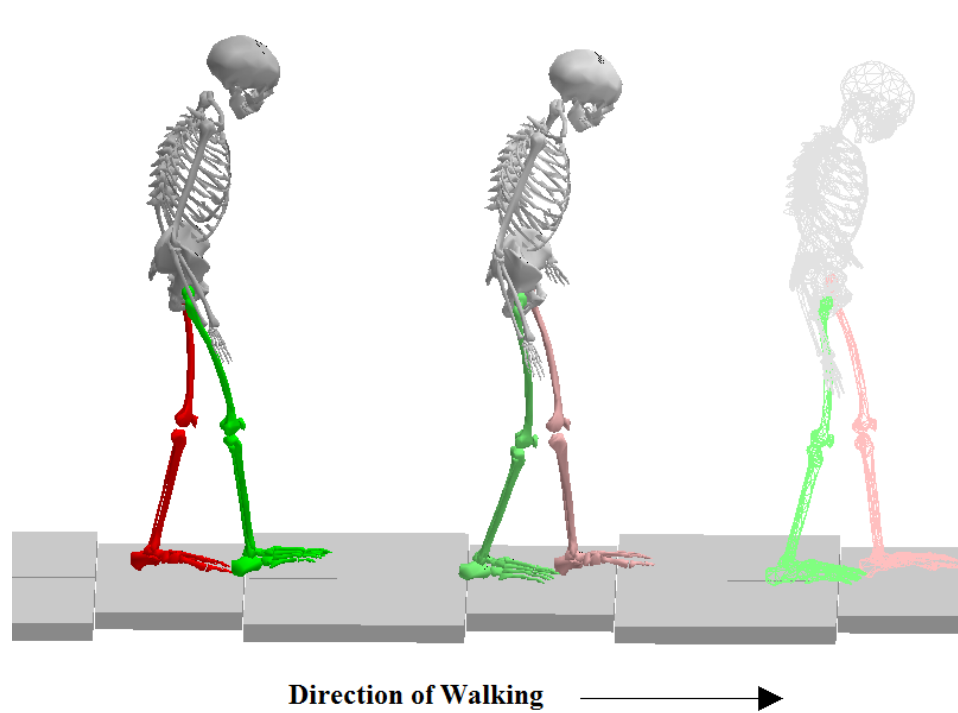
Figure 4.4.5: Functional diagram of over-ground tandem walking task.

Next a simple "T" constructed from white paper tape was placed on force plate 9, which is approximately the location of least parallax from the sagittal plane video camera and halfway in the walkway (Figure 4.4.6). The subject was instructed to walk normally at a self-selected speed toward the "T" and upon reaching the mark, made a 90° turn to either the left or right. Each subject performed a minimum of one and maximum three turns per side.
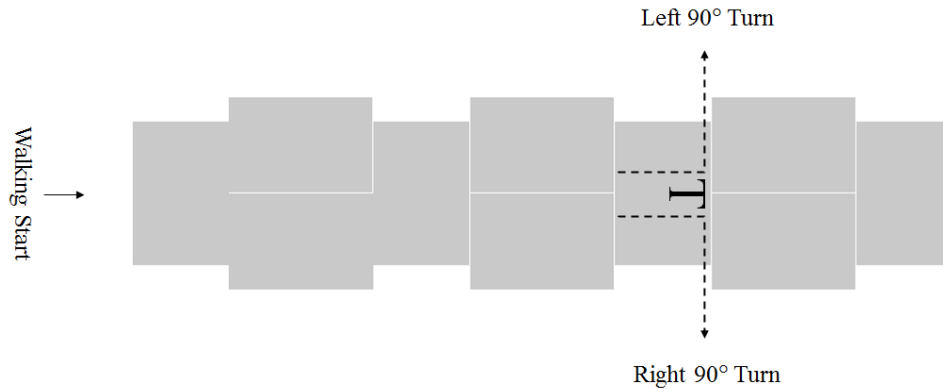
Figure 4.4.6: Diagram of 90° walking task setup with the 'T' tape target indicating where to initiate the turn (transverse view).

4.4.1.4 Prospective Unimpaired Subject: Treadmill Walking Task

To determine each prospective subject's preferred walking speed for the treadmill tasks, the mean over-ground walking speed from three trials was calculated for each subject. This average over-ground walking speed was then used to set the treadmill belt speed for this task. Each prospective subject walked for at least 3 minutes on the treadmill with the belt speed set at this mean Vss.

4.4.1.5 Prospective Unimpaired Subject: Changes in Walking Speed Task

The effects of changes in walking speed on coordination dynamics were examined for level treadmill walking. The subject's average Vss was used to calculate walking speeds that are 10 and 20 percent slower and faster than Vss (Table 4.5). Alternatively described, the subject walked on the treadmill with a belt speed of 80%, 90%, 110%, and 120%. Walking speeds faster than 120% were not included in order to adequately avoid the transition (and therefore change in gait pattern) from walking to running, which occurs at approximately 130-140% of Vss [13].

Table 4.4.3: Changes in walking speed conditions for unimpaired prospective subjects.

Belt Speed	Task	Duration
80% of VSS	Level treadmill walking	3 minutes
90% of VSS	Level treadmill walking	3 minutes
110% of VSS	Level treadmill walking	3 minutes
120% of VSS	Level treadmill walking	3 minutes

4.4.1.6 Prospective Unimpaired Subject: Changes in Assistive Forces Task

The effect of adding assistive external forces to the advancing swing leg during the task of swing limb advancement on coordination was performed on the treadmill using a leg swing extension assist device (LSEAD). The LSEAD device assists swing limb advancement by using a linear spring and pulley system to pull the subject's leg forward during swing and thereby providing an assistive force. Each subject walked for 3 minutes with the LSEAD device attached to the subject's shoes. If the 5lbf linear spring was too much force for the subject to walk safely and for the allotted task duration, then the 3lbf linear spring was used instead.

4.4.1.7 Prospective Unimpaired Subject: Changes in Resistive Forces Task

The effect of adding resistive external forces to the advancing swing leg during the task of swing limb advancement on coordination was performed on the treadmill using the LSEAD. In this condition, the LSEAD attaches to the subject's shoes as the subject walks in the opposite direction from the previous LSEAD walking task. When walking in this direction, the LSEAD device resists

swing limb advancement by using a linear spring and pulley system to pull the subject's leg backward during swing. The same linear spring force as in the assistive condition was also used in this resistive condition. Each subject walked for 3 minutes with the LSEAD device attached to the subject's shoes.

4.4.1.8 Prospective Unimpaired Subject: Changes in Joint Range of Motion Tasks

The effects limiting the range of motion for knee and ankle joints on coordination were simulated by having the unimpaired subject wear passive braces on the knee and ankle joints during level treadmill walking at Vss. This commonly employed method of creating a temporary impairment in an unimpaired subject was included in order to simulate stiff knee and crouch gait patterns in subjects with an intact nervous system. Prior investigations of pathological gait have shown significant changes in kinematics and temporal spatial measures in subjects before and after surgical interventions that afforded subjects with an increased range of motion [7].

Limitation of the knee joint's range of motion was accomplished by having each subject wear a hinged knee brace while walking on the treadmill for 3 minutes. The two knee range of motion limitations will simulate a stiff knee gait pattern (fixed at 180° extension) and a crouch gait pattern (fixed at 60° extension) [11]. The knee brace pins were used to set the flexion and extension ranges for each condition and ensured the brace remained fixed in the desired position. Limitation of the ankle joint's range of motion was accomplished by having each subject wear a solid (non-articulating) walking ankle boot to prevent plantar/dorsi-flexion (0° dorsi/plantar-flexion). The following table provides a summary of this task's conditions, range of motion, and applicable side(s).

Table 4.4.4: Joint range of motion limitations for unimpaired prospective subjects.

Joint	Task	Side & Duration
A. Knee	A1. 180°	A1. Dominant leg, 3 minutes
	A2. 60°	A2. Dominant leg, 3 minutes
B. Ankle	B1. 0°	B1. Dominant leg, 3 minutes

Among the available brace sizes, each subject was fitted to an appropriately sized brace for these treadmill walking tasks. The knee and ankle braces utilized for this task were obtained from the Orthopedic Clinic at Children's Hospital Colorado (pediatric sizes) and the Department of Physical Therapy at the University of Colorado (adult sizes).

4.4.1.9 Prospective Unimpaired Subject: SCALE Exam and Modified ICARS Task

Prior to performing the Selective Control Assessment of the Lower Extremity (SCALE) exam on any prospective subjects, I reviewed the clinical training videos, accompanying worksheet, and

presentation to learn how to properly instruct a subject and perform each task. This investigator reviewed the trials to verify each prospective subject's SCALE score and achieved procedural fidelity with a clinical advisor and co-investigator experienced in neurological physical therapy. Although a detailed description of the SCALE tasks and scoring criteria is provided in Appendix B, the following general descriptions offer an overview of the tasks and experimental protocol for all prospective subjects.

After removing all passive retro-reflective markers, each prospective subject lay on his/her side and sat on an exam table in the treadmill motion capture environment for these performance measures. Each subject performed the selective voluntary movement tasks at the hip, knee, and ankle after the examiner demonstrated each joint's task by passively moving the joint through the desired motion. Each task was verbally explained and demonstrated to the subject prior to the subject performing the task. The subject was then given a verbal cue to perform the task along with a three-second verbal cadence by the examiner. The subject's comfort was also monitored throughout the passive demonstration of these tasks by asking each subject if he/she was experiencing any pain. The following figure provides the flow chart used for this portion of the prospective subject data capture.
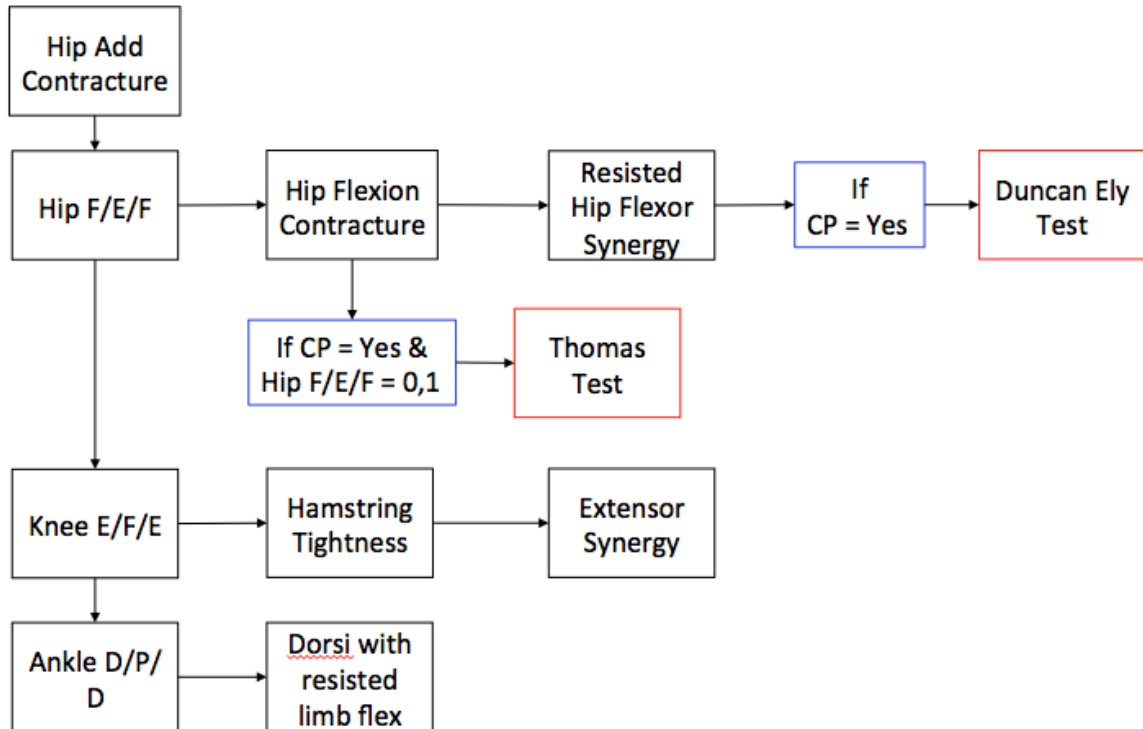
Figure 4.4.7: Flowchart of the SCALE tasks performed for each prospective subject.

The subject's hip range of motion for flexion and extension was passively demonstrated by the examiner and then actively performed by the subject while lying on his/her side. This task was performed for each leg. The examiner assessed the subject's passive hip abduction range of motion while the subject lay on his/her side. The Thomas test was performed to asses the tightness of the muscles involved in or effecting hip flexion (e.g. rectus femoris, illiopsoas) [141]. Next the subject's knee flexion/extension range of motion was passively and actively assessed while the subject sat on the edge of the exam table. Lastly, the subject's ankle plantarflexion/dorsiflexion passive range of motion was assessed by the examiner and then actively performed by the subject.

Video of the task was recorded and used after the subject's data capture visit to score the subject's ability to perform the various SCALE exam tasks. While the original SCALE exam includes measures for the subtalar joint and toes, these segments were not included because this body of work is examining segmental coordination dynamics and characterized the foot as one segment. Furthermore, since the prospective subjects wore shoes for all walking conditions the ability to accurately distinguish a multi-segmented foot would not be possible with the currently available and validated motion capture models. A SCALE score for each limb is obtained by summing the points assigned to each joint. Since only the hip, knee, and ankle, joints are being measured for this research project, a maximum limb score of 6 points is possible.

The knee-tibia slide test from the ICARS/SARA exams was then performed in a supine position (laying on the exam table) with the head tilted so that visual input was possible. Before the subject performed the task it was first explained and demonstrated. After receiving a verbal cue to begin the task, the subject raised placed the right heel on the left knee, and then slid the right heel down the anterior tibial crest/surface of the resting left leg until reaching the left ankle. Once the right heel was at the left ankle, the subject raised the heel off the left leg and repositioned the right heel on the left knee. The subject repeated this knee-heel sliding motion three times with the right leg and then three times with the left leg. Video of the task was recorded and used after the subject's data capture visit to confirm the score for this task, which reflected the subject's ability to perform the task. The task was scored by two different requirements, which total a maximum possible score of 8. The first requirement scored the subject on his or her ability to perform the task (0 = unable to perform and 4 = no impairment) and the second requirement scored the subject on the amount of action tremor during the task (0 = uninterrupted tremor and 4 = no tremor). A more detailed description for the scoring criteria is located in Appendix B.

4.4.2 Experimental Protocol for Prospective Subjects with an Atypical Gait Pattern

The following table outlines the order of experiments (detailed below), data capture environment for each prospective subject with either a lower limb amputation (LLA) or cerebral palsy (CP) and corresponding instrumentation associated with each task. Prior to placing markers on a prospective subject, the investigator measured each subject's anthropometric data.

Table 4.4.5: Overview of the location and instrumentation used for experiments for the prospective subjects with an atypical gait pattern.

Location	Task	Instrumentation
Clinical Exam Room	Anthropometric Data	Calipers, tape measure, scale
Over-ground MoCap Environment	1. Walk at Vss 2. Speed-Accuracy Task 3. Modified ICARS Tasks	1-3. Full body marker set Biplanar HD Video
Treadmill MoCap Environment	4. Level walking at Vss 5. SCALE & ICARS Tasks	4-5. Full body marker set Biplanar HD Video

4.4.2.1 Prospective Atypical Subject: Over-Ground Walking Task

Each prospective subject walked in the main motion capture laboratory while wearing a full body marker set to establish the baseline over-ground gait pattern. Each subject walked at a self-selected walking speed (Vss) on the level over-ground surface for approximately 3 minutes. If a subject was unable to walk for a cumulative amount of 3 minutes, then the subject was asked to walk until he/she began to feel tired. Rests were taken as needed to try to reduce fatigue. Aside from the subject dependent modifications mentioned here, the procedures, measures, and equipment for these subjects were the same as that detailed by the subjects with an unimpaired gait pattern above for this task.

4.4.2.2 Prospective Atypical Subject: Speed-Accuracy Task

Each prospective subject with an atypical gait pattern performed the lower extremity speed-accuracy task to characterize any impairment in the subject's accuracy of voluntary reciprocal movements. In the event a subject was unable to physically reach the targets when placed a distance apart equal to the mean step length, the target distance was systematically reduced (increments of 1cm) until the subject was able to reach both foot targets. Subjects were instructed to position themselves in order to see each target prior to a foot tap and so as to reduce the influence of obscured vision, which could hinder the subject's accuracy. For safety and subject stability, all subjects used both hands to hold onto a fixed support bar while performing the task. The duration

of each trial was fixed to 30 seconds. Depending on the severity of gait impairment each subject performed this task a minimum of one and maximum of three times for each set of foot targets. Aside from the subject dependent modifications mentioned here, the procedures, measures, and equipment for these subjects were the same as that detailed by the subjects with an unimpaired gait pattern above for this task.

4.4.2.3 Prospective Atypical Subject: Modified ICARS/SARA Tasks

In the main motion capture environment, all prospective subjects performed the tandem walking and 90° turning tasks. Each subject performed this task a maximum of four times on the same walkway as the over-ground walking tasks. If subjects were unable to safely walk independently, the investigator held their hands to prevent falling. If subjects were unable to touch a heel to a toe, they were instructed to get as close as possible. Aside from the subject dependent modifications mentioned here, the procedures, measures, and equipment for these subjects were the same as that detailed by the subjects with an unimpaired gait pattern above for this task.

As with the unimpaired prospective subjects, a simple "T" constructed from white paper tape was placed on force plate 9, at approximately the location of least parallax from the sagittal plane video camera and half the length of the total motion capture walkway. The subject was instructed to walk normally at a self selected pace toward the "T" and upon reaching the mark, make a 90 degree turn to either the left or right. Depending on the subject's walking ability, each subject performed a minimum of one left and right turn to a maximum of three left and three right turns for this task. Aside from the subject dependent modifications mentioned here, the procedures, measures, and equipment for these subjects were the same as that detailed by the subjects with an unimpaired gait pattern above for this task.

4.4.2.4 Prospective Atypical Subject: Treadmill Walking Task

The mean over-ground walking speed from three trials was calculated for each prospective subject. This average over-ground walking speed was then used to set the treadmill belt speed for this task. Each subject walked for a minimum of 30 seconds and a maximum of 3 minutes on the treadmill with the belt speed set at this mean self-selected walking speed (Vss). For individuals who were unable to walk on the treadmill at the same speed as their over-ground walking trials (as is common for individuals with cerebral palsy), the treadmill belt speed was systematically lowered in 10% increments until the subject was able to walk safely, in a controlled manner, and without the assistance of the bodyweight support harness. In such situations, the reduced belt speed was

recorded. Aside from the subject dependent modifications mentioned here, the procedures, measures, and equipment for these subjects were the same as that detailed by the subjects with an unimpaired gait pattern above for this task.

4.4.2.5 Prospective Atypical Subject: SCALE and Modified ICARS Tasks

Prior to performing the SCALE exam on any prospective subjects, this investigator reviewed the clinical training videos, accompanying worksheet, and presentation to learn how to properly instruct a subject and perform each task. As with the unimpaired prospective subjects, this investigator reviewed the trials of the prospective subjects with an atypical gait pattern and achieved procedural fidelity with a clinical advisor and co-investigator experienced in neurological physical therapy.

4.4.3 Retrospective Subject Motion Capture Data

As previously mentioned, the motion capture data of the retrospective subjects in this investigation was obtained from the retrospective subject database at CGMA. The motion capture for all retrospective subjects from the CGMA database contains a subject's anthropometric data , biplanar video, and tri-planar lower body marker trajectories. To establish each retrospective subject's baseline over-ground measures of gait, all unassisted walking trials were concatenated using foot strike as the common joining temporal event. The subject's representative walking trial was then assessed with the same motion capture model and Matlab analyses as the prospective subjects over-ground walking gait data. Clinical IGA from the CGMA retrospective database usually only contains motion capture data for the task of over-ground walking. Therefore, over-ground walking is the only common motion capture task between all retrospective and prospective subjects in this dissertation and comparisons of the other prospective motion capture tasks to retrospective subjects were not possible.

4.4.4 Mathematical Software Model of a Compound Pendulum

The Lagrangian approach was used to solve for a double pendulum's equations of motion. Initially, the equations of motion were calculated for a pendulum without damping or inertia terms and then again including these terms (Appendix C). The later set of equations of motion was implemented into the Matlab model and used for all analyses.

The baseline mathematical, two-dimensional pendulum model consists of a fixed pivot and two linkages. This pendulum model provided a theoretical analogue to the sagittal motion of the thigh and shank segments during level over-ground walking. The length, center of mass location, initial

angular displacement, initial angular velocity, and mass for the pendulum linkages were calculated from the mean of the corresponding variables from the retrospective unimpaired subjects, all subjects with stiff knee gait and crouch gait patterns, and all subjects with either a transtibial or transfemoral amputation. These subject-derived variables were used in an effort to create a pendulum model that is based upon the initial conditions of human subjects at the beginning of swing period. The pendulum model was created in Matlab using the code provided in Appendix C to solve for each linkage's angular displacement and angular velocity.

4.4.4.1 Compound Pendulum Software Model

A mathematical, two-dimensional compound pendulum software model consisting of a fixed pivot and two linkages provided a theoretical analogue to the sagittal motion of the thigh and shank segments during level over-ground walking. The resulting motions of this pendulum model for various damping cases served as a theoretical comparison to the swing limb advancement dynamics of the various subject cohorts in this study. The variables for the initial conditions of the software model were generated from each cohort's mean of the variables listed in Table 4.8. The subject cohorts used for the pendulum model consisted of all unimpaired subjects (N), all subjects with a stiff knee gait pattern (SKG), all subjects with a crouch (C) gait pattern, all subjects with a below knee amputation (BK), and all subjects with an above knee amputation (AK).

Table 4.4.6: Pendulum model parameters, model's initial conditions, and the subject instrumented gait analysis data from which they are derived. The subject data variables are mean values for each of the study's cohorts and FO indicates the instance of foot off during the gait cycle.

Model Variables	Subject Data
1. Length of proximal linkage	1. Thigh length
2. Length of distal linkage	2. Shank length
3. Mass of proximal linkage	3. Thigh mass
4. Mass of distal linkage	4. Shank mass
5. Center of mass location of proximal linkage	5. Thigh center of mass location
6. Center of mass location of distal linkage	6. Shank center of mass location
7. Initial angular displacement of proximal linkage	7. Thigh angular displacement at FO
8. Initial angular velocity of proximal linkage	8. Thigh angular velocity at FO
9. Initial angular acceleration of distal linkage	9. Shank angular acceleration at FO
10. Initial angular displacement of distal linkage	10. Shank angular displacement at FO
11. Initial angular velocity of distal linkage	11. Shank angular velocity at FO
12. Initial angular acceleration of distal linkage	12. Shank angular acceleration at FO
13. Duration of model simulation	13. Swing period duration

The pendulum model was run for four different damping conditions for each subject cohort, totaling twenty simulations. The proximal and distal linkages' damping coefficient for each condition were set equal to each other. Table 4.9 lists the four classical dynamics damping cases used for each

cohort's pendulum analysis.

Table 4.4.7: Description of the four damping conditions and corresponding linkage damping coefficient values.

Damping Coefficient	Damping Condition	Cohort Comparison
1. $\xi_{Prox} = \xi_{Dist} = 0$	1. Un-damped	1. N, SKG, C, BK, AK
2. $\xi_{Prox} = \xi_{Dist} = 0.5$	2. Under damped	2. N, SKG, C, BK, AK
3. $\xi_{Prox} = \xi_{Dist} = 1$	3. Critically damped	3. N, SKG, C, BK, AK
4. $\xi_{Prox} = \xi_{Dist} = 1.5$	4. Over damped	4. N, SKG, C, BK, AK

The pendulum model's initial conditions were calculated from each subject's representative trial using the Matlab algorithm detailed in Appendix E. A cohort's ensemble average was then calculated using each subject's initial conditions and this ensemble cohort average provided the pendulum model's input for each gait pattern simulation. A gait pattern simulation for the pendulum model was run for the retrospective normative cohort, all subjects with a stiff knee gait pattern, all subjects with a crouch gait pattern, all subjects with a below knee amputation, and all subjects with an above knee amputation.

The model used a cohort's initial conditions and the equations of motion provided in Appendix B to solve the compound pendulum's differential equations with Matlab's ode45 function. This Matlab function applies the Runge-Kutta 4,5 method to solve the models' ordinary differential equations of motion. This ordinary differential equation solver returns the angular displacement, angular velocity, and angular acceleration of the two pendulum linkages in the PEGASUS model's coordinate system (Figure 4.5.2). The resulting positions of the linkages were then used to calculate a phase portrait for each linkage and the resulting CPRD for the two linkages, which are in the DIONYSOS model's coordinate system (Figure 4.5.2). The pendulum model's PPs and CPRDs for each cohort and each cohort's damping case were then compared to the actual cohort's mean PPs for the thigh and shank and the thigh-shank CRPD. All phase portraits and continuous relative phase diagrams for this experiment were normalized to swing period, which had 100 time epochs (e.g. points).

For each damping condition, the normalized root mean square error (NRMSE) of the residual between the angular displacement and angular velocity of the pendulum model's linkages and a cohort's thigh and shank angular displacement and angular velocity were calculated for each time epoch in Matlab. The summation of the NRMSE values for all curves were then calculated and used to rank the damping cases for each cohort. The damping condition with the smallest summed NRMSE for a cohort was deemed as the closest of the four damping conditions to that cohort's actual motion. In addition to ranking the damping conditions for each cohort, the cohorts were also ranked with respect to each other for the four damping conditions. To determine if there was a

significant difference between the rankings between cohorts and intra-cohort rankings, a Wilcoxon signed-rank test was performed.

4.4.4.2   Additional Investigations of the Pendulum Model

A nonlinear approach to solving the compound pendulum's differential equations and variable damping coefficients used a numerical solution at each percentage of swing period by calling the Matlab ode45 function, which applies the Runge-Kutta 4,5 solver. This additional investigation into the pendulum model was implemented to determine if the damping coefficient for each of the pendulum's linkages could be calculated for each percent of swing period instead of using a constant damping coefficient for the entire simulation.

A second linear approach to solving the compound pendulum's differential equations and variable damping coefficients used the analytic solution for $\dot{\theta}_{\text{proximal}}$ and $\dot{\theta}_{\text{distal}}$ by calling the Matlab function lsqcurvefit. This built in Matlab function enables the code to fit parameterized linear functions to data easily. This approach requires the parameterization of the pendulum's equations of motion. Unfortunately, it is not possible (refer to equations of motion in Appendix B) to parameterize the two equations of motion for these two variables because of the inherent coupling between the two linkages in a double pendulum.

4.5   Hypothesis Testing and Data Analysis

Table 4.10 lists the primary outcome measures for this descriptive research study and the aims and hypotheses to which they directly relate. Also, the source of the data and motion capture environment for these primary outcome measures is provided.

Table 4.5.1: Primary sagittal plane outcome measures, their corresponding aims and hypotheses, and motion capture (MoCap) environment (OG=over-ground, TM=treadmill) that provides the source data for these measures.

Primary Outcome Measure	Aims & Hypotheses	Source
PPs: Pelvis, Thigh, Shank, & Foot	Aim 1	
• Extrema	Aim 3, H3A, H3B, H3C	OG/TM MoCap
• Zero-crossings	Aim 4, H4A	
CRPD: Pelvis-Thigh, Thigh-Shank, Shank-Foot, & Thigh-Foot		
• Extrema	Aim 1	
• Zero-crossings	Aim 3, H3A, H3B, H3C	OG/TM MoCap
• Slopes	Aim 4, H4A	
• Inflection points		

Table 4.11 lists all the secondary outcome measures for this descriptive research and the corresponding aims and hypotheses. Additionally, the source of the data for these secondary outcome

measures is also provided.

Table 4.5.2: Secondary outcome measures, their corresponding aims and hypotheses, and source of the data for these measures (e.g. motion capture environment = MoCap).

Secondary Outcome Measure	Aims & Hypotheses	Data Source
Speed-Accuracy Task		
• % of successful target taps	Aim 2, H2A	OG MoCap
• advancing limb's forward speed		
SCALE Score	Aim 2, H2B	Exam room video
ICARS/SARA Score		
• Turn curvature	Aim 2, H2C	OG MoCap
• Base of support width		
Temporal-spatial Measures		
• Cadence	Aim 1	
• Walking speed	Aim 3, H3A, H3B, H3C	OG/TM MoCap
• Stride length, stride time, step time	Aim 4, H4A	
• Gait cycle phases, tasks, periods, events		
Sagittal plane kinematic curves	Aim 1	
• Pelvis, hip, knee, ankle	Aim 4, H4A	OG/TM MoCap
Angular displacement & angular velocity		
• Pendulum model's proximal linkage		
• Pendulum model's distal linkage	Aim 3, H3A, H3B, H3C	OG/TM MoCap
• Thigh segment		
• Shank segment		

4.5.1 Aim 1 Data Analysis Methods and Measures

The purpose of Aim 1 was to construct a normative reference for the other aims and demonstrate the proposed measures of coordination dynamics characterize an unimpaired gait pattern. Since the unimpaired retrospective subjects were barefoot and the prospective subjects wore shoes, two normative reference datasets were constructed from these two groups.

Mean sagittal PPs and ensemble CRPDs for the lower extremity segments were created from the two unimpaired cohorts using the methods described in Chapter 3 for the entire gait cycle. The coefficient of variance (CV) for each of the cohorts' segment PPs and CRPDs variables was calculated using the following equation (Winter, 1983).The CV was calculated to quantify the extent of variability for each of the coordination curves' variables with respect to the mean of these curves across all time in the ensemble average and is shown within each PP and CRPD.

Algorithm 4.1 Coefficient of variation (CV).

$$CV = \sqrt{\frac{\frac{1}{N}\sum_{i=1}^{N}\sigma_i^2}{\frac{1}{N}\sum_{i=1}^{N}|X_i|}}$$

The group's mean percent gait cycle for foot strike, opposite foot on, opposite foot off, and foot off were also calculated. The corresponding relative phase angle for each of these essential

footfall events was found and a 95% confidence interval (CI) for each relative phase angle value was calculated to provide an estimate of the normal limits for a population free of gait pathology.

4.5.2   Aim 2 Data Analysis Methods and Measures

The experiments associated with Aim 2 and its hypotheses are designed to explore the relationship between the proposed measures of coordination dynamics (e.g. PP, CRPD) and select clinical performance measures that characterize aspects of coordination. These are not direct analogues to the measures of the proposed coordination dynamics during gait and are instead used as descriptive performance measures.

Hypothesis 2A uses the voluntary reciprocal movements in a speed-accuracy task to characterize a subject's selective motor control in relation to any task specific coordination deficits. Two measures were calculated to test this hypothesis. First, to quantify a subject's ability to successfully tap a foot on the a target, the number of foot taps that were on a target was divided by the number of foot taps outside of a foot target and used as the percentage of hits (e.g. tapping accuracy). It was anticipated that subjects with an atypical gait pattern would have decreased target accuracy compared to the unimpaired subjects. Secondly, the speed of the swinging limb when it moved from the aft to forward target was calculated by the distance covered between foot taps and divided by the time it took the swinging leg to traverse that distance. A mean forward swinging limb speed for this task was calculated for each subject. This forward swinging limb speed was then compared to the mean swing limb advancement speed during the subject's representative over-ground walking trial. Since subjects with impaired swing limb advancement are known to have slower walking speeds, then it was anticipated that the speed of the swinging limb would be slower for individuals with a coordination deficit compared to the unimpaired subjects. The timing and magnitude of coordination events (minimum near foot of, zero crossing, inflection point, maximum instantaneous slope) from each prospective subject's thigh-shank and thigh-foot CRPDs were extracted since these events capture the dissociation of the extension synergy at foot off. Student's t-tests were calculated to test for significant differences between the mean accuracy and forward swing limb speed for the unimpaired prospective subjects' and prospective subjects with cerebral palsy.

Hypothesis 2B uses the SCALE assessment to characterize the degree of selective motor control impairments in a subject's lower extremities. As previously discussed, the SCALE score for each prospective subject's leg only included the hip, knee, and ankle joint tasks and thus resulted in a total possible limb score of 6. For retrospective subjects with an atypical gait pattern the SCALE score was calculated for each affected limb. For the unimpaired prospective subjects, although the left and

right limbs performed the SCALE tasks, only the right limb's score was used for analysis. Since curve features from CRPDs (e.g. extrema, slope, inflection point, zero crossing) capture various aspects of inter-segmental coordination, the CRPD curve features near foot off for the thigh-shank and thigh-foot CRPDs were examined in an exploratory analysis. The ability to dissociate the thigh-foot extension synergy at foot off during gait is an important motor control task to successfully achieve swing limb advancement. Since the SCALE score characterizes an individual's ability to voluntarily dissociate segments, then it was hypothesized that this same ability during walking should be captured by various curve features from CRPDs. The timing and magnitude of a CRPD extremum quantifies the dissociation of synergies between two segments. Therefore the timing and magnitude of the minimum near foot off on the thigh-shank and thigh-foot CRPDs were extracted from each prospective subject's affected side (right side only for unimpaired subjects). Additionally, the rate at which these segments dissociated from this minimum to the next local maximum (maximum instantaneous slope) was calculated. Lastly, the timing and magnitude of the inflection point and zero crossing that occurred from this minimum to the next local maximum were calculated for each subject. It was anticipated that the timing, magnitude, and slope of these curve features would follow a similar trend to a subject's SCALE score. T-tests were used to test if there was a significant difference between prospective cohorts' mean timing, magnitude, and slope for these coordination events. A t-test was also used to determine if there was a significant difference in the SCALE scores for the prospective unimpaired subjects and prospective subjects with cerebral palsy.

Hypothesis 2C uses gait tasks from the ICARS and SARA assessments to characterize a prospective subject's spatial accuracy during a movement and dynamic balance. While there are numerous methods for characterizing dynamic balance during gait, the following two measures were calculated for to test this hypothesis and characterize this aspect of gait. First, a Matlab special function was written to calculate the curvature for the 90° turns from a subject's center of mass trajectory with the following equation. A plane curve created by subject's center of mass (CoM) trajectory in $\Re 2$ space can be parametrically defined in Cartesian coordinates for each time epoch with the following equation.

Algorithm 4.2 Parametric equation for center of mass (CoM) two-dimensional trajectory.

$$r_{CoM}(t) = (CoM_x(t), CoM_y(t))$$

The curvature ($\varkappa$) of this transverse plane CoM curve (e.g. trajectory) was then calculated with the first and second derivatives of the CoM x and y trajectory using the following equation.

Algorithm 4.3 Curvature for two-dimensional parametric curve.

$$\varkappa = \frac{|\dot{x}\ddot{y} - \dot{y}\ddot{x}|}{(\dot{x}^2 + \dot{y}^2)^{3/2}}$$

Along with joint centers, the center of mass trajectory is automatically calculated in Vicon's Plug-In-Gait motion capture full body model. The transverse plane trajectory coordinates (zeroed height) for this virtual marker were used to calculate a subject's curvature during each of the 90° turning tasks. A mean curvature was calculated for all turns associated with a subject's affected sides or in the case of unimpaired subjects, the right side only. It was anticipated that a larger curvature would corresponded to an increased dynamic balance impairment because subjects. A correlation matrix was calculated using each prospective subject's mean left and mean right curvature and mean cadence, mean stride length, and mean walking speed from the subject's representative over-ground walking trial.

Secondly, a custom Matlab function was written to calculate the mean base of support (BoS) for each subject's over-ground walking trials and tandem walking trial(s). Other research studies have reported the base of support as a measure of dynamic balance during walking and the trend that a larger base of support corresponds to increased difficulty with dynamic balance and thus acts as a compensatory mechanism to provide more stability. Therefore it was anticipated that the study's subjects with an atypical gait pattern would have a larger base of support than the subjects free of gait pathology. The following figure illustrates the definition of base of support width used for this analysis.
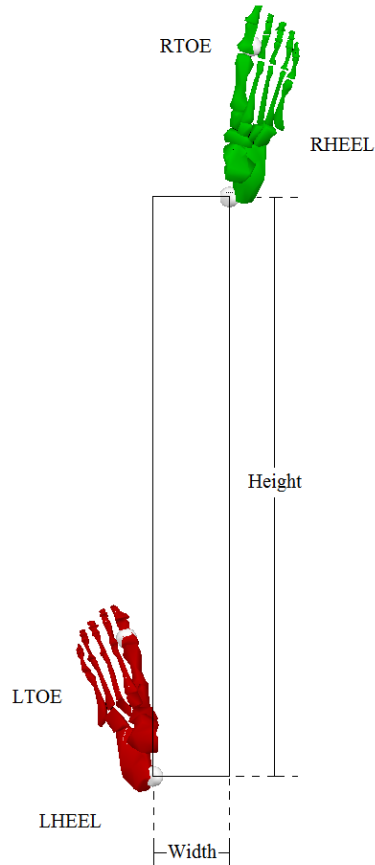
Figure 4.5.1: Definition of the base of support width during double limb support.

The width of the base of support was calculated for each instance of double limb support during a subject's representative over-ground walking trial. Double limb support is defined as the instance in the gait cycle when both feet are in contact with the ground. The transverse plane heel marker locations during the onset of each double limb support were used to create the base of support rectangle (shown above in Figure 4.5.1). The mean width of this rectangular base of support was calculated for each subject. A cohort mean base of support width was calculated for the prospective and retrospective subjects with cerebral palsy, free of gait impairment, and all retrospective subjects with a lower limb amputation. T-tests were calculated to test for significant differences between the cohorts's mean base of support width. As a reference to the tandem walking task BoS calculations, the BoS was calculated for each prospective and retrospective subject's representative over-ground walking trial.

4.5.3   Aim 3 Data Analysis Methods and Measures

The purpose of Aim 3 and its corresponding hypotheses is to compare the motion of a compound pendulum to the motion of the thigh and shank for various gait patterns during the swing period of gait. The measures of coordination dynamics used in this investigation were derived with respect to the global coordinate system of the motion capture environment and are calculated with respect to the horizontal (DIONYSOS). The software pendulum model was defined with respect to the vertical of a two dimensional coordinate system (PEGASUS). The differences in these two models and their outcome measures are depicted in following figure.
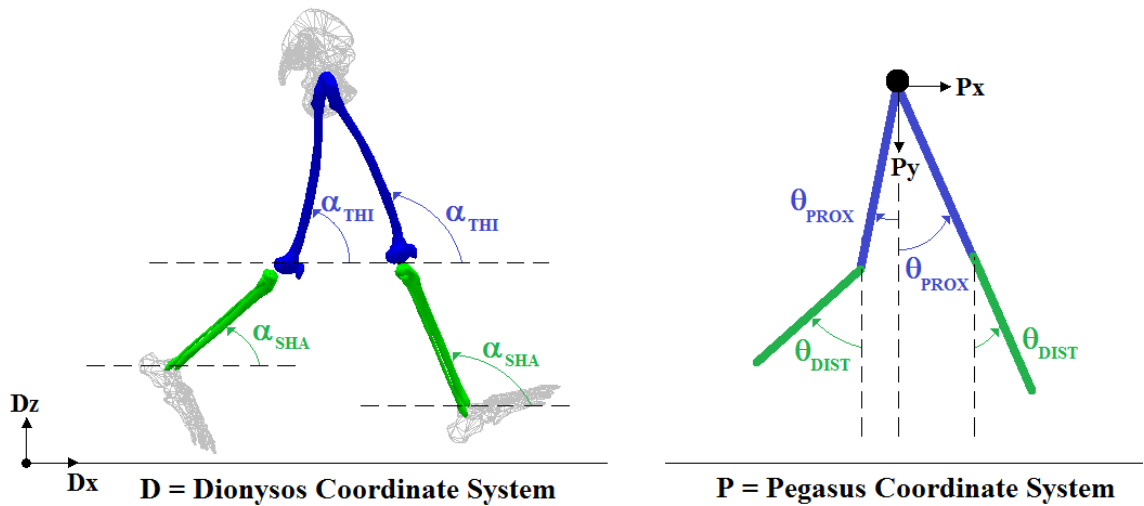
Figure 4.5.2: Comparison of coordination systems for nonlinear measures (left) and pendulum model (right).

A special function was written in Matlab to convert between the coordinate systems so the phase portraits and continuous relative phase diagram of the double pendulum could be compared to the cohort's coordination measures. However, after generating these PPs and CRPDs from the pendulum model for the different ensemble cohort based initial conditions and damping conditions, it was realized that because the pendulum's pivot (i.e. virtual pelvis) was stationary and did not oscillate like an actual subject walking the magnitude of these PPs and CPRDs would not be the same as the human motion capture data. Therefore, the angular displacement and angular velocity of the cohort's thigh and shank segments for the entire duration of swing period were calculated using the PEGASUS coordinate system convention. This provided a means to compare the two models (e.g. subject based and theoretical pendulum) and did not require additional scaling or coordinate system transformations.

The root mean square error (RMSE) between the theoretical pendulum linkages' motions and the actual subject ensemble cohort motions was calculated. Since this analysis' output variables (e.g. angular displacement and angular velocity) have different units, the RMSE was normalized to the mean of the cohort's variable. The following equation for the normalized RMSE is also commonly known as the coefficient of variation of the RMSE. For this application of NRMSE, the number of time epochs in swing period (n) was 100, the predicted values (y_{PEND}) were the pendulum model's angular displacement or angular velocity of both linkages in PEGASUS coordinates, and the reference values (y_{SUBJ}) from a cohort's actual mean angular displacement or angular velocity of the thigh and shank during the swing period of gait. As previously discussed, the NRMSE was calculated for each damping condition (ξ) for each subject cohort comparison.

Algorithm 4.4 Normalized root mean square error (NRMSE)

$$NRMSE_d = \frac{(1/n)\sqrt{(y_{PEND}-y_{SUBJ})^2}}{\bar{y}_{SUBJ}}$$

The sum of the four output variables from each pendulum versus cohort simulation was calculated and then used to rank the damping conditions within each cohort and amongst the cohorts (Figure 4.5.3).
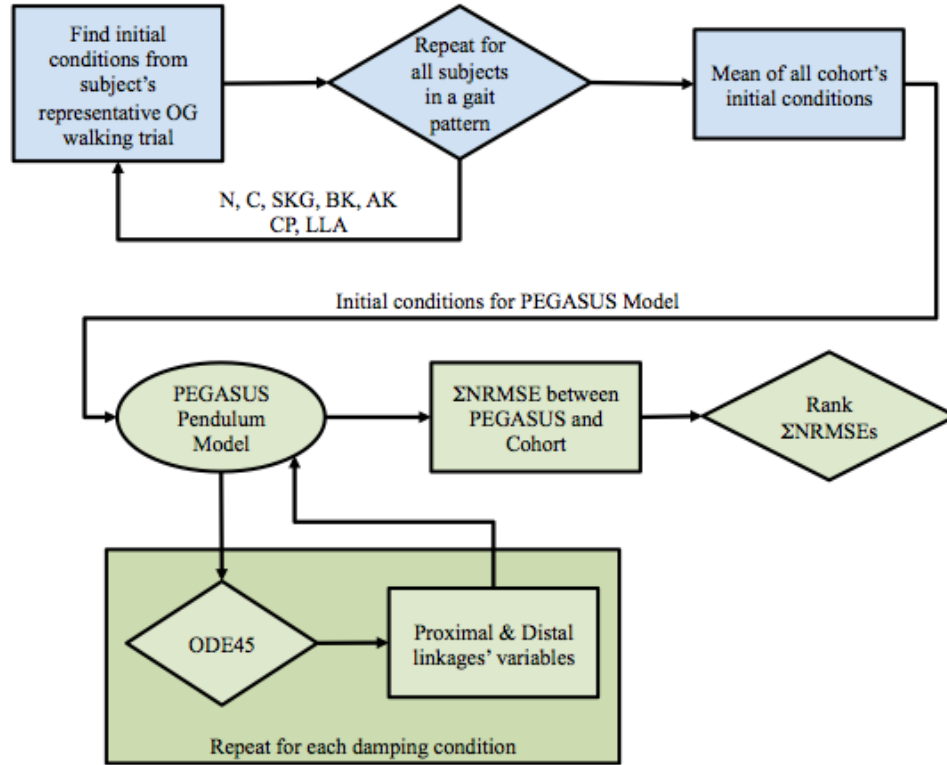
Figure 4.5.3: Flowchart of theoretical pendulum model to a gait pattern cohort's actual thigh and shank segment motions during the swing period of gait.

The ranking of the summed NRMSE variables for each cohort's damping condition was used to test hypotheses for this aim. A Wilcoxon signed-rank test was run on the rankings for each damping condition to determine assess whether the cohort's ranks were statistically different from each other.

4.5.4   Aim 4 Data Analysis Methods and Measures

The purpose of Aim 4 and its hypothesis was to demonstrate the proposed measures of coordination dynamics are able to distinguish between different gait pathologies and patterns associated with altered limb advancement during the swing period of gait. However, since there is currently not a gold standard measure for coordination dynamics nor is there a variable that encompasses these eight coordination curves it was determined that a metric that satisfies this need must be created. Additionally, due to the number of curves for each cohort, variables characterizing a curve, and the number of subject groups that the number of t-tests would increase the chances of a hypothesis being significant (type II error) when it actually is false. Two different approaches were taken to generate an index of coordination dynamics so that the various subject groups could be compared and test this aim's hypothesis: the gait patterns studied in this body of work are distinguishable with

the nonlinear dynamic systems theory based measures (e.g. PPs, CRPDs). The two coordination indices were calculated for all subjects and prospective experimental walking tasks. Comparisons between the two indices were performed using paired t-tests. The results from these t-tests and the additional analyses for regression model based index were used to test this aim's hypothesis. In regards to satisfying the objective of Aim 4 and testing its hypothesis, the two novel coordination indices were used to show how each gait pathology considered in this study is different from the unimpaired cohort, as well as how the various cohorts are different from each other.

4.5.4.1 Coordination Deviation Index (CDI)

Application of the gait deviation index (GDI) is continuing to grow in instrumented gait analysis as a measure of how close a subject's joint angles are to a normative reference [103]. Since the GDI quantifies changes in an overall joint angle pattern, it is a valuable metric especially when considering the hypothesis that one behavioral goal of ambulation is to maintain joint angle patterns [137]. In order to quantify how changes in segment positions and timings contribute to a gait pattern, another level of analysis for marker-based data that characterizes the underlying coordination dynamics and enriches existing gait pattern descriptors was incorporated. Employing the GDI methodology, a coordination deviation index (CDI) was created that uses sagittal plane phase portraits and continuous relative phase diagrams instead of joint angles. This portion of the analysis used the CDI to examine the coordination dynamics in the two clinical cohorts with distinct gait impairments affecting their ability to successfully complete swing limb advancement with reference to a group of healthy subjects free of gait pathology (N). In addition to the unimpaired subjects, CDI scores were generated for subjects with spastic cerebral palsy (CP) with either the hemiplegic (H) or diplegic (D) distribution and either stiff knee gait (SKG) or crouch (C) gait pattern, and lower limb amputees (LLA) with an amputation either above (AK) or below (BK) the knee Table 4.12.

Table 4.5.3: Subject classification for coordination deviation index analysis.

Population	Designation
Unimpaired	N
Cerebral Palsy	CP
Hemiplegia	H
Diplegia	D
Stiff Knee Gait	SKG
Crouch Gait	C
Lower Limb Amputation	LLA
Below Knee Amputation	BK
Above Knee Amputation	AK

The overall objective of this sub-investigation was to explore the applicability of the CDI in describing gait pathology. The specific objectives of this analysis were to 1) generate a coordination deviation index using the GDI methodology for these groups, 2) compare CDI scores of the groups using the GDI as a benchmark to describe varying degrees of gait performance in these distinct groups, and 3) demonstrate that the magnitude of coordination impairment (CDI) corresponds to the magnitude of joint angle impairment (GDI).

Creating an index from PPs and CRPDs, which describes movement at the level of coordination, provides clinicians and researchers with a metric that may be more meaningful and appropriate when studying a gait pattern's underlying coordination dynamics. Additional insights provided by the CDI complements the GDI by elucidating underlying individual segment positions and timing that contributes to a gait pattern. For example, inter-segmental coordination describes selective motor control impairments in individuals with CP and quantifies coordination strategies that are adopted and reorganization of segments by individuals with a LLA as a result of the inertial consequences due to an amputation and wearing a prosthetic.

A custom Matlab program was written to reproduce the calculations of the GDI detailed in the article by Schwartz et al., 2008. The accompanying normative gait features reference from this article was used for each subject's GDI calculation. A GDI was calculated for each affected leg in the subjects with CP or a LLA and only the right leg was used for each unimpaired subject. Additional staff at CGMA and a co-author of the original article that presented this methodology validated this GDI Matlab program. An explanation of the methodology for this feature based analysis, originally provided by Schwartz et al., 2008, that uses the coordination dynamics measures instead of the GDI's kinematic curves from all three planes of motion is provided in the following paragraphs and Appendix E.

Although displayed as a two-dimensional curve, the segment PPs were separated into two curves, one for angular displacement and the other for angular velocity. Thus each subject's coordination dynamics vector was constructed from eight phase portrait curves and four CRPD curves. Sagittal plane PPs (pelvis, thigh, shank, foot) and CRPD (pelvis-thigh, thigh-shank, shank-foot, thigh-foot) were calculated in 2% increments throughout the entire gait cycle and form the coordination dynamics vector for each subject. One coordination dynamics vector contains twelve curves that are sampled at 51 points and thus create a vector of length 612. The complete process and equations used to construct the normative control features and a subject's CDI are located in Appendix E.

Theoretically, an individual without any deviations from the normative reference would have a perfect CDI score of 100. Every 10-point increment below the theoretical perfect score corresponds to

an increasing number standard deviations away from the normative reference. Therefore, a subject's CDI value can be interpreted as follows:

- CDI ≥ 100 indicates the subject's (sagittal plane) coordination dynamics is at least as close to the unimpaired average as that of a randomly selected unimpaired subject. A CDI greater than or equal to 100 indicates the absence of (sagittal) coordination pathology.

- Every 10 points the CDI falls below 100 corresponds to one standard deviation away from the unimpaired mean. For example, a subject with a CDI of 75 means the coordination dynamics of that subject (s) is 2.5 standard deviations away from the unimpaired mean.

A CDI score was calculated for all prospective and retrospective subjects affected side (right leg only for unimpaired subjects) and like the subjects' GDI scores represents the coordination dynamics for the entire duration of the gait cycle (e.g. stance and swing). The groups' mean CDI and GDI scores were then compared using paired t-tests to determine if there were significant differences between the subject classifications.

While the manifestation of motor disorders in individuals with cerebral palsy is complex and uniquely expressed, there are common gait patterns [69] used to describe this group's inability to achieve various spatial and temporal aspects of gait (e.g. gait events and tasks [26,143], decreased step length and walking speed [26,29,143]). Motor deficits in individuals with a lower limb amputation, while from a different etiology than CP, are similarly expressed in visually recognizable gait patterns [78,82,98]. Due to the lack of neurological control below the level of amputation, these subjects also struggle to achieve critical gait events [78,82]. Molloy et al., 2010 evaluated the relationship of the GDI and gross motor function by using the Gross Motor Function Classification System (GMFCS) and demonstrated the GDI distinguishes between different GMFCS levels in individuals with CP. To evaluate the CDI's ability to stratify gait pathology related to coordination, we also analyzed the relationship between the GMFCS levels for individuals with CP. Since increasing amputation level for individuals with a LLA has been shown to decrease functional gait abilities [82], the CDI's ability to detect differences in coordination due to amputation level was also examined. Therefore, a one-way analysis of variance (ANOVA) test was performed on the cohort's mean CDIs, GDIs, and GMFCS levels (for subjects with CP). Matlab's built-in Kolmogorov-Smirnov function was use to verify the assumption of normality in the GDI and CDI values for all unimpaired subjects.

4.5.4.2 Coordination Performance Score (CPS)

Employing a similar methodology to the gait performance score presented by Baker et al, 2008, statistically significant curve features from PPs and CRPDs were identified and used to create a second index: the coordination performance score (CPS). Additionally, these significant coordination events were used to create two nominal regression models capable of distinguishing between unimpaired and impaired gait patterns for individuals with cerebral palsy.

The gait performance score (GPS) uses an alternative interpretation of the Euclidean difference measures from the GDI methodology and creates an un-scaled index from nine kinematic curve features (e.g. maximum sagittal knee flexion) that have been found to significant measures of gait pathology in numerous gait studies [138]. Following this logic, a coordination performance score (CPS) was then calculated with a custom Matlab program for each subject's affected limb (right only for unimpaired subjects). No statistical analysis was presented by Baker et al., 2008, in regards to the statistical significance for selecting the nine kinematic curve features used to create the GPS. Since a major objective of this dissertation is to establish a normative reference (Aim 1) and find meaningful measures from this model of coordination dynamics, then determining if essential or critical coordination events exist is a logical analysis. Two different precursory analyses were performed on swing period coordination events from the sagittal plane PPs (pelvis, thigh, shank, foot) and CRPDs (pelvis-thigh, thigh-shank, shank-foot, thigh-foot) to determine which (if any) coordination events were statistically significant and thus justify their inclusion in the calculation of the coordination performance score.

Perry's critical and temporal gait events have been used to delineate the essential phases, tasks, and joint motions of the gait cycle necessary to achieve a normal gait pattern and provide a framework for conventional instrumented gait analysis measures [26,137]. As Perry's gait events provide a framework for conventional instrumented gait analysis measures, the existence of essential coordination events from the cohort's mean normal gait pattern can serve as an initial normative reference for important curve features and framework for clinical and research applications using PPs and CRPDs in addition to serving as a means to create a coordination dynamics index. By identifying critical coordination events during the swing period of gait for a large cohort of unimpaired subjects, these methods provide a means to enhance the understanding of various motor control strategies employed in the swing period gait. Also, extracting specific curve features from these nonlinear curves to identify coordination events demonstrates the clinical utility of these measures as a complement to conventional instrumented gait analysis measures.

The following two sections describe two different methodological approaches to identifying critical coordination events on phase portraits and continuous relative phase diagrams during the swing period of gait. Using critical coordination events to construct a consolidated index of an individual's PPs and CRPDs offers 1) a quantitative means to satisfy Aim 4 and test its hypothesis, 2) show how each gait pathology considered in this study is different from the unimpaired cohort, and 3) a metric that can be used to characterize how the coordination dynamics of the various subject cohorts are different from each other.

First Approach to Identify Critical Coordination Events. The first approach to identifying critical coordination events began with generating the sagittal plane PPs (pelvis, thigh, shank, foot) and CRPDs (pelvis-thigh, thigh-shank, shank-foot, thigh-foot) for each unimpaired prospective and retrospective subject. Then three categories of curve features were chosen as coordination events in swing: extremum, zero-crossing, and inflection point. The built-in Matlab functions for identifying the maximum and minimum of a variable were used to identify the percent gait cycle of each extremum. Another custom Matlab function calculated zero-crossings of CRPDs and inflection points on CRPDs as the instant when the curve's derivative equals zero. In cases when a zero crossing did not fall exactly on a sampled percent gait cycle, the function selected the previous closest percent gait cycle as the instance of the zero-crossing. The percent gait cycle at which these three curve features occurred on each subject's set of coordination dynamics curves was found. Of the forty-four possible coordination events, thirty-seven were found to always exist in the unimpaired cohort's coordination curves. These thirty-seven coordination events were used for the remainder of this analysis.

The question of whether any of these thirty-seven coordination events (CE) were independent and invariant for an unimpaired walking pattern for various demographics/anthropometrics was then posed. To determine if any of the CEs were independent and invariant for an unimpaired walking pattern, the cohort was sorted into the following demographic categories for each gender individually and both genders combined: age (2year increments), weight (10kg increments), and leg length (50mm increments). For each of these nine demographic categories, the r-square value and corresponding Pearson correlation coefficient (ρ) were calculated for the percent gait cycle when each of the thirty-seven coordination events occurred. The r-square and ρ values for comparing each demographic and anthropomorphic category to a coordination event was calculated using the corresponding MiniTab functions. A coordination event was deemed "critical" if the percent gait cycle at which it occurred was invariant if $r^2 \leq 2.5\%$ and independent if the Pearson correlation coefficient threshold of was equal to or less than 0.2 for all of these demographic/anthropomorphic

categories.

Subsequent analyses were then performed on this data set to investigate the potential influences of barefoot versus shod walking on the initial results. The barefoot over-ground walking trials (e.g. retrospective normative subjects) and the shoe over-ground walking trials (e.g. prospective normative subjects) were separated into two cohorts and this analysis was repeated for these two subgroups. Next, confidence intervals for the critical coordination events from these two normative cohorts were calculated to determine if age had an affect on the timing of these coordination events. The third subsequent analysis, the means and standard deviations of the timing for these critical coordination events and the timing of critical gait and temporal events were calculated and compared to determine if any coordination events occurred at the same time as conventional gait events.

After examining the sagittal plane coordination dynamics curves for the various subject cohorts, it is qualitatively clear there are essential curve features present in different gait patterns. A second approach to identifying significant coordination events was performed and formed the basis for the second coordination dynamics index. Additionally, this second approach is appealing because it captures the number of measures represented in these low dimensional PPs and CRPDs and it accounts for both the timing and magnitudes of points on these curves. The first approach to identifying critical coordination events only accounts for the timing of the points in the PP and CRPD curves.

Second Approach to Identify Critical Coordination Events. The second approach to finding the potential existence of critical coordination events used two sets of regression models: 1) a stepwise backward regression was used to determine if a subset of coordination events could distinguish between pathological and pathology free gait and 2) a nominal regression model to determine if this subset of coordination events could distinguish between different gait patterns. This second approach defined the same three types of coordination dynamics curve features (extrema, zero crossings, and inflection points) as coordination events. Thirty-seven coordination events were found in the swing period of the sagittal plane PPs and CRPDs of all unimpaired subjects. The timing and magnitude for each of these thirty-seven coordination events were extracted from all prospective and retrospective subjects. One dataset was created for the timing of these coordination events and a second was created for the magnitude of theses coordination events. A backward stepwise regression in JMP was run on each dataset with the following parameters to determine if any of these events were statistically significant ($p \leq 0.05$) in distinguishing whether a subject's gait pattern was unimpaired or atypical. The following table lists the variables used in this backward stepwise regression.

Table 4.5.4: Variables used to create the backward stepwise regression models.

Model Variable	Type	Description
Gait Pathology	Dependent	0=No, 1=Yes
Gender	Control	F=female, M=male
Leg Length	Control	Value (mm)
Weight	Control	Value (kg)
Coordination Events	Independent	Timing (%GC) or Magnitude

The remaining coordination events from each stepwise regression model (timing, magnitude) that were statistically significant were then used to create a nominal regression model. The nominal regression model from these significant coordination events was created to determine if this model could be used to distinguish between different gait patterns. The following table provides the parameters used to create the nominal regression models.

Table 4.5.5: Variables used to create the nominal regression models.

Model Variable	Type	Description
Gait Pattern	Dependent	0=N, 1=SKG, 3=C, 4=BK, 5=AK
Gender	Control	F=female, M=male
Leg Length	Control	Value (mm)
Weight	Control	Value (kg)
Significant Coordination Events ($p \leq 0.05$)	Independent	Timing (%GC) or Magnitude

This process of generating a regression model was conducted for a third time to determine if all of the significant coordination events (both timing and magnitude) from the previous two stepwise regression models were necessary to accurately predict the presence of gait pathology and distinguish different gait patterns. The resulting nine significant combined coordination events that were statistically significant ($p \leq 0.05$) were then used to create a third nominal regression model, which was used to determine how well these coordination events were able to distinguish between different gait patterns. For clarity of this methodology, Figure 4.5.4 provides a flow chart depicting all the regression models created for this portion of the CPS analysis. The nine coordination events were then used as the variables for the CPS.
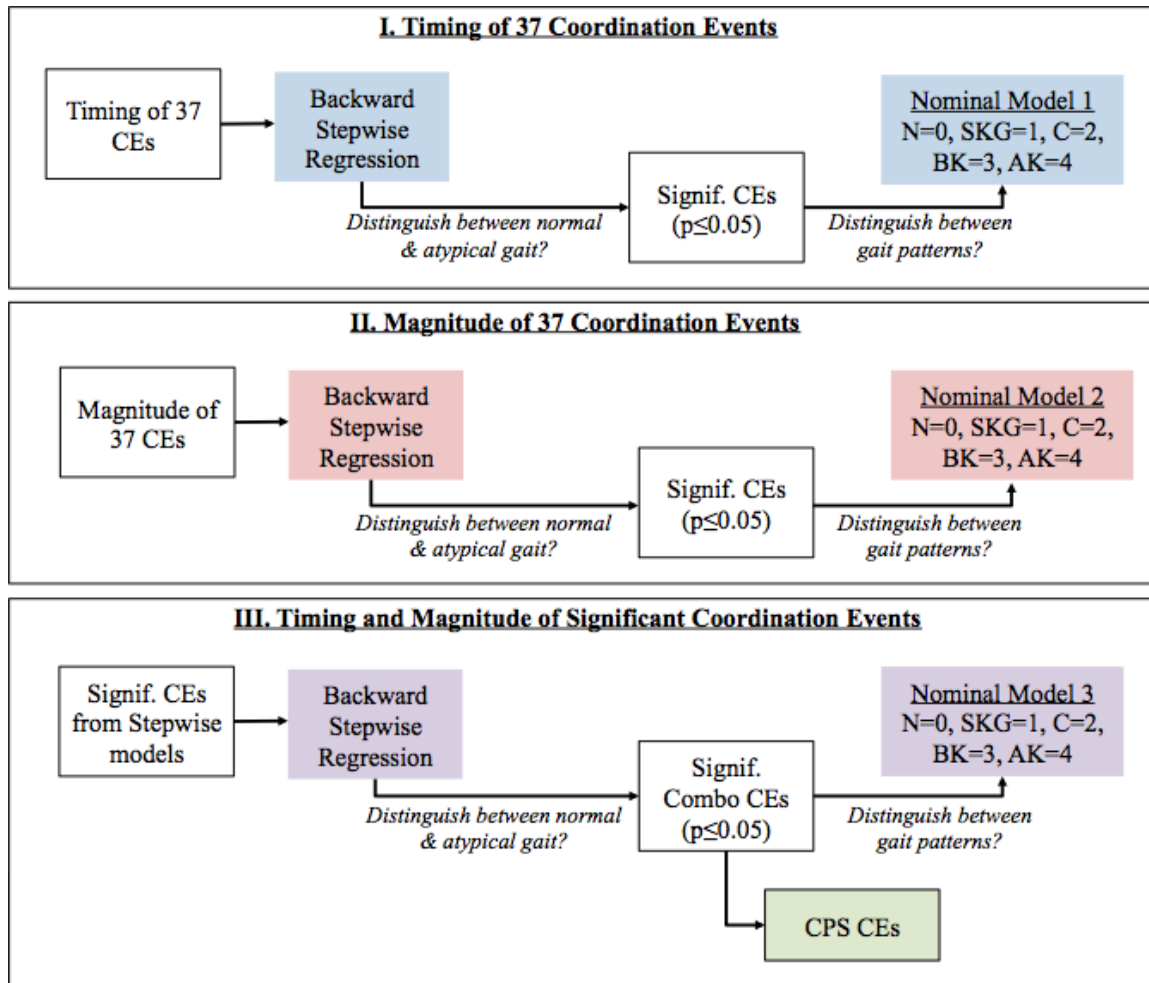
Figure 4.5.4: Flow chart of process using regression models to identify significant swing period coordination events.

Unlike conventional IGA measures, there has not been an investigation to determine which coordination curve features are significant during gait. Therefore, we first defined a coordination event (CE) as one of the three following categories of curve features: extremum, zero-crossing, or inflection point. Built-in and custom Matlab functions were used to identify the percent gait cycle and magnitude of all possible swing period CEs on the sagittal plane PPs and CRPDs, yielding thirty-seven CEs total. Using JMP software, a backward stepwise regression models was created using the timing and magnitude of these CEs as the model's independent variables. The subjects' age, gender, leg length, and weight were provided as control variables for this regression model. The presence of gait pathology was used as the model's nominal predictor by designating each unimpaired subject as typical and each subject with CP as atypical. The minimum p-value (probability to leave) of 0.05 was set as the threshold for which a CE was removed from the model during a backward

step. Nine significant CEs were identified using this stepwise regression model.

The variance inflation factor (VIF) and tolerance for these nine significant CEs were calculated in SAS 9.4 to determine the potential presence of multicollinearity between these CEs. A CE with a tolerance less than 0.4 and/or a VIF greater than 2.5 was deemed as indicative of multicollinearity. The unimpaired cohort's mean timing of all nine CEs was calculated and used to determine if any of the CEs occurred at the same time in swing. Of the CEs with VIF and tolerance values above the given thresholds, three were found to occur at the same time as other CEs in the set of nine significant CEs. These three CEs were removed and the VIF and tolerance were recalculated to ensure there was no multicollinearity associated with the parameter estimates of the remaining six CEs.

Calculation of the Coordination Performance Score. The following procedures were adapted from the article by Baker et al, 2008 using the final six significant CEs. The GDI is fundamentally based on the root mean square (RMS) difference between the coordination dynamics vector and the average coordination dynamics vector for individuals free of gait pathology. The Euclidean distance (e.g. difference) between a coordination event of any subject (CE^S) and the mean normative reference coordination event (CE^N) can be calculated with the following equation, using similar notation from the CDI section.

Algorithm 4.5 Difference of coordination event between subject (s) and mean normative reference (N).

$$\Delta CE^{s,N} = CE^s - \bar{CE}^N$$

This difference can be used to calculate a similar quantity for a single coordination dynamics variable rather than the entire coordination dynamics vector. The average root mean square of all the coordination value scores (CVS) for a particular side equal the CPS calculated from a the entire coordination vector using each of the significant coordination events (n_{CE}).

Algorithm 4.6 Equation for a subject's Coordination Performance Score (CPS).

$$CPS_s = \sqrt{\frac{1}{n_{CE}}(CVS^2_{CE1} + CVS^2_{CE2} + \ldots + CVS^2_{CEn})}$$

The CPS was calculated for each subject's affected side and the right side only for all unimpaired subjects. The mean and standard deviation for each subject cohort classifier (N, CP, LLA, SKG, C, H, D, BK, AK) was calculated. T-tests were used to test for statistical significance between the cohorts' mean CPS scores. Lastly, the CPS was subtracted from 100 for ease of comparison to the CDI and GDI subject scores and to display these scores in the same scale.

Algorithm 4.7 Scaled coordination performance score (*CPS).

$$CPS^* = 100 - \text{CPS}_s$$

It is important to note that this scaling of the CPS does not follow the same convention as the CDI and GDI, where every 10-point decrement away from 100 is equal to a standard deviation away from the normative mean. Instead the further a subject's scaled CPS score is from the maximum (100), then the further away the subject's coordination events are from the maximum. By scaling the CPS, the indices convention of "bigger is better" is maintained, as is the convention for the CDI and GDI scores.

Regression Models for Distinguishing Coordination of Different Gait Patterns. The first regression model determined which of the six significant CEs were necessary for distinguishing between an unimpaired and impaired gait pattern. A second regression model determined which of the six CEs events were necessary to distinguish between a stiff knee or crouch gait pattern. These two regression models offer an additional means to demonstrate how each gait pathological pattern considered in this study is different from the unimpaired cohort and these models can be used to characterize how the coordination dynamics of the various subject cohorts are different from each other (Aim 4). Unfortunately, due to the small sample size of limbs with an amputation (n=19), it was not possible to build a satisfactory regression model for distinguishing the gait patterns of either a below knee or above knee amputation. The first regression model was designed to distinguish between the presence or absence of gait pathology and the second model was designed distinguish between a stiff knee gait or crouch gait pattern.

To determine which of the six significant coordination events were necessary for the two regression models, the affects on the model for the addition of each coordination event was assessed and for all combinations. In order for a coordination event to be added to a model the following criteria had to have been meet. First, the addition of a CE must increase the significance related to the outcome of interest. Second, the addition of a CE must improve the area under the curve of the receiver operator characteristic curve. And third, the addition of a CE must not violate and errors (e.g. variance inflation factor, tolerance). The correlation matrix p-values of the six coordination events was used to rank the importance of the coordination events and ensure there wasn't any multicolinearity between coordination events. After assessing the inclusion of coordination events into each of the two regression models, the inclusion of nuisance (e.g. control) variables were used to assess if the addition of these variables improved the overall model. Leg length, age, weight, and gender of all subjects were used as nuisance variables.

The area under the curve (AUC) from the receiver-operator curves for the two nominal regression models (timing and magnitude of significant coordination events) was calculated in JMP and Statistical Analysis Software (SAS) along with the confusion matrix and confidence intervals. The leave-one-out method in SAS was used to create a randomly selected subset of the available 226 samples and compare the area under the curve (AUC) of the receiver operator characteristic (ROC) curve to the ROC of all the samples.

4.5.4.3 Curve Feature Trends by Gait Pattern

While visually examining the various cohorts' coordination curves generated for the different experiments and aims discussed above, there appeared to be trends in which certain gait patterns were missing certain PP and CRPD curve features. Similar to the visual use of kinematic curves to identify a particular gait pattern, it was postulated that certain curve features from PPs and CRPDs could be used to identify certain coordination impairments. Additionally, it was postulated that there might be trends in which common curve features (e.g. zero-crossing, inflection point, extremum) were missing for various atypical gait patterns. Portions of this dissertation has been presented at professional conferences and often members of the gait community have expressed a common reason for the hesitancy to adopting PPs and CRPDs is that these curves are unfamiliar and that the correlations between these nonlinear curves' features and a subject's gait pattern are unknown. Therefore, this secondary analysis, designed to address Aim 4, was conducted in an effort to resolve the unfamiliarity of these coordination measures and provide a primer for curve features for sagittal plane PPs and CRPDs in the following gait patterns: unimpaired, stiff knee gait, crouch, below knee amputation, and above knee amputation.

First, the timing and magnitude of every subject's thirty-seven swing period coordination events was manually checked to ensure the algorithms for detecting these events had sufficient criteria for identifying these events, even for the more extreme aberrant gait patterns. When the Matlab program did not detect a coordination event, this manual process of checking the timings and magnitudes of all coordination events also served as a means to confirm if an event truly did not exist for a particular subject. Once the timings and magnitudes of all thirty-seven swing period coordination events were confirmed for all prospective and retrospective subjects (n=265 legs), they were then coded as either present (1) or absent (0) and organized topographically (e.g. hemiplegia or diplegia for subjects with CP), by gait pattern (e.g. SKG or Crouch for subjects with CP), level of amputation (e.g. below knee, above knee), and by number of affected sides (e.g. unilateral or bilateral for subjects with a LLA). The percentage of subjects missing one or more coordination

events for each gait pattern category, including the unimpaired group, was then calculated. These percentages were used to determine if there was a trend for the subjects missing a coordination event(s) and their gait pattern or diagnosis. Next, the percentage of subjects in a gait category that were unable to achieve a missing coordination event was calculated. These percentages were used to determine if a gait pattern or diagnosis was associated with the inability to achieve specific coordination events.

4.6 Experimental Limitations Associated with Human Subjects

Recalling the overview presented in Chapter 2 of the subsystems involved with walking and complex physiological interactions required to perform this elegant motor task, it becomes apparent that instrumented gait analysis is currently unable to measure all of these elements. The use of human subjects provides more accurate data than models even more complex than the theoretical pendulum model created for this dissertation. Theoretical forward modeling programs are challenged even more when tasked with predicting the gait pattern of a subject with a complex and uniquely expressed neuromuscular impairment, such as cerebral palsy. Although many of the more advanced modeling programs are increasing the use of subject data from instrumented gait analysis to enhance their outcome measures, there are still significant limitations, often due to the simplifying assumptions, to these models. Thus the need for collecting human motion capture data remains valuable and second to none, especially for clinical decision making and patient care applications. While motion capture data for a subject is typically far more accurate than a model, there are still significant challenges associated with human subjects.

Numerous factors associated with using human subjects (e.g. endurance, strength, time) for prospective experiments affect the experimental protocol, duration, and variables that can be measured. Instrumented gait analysis requires a considerable amount of time for data capture and significantly even more time to process the motion capture data to the point where it can be used to generate measures of gait (e.g. kinematics, temporal-spatial, coordination). On average the prospective unimpaired subject protocol in this body of work required on 3 hours of a subject's time, from consent to completion of data capture. As it is hopefully clear from the discussion in Chapter 3, it is also not practical to measure all variables associated with walking or even the constitutive element of coordination, which itself is highly complex and contains numerous variables. The gait measures and proposed coordination measures selected in this body work describe the resulting behavior of numerous subsystems and are intended to describe the system of walking at a more macroscopic, sys-

tem level. However, future work may reveal promising findings when these measures of coordination are paired with more specific measures of human performance (e.g. surface electromyography).

Experimental limitations associated with human performance are further confounded in subjects with a gait impairment. As discussed in Chapter 2, due to the nature of cerebral palsy each subject presents different functional limitations and thus requires flexibility to be incorporated into the design of experiments. Often subjects' with impaired gait have diminished endurance and strength, thus placing a limit on the duration of an experiment and the subject's visit. The data capture duration for a prospective subject with a gait impairment lasted an average of two hours. Although the subjects were given breaks for rest whenever they needed, it is clear a motion capture visit longer than two hours would have significantly diminished the quality of motion capture data due to subject fatigue, both mentally and physically. Other experimental considerations must be taken for subjects with a gait impairment. For example, a subject with cerebral palsy may be able walk independently over-ground for at least 6 minutes, but that same subject may not be able to safely walk on a treadmill at the same speed or duration due to the nature of the neuromuscular impairment. Although an effort was made to anticipate limitations in a subject's ability to perform any of the prospective experiments, a few adaptive adjustments were made to the protocol so the subjects could perform the task. These adjustments are reflected in the previous sections. Most significantly, was the reduction of the treadmill belt speed for the prospective subjects with cerebral palsy. All the retrospective normative subjects walked barefoot over-ground. However, the prospective normative subjects walked with shoes for all motion capture trials because of the treadmill walking task. Additionally, having the prospective normative subjects walk with shoes made for a more consistent comparison to the prospective subjects with an atypical gait pattern because they also performed all motion capture tasks with shoes. Comparisons between the potential differences of barefoot and shod walking are detailed above and the results presented in Chapter 5.

The retrospective database consists of motion capture data from two different motion capture laboratories. The first and older lab was located at the Children's Hospital in Denver, Colorado prior to the hospital's relocation to the Fitzsimmons campus in 2008. The second set of retrospective subjects' motion capture data was collected at the new Children's Hospital campus in Aurora, Colorado. Only subjects with the same maker sets for both motion capture locations were included in the study. Most of the staff members who collected the retrospective normative subject dataset at both locations also helped train myself, who was the sole person responsible for all prospective subjects marker placement. The subject of marker placement and associated error is a topic of considerable debate in the motion capture community and numerous articles have been published

106

that investigate different marker sets, checks to validate placement, error correction algorithms, and marker placement protocols. The knowledge and experience gained from participating in such discussions and experiments at the Center for Gait and Movement Analysis laboratory prior to starting this dissertation was of significant benefit and influence to my marker placement training and protocol used in the prospective experiments. Great care was taken to ensure marker placement for each subject was as accurate as possible since all of the study's motion capture based variables are derived from marker trajectories. For example, clinical staff members with many more years of marker placement and gait analysis offered training in marker placement, demonstrated palpation techniques to correctly identify bony landmarks, and validation of marker placement (e.g. static trial marker placement) for several prospective subjects. In addition to these efforts, each prospective subject's static to dynamic trial transition was checked to ensure the thigh and shank rotation offsets were within acceptable limits and that there was no cross talk between the sagittal and coronal planes of motion at the knee joint.

5   Results

After approval to conduct this research was granted by the Colorado Medical Internal Review Board (COMIRB), prospective subject data capture occurred from July 2013 to November 2014. Identification and analysis of retrospective subject data was conducted in tandem with prospective subject data capture and analysis. This chapter reports the results from the prospective subject experiments, retrospective subject analyses, analyses combining prospective and retrospective subject cohorts, and the analyses for the four aims and their respective hypotheses.

5.1   Subject Demographics

Each prospective unimpaired subject's motion capture study was approximately 3 hours in duration, from consent/assent to completion of data capture. The study visit for prospective subject with an atypical gait pattern lasted an average of 2 hours, from consent/assent to completion of data capture. Table 5.1 provides the average time spent for each prospective subject's data capture, motion capture data processing, and Matlab processing necessary to generate PPs and CRPDs. These time estimates do not include the additional analyses in Matlab for testing the various aims and hypotheses or secondary investigations.

Table 5.1.1: Average times for prospective subject data capture and analysis.

Prospective Subject	Data Capture	Vicon Processing	Matlab Processing	Total
Unimpaired	3 hours	15 hours	2 hours	20 hours
Cerebral Palsy	2 hours	10 hours	1 hour	13 hours

While each retrospective subject did not require time for data capture, the motion capture trials captured from each retrospective subject's instrumented gait analysis was reprocessed to ensure the same motion capture marker set, motion capture model (e.g. Plug-in-Gait), gait events, and filtering methods were consistent with those used for all prospective subjects. Additionally, the diagnosis of each prospective subject was verified by examining and confirming consistency between the diagnosis listed in each clinical patient's instrumented gait analysis clinical report with the patient's diagnosis in his/her electronic medical records. Further visual confirmation of a retrospective subject's motion capture data was performed by examining each retrospective subject's multimedia instrumented gait analysis report (e.g. Vicon Polygon), which includes bi-planar video, kinematics, kinetics, temporal-spatial, and when applicable, dynamic surface electromyographic data. On average time spent identifying, confirming, and of processing motion capture data for retrospective subject with an atypical gait pattern was 3 hours.

As anyone familiar with prospective experiments with human subjects can attest, one of the challenges in this area of biomedical research is recruiting a large number of subjects who meet the study's inclusion criteria and are interest in participating in research. Numerous efforts were made to recruit prospective subjects with either spastic cerebral palsy or a lower limb amputation by applying new techniques and lessons learned from previous experience with recruiting prospective subjects. Potential prospective subjects were recruited by attending four cerebral palsy clinics and five lower limb amputee clinics at either the main campus of Children's Hospital Colorado or one of the satellite locations. Flyers were posted throughout the community, Fitzsimmons Medical Campus, Children's Hospital Colorado clinical areas, and on several electronic research sites/email listings. During this phase of subject recruitment, four individuals with a lower limb amputation were identified, but canceled their scheduled study visit due to recent development of musculoskeletal impairments (2 individuals) affecting their ability to walk, cardiovascular problems limiting endurance (1 individual), and personal scheduling conflicts (1 subject). There were several individuals with cerebral palsy who were interested in participating as a prospective subject but did not meet the study's inclusion criteria due to concomitant neurological disorders affecting gait (4 individuals), inability to ambulate independently without an assistive device (2 individuals), recent musculoskeletal surgery (1 individual), and orthopaedic injury affecting gait (1 individual). Additionally, one individual with cerebral palsy had to cancel a scheduled data capture visit due to increased pain that significantly affected his/her gait pattern and duration, which also prevented rescheduling of the data capture visit. The following three tables provide the general subject demographics of the three subject cohorts studied in this body of work: unimpaired, cerebral palsy, and lower limb amputation.

Table 5.1.2: Prospective and retrospective demographics for all subjects free of gait pathology, with mean (standard deviation) values reported.

UNIMPAIRED	Retrospective	Prospective
Males	56	9
Females	64	11
Age (yr)	21.03 (12.58)	25.95 (10.69)
Range (yr)	7 to 66	9 to 54
Leg Length (mm)	851.41 (94.26)	877.45 (80/25)
Weight (kg)	59.25 (19.49)	65.43 (17.34)
# Subjects	120	20
# Legs	120	20

Table 5.1.3: Prospective and Retrospective demographics for all subjects with cerebral palsy, with mean (standard deviation) values reported.

CEREBRAL PALSY	Retrospective	Prospective
Males	32	2
Females	23	2
Age (yr)	11.73 (4.89)	21.25 (13.94)
Range (yr)	7 to 66	7 to 36
Leg Length (mm)	716.28 (96.25)	735.83 (99.62)
Weight (kg)	33.21 (12.74)	50.73 (22.38)
# Subjects	55	4
# Legs	100	6
SKG (# Legs)	54	6
Crouch (# Legs)	46	0
Hemiplegic (# Subjects)	10	2
Diplegic (# Subjects)	45	2

Table 5.1.4: Retrospective demographics for all subjects with a lower limb amputation, with mean (standard deviation) values reported.

LOWER LIMB AMPUTATION	Retrospective
Males	9
Females	6
Age (yr)	17.33 (8.35)
Range (yr)	7 to 66
Leg Length (mm)	832.37 (147.74)
Weight (kg)	53.59 (24.31)
# Subjects	15
# Legs	19
Transtibial (# Legs)	9
Transfemoral (# Legs)	6
Unilateral (# Subjects)	11
Bilateral (# Subjects)	4

5.2   Prospective Experimental Results

While PP and CRPD are low-dimensional descriptors, since there are four PPs and four CPRDs for each experimental condition there is still a large amount of data associated wtih these measures and conditions. Therefore developing a means to reduce these measures of coordination and provide a simple metric to describe the deviation of a cohort or experimental condition from a reference becomes desirable. Developing a quantitative means of further consolidating the information in these curves was solved by created two indices based upon elements of these coordination curves. In addition to using these two coordination indices, the gait deviation index was also calculated for a comparison to a commonly used joint angle descriptor. The justification and analytical results from testing these new coordination indices is addressed in section 5.3.4 as part of the Aim 4 hypothesis testing. Although the focus of this body of work and prospective experiments is to examine changes in coordination dynamics for various subject groups and walking conditions, conventional swing

period temporal-spatial measures, temporal events, and critical events were also calculated for all subjects and provided for reference in Appendix G.

5.2.1 Prospective Subjects: Over-Ground Walking Task

To establish each prospective unimpaired subject's baseline gait for over-ground walking, each subject walked in the main motion capture laboratory while wearing a full body marker set. The mean phase portraits and ensemble continuous relative phase diagrams for this cohort are presented in Figure 5.2.1 with the retrospective unimpaired cohort's mean coordination curves.
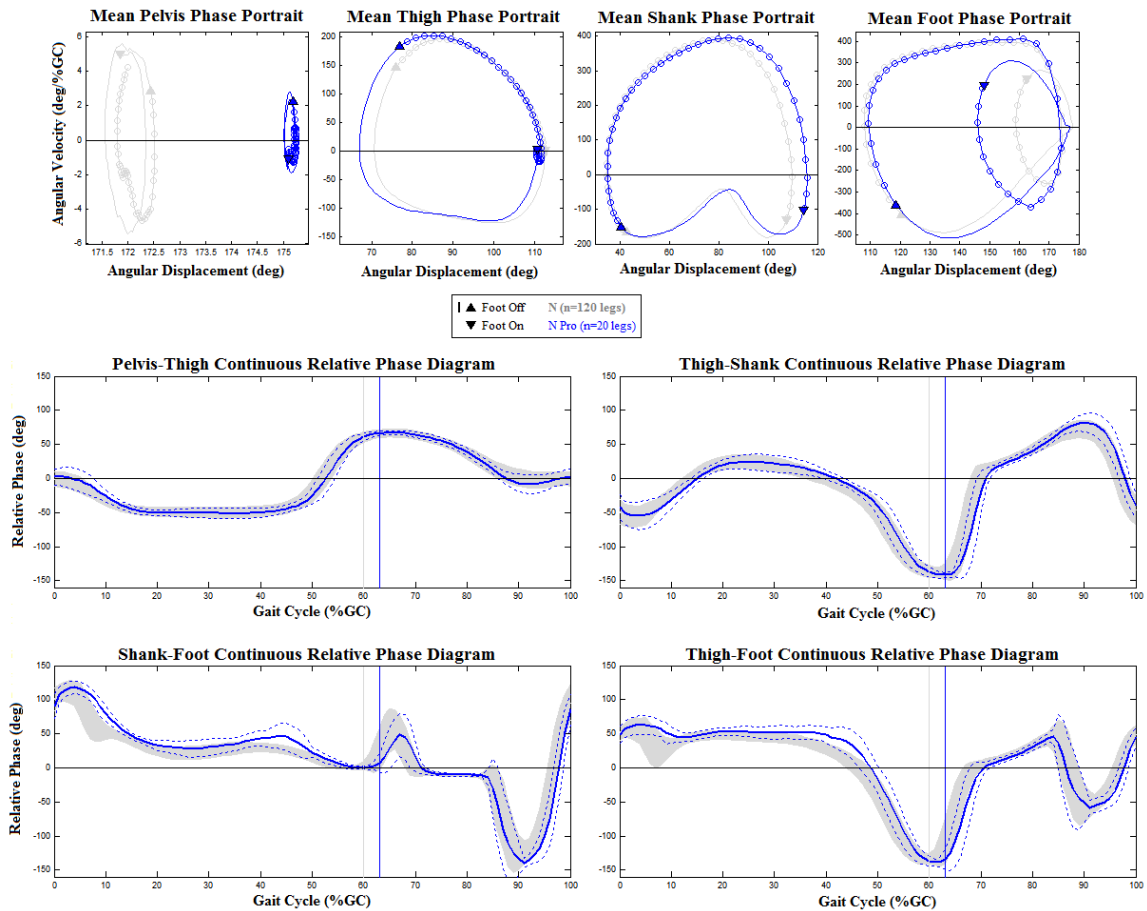
Figure 5.2.1: Unimpaired prospective subjects' (blue) mean phase portraits and ensemble continuous relative phase diagrams with the retrospective unimpaired cohort's mean coordination curves (grey).

In Appendix G, Table G1.1 provides the mean over-ground walking speed, mean step length, conventional temporal-spatial measures, and timing of critical and temporal gait events for the unimpaired subjects, subjects with cerebral palsy, and subjects with a lower limb amputation. The mean and standard deviations for the GDI, CDI, and scaled CPS values for each subject group were

calculated and listed in the table below.

Table 5.2.1: Mean and standard deviation values for the GDI, CDI, and scaled CPS of the unimpaired subjects, subjects with CP, and subjects with a lower limb amputation for over-ground walking.

Cohort	# Subjects	GDI	CDI	CPS*
N (Retro)	120	101.87 (8.38)	98.17 (8.48)	97.15 (1.25)
N (Pro)	20	92.67 (5.00)	92.37 (7.74)	97.08 (0.68)
CP (Pro)	4	75.95 (10.16)	84.25 (5.44)	87.557 (9.12)
CP (Retro)	55	70.43 (17.46)	84.73 (6.52)	82.56 (8.79)
LLA (Retro)	15	78.79 (12.68)	85.69 (7.21)	89.03 (5.86)

Table 5.2.2: The coefficient of variation (CV) and variance ration (VR) for the angular displacement (AD), angular velocity (AV) and continuous relative phase diagrams for all unimpaired retrospective (n=120) and prospective (n=20) subjects during over-ground walking.

Coordination Curve	CV		VR	
	Retro	Pro	Retro	Pro
Pelvis AD	2.7120	2.06	1.0047	1.05
Pelvis AV	365.5103	913.42	0.9220	1.03
Thigh AD	4.1143	3.63	0.0602	0.04
Thigh AV	31.7030	27.98	0.0626	0.05
Shank AD	5.4048	4.52	0.0308	0.02
Shank AV	26.1728	21.96	0.0440	0.03
Foot AD	4.0283	3.65	0.0783	0.07
Foot AV	55.8985	54.49	0.1504	0.14
Pelvis-Thigh CRPD	27.2504	25.64	0.0517	0.05
Thigh-Shank CRPD	36.0529	33.07	0.0730	0.06
Shank-Foot CRPD	50.5218	42.38	0.1388	0.10
Thigh-Foot CRPD	43.7863	38.27	0.1173	0.10

5.2.2 Prospective Subjects: Treadmill Walking Tasks

All unimpaired prospective subjects walked over-ground at a self-selected walking speed and then on the treadmill at slower and faster walking speeds (Vss). The next table provides the GDI, CDI, and scaled CPS for each condition's representative trial was used to calculate the cohort's mean and standard deviation index values. Marker dropout for one subject during the 80% Vss walking condition was unable to be filled and thus resulted in 19 subjects contributing to the index means.

Table 5.2.3: Mean and standard deviation values for the GDI, CDI, and scaled CPS of the unimpaired prospective cohort for various walking conditions.

Task	# Subjects	GDI	CDI	CPS*
Over-ground Walk	20	92.67 (5.00)	92.36 (7.74)	97.08 (0.68)
Treadmill 80% Vss	19	78.53 (8.07)	85.27 (5.98)	92.15 (1.31)
Treadmill 90% Vss	20	78.31 (7.67)	88.24 (6.67)	91.99 (0.61)
Treadmill 100% Vss	20	77.38 (8.44)	96.98 (12.17)	92.32 (0.58)
Treadmill 110% Vss	20	78.91 (9.23)	97.44 (9.44)	92.09 (0.71)
Treadmill 120% Vss	20	80.74 (9.02)	100.29 (9.76)	92.09 (0.61)

The sagittal plane PPs and CRPDs for the unimpaired prospective cohort's different treadmill walking conditions are provided in the figure below. A zoomed in view of the sagittal plane PPs and

CRPDs for the unimpaired prospective cohort's different treadmill walking conditions are provided in Appendix G.
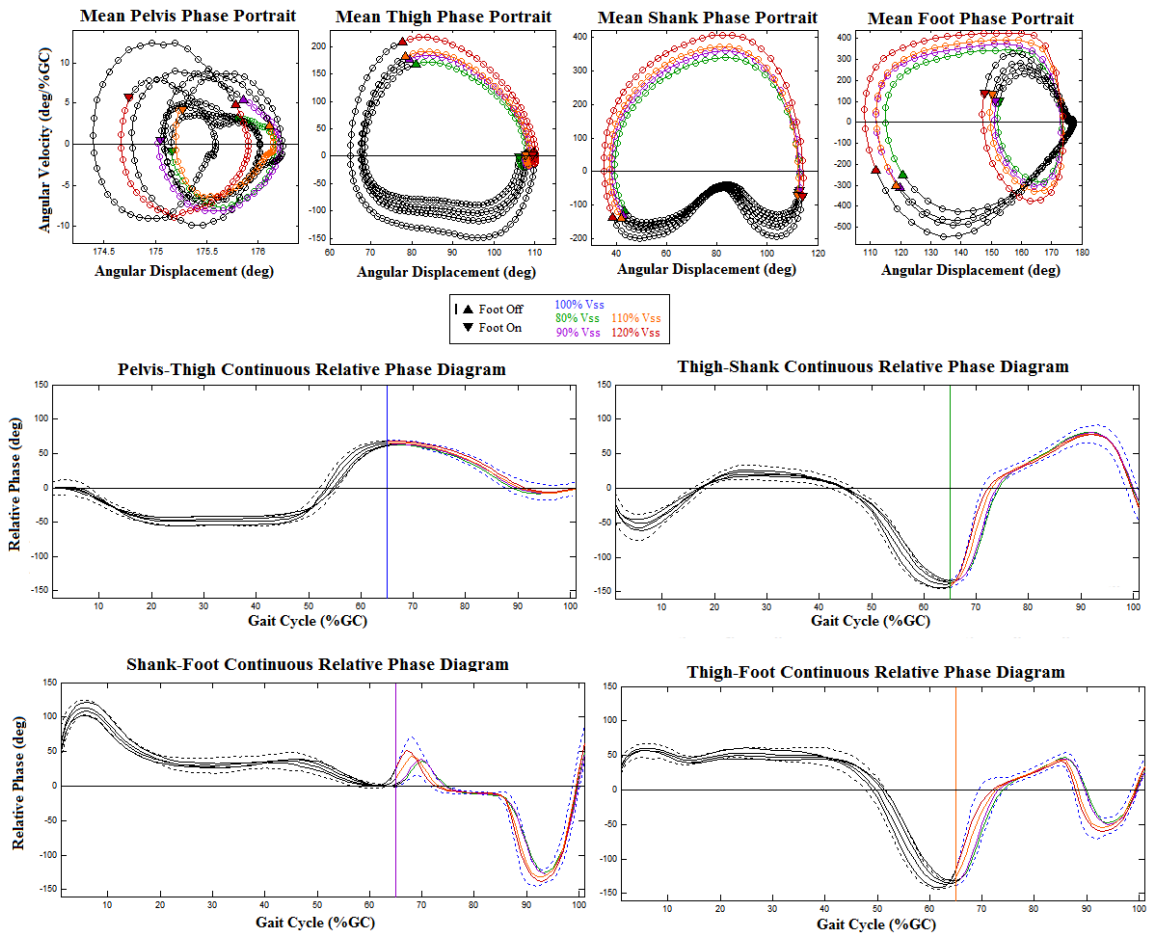
Figure 5.2.2: Phase portraits and continuous relative phase diagrams for treadmill walking conditions of the unimpaired prospective subjects (green=80%Vss, purple=90%Vss, blue=100%Vss, orange=110%Vss, red=120%Vss).

All prospective subjects with CP walked over-ground at a self-selected walking speed and then on the treadmill at as close to the over-ground walking speed (Vss) as possible. The table below provides the GDI, CDI, and scaled CPS for each condition's representative trial was used to calculate the cohort's mean and standard deviation index values.

Table 5.2.4: Mean and standard deviation values for the GDI, CDI, and scaled CPS of the prospective subjects with CP for over-ground and treadmill walking conditions.

Task	# Subjects	GDI	CDI	CPS*
Over-ground Walking	4	78.79 (12.68)	85.69 (7.21)	82.56 (8.79)
Treadmill Walking	3	65.10 (3.58)	82.74 (10.87)	88.41 (7.25)

The sagittal plane PPs and CRPDs for over-ground and treadmill walking conditions are provided

in following figure for the prospective subjects with cerebral palsy. The sagittal plane kinematics for the prospective subjects with CP for over-ground and treadmill walking conditions are provided in Appendix G. Additionally, a table of conventional instrumented gait analysis measures for the subjects with CP is provided in Appendix G.
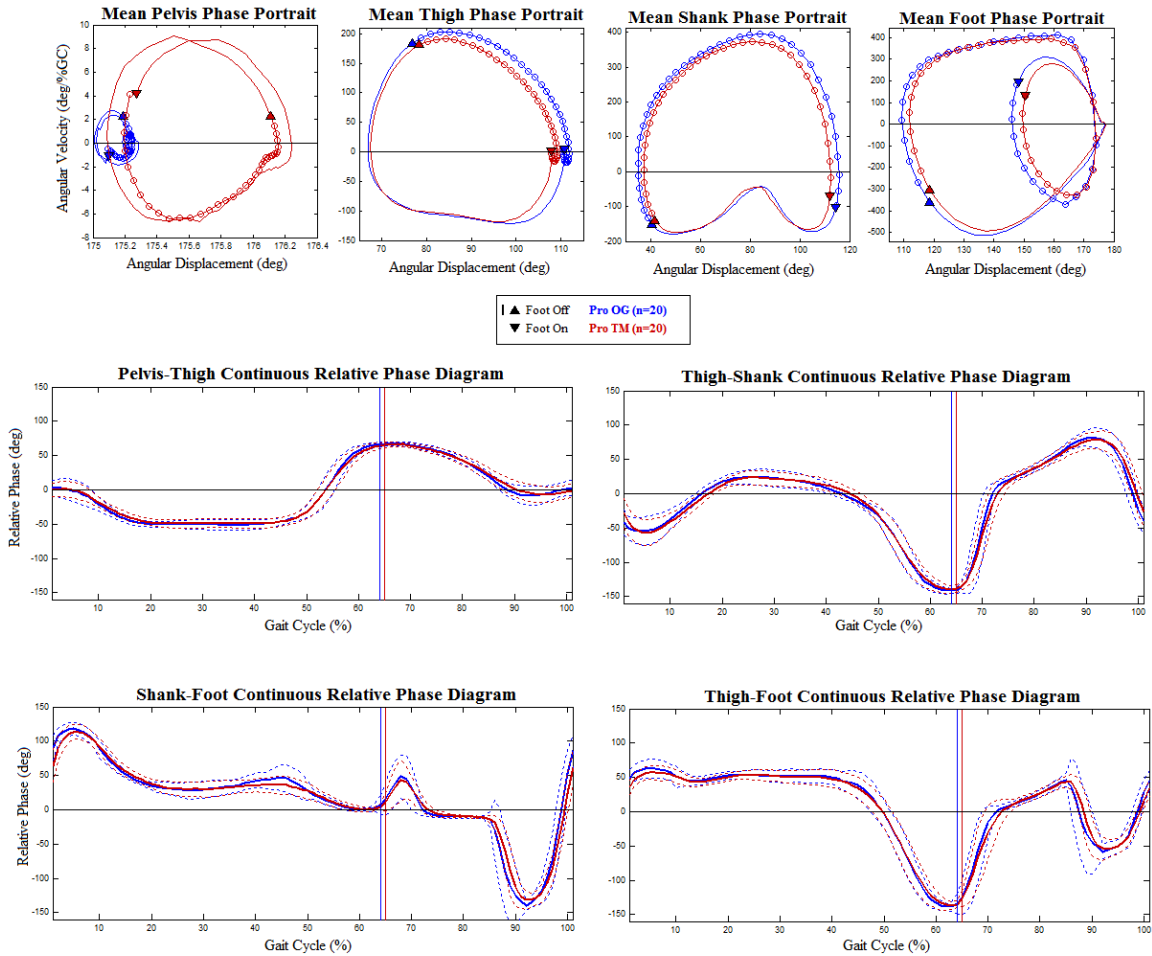
Figure 5.2.3: Phase portraits and continuous relative phase diagrams for over-ground (OG) and treadmill (TM) walking conditions of prospective subjects with CP (blue=OG, red=TM).

5.2.3 Unimpaired Prospective Subjects: Changes in Assistive/Resistive Forces Task

The following table lists the mean and standard deviation for the GDI, CDI, and scaled CPS values for the treadmill walking tasks with swing limb assistance and swing limb resistance were calculated. Marker dropout for two subjects during the both of these treadmill walking conditions were unable to be filled and thus resulted in 18 subjects contributing to the indices means. For both of these treadmill walking conditions, the treadmill belt speed was set to the average over-ground walking speed for each subject.

Table 5.2.5: Mean and standard deviation values for the GDI, CDI, and scaled CPS of the unimpaired prospective cohort for two walking treadmill conditions.

Task	# Subjects	GDI	CDI	CPS*
Swing Limb Assist	18	90.99 (13.72)	94.07 (9.32)	92.72 (1.35)
Swing Limb Resist	18	91.36 (9.85)	94.04 (1.41)	89.98 (1.70)

5.2.4   Unimpaired Prospective Subjects: Over-ground vs. Treadmill Walking

Comparisons between the prospective unimpaired subjects' over-ground and treadmill walking were made using conventional instrumented gait analysis measures, the two novel indices of coordination dynamics, phase portraits, and continuous relative phase diagrams. The figure below contains mean ensemble sagittal kinematic curves were generated from the prospective unimpaired group's OG and TM walking trials.
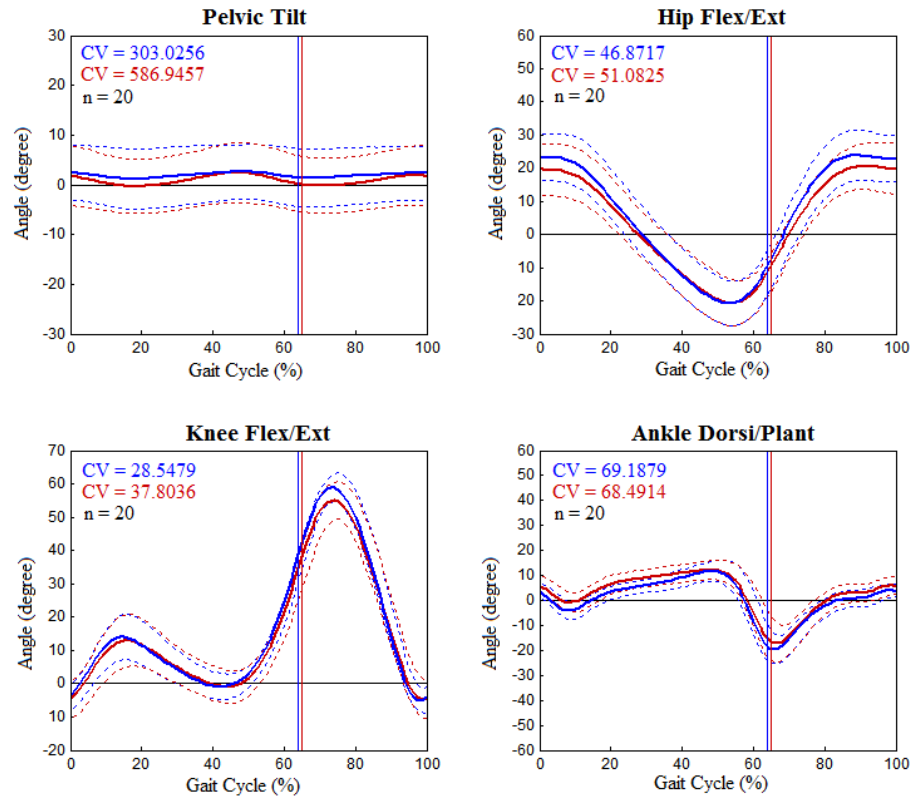
Figure 5.2.4: Sagittal plane kinematic curves for prospective unimpaired subjects during over-ground (OG, blue) and treadmill (TM, red) walking conditions, with coefficients of variation (CV).

The conventional temporal-spatial, gait events, and kinematic descriptors of gait for these two walking conditions is provided in the following table.

Table 5.2.6: Conventional Temporal-Spatial, Gait Events, and Kinematic Descriptors of Gait The mean, standard deviation, and p-values for temporal-spatial, kinematic, and critical gait events from the cohort's over-ground (OG) and treadmill (TM) walking conditions. * Significantly different from over-ground walking, p ≤ 0.05. 1 Calculated as distance walked divided by time to walk corresponding distance.

Gait Measure	OG	TM	p-value
Cadence (steps/min)	110.6 (7.19)	113.43 (7.61)	0.2339
Walking Speed (m/min)1	81.20 (11.35)	71.60 (11.20) *	0.0105
Step Length (m)	0.73 (0.08)	0.64 (0.09) *	0.0009
Step Time (sec)	0.54 (0.04)	0.53 (0.04)	0.1566
Stride Length (m)	1.47 (0.16)	1.28 (0.17) *	0.0011
Stride Time (sec)	1.09 (0.07)	1.06 (0.07)	0.2739
Stance Time (sec)	0.70 (0.05)	0.69 (0.05)	0.8838
Swing Time (sec)	0.39 (0.03)	0.37 (0.02) *	0.0074
Foot Off (%GC)	64 (1.65)	65 (1.45) *	0.0015
Feet Adjacent (%GC)	78 (1.35)	79 (1.14) *	0.0178
Tibia Vertical (%GC)	86 (1.50)	82 (6.53) *	0.0222
Knee to 40° Flexion (%GC)	65 (1.33)	66 (1.84) *	0.0046
Peak Rate of Ankle Flexion (°/%GC)	-2.10 (0.39)	-1.78 (0.52) *	0.0312
Max Knee Flexion (%GC)	73 (1.43)	74 (1.41)	0.1021
Max Knee Flexion (°)	59 (4.47)	55 (5.27) *	0.0009
Max Hip Flexion (%GC)	92 (5.66)	93 (4.06)	0.4936
Max Hip Flexion (°)	25.12 (7.47)	21.20 (5.14)	0.0724
Knee to Neutral (%GC)	95 (2.24)	92 (4.76) *	0.0429
Ankle to Neutral (%GC)	84 (5.81)	82 (7.54)	0.0700
Minimum Ankle Dorsiflexion (°)	-21 (5.74)	-19 (7.57) *	0.0231
Hip Range of Motion (°)	46.02 (4.74)	41.87 (5.07) *	0.0484
Knee Range of Motion (°)	65.52 (5.34)	60.83 (5.19) *	0.0162
Ankle Range of Motion (°)	33.42 (4.90)	31.67 (5.83)	0.4244

Paired t-tests were calculated for the timing and magnitude of the thirty-seven coordination events in the swing period of gait. False discover rate (FDR) is a multiple hypothesis error measures that was used to reduce the likelihood of false positive findings. FDR is the quantity of expected proportion of false positive findings among all the rejected hypotheses. Since FDR does not suffer from the overly strict criteria in the Bonferroni adjusted significance level, it is a more appropriate error rate to control in the testing of multiple hypotheses. Of the thirty-seven coordination events, the following tables list the four coordination events that were found to be significantly difference using the false discovery rate method and adjusted p-values less than or equal to 0.0091.

Table 5.2.7: Swing period coordination events with significant changes in timing and magnitude. The mean, standard deviation, and p-value for the magnitude and/or timing (percent gait cycle = %GC) of swing period coordination events that were significantly different (adjusted p ≤ 0.0091) between the cohort's over-ground and treadmill walking conditions. Each CE is also associated with a mechanism category.

Coordination Event	OG	TM	Adj. p value
1. Foot max AD (°)	178.45 (0.54)	175.15 (1.44)	0.0000
2. Foot min AV (%GC)	88 (1.79)	91 (1.10)	0.0000
Foot min AV (°/%GC)	-444.18 (58.93)	-375.59 (61.26)	0.0009
3. Shank-Foot abs. swing min (%GC)	88 (1.77)	91 (1.17)	0.0000

Mean sagittal PPs and ensemble CRPDs for the right thigh, shank, and foot were generated from the cohort's OG and TM walking trials (Figure 5.2.5). The four coordination events that were significantly between these two walking conditions are indicated in the figure below. The numbering of statistically significant coordination events listed in Table 5.11 corresponds to the numbers shown in the PPs and CRPDs.
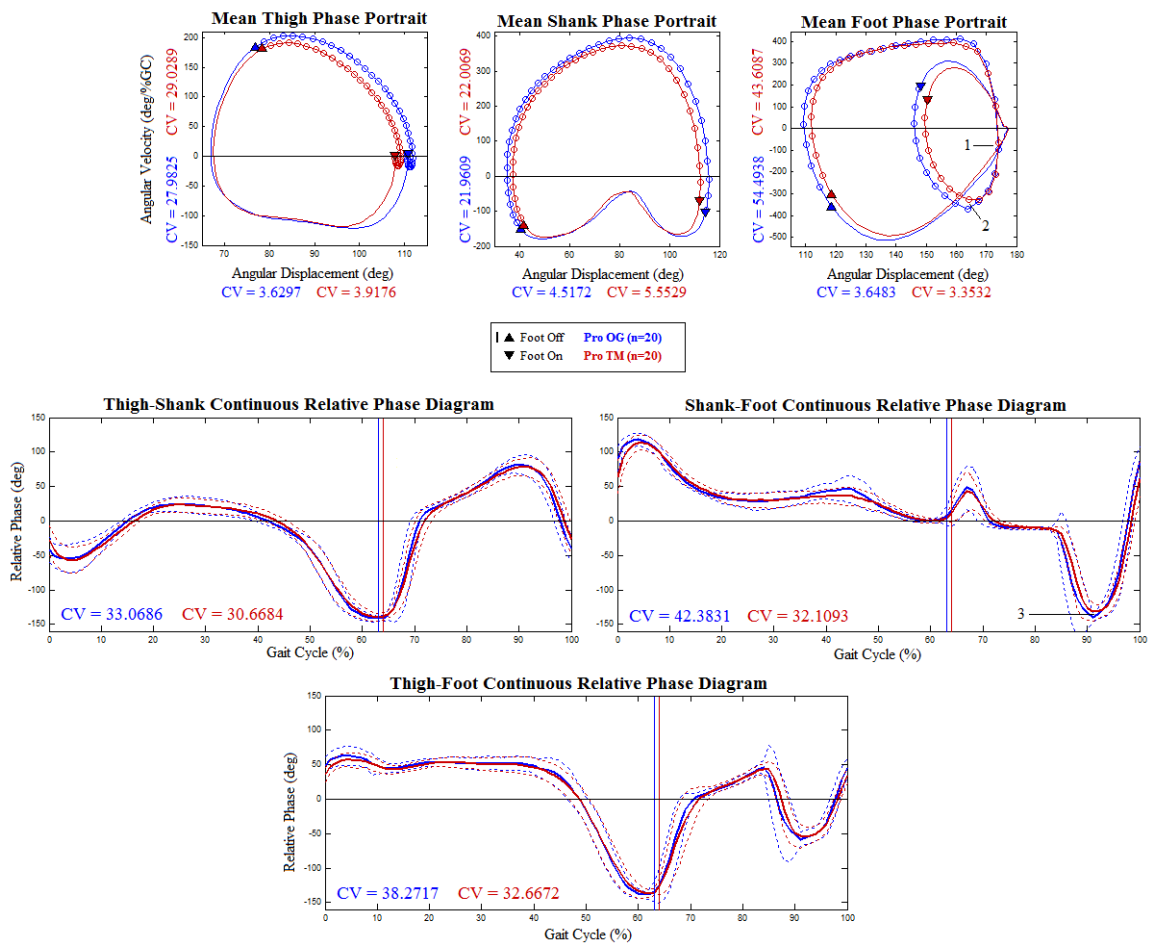
Figure 5.2.5: Mean phase portraits and continuous relative phase diagrams for unimpaired prospective subjects over-ground (OG, blue) and treadmill (TM, red) walking conditions and significant coordination events.

The coefficient of variation (CV) for each PP variable and CRPD are also provided in figure above.

5.2.5 Unimpaired Prospective Subjects: Changes in Assistive/Resistive Forces Task

The next table lists the mean and standard deviation for the GDI, CDI, and scaled CPS values for the treadmill walking tasks with swing limb assistance and swing limb resistance were calculated. Marker dropout for two subjects during the both of these treadmill walking conditions were unable to be filled and thus resulted in 18 subjects contributing to the indices means. For both of these treadmill walking conditions, the treadmill belt speed was set to the average over-ground walking speed for each subject.

Table 5.2.8: Mean and standard deviation values for the GDI, CDI, and scaled CPS of the unimpaired prospective cohort for two walking treadmill conditions.

Task	# Subjects	GDI	CDI	CPS*
Swing Limb Assist	18	90.99 (13.72)	94.07 (9.32)	92.72 (1.35)
Swing Limb Resist	18	91.36 (9.85)	94.04 (1.41)	89.98 (1.70)

5.2.6 Unimpaired Prospective Subjects: Changes in Joint Range of Motion Tasks

The following table provides the mean and standard deviation for the GDI, CDI, and scaled CPS for the treadmill walking tasks a knee brace fixed to full extension (180°), a knee brace fixed to 60° of flexion, and an ankle boot fixed to neutral dorsiflexion was also calculated for all unimpaired prospective subjects. Marker dropout for one subject during these treadmill walking conditions was unable to be filled and thus resulted in 19 subjects contributing to the indices means. For these three treadmill walking conditions, the treadmill belt speed was set to the average over-ground walking speed for each subject.

Table 5.2.9: Mean and standard deviation values for the GDI, CDI, and scaled CPS of the unimpaired prospective cohort for two walking treadmill conditions.

Task	# Subjects	GDI	CDI	CPS*
Knee Fixed 180°	19	73.69 (7.86)	80.72 (5.24)	86.25 (3.27)
Knee Fixed 60°	19	75.53 (7.08)	85.08 (7.00)	84.95 (4.35)
Ankle Fixed 0°	19	89.92 (10.56)	89.35 (8.12)	90.99 (1.37)

Since the purpose of the experiment with one of the unimpaired subjects knees being fixed in full extension was to compare the coordination dynamics of the unimpaired subjects to the coordination dynamics of subjects with a stiff knee gait pattern, the sagittal plane PPs and CRPDs for these two subject groups are provided in the figure below.
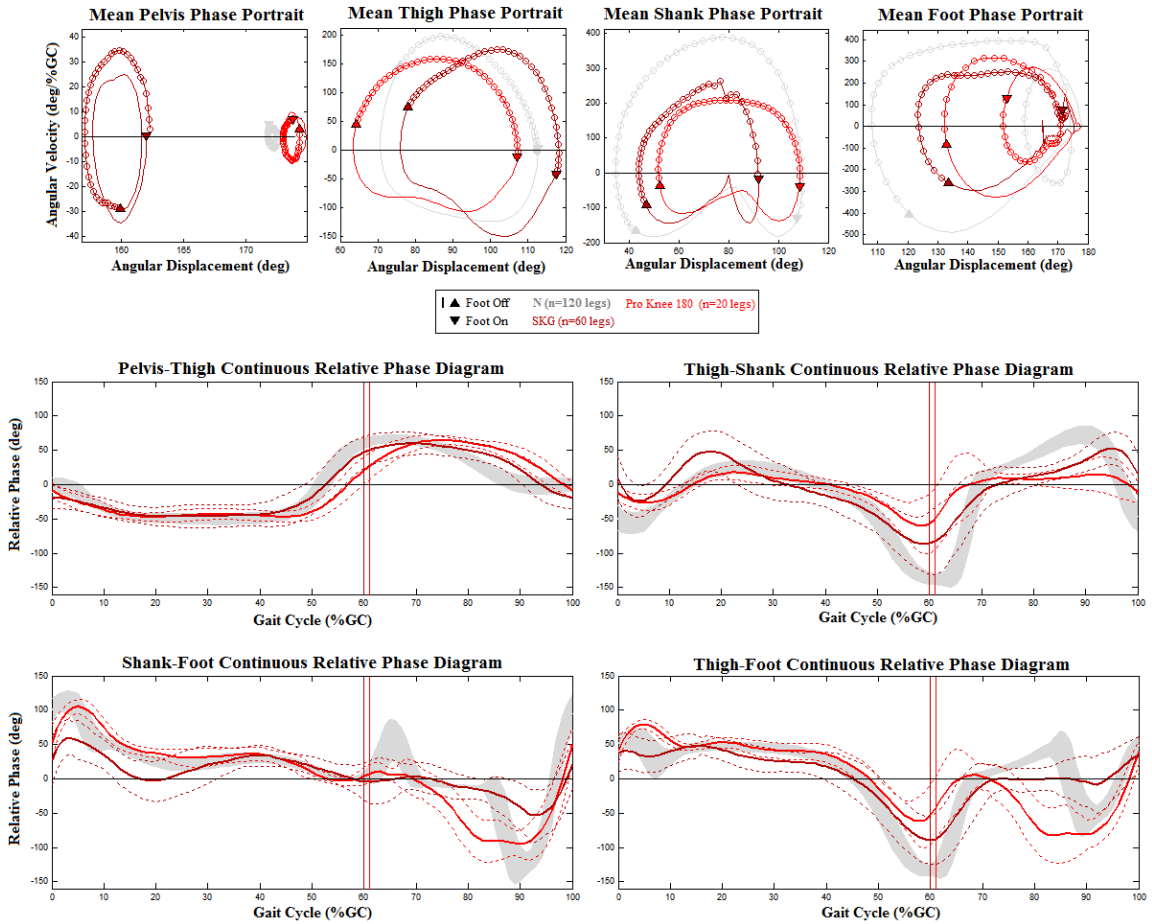
Figure 5.2.6: Phase portraits and continuous relative phase diagrams for unimpaired prospective subjects walking on the treadmill with fixed 180° knee extension (light red), over-ground walking of all subjects with a stiff knee gait pattern (dark red), and over-ground walking for all retrospective unimpaired subjects (grey).

Similarly, the purpose of the experiment with one of the unimpaired subjects knees being fixed in flexion was to compare the coordination dynamics of the unimpaired subjects to the coordination dynamics of subjects with a crouch gait pattern. The sagittal plane PPs and CRPDs for these two subject groups are provided in the following figure.
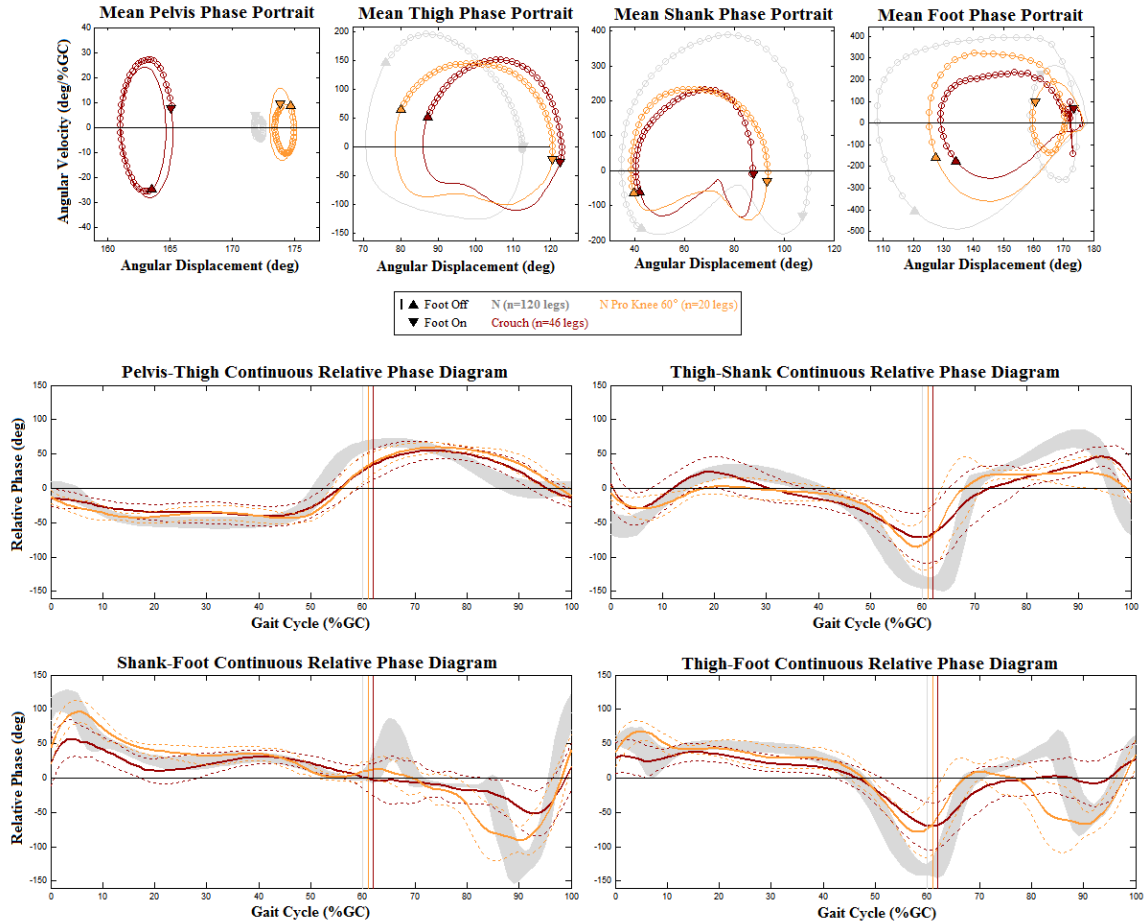
Figure 5.2.7: Phase portraits and continuous relative phase diagrams for unimpaired prospective subjects walking on the treadmill with fixed 60° knee flexion (orange), over-ground walking of all subjects with a crouch gait pattern (red), and over-ground walking for all retrospective unimpaired subjects (grey).

Similarly, the purpose of the experiment with one of the unimpaired subjects ankles being fixed in neutral dorsiflexion was to compare the coordination dynamics of the unimpaired subjects to the coordination dynamics of subjects with a below knee amputation. Phase portraits and continuous relative phase diagrams for these various subject groups are presented in the next figure.
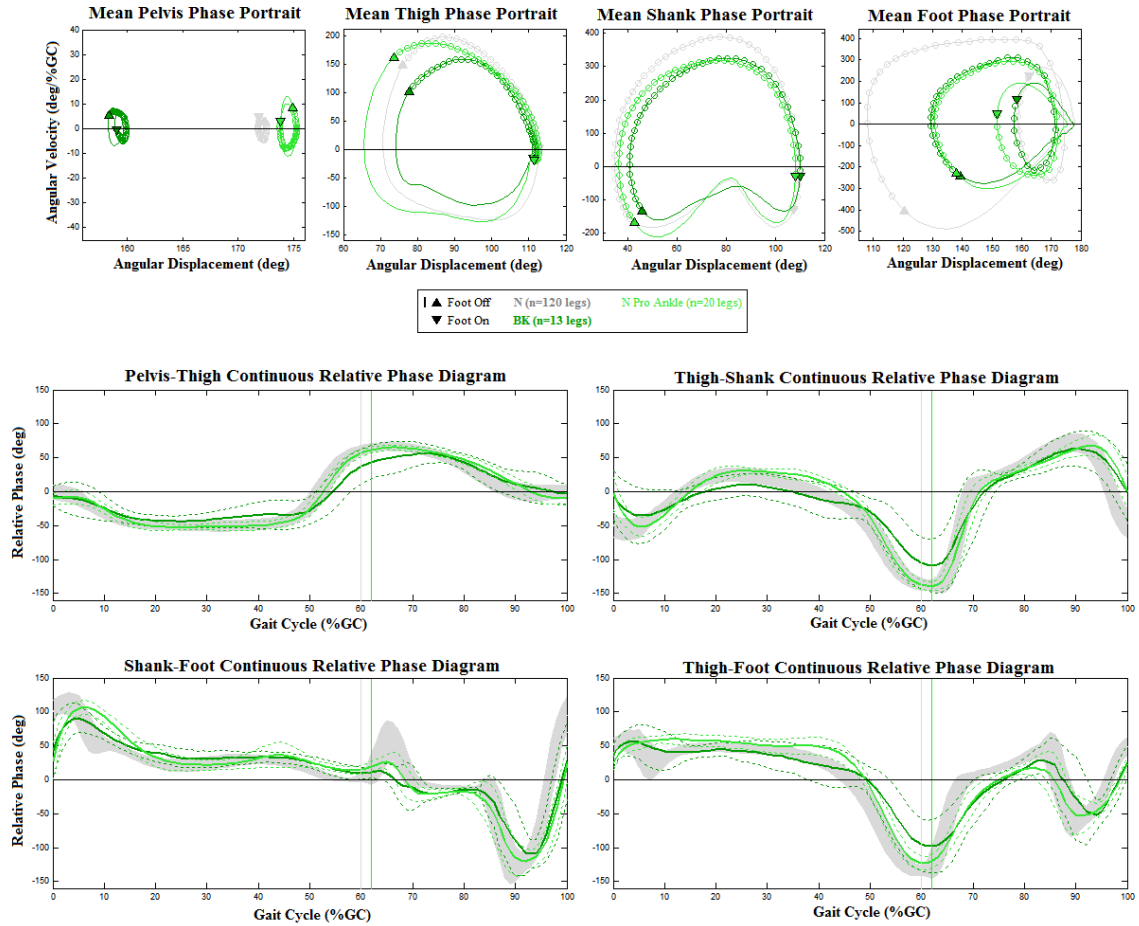
Figure 5.2.8: Phase portraits and continuous relative phase diagrams for unimpaired prospective subjects walking on the treadmill with fixed ankle dorsiflexion (light green), over-ground walking of all subjects with a transtibial amputation (dark green), and over-ground walking for all retrospective unimpaired subjects (grey).

5.3 Aims and Hypotheses Test Results

5.3.1 Aim 1 Results

As discussed in Chapter 1 and 3, the purpose of Aim 1 was to construct a normative reference from a large cohort of individuals free of gait pathology, which would serve as the reference for the other three aims. As mentioned in Chapter 4, two normative reference datasets were constructed because the unimpaired retrospective subjects were barefoot and the prospective subjects wore shoes. Mean sagittal PPs and ensemble CRPDs for the lower extremity segments were created for the prospective and retrospective unimpaired subjects using the methods described in Chapters 3 and 4 (Figure 5.2.1).

The following table provides the coefficient of variation (CV) and variance ratio (VR) were

calculated to quantify the extent of variability for the angular displacement (AD), angular velocity (AV), and relative phase angle with respect to the mean of these curves across all time in the ensemble average.

Table 5.3.1: Coefficient of variation (CV) and variance ratio (VR) for unimpaired retrospective cohort's mean angular displacement (AD), mean angular velocity (AV), and relative phase angles.

Coordination Curve	CV		VR	
	Retro	Pro	Retro	Pro
Pelvis AD	2.7120	2.06	1.0047	1.05
Pelvis AV	365.5103	913.42	0.9220	1.03
Thigh AD	4.1143	3.63	0.0602	0.04
Thigh AV	31.7030	27.98	0.0626	0.05
Shank AD	5.4048	4.52	0.0308	0.02
Shank AV	26.1728	21.96	0.0440	0.03
Foot AD	4.0283	3.65	0.0783	0.07
Foot AV	55.8985	54.49	0.1504	0.14
Pelvis-Thigh CRPD	27.2504	25.64	0.0517	0.05
Thigh-Shank CRPD	36.0529	33.07	0.0730	0.06
Shank-Foot CRPD	50.5218	42.38	0.1388	0.10
Thigh-Foot CRPD	43.7863	38.27	0.1173	0.10

The following table provides the mean, standard deviation, and 95% confidence intervals for the relative phase angles from each CRPD at the four essential footfall conditions of the normal gait cycle from the unimpaired retrospective cohort.

Table 5.3.2: Mean, 1 standard deviation, and 95% confidence intervals for the relative phase angles (degrees) at common temporal gait events for unimpaired prospective subjects. The prospective cohort's mean and 1 standard deviation for the percent gait cycle for each temporal gait event is also reported.

CRPD	Foot Strike 0% ($\pm$0.00%)		Opposite Foot Off 10% ($\pm$2.49%)	
Pelvis-Thigh	0.70 (SD 11.23)	-1.28 to 2.68	-32.17 (SD 7.43)	-33.48 to -30.86
Thigh-Shank	-48.05 (SD 19.16)	-51.44 to -44.66	-23.29 (SD 9.78)	-25.02 to -21.56
Shank-Foot	98.12 (SD 17.76)	94.98 to 101.26	57.30 (SD 14.68)	54.71 to 59.89
Thigh-Foot	50.07 (SD 10.77)	48.17 to 51.97	34.01 (SD 13.20)	31.68 to 36.34

CRPD	Opposite Foot On 49% ($\pm$0.92%)		Foot Off 60% ($\pm$2.14%)	
Pelvis-Thigh	-27.17 (SD 12.73)	-29.42 to -24.92	62.20 (SD 6.35)	61.08 to 63.32
Thigh-Shank	-40.14 (SD 15.24)	-42.83 to -37.45	-137.69 (SD 7.51)	-139.02 to -136.36
Shank-Foot	19.29 (SD 9.02)	17.70 to 20.88	5.81 (SD 10.07)	4.03 to 7.59
Thigh-Foot	-20.85 (SD 20.87)	-24.54 to -17.16	-131.88 (SD 10.69)	-133.77 to -129.99

5.3.2   Aim 2 Results

As presented in Chapter 1 and 3, the purpose of Aim 2 and its hypotheses was to explore the relationship between the proposed measures of coordination dynamics (e.g. PP, CRPD) and select clinical performance measures that characterize aspects of coordination. Recall from the methods discussion in Chapter 4, that the results from these tests and analyses are only for the study's

prospective subjects.

5.3.2.1 Hypothesis 2A Results

Hypothesis 2A was tested by two measures derived from the voluntary reciprocal movements of each subject's legs in the speed-accuracy task, which was designed to characterize a subject's selective motor control in relation to any task specific coordination deficits. The average percentage of foot taps that were within a target's boundary (e.g. hit accuracy) for the prospective subjects with cerebral palsy and an unimpaired gait are displayed with a trend line in the following figure.
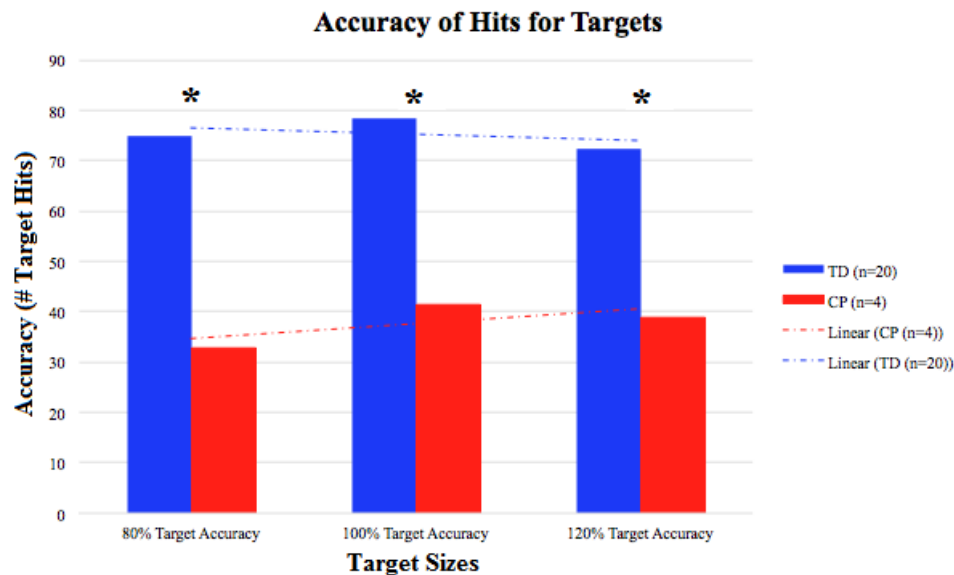
Figure 5.3.1: Mean percentage of hits (accuracy) for the prospective unimpaired subjects (blue) and subjects with cerebral palsy (red) for the three foot target sizes (80%, 100%, 120%) . A linear trend line is provided and * indicates a significant ($p<0.05$) difference between the two subject groups.

For each of the three target sizes, Student's t-tests were conducted to test if there was a significant difference between the unimpaired subjects' mean accuracy and the mean accuracy of the subjects with cerebral palsy. As indicated in the figure above, there was a statistically significant ($p<0.05$) difference between the two subject groups' ability to accurately tap the target.

The second measure used to test the hypothesis 2A was the speed of the swinging limb when it moved from the aft target to the forward target. For each of the three target sizes, Student's t-tests were conducted to test if there was a significant difference between the unimpaired subjects' mean swing leg forward speed and the mean forward speed of the swinging leg of the subjects with cerebral palsy. As indicated in the figure below, there was a statistically significant ($p<0.05$) difference between the two subject groups' ability to accurately tap the target.

Forward Speed of Swing Leg
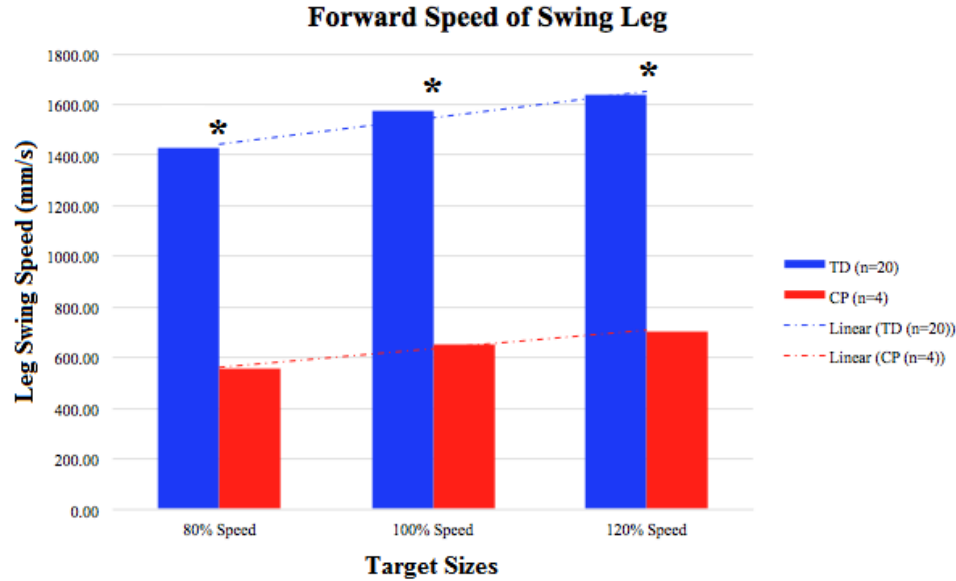
Figure 5.3.2: Mean speed of the forward swinging leg for the prospective unimpaired subjects (blue) and subjects with cerebral palsy (red) for the three target sizes (80%, 100%, 120%). A linear trend line is provided and * indicates significant ($p<0.05$) differences between the two subject groups.

Since the forward motion of the swinging leg in this reciprocal tapping task mimics the forward motion of the swing leg during gait, coordination events related to a subject's ability to dissociate the hip extension and ankle plantarflexion synergy near foot off and during initial swing were compared to each prospective cohort's swinging leg speed. As mentioned in Chapter 4, t-tests were calculated for each cohort's mean timing (%GC) and magnitude for coordination events during initial swing on the thigh-shank and thigh-foot continuous relative phase diagrams. The coordination events were a minimum, maximum instantaneous slope (MiS), inflection point (IP), and a zero crossing (0x). The timing and magnitude of the maximum instantaneous slope of the thigh-shank CRPD was the only statistically significant coordination event. The following table provides the means and standard deviations for this thigh-shank CRPD coordination event in initial swing.

Table 5.3.3: Mean timing (%GC) and magnitude of the maximum instantaneous slope (MiS), with its standard deviation, for the two prospective cohorts' thigh-shank continuous relative phase diagram.

Pro. Groups	Thigh-Shank CRPD MiS (%GC)	Thigh-Shank CRPD MiS (°/%GC)
N (n=20)	70 (±1.28)	52.00 (±5.55)
CP (n=6)	74 (±5.04)	21.85 (±11.42)

Additionally, below is a plot of the two mean ensemble thigh-shank CRPDs for the two prospective subject cohorts. As the two black arrows on the figure indicate, the maximum instantaneous slope for the subjects with CP is considerably shallower, delayed, and overall attenuated.

124

Thigh-Shank Continuous Relative Phase Diagram

	▲ Foot Off	N (n=120 legs)	CP (n=6 legs)
	▼ Foot On	N pro. (n=20 legs)	■ 1) Max Inst. Slope
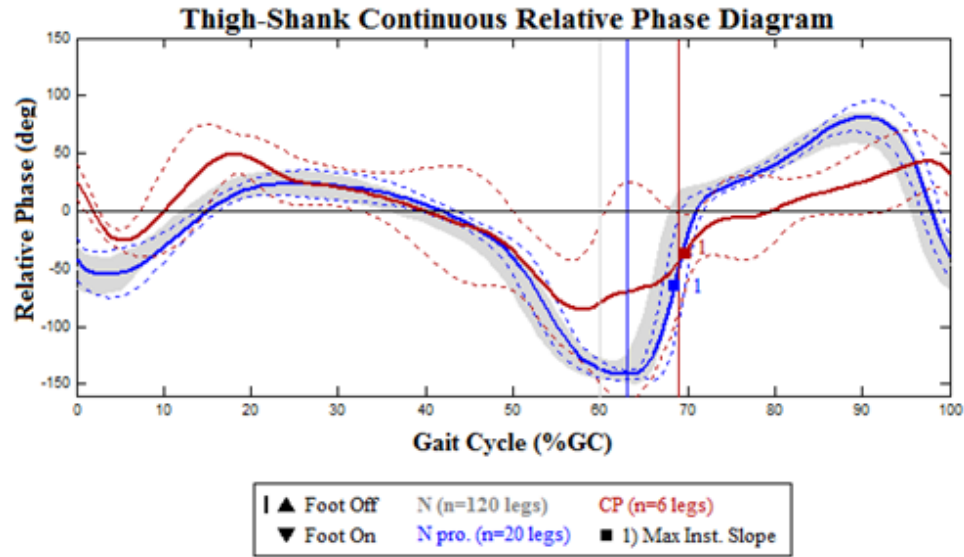
Figure 5.3.3: Mean ensemble thigh-shank CPRD for the unimpaired retrospective subjects (grey), unimpaired (blue) prospective subjects, and prospective subjects with CP (red) with the significant coordination event. Vertical lines indicate the mean occurrence of foot off for each group.

5.3.2.2   Hypothesis 2B Results

All prospective subjects were given a score for each limb based on the Selective Control Assessment of the Lower Extremity (SCALE) to characterize each subject's degree of selective motor control impairment. A maximum of 6 points for each limb were possible; 2 points per joint. The SCALE scores for all prospective subjects with CP are provided in Appendix G. All of the unimpaired prospective subjects score a maximum possible score of 6 points. The subjects with CP had various scores ranging from the maximum possible to 2 points per limb. There was a significant difference (p=0.013) between the mean unimpaired subjects SCALE score and the mean SCALE score for the subjects with CP.

To determine if there was a significant relationship between a subject's ability to perform the select voluntary motor control joint tasks of the SCALE and a subject's ability to perform swing limb advancement while walking over-ground, the SCALE scores were compared to coordination events in initial swing that are related to a subject's ability to dissociate the hip extension and ankle plantarflexion synergy near foot off and initiate a hip flexor synergy. As mentioned in chapter 4, t-tests were calculated for each cohort's mean timing (%GC) and magnitude for coordination events during initial swing on the thigh-shank and thigh-foot continuous relative phase diagrams. The coordination events analyzed were a minimum, maximum instantaneous slope, inflection point, and a zero crossing. Three coordination events were found to be significantly (p < 0.05) different between

the two subject groups. While complete tables of these t-tests for all the considered coordination events are provided in Appendix G, the following table provides the means and standard deviations for these three coordination events.

Table 5.3.4: Mean timing (%GC) and magnitude of the maximum instantaneous slope (MiS), minimum (Min), and inflection point (IP) with standard deviation, for the prospective cohorts' thigh-shank and thigh-foot continuous relative phase diagrams (CRPDs).

Pro. Group	Thigh-Shank CRPD Min (%GC)		Thigh-Shank CRPD MiS (deg/%GC)	
	(%GC)	(°)	(%GC)	(°)
N (n=20)	64 (±1.21)	-142.53 (±4.03)	52.00 (±5.55)	69 (±1.67)
CP (n=6)	70 (±6.0)	-85.57 (±44.32)	21.85 (±11.42)	76 (±5.92)

The following plot of the mean ensemble thigh-shank and thigh-foot CRPDs for the two prospective subject cohorts with the three coordination events that were significantly different ($p < 0.05$) for these two cohorts.
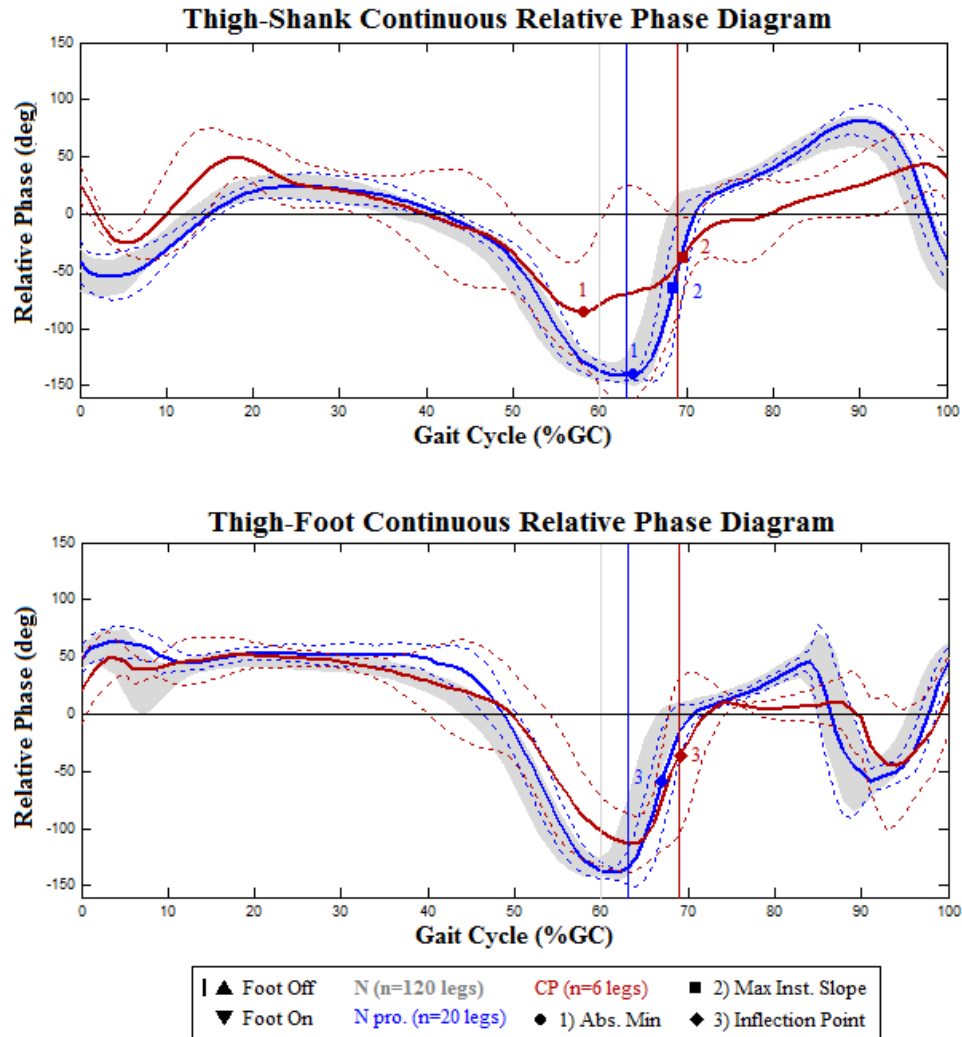
Figure 5.3.4: Mean ensemble thigh-shank (top) and thigh-foot (bottom) CPRD for the unimpaired retrospective subjects (grey), unimpaired (blue) prospective subjects, prospective subjects with CP (red), and the significant coordination events. Vertical lines indicate the mean occurrence of foot off for each group.

Since all unimpaired prospective subjects scored the maximum possible points for this metric, correlations for these subjects' SCALE scores and other measures were not calculated. However, a correlation matrix for the prospective unimpaired subjects' significant coordination events is provided in Appendix G. Additionally, a correlation matrix for the same variables and SCALE score for the prospective subjects' with CP is provided in Appendix G.

5.3.2.3   Hypothesis 2C Results

Gait related tasks from the International Cooperative Ataxia Rating Scale (ICARS) and Scale for the Assessment and Rating of Ataxia (SARA) exams were used to characterize cerebellar based

impairments in spatial accuracy of movement and dynamic balance for all prospective subjects. A maximum of 40 points for each limb was possible for this metric. While Figure 5.12 provides a scatter plot of the prospective subject's scores, the ICARS/SARA scores for all prospective subjects with cerebral palsy are provided in Appendix G. There was not a statistically significant difference (p=0.1040) between the unimpaired prospective subjects and subjects with cerebral palsy. This may be partially due to the fact that all unimpaired prospective subjects scored the maximum possible value for this metric and the small sample size of subjects with CP.
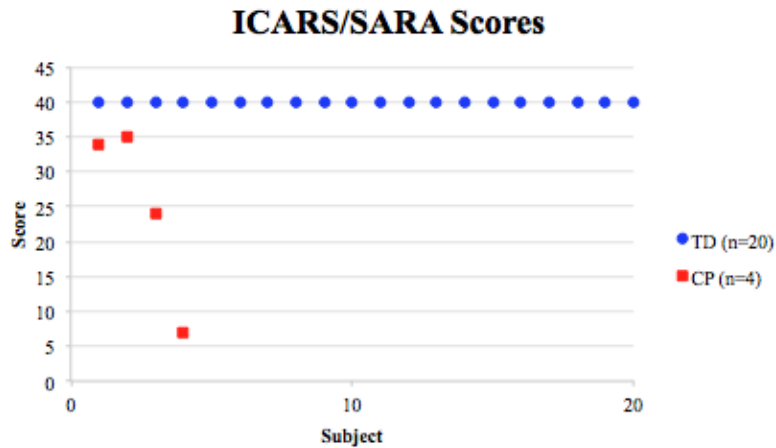
Figure 5.3.5: ICARS/SARA scores for all unimpaired prospective subjects (blue circle) and all prospective subjects with cerebral palsy (red square).

As detailed in Chapter 4, two additional analyses were conducted on the motion capture data for the experiments related to this hypothesis. First, the mean base of support (BoS) was calculated for each prospective subject's representative over-ground walking trial and mean of all tandem walking trial(s). Of the four prospective subjects with cerebral palsy, only one subject was able to complete the tandem walking task. The other three subjects were unable to complete this task for various reasons: required assistance (1 subject), heel/toe markers kept falling off due to walking pattern (1 subject), and unable to perform task (1 subject). There was not a statistically significant difference (p=0.0672) between the over-ground BoS walking trials for the prospective subjects with CP and the BoS for the unimpaired prospective subjects. However, when comparing the BoS for over-ground walking of all the study's subjects, both prospective and retrospective, there were significant differences between the unimpaired subjects and subjects with CP (p=2.96E-12) and between subjects with CP and subjects with a LLA (p=0.01). There was not a significant difference in the BoS width between the unimpaired subjects and subjects with a LLA (p=0.27).

Secondly, the center of mass curvature during the turning tasks was calculated for all prospective

subjects and t-tests were run to determine if there were significant differences between the cohorts. Recall a larger curvature ($\varkappa$) corresponds to a tighter turn. There were not any statistically significant differences between the mean maximum curvature for each prospective cohort's right and left turns (figure below). Again, this could in part be due to the small number of prospective subjects with CP. Also, it is important to note that of the four prospective subjects with CP, two subjects were affected on both sides (e.g. diplegic) and two were affected on only one side (e.g. hemiplegic). Therefore, of the four legs corresponding to the four right turns, all of the legs were affected and of the four legs corresponding to the four left turns, only two were affected.
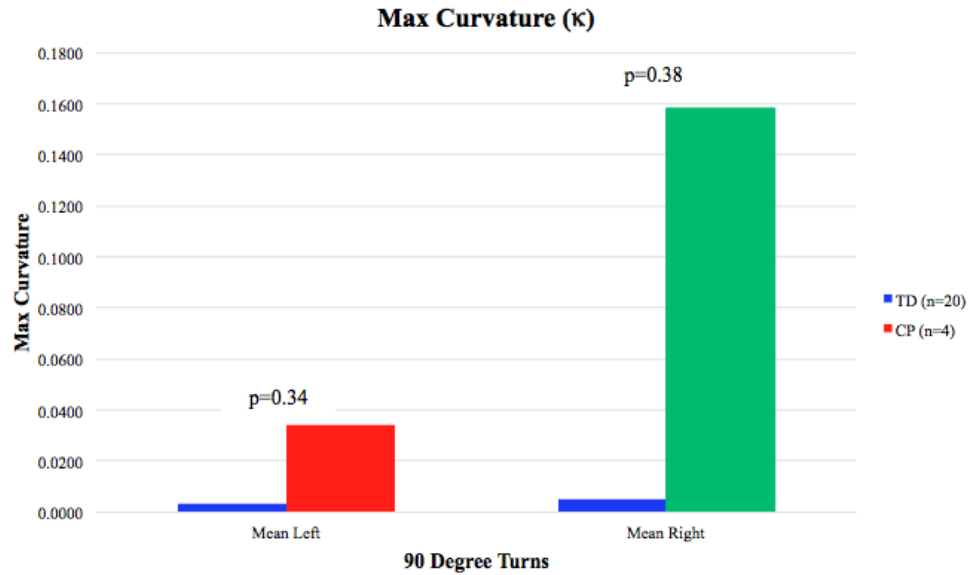
Figure 5.3.6: Mean maximum curvature (K) for left (red) and right (green) turns for all unimpaired prospective subjects (n=20) and prospective subjects with CP (n=4).

The next figure depicts the mean center of mass (CoM) trajectory for the left and right turns of both prospective subject groups. This figure clearly shows there are differences in the turning curvature and the influence of subjects with hemiplegia and diplegia on these results and observed turning strategies for these two cohorts will be discussed in Chapter 6.
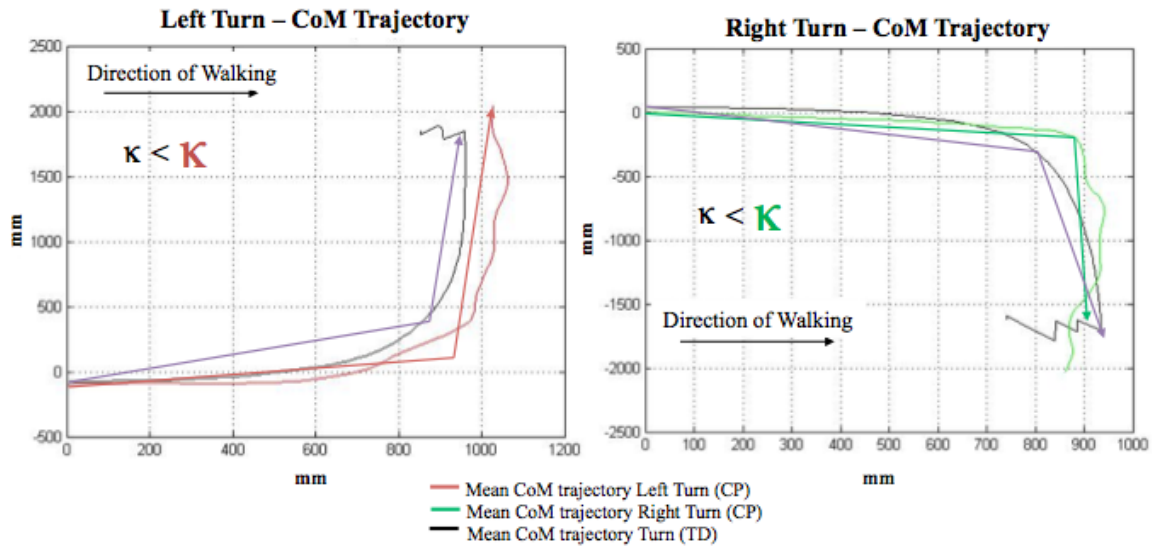
Figure 5.3.7: Mean Center of Mass (CoM) trajectories for left (red) and right (green) turning tasks of prospective subjects.

Since all unimpaired prospective subjects scored the maximum possible points for this metric, correlations for these subjects' ICARS/SARA scores and other measures were not calculated. However, a correlation matrix for the prospective unimpaired subjects' maximum curvature and conventional temporal-spatial measures of gait is provided in Appendix G. Additionally, a correlation matrix for the same variables and ICARS/SARA score for the prospective subjects' with CP is provided in Appendix G.

5.3.3 Aim 3 Results

As presented in Chapter 1 and 3, the purpose of Aim 3 was to construct a mathematical software model of a double pendulum, using initial conditions and model parameters derived from subject motion capture data, and compare the motion of the model's two linkages to the sagittal plan motion of the thigh and shank from actual subject data. Recalling from the methodology outlined in Chapter 4, the first version of the model used the Matlab function ode45 to solve the equations of motion and compare the four different damping cases to the actual motion of each cohort's thigh and shank sagittal plane trajectories. The table below presents the ranking of the general subject cohorts (e.g. N, CP, LLA) for each damping case. A larger summed normalized root mean square error (NRMSE) indicates a greater difference between the pendulum model's motion and the cohort's motion, thus resulting in a lower ranking.

Table 5.3.5: Rankings of the three general subject cohorts for 4 different pendulum model damping conditions. The subject group with the lowest ranking for each damping case is indicated with a rectangle surrounding the summed normalized root mean square error (ΣNRMSE). Three subject cohorts were considered: unimpaired (N), cerebral palsy (C), and alower limb amputation (LLA).

Group	Undamped		Under Damped		Critically Damped		Over-Damped	
	$\sum$NRMSE	Rank	$\sum$NRMSE	Rank	$\sum$NRMSE	Rank	$\sum$NRMSE	Rank
N	23.32	2	25.58	1	26.30	1	26.17	1
C	31.57	3	35.80	3	34.52	3	34.56	3
LLA	19.97	1	26.58	2	26.81	2	26.37	2

The next table provides the summed NRMSE ranking for each of the four damping conditions that was calculated for the five gait patterns considered in this body of work.

Table 5.3.6: Gait pattern cohort rankings for 4 different pendulum model damping conditions. Five gait patterns were considered: unimpaired (N), stiff knee gait (SKG), crouch (C), below knee amputation (BK), and above knee amputation (AK).

Group	Undamped		Under Damped		Critically Damped		Over Damped	
	$\sum$NRMSE	Rank	$\sum$NRMSE	Rank	$\sum$NRMSE	Rank	$\sum$NRMSE	Rank
N	23.32	3	25.58	2	26.30	2	26.17	3
SKG	35.30	4	33.02	4	30.66	4	30.69	4
C	38.52	5	38.39	5	38.11	5	38.13	5
BK	20.45	1	26.38	3	26.34	3	25.77	2
AK	22.44	2	24.45	1	25.34	1	25.36	1

The summed NRMSE and corresponding rankings for each subject cohort for each of the four damping conditions are provided in Appendix G. To determine if the various rankings for the three different subject groups were significantly different, a Wilcoxon signed-rank test was conducted in Matlab. None of the p-values from the various Wilcoxon signed-rank tests were significantly different.

As indicated in previous table, a subject with a lower limb amputation, specifically those with a transtibial amputation, had coordination dynamics measures with the smallest residual when compared to a passive double pendulum (Hypothesis 3A). And when considering subjects with a lower limb amputation as a group, this cohort had the lowest residual when compared to an un-damped pendulum (Table 5.13). In general, the residual between the coordination dynamics measures of subjects with cerebral palsy and an over-damped double pendulum were the largest of the three groups (Hypothesis 3B). However, when dividing subjects further into gait pattern, the subjects with either stiff knee gait or crouch were the furthest from any of the pendula damping conditions. In general, the unimpaired subject group had the smallest residual when compared to a critically damped pendulum (Hypothesis 3C), but they also had the smallest residual for all damping cases. When compared to the various gait patterns, this cohort had either the second or third smallest residual for all damping cases.

5.3.4   Aim 4 Results

Recall the object of Aim 4 was to demonstrate the proposed measures of coordination dynamics are able to distinguish between different gait pathologies and patterns associated with altered limb advancement during the swing period of gait. In an effort to consolidate the large amount of variables and data associated with the proposed measures of coordination dynamics two novel indices were created. These indices were used to determine if there are statistically significant difference between the coordination dynamics for unimpaired subjects and subjects with either a stiff knee, crouch, and mechanically altered gait pattern. The following section presents the results for various analyses testing the validity of these new indices and the hypothesis test results.

5.3.4.1   Coordination Deviation Index Results

Two novel indices were created to address Aim 4 and its hypothesis. The first index, the coordination deviation index (CDI), was calculated for all prospective and retrospective subjects and compared to the GDI and Gross Motor Function Classification System (GMFCS) level of individuals with varying degrees of motor impairment. The overall objective of this investigation was to explore the applicability of the CDI in describing gait pathology for two clinical cohorts (CP, LLA) with different reasons for coordination deficits. The specific aims of this index's investigation were to 1) generate a coordination deviation index using the GDI methodology for the subject groups, 2) compare CDI scores of the groups using the GDI as a benchmark to describe varying degrees of gait performance in these distinct groups, and 3) demonstrate that the magnitude of coordination impairment (CDI) corresponds to the magnitude of kinematic impairment (GDI).

In Appendix G, Table G.4.1 provides the means and standard deviations of demographic characteristics, GDIs, and CDIs for the subjects. Using the equation of variance accounted for in Schwartz et al, 2008 six coordination features were found to be necessary for reconstructing the coordination curves with 98% reconstruction quality (Appendix G, Figure 1). Figure 5.3.8A displays the mean GDI and CDI values for the different subject cohort categories. For all of the subject groups, there was a significant difference ($p \leq 0.001$) between their GDI and the unimpaired group's GDIs and a significant difference ($p \leq 0.001$) between group's CDI and the unimpaired group's CDIs. Except for the AK subject group, there was a significant difference ($p \leq 0.001$) between a group's CDIs and GDIs. Note the pattern for reduced CDI in clinical groups follows a similar downward trend as the GDI. Figure 5.3.8B presents the mean GDIs and CDIs for the unimpaired subjects and subjects with CP when organized by GMFCS level. There were significant differences ($p \leq 0.05$) between

the mean CDIs and each GMFCS level and between the mean CDIs for GMFCS levels I and III.
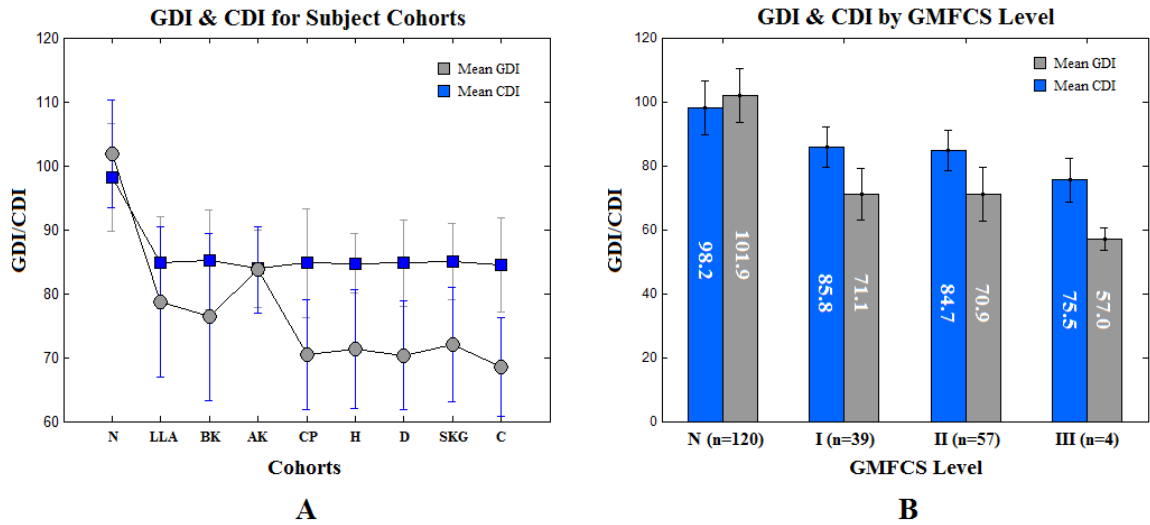
Figure 5.3.8: A) Comparison of GDI (grey square) and CDI (blue square) mean scores for each subject group: unimpaired (N), lower limb amputation (LLA), below knee amputation (BK), above knee amputation (AK), cerebral palsy (CP), hemiplegia (H), diplegia (D), stiff knee gait pattern (SKG), and crouch gait pattern (C). B) Mean GDI (grey) and CDI (blue) values for N and CP subjects with confidence intervals with 95% confidence intervals are presented by GMFCS level. Significant differences between groups (p≤0.05) and between GMFCS levels I and III.

Figure 5.3.9A shows the relationship between the GDI and CDI values for all of the study's subjects, with a dashed line indicating the ideal unimpaired subject index value. Figure 5.3.8B illustrates the empirical normal distribution of the GDI and CDI scores in relation to a theoretical cumulative distribution function. The Kolmogorov-Smirnov test confirmed the GDI and CDI values for this study's subjects were normally distributed.
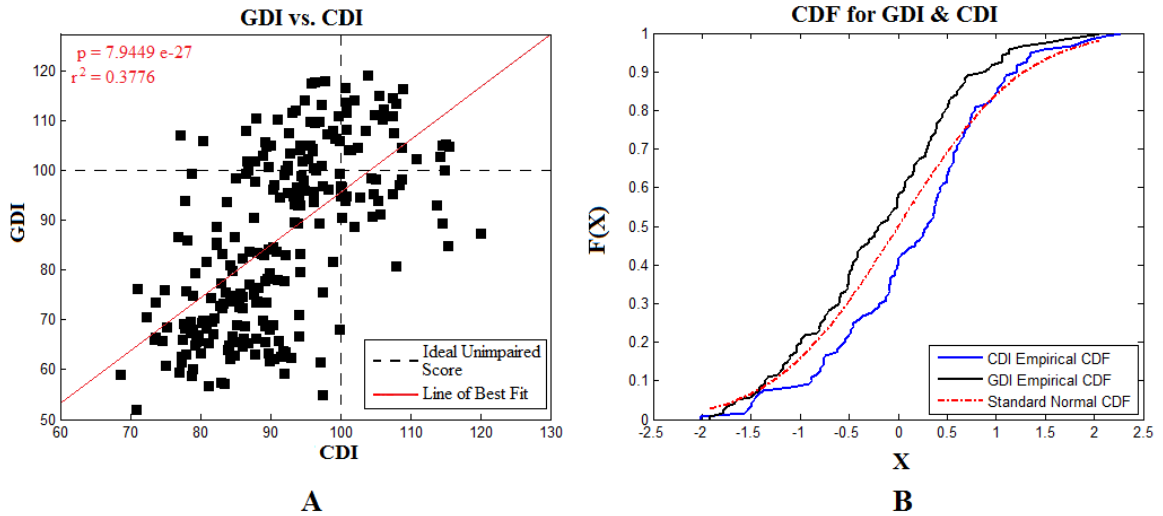
Figure 5.3.9: A) Scatter plot of all GDI scores against all CDI scores with the line of best fit (red). B) Cumulative distribution functions (CDF) for the GDI (black) and CDI (blue) in comparison to the theoretical normal CDF (red).

5.3.4.2 Coordination Performance Score Results

Recall from Chapter 4 that six coordination events (CEs) during swing period were identified using a backward stepwise regression model as significant. Table 5.20 provides a list of the six significant CEs, a brief description of each CE, the mean, standard deviation, and 95% confidence intervals from the unimpaired subjects.

Table 5.3.7: Description of the six significant coordination events listed in order of occurrence during swing period with the normative cohort's mean (standard deviation) value for each CE, and 95% confidence interval (CI) from the normative cohort. The gait cycle was indexed from 1 to 101%.

Coordination Event	Description	Mean (SD)	95% CI
1) Thigh-Foot CRPD	Absolute minimum (%GC)	-137.14° (6.38)	-149.65° to -124.63°
2) Thigh PP	Max angular velocity (%GC)	67% (1.70)	64.05% to 70.41%
3) Pelvis PP	Max angular displacement (°)	173.59° (4.61)	164.56° to 182.62°
4) Pelvis PP	Min angular displacement (°)	171.51° (4.54)	162.62° to 180.41°
5) Foot PP	Max angular displacement (°)	89% (1.83)	85.00% to 92.16%
6) Thigh-Foot CRPD	Last inflection point in swing (°)	98% (1.25)	95.29% to 100.19%

Of the six significant coordination events identified, three swing period coordination events were used for this first regression model (atypical vs. typical gait pattern). The magnitude of the thigh-foot CRPD minimum near foot off (TF1), the magnitude of the pelvis PP's minimum angular displacement (P1), and the percent gait cycle of the foot PP's maximum angular displacement (pF2). All of the available 246 observations (legs) were used in the construction of the two regression models based upon the coordination events used to construct the CPS metric. The final regression model for distinguishing between an impaired and unimpaired gait pattern is provided in the equation below.

134

The area under the receiver operator characteristic (ROC) curve was 0.9767. Appendix G contains additional results from this model's analyses in SAS.

Algorithm 5.1 Regression model for distinguishing between an unimpaired (N) and cerebral palsy (CP) gait pattern.

$$Y_{CPvN} = 8.74246 - 0.04577X_{P1} + 0.03298X_{TF1} + 0.03815X_{F2}$$

Using this equation, it is possible to solve for the probability that a subject's gait pattern is atypical. This further supports the ability of the proposed measures of coordination dynamics to distinguish between various gait patterns (Aim 4). None of the nuisance variables considered (e.g. leg length, weight, age, gender) had a significant influence on this model and were not included because they did not strengthen the model or improve the area under the curve of the receiver operator characteristic curve.

Of the six significant coordination events identified, two swing period coordination events were used for this second regression model (stiff knee gait vs. crouch gait pattern). The final regression model for distinguishing if a subject with cerebral palsy has either a stiff knee gait or crouch gait pattern is provided in the following equation. The area under the receiver operator characteristic (ROC) curve was 0.6377. None of the nuisance variables considered (e.g. leg length, weight, age, gender) had a significant influence on this model and were not included because they did not strengthen the model or improve the area under the curve of the receiver operator characteristic curve. Appendix G contains additional results from this model's analyses in SAS.

Algorithm 5.2 Regression model for distinguishing between a stiff knee gait (SKG) and a crouch (C) gait pattern.

$$Y_{SKGvC} = 7.8164 - 0.0564X_{TF1} - 0.0147X_{P1}$$

Mean sagittal PPs and ensemble CRPDs with the six significant coordination events were created for the retrospective unimpaired subjects and subjects with either a stiff knee gait or crouch gait pattern (Figure 5.3.10). PPs are read in a clockwise progression through the gait cycle starting at foot strike, indicated with a solid downward arrow. Foot off is indicated with a solid upward arrow on each PP and vertical line on the CRPD. For visual clarity, standard deviation bands for the PP curves are not depicted. Each percent gait cycle is indicated with a circle on the PPs.
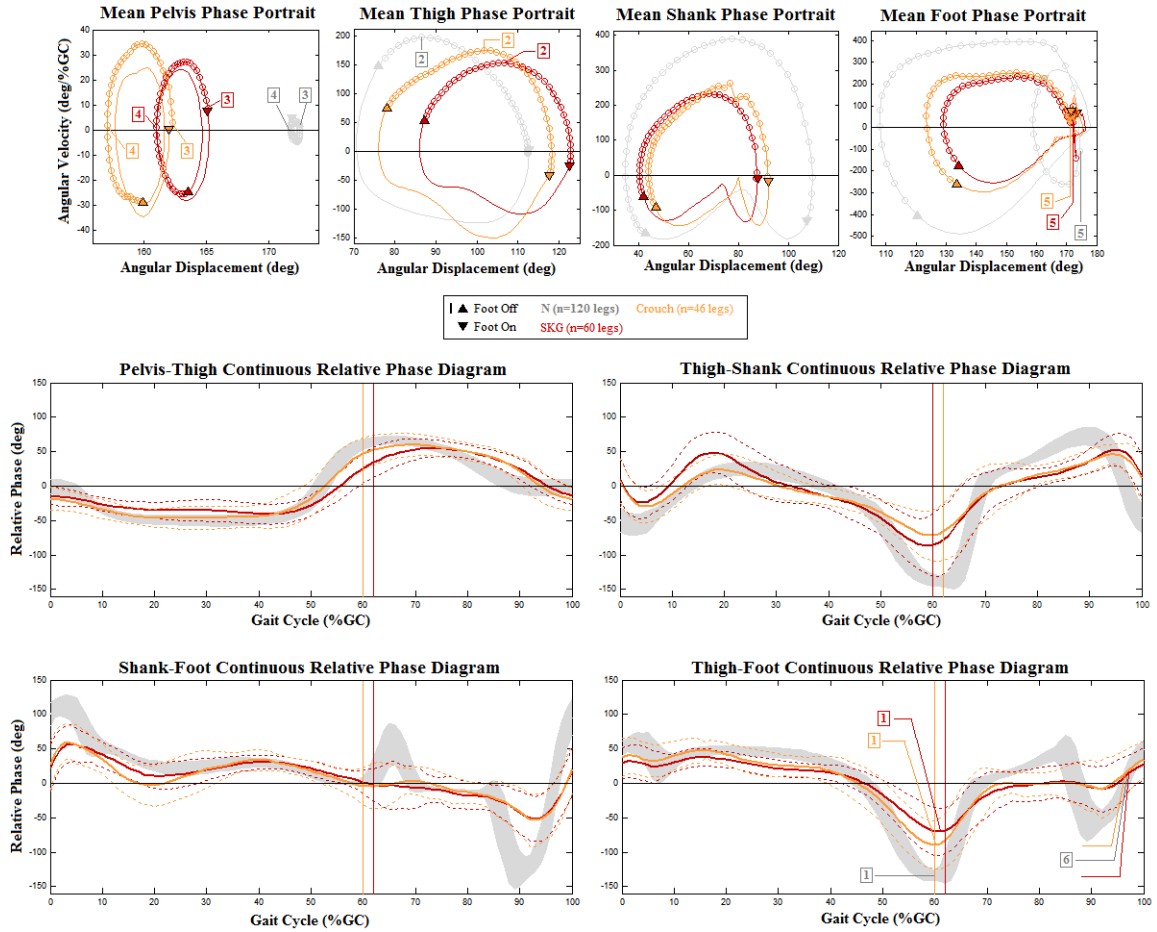
Figure 5.3.10: The six significant CEs are indicated on each cohort's corresponding PPs and ensemble CPRDs, where grey corresponds to the unimpaired subjects, red corresponds to subjects with a SKG pattern, and orange corresponds to subjects with a crouch gait pattern.

The mean (unscaled) CPS score for each gait pattern and subject group are depicted in the following figure.
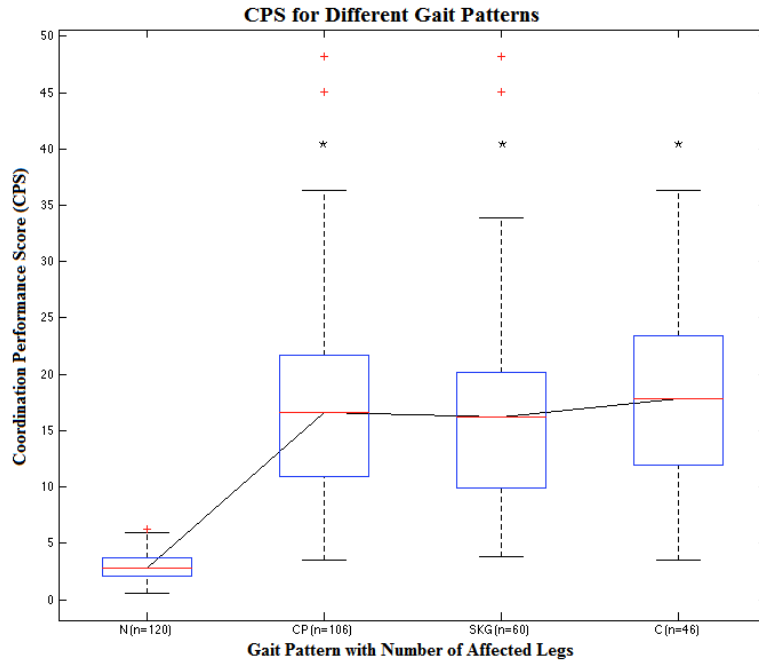
Figure 5.3.11: A box-plot of each cohort's Coordination Performance Score (CPS) is provided, where outliers are indicated with a red + and a black * indicates mean cohort CPSs that were significantly (p<0.001) from the unimpaired cohort's mean CPS.

5.3.4.3 Comparison of Two New Coordination Indices

The processes discussed in section 5.3.4.1 were also used to assess the CDI the scaled coordination performance score (CPS). Figure 5.3.12A displays the mean GDI, CDI, and CPS values for the different subject cohort categories. For all of the subject groups, there was a significant difference (p≤0.001) between their GDI and the TD group's GDIs and a significant difference (p≤0.001) between group's CDI and the TD group's CDIs. Except for the AK subject group, there was a significant difference (p≤0.001) between a group's CDIs and GDIs. Note the pattern for a reduced CDI and CPS in clinical groups follows a similar downward trend as the GDI. Figure 5.3.12B presents the mean GDI, CDI, and CPS values for the unimpaired subjects and subjects with CP when organized by GMFCS level. There were significant differences (p ≤ 0.05) between the mean scaled CPS values and each GMFCS level and between the mean scaled CPS for GMFCS levels I and III.
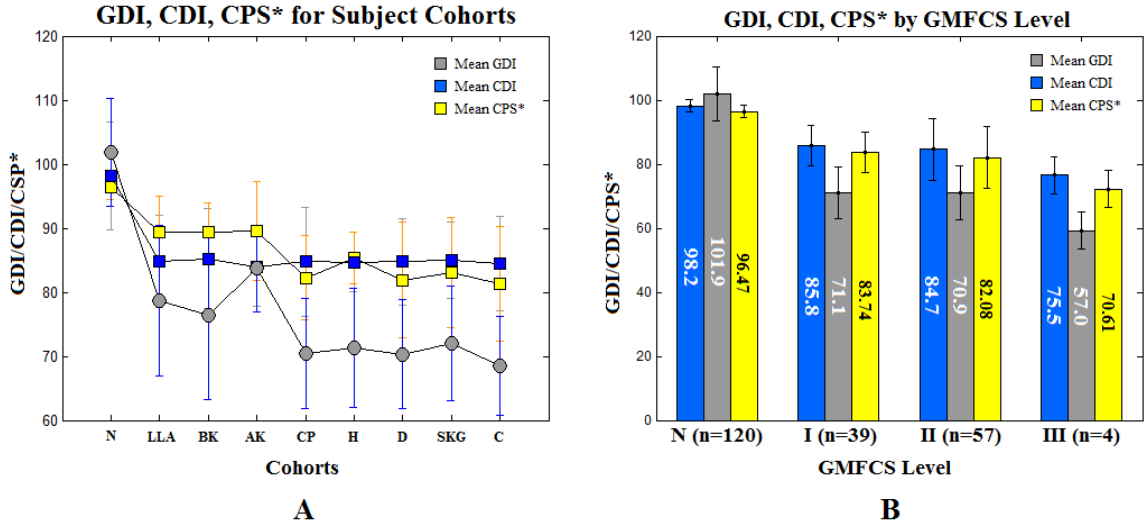
Figure 5.3.12: A) Comparison of GDI (grey square), CDI (blue square), and scaled CPS (yellow square) mean scores for each subject group: unimpaired (TD), lower limb amputation (LLA), below knee amputation (BK), above knee amputation (AK), cerebral palsy (CP), hemiplegia (H), diplegia (D), stiff knee gait pattern (SKG), and crouch gait pattern (C). B) Mean GDI (grey), CDI (blue), and CPS (yellow) values for TD and CP subjects with confidence intervals with 95% confidence intervals are presented by GMFCS level. Significant differences between groups (p≤0.05) and between GMFCS levels I and III.

Figure 5.3.13A shows the relationship between the GDI and scaled CPS values for all of the study's subjects, with a dashed line indicating the ideal unimpaired subject index value. Figure 5.3.13B illustrates the empirical normal distribution of the GDI, CDI, and scaled CPS values in relation to a theoretical cumulative distribution function. The Kolmogorov-Smirnov test confirmed the GDI, CDI, and scaled CPS values for this study's subjects were normally distributed.
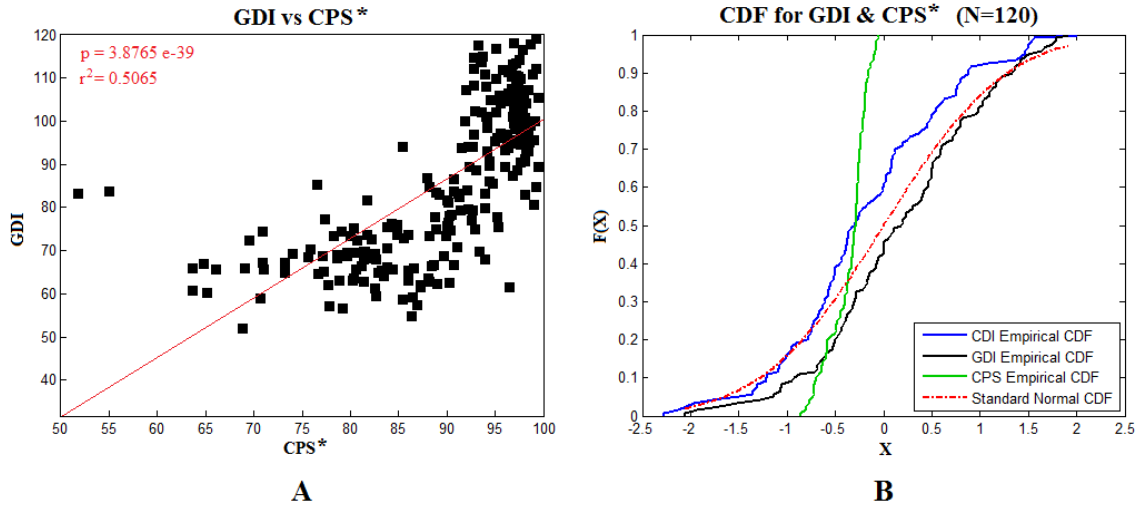
Figure 5.3.13: A) Scatter plot of all GDI scores against all scaled CPS values with the line of best fit (red). B) Cumulative distribution functions (CDF) for the GDI (black), CDI (blue), and scaled CPS (green) in comparison to the theoretical normal CDF (red).

5.3.4.4 Missing Coordination Events by Gait Pattern

In an effort to determine if there were certain gait patterns, diagnoses, or gait categories associated with the inability to achieve specific coordination events, an investigation into missing coordination events for all subjects was performed. While this investigation did not directly address Hypothesis 4A, it does contribute to the utility of these coordination measures, their interpretation for various gait patterns, and ability to isolate specific coordination dynamics critical for the completion of swing limb advancement. The percentage of subjects missing one or more coordination events for each gait pattern category, including the unimpaired group, was calculated.

For all unimpaired subjects, three different swing period coordination events did not exist for 6.34% (or 9 subjects) of this 140-subject cohort. The three missing coordination events for this cohort was the zero-crossing after absolute maximum in late swing on the pelvis-thigh CRPD (e.g. PelvThi3), inflection point between opposite foot on and the swing maximum on the pelvis-thigh CRPD (e.g. PelvThi4), and zero-crossing after the swing maximum on the thigh-shank CRPD (e.g. ThiSha4). It is interesting to note that these three coordination events were also found missing in several of the subjects with CP and subjects with a LLA. Four subjects were missing the PelvThi3 coordination event, three subjects were missing the PelvThi4 coordination event, and two subjects were missing the ThiSha4 coordination event. The following figure provides the percentages unimpaired subjects that did not have these three coordination events. The impact of not having these curve features is discussed in the next Chapter. It is worth noting that none of the missing

coordination events were selected by the regression models for use in the CPS index.
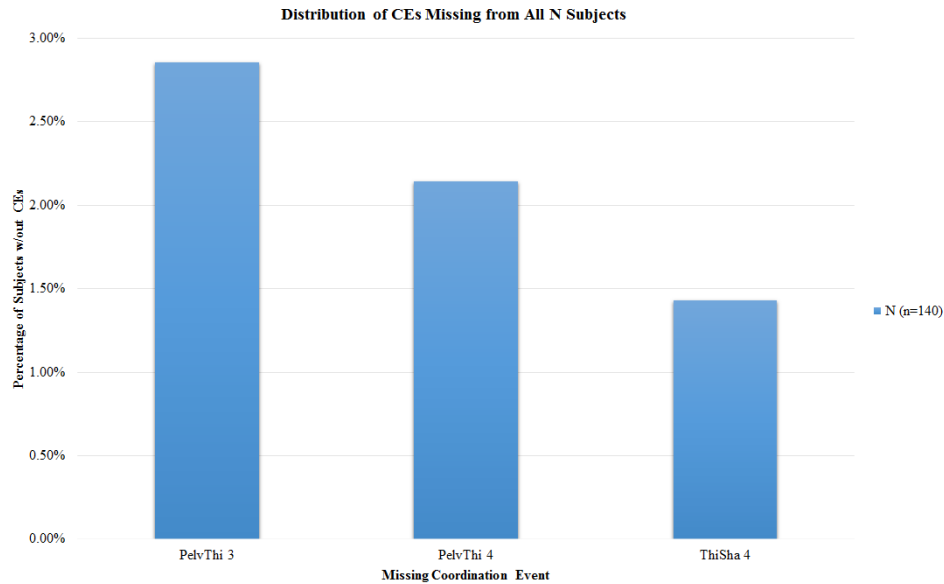
Figure 5.3.14: Percentage of coordination events (CE) missing from all unimpaired (N) subjects.

For all subjects with CP, the subjects were organized by gait pattern, topographically, and as a group. The percentage of subjects with CP that were missing at least one coordination event for each of these categories was calculated and presented in the next figure.
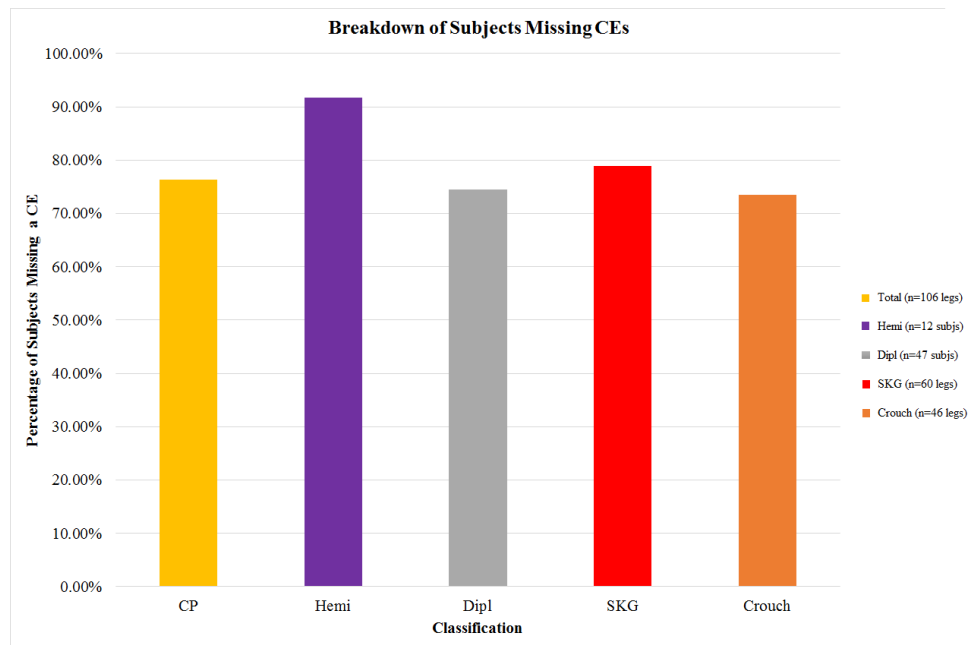
Figure 5.3.15: The percentage of subjects with CP missing at least one coordination event (CE) are displayed for each gait category: all subjects with CP, hemiplegic (hemi), diplegic (dipl), stiff knee gait pattern (SKG), and crouch gait pattern.

While further elaboration into the significance of these trends and missing coordination events for this cohort will be provided in the next chapter, it is interesting to note that over 70% of subjects of with CP were missing a least one coordination event, regardless of gait category. For the subjects with CP, ten coordination events were found to be missing and are presented in the table below.

Table 5.3.8: Description of the ten swing period coordination events missing in subjects with CP, where a superscript L and N indicate this coordination event is also missing in subjects with a LLA and unimpaired subjects, respectively.

Coordination Event	Abbreviation	Description
1) Pelvis-Thigh CPRD	PelvThi2	1st 0x in Swing
2) Pelvis-Thigh CPRD^{N,L}	PelvThi3	1st 0x after abs. max in Swing
3) Pelvis-Thigh CRPD^{N}	PelvThi4	Inflection point btwn opposite foot on and max
4) Thigh-Shank CRPD	ThiSha3	1st 0x after foot off
5) Thigh-Shank CRPD^{N,L}	ThiSha4	1st ox after swing max
6) Shank-Foot CRPD	ShaFoot3	Inflection point after swing abs. min
7) Shank-Foot CRPD^{L}	ShaFoot4	Last zero-crossing in swing
8) Thigh-Foot CRPD	ThiFoot3	2nd zero-crossing after foot off
9) Thigh-Foot CRPD	ThiFoot4	Abs. max between 1st & 2nd 0x post FO
10) Thigh-Foot CRPD	ThiFoot6	Last zero-crossing in swing

The next figure presents the distribution of missing coordination events for the various gait categories of subjects with cerebral palsy.
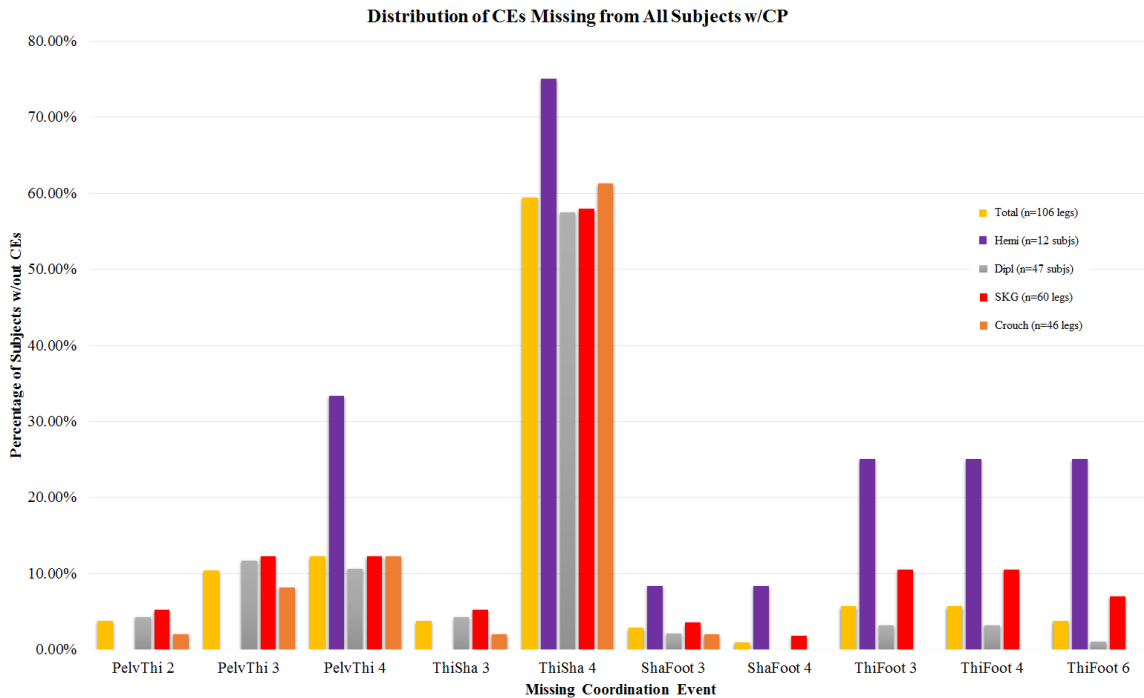
Figure 5.3.16: Percentages of coordination events missing from subjects with CP who are organized by five gait categories: all subjects with CP, hemiplegic (hemi), diplegic (dipl), stiff knee gait pattern (SKG), and crouch gait pattern.

Subjects with a LLA were organized into the following five categories: all subjects with a LLA, unilateral amputation, bilateral amputation, below knee amputation, and above knee amputation. The percentage of subjects with a LLA that were missing at least one coordination event for each of these categories was calculated and provided in the next figure.
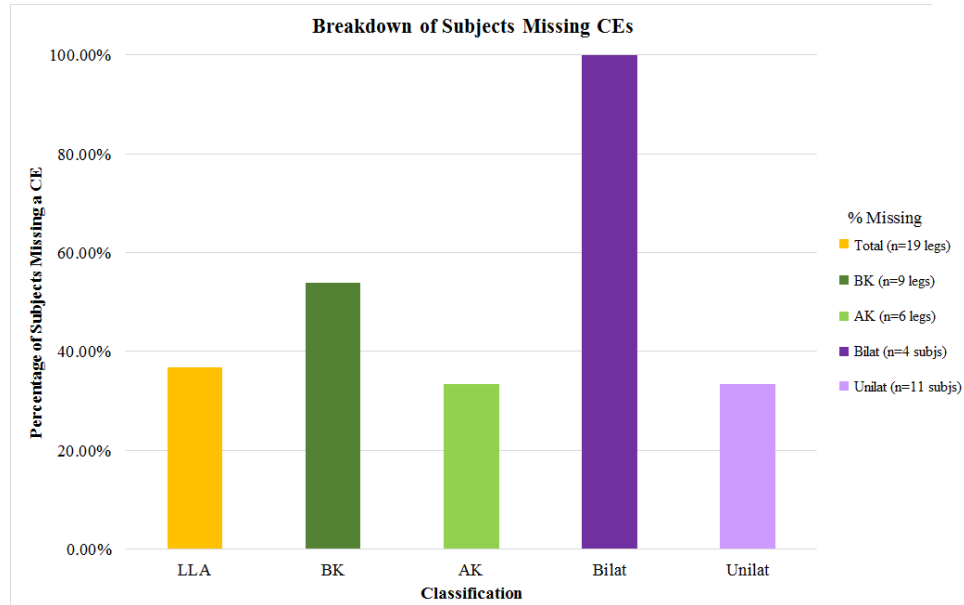
Figure 5.3.17: The percentage of subjects with a LLA missing at least one coordination event (CE) are displayed for each gait category: all subjects with a LLA, below knee amputation (BK), above knee amputation (AK), bilateral amputation (Bilat), and unilateral amputation (Unilat).

Further elaboration into the significance of these trends and missing coordination events for this cohort will be provided in the following chapter. As depicted in the following figure, for the subjects with a LLA, three coordination events were found to be missing: PelvThi3, ThiSha4, and ShaFoot4. The figure below presents the distribution of these three missing coordination events for the various gait categories of subjects with a lower limb amputation.
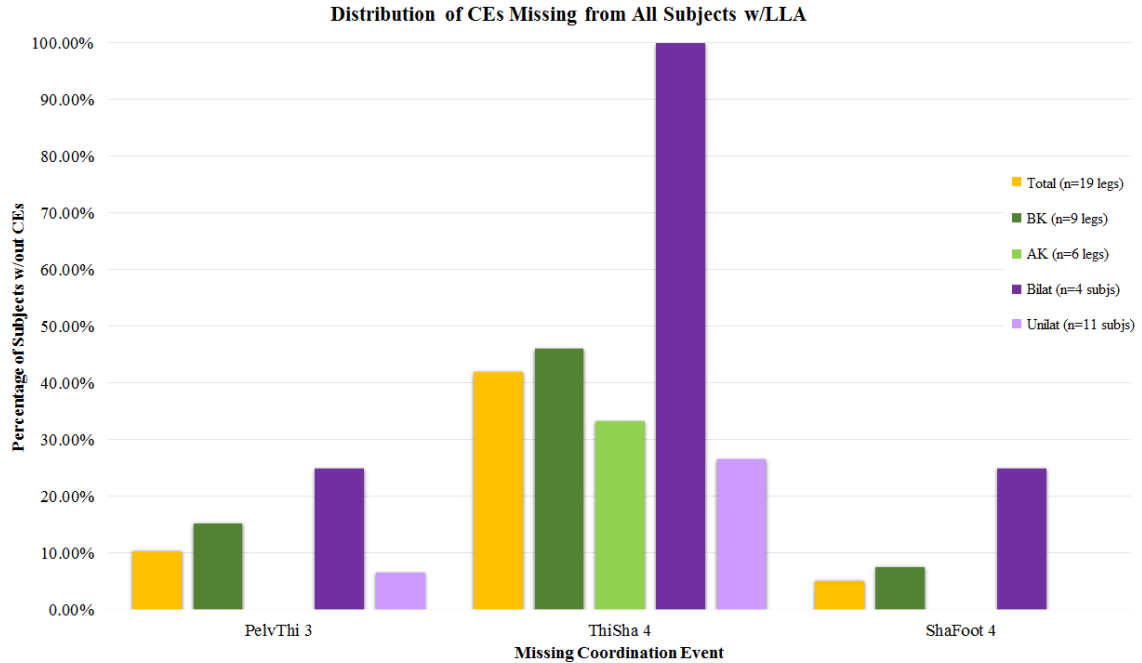
Figure 5.3.18: Percentages of coordination events missing from subjects with a LLA who are organized by five gait categories: all subjects with a LLA, below knee amputation (BK), above knee amputation (AK), bilateral amputation (Bilat), and unilateral amputation (Unilat).

5.3.4.5   Exploratory Investigation to Identify Critical Coordination Events

As discussed in section 4.5.4.2.1 of Chapter 4, three additional analyses were conducted to determine if there were salient coordination events in the swing period of gait. Results for these analyses are provided in Appendix G. The first of these analyses divided the unimpaired prospective subjects (n=20), who walked over-ground with shoes, and the unimpaired retrospective subjects (n=120), who walked barefoot over-ground. Out of thirty-seven possible coordination events, four critical coordination events (Table 5.17) met the criteria for being both independent (P$\leq$0.2) and invariant (r^2$\leq$2.5%). The mean timing, with standard deviation, and variance for each of these critical coordination events is provided in the table below and was calculated from the 120 unimpaired retrospective subjects.

Table 5.3.9: The mean timing (standard deviation) and variance for the 120 unimpaired retrospective subjects' four critical coordination events are provided along with a description of each event.

Coordination Measure	Coordination Event	Mean (SD)	Variance
1) Foot PP	Timing of maximum angular velocity	83% ($\pm$3%)	13.12%
2) Thigh-Foot CPRD	Last local minimum	89% ($\pm$2%)	4.60%
3) Thigh-Foot CRPD	Last zero-crossing	98% ($\pm$1%)	1.38%
4) Shank PP	1st zero crossing after foot off	98% ($\pm$1%)	1.34%

It is worth noting that the last inflection point of the thigh-foot CRPD was identified as a critical

coordination event by this methodology and the stepwise regression model used in the coordination performance score methods. The results supporting the following findings from the additional analyses of the critical CEs are provided in Appendix G. The timing of these four critical CEs was not found to be clinically different between these two unimpaired group samples. Secondly, it was found that age does not affect the timing of these four critical CEs. Thirdly, the four critical CEs were found to be unique and did not coincide with other gait events (e.g. temporal, critical).

5.3.5   Hypothesis 4A Results

Referring to Figure 5.3.8A, when organized by gait pattern, level of amputation, and topographically there was a significant difference ($p \leq 0.001$) between a cohort's mean CDI and GDI, except for the subjects with a transfemoral amputation. Additionally, when organized by gait pattern, level of amputation, and topographically there was a significant difference ($p \leq 0.001$) between a cohort's mean scaled CPS value and the unimpaired cohort's mean scaled CPS value. Therefore, as a consolidated index of the proposed measures of coordination dynamics, the CDI and scaled CPS detect statistically significant differences ($p \leq 0.05$) between the coordination dynamics of individuals with unimpaired, stiff knee, crouch, and mechanically altered gait patterns (Hypothesis 4A). The phase portraits and continuous relative phase diagrams for the three general subject groups (unimpaired, CP, LLA) are provided below in figure below. The phase portraits and continuous relative phase diagrams for additional subject comparisons and organizations (e.g. affected side, amputation level, topographical) are provided in Appendix G.
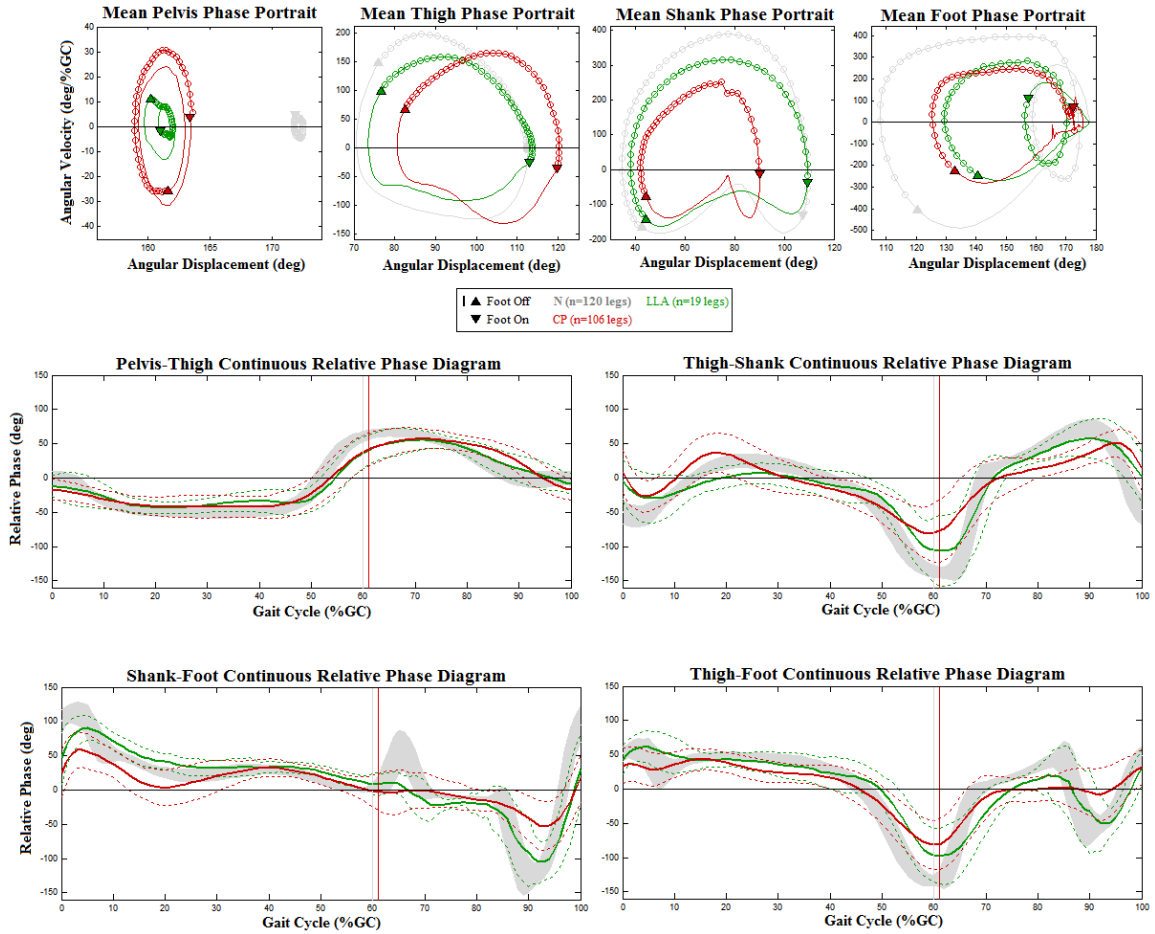
Figure 5.3.19: Phase portraits and continuous relative phase diagrams for over-ground walking for all subjects with CP (red), all subjects with a LLA (green), and all retrospective unimpaired subjects (grey).

5.4 Transtibial Amputation Case Study Results

Results for this case study are located in Appendix G.

6 Discussion

The main goals of this body of work were to 1) create a normative dataset for the proposed measures of coordination from an unimpaired cohort, 2) compare the proposed model of coordination to three clinical performances measures that describe aspects of motor control, 3) compare the motion of a theoretical compound pendulum to actual human gait data, and 4) use the proposed measures to study and compare the coordination dynamics of different clinical populations who have varying abilities to successfully and efficiently perform swing limb advancement. In addition to the retrospective subject motion capture data, prospective motion capture data was collected for the different experiments discussed in Chapter 4. The prospective experiments were designed to study the potential effects on the coordination strategies of the unimpaired subjects by varying temporal and spatial constraints during walking tasks. Additionally, potential differences in coordination strategies were studied for both over-ground and treadmill walking conditions in the prospective subjects with an atypical gait pattern. In reference to the results presented in Chapter 5 and Appendix G, the following sections discuss the results for these four different aims and the additional prospective experiments.

6.1 Discussion of Prospective Experiments

6.1.1 Over-Ground Walking Task

The unimpaired subject cohort consisted of over-ground walking data for both retrospective and prospective subjects. The measures of coordination dynamics were generated for the entire unimpaired cohort, the retrospective subjects who were barefoot for their over-ground walking, and the prospective subjects who wore shoes for their over-ground walking. The continuous relative phase diagrams (CRPD) for the prospective subjects were within one standard deviation band of the larger retrospective unimpaired cohort, indicating that there were little to no differences in the coordination strategies for barefoot and shod walking employed by these two groups. While there are some subtle differences the between prospective and retrospective subjects PPs and CRPDs, perhaps the most striking difference is in the pelvis phase portrait center location. This difference in center location of the pelvis phase portrait is most likely due to differences in placement of the sacral marker. While the marker placement of several random subjects was confirmed by clinicians experienced in motion capture, the sacrum marker could have easily been placed a few millimeters below the sacrum, thus resulting in an increase in a few degrees of posterior pelvic tilt. It was originally speculated

that some of the other more subtle differences in the prospective and retrospective subjects PPs and CRPDs maybe due to the fact that the prospective subjects wore shoes and the retrospective subjects were barefoot. The results from subsequent investigations into potential differences in these two unimpaired subject groups is addressed later in this Chapter in section 6.3.1.

Table G.1.3 in Appendix G provide the mean, standard deviation, and 95% confidence intervals for the relative phase angles at common foot floor contact events for the unimpaired prospective subjects. Not all of the unimpaired prospective cohort's mean CRPD values at essential foot contact conditions fell within the 95% confidence intervals of the unimpaired retrospective subjects' CRPD foot contact events. When examining the CRPD plots, it seems less likely that the CRPD values from the prospective subjects that were outside of these limits were because of a different coordination strategy employed while walking barefoot verses with shoes. The difference in subject sample size may skew these values and it would be interesting to see if future collection of more prospective subjects might bring these values within the retrospective subject's confidence intervals.

The CDI and scaled CPS values were calculated for the unimpaired prospective and retrospective subjects as another means for comparing their coordination curves. The GDI and CDI values for the unimpaired prospective and retrospective subjects were within one standard deviation away from the normative reference, indicating that any deviations from the reference are still within the "unimpaired" range. Similarly, the scaled CPS values for these two unimpaired subject subgroups varied only a small amount from each other and were close to the normative reference. When considering the coordination and gait indices, coordination curves, and additional analyses below comparing coordination events between these two unimpaired subject groups, there does not appear to be any clinically significant differences in the coordination dynamics. As mentioned in Chapter 4, the prospective subjects needed to wear shoes because of the treadmill walking tasks. Therefore, having different unimpaired subjects groups allows for more consistent comparisons and references for the prospective experiments and other analyses conducted to address Aims 2, 3, and 4.

6.1.2 Treadmill Walking Tasks

In general, the difference in the prospective subjects' pelvis phase portrait range of motion and angular velocity may in part be due to the fact they were wearing a harness and attached to the body weight support system. The differences in the CPRDs for these two walking conditions is indistinguishable in the unimpaired subjects, indicating that these subjects were able to adapt to the changing task constraints of walking on a treadmill verses over-ground and maintain the same inter-segmental coordination dynamics (e.g. spatio-temporal organization). For the unimpaired subjects,

the subtle differences (e.g. reduced swing period limit cycle radius, diverge to a smaller phase portrait orbit in swing) in the thigh, shank, and foot PPs appear to be the compensatory changes at the segment level that allowed the subjects to maintain a similar inter-segmental coordination dynamics between these two walking conditions. The following sections delve into more specific differences for the various prospective subject cohorts and walking tasks.

6.1.3 Prospective Unimpaired Subjects: Over-ground and Treadmill Walking

One of the experiments for the 20 unimpaired prospective subjects was to walk over-ground with shoes at a self-selected speed and then walk on a split belt instrumented treadmill at a belt speed equivalent to each subject's over-ground walking speed. One of the motivations for this experiment was to use PPs and CRPDs, which offer an alternative level of analysis and perspective of marker based motion capture data, to characterize the underlying coordination strategies employed by healthy individuals as they maintain a normative gait pattern for these two similar, yet different walking conditions. Treadmill gait training is an appealing modality for rehabilitation of patients with a neuromuscular impairment because it offers a means for task-specific gait training, repetition, manually and robotically guided assistance, systematically controlled progression of walking speed, and the option for partial body weight support. Although numerous studies have examined potential differences between over-ground (OG) and treadmill (TM) walking in order to assess the validity of this OG walking analogue, the findings from these studies are often inconclusive and conflicting [145-150]. Therefore, the motivation for this exploratory comparison was to use the proposed measures of coordination, which offer an alternative level of analysis and perspective of marker based motion capture data, to characterize the underlying coordination strategies employed by healthy individuals as they maintain a normative gait pattern for these two similar, yet different walking conditions.

From the Bernstein perspective, the central nervous system's organization of individual variables into a larger group (e.g. synergy) during a movement decreases the degrees of freedom in the system and allows for simpler control strategies, which in the case of bipedal gait result in complex oscillatory patterns [7-10]. A fundamental principle from the dynamic systems theory perspective of motor control is that the task, environment, and individual all influence the resultant motor behavior [109]. Small changes in any of these elements can result in an altered movement pattern. For example, during treadmill walking the moving belt drives the support limb backwards under the relatively stationary center of mass as opposed to over-ground walking where the center of mass is rotated over the stance limb, much like an inverted pendulum [56]. In addition to differences in task constraints, environmental changes contribute to differences in sensory information (e.g. optic flow

information) and have been shown to alter an individual's gait pattern [151,152]. Findings from Lee et al proposed the changes in muscle activations and kinetics could be attributed to how subjects are able to achieve a walking pattern, characterized by temporal gait parameters and kinematics (i.e. joint angles), that is similar between over-ground and treadmill walking. While walking, individuals with an intact nervous system are able to integrate this large amount of information about the orientation of limb segments, task, and environment and develop a motor plan that consolidates these elements and organizes the position and timing of the leg into a coordinated gait pattern.

Carollo, et al (2002) proposed the hypothesis that one behavioral goal of ambulation is to maintain kinematic patterns. When considering this hypothesis and the Bernstein perspective of motor control, it is then perhaps of no great surprise that often little to no statistically significant differences in kinematic curves between over-ground and treadmill walking for healthy individuals are reported. Incorporation of dynamic systems theory measures as a complement to traditional instrumented gait analysis measures provides valuable insights in into the underlying coordination strategies that contribute to an asymmetrical or atypical a gait pattern. As previously discussed in Chapter 3, phase portraits and continuous relative phase diagrams from dynamic systems theory provide a different perspective for studying a gait pattern by describing individual segments in phase space and coordination dynamics (e.g. position and timing) between any two segments; adjacent or non-adjacent [137]. To quantify the complex coordination dynamics used to maintain a normative gait pattern during these two different walking conditions, low dimensional measures encapsulating the position and timing of both individual and multiple segments are required. Measures that quantify the underlying coordination dynamics contributing to an aberrant gait pattern are essential to capitalize upon the rehabilitative benefits of treadmill gait training.

The kinematic curves for these prospective subjects are within the expect ranges for a normal gait pattern. The coefficient of variation values for this group's kinematic curves similar to those reported by Winter (1983), supporting the hypothesis that subjects try to maintain a normative kinematic pattern during these two walking conditions. In general, the magnitude of kinematic variables during treadmill walking were reduced, which supports the position that changes in amplitude of spatial variables were made by the subjects in order to comply with the reduced swing time. While there are statistically significant differences between some of these conventional measures, it is difficult to determine if differences are also clinically significant. Consistent with previously reported studies, the subjects had shorter step lengths, shorter stride lengths, reduced swing time duration, and slower walking speeds during TM walking [146,153]. Changes in the subjects' gait patterns described by conventional instrumented gait analysis measures are proposed to be accomplished by altering the

timing and organization of the following four mechanisms, elucidated by coordination dynamics, that are essential for successful completion of swing limb advancement.

The remaining paragraphs of this section discuss how the inclusion of PPs and CRPDs to examine the gait of these individuals for these two different walking tasks provides an alternative level of analysis and perspective into the underlying coordination dynamics of a gait pattern. As the thigh PP trajectory rate of change decreases and approaches an abscissa zero-crossing (e.g. maximum angular displacement), the foot PP trajectory is accelerating as the foot approaches a horizontal orientation with respect to the floor and transitions from plantarflexion to dorsiflexion (e.g. near ankle kinematic zero-crossing). This change in relationship between these two segments manifests as a local maximum on the thigh-foot CRPD, which is predominantly influenced by the foot PP phase angle because the thigh PP phase angle is approximately zero. The attenuation of this extremum during treadmill walking means the subjects increased the rate of change in the foot PP trajectory (e.g. position and velocity) in order to sufficiently advance the foot in time for the up-coming foot strike and compensate for an overall reduced swing period duration.

Once the foot is located ahead of the hip joint center, the pendular motion of the leg segments and momentum from hip flexion contributes to completion of swing limb advancement (e.g. passive knee extension) [26]. A significant reduction in the magnitude of the shank's maximum angular velocity during treadmill walking coincides with the PP trajectory beginning to noticeably diverge to a smaller orbit from the over-ground trajectory causing a reduced pendular velocity and displacement of the shank for the remainder of swing period. Other studies reporting shorter swing period duration have also observed increased cadence and shorter step length, all of which can be attributed to decreased hip and knee extension, in part as a result of the altered pendular motion of the contralateral support limb as moves backward by the tread and rotates about the hip instead of the inverted pendular motion about the ankle during OG walking [143,145,153]. Considering these altered pendular mechanics of the legs, the temporal-spatial and kinematics of the leg segments during terminal swing can be further expounded upon by the abated shank PP trajectory during treadmill walking. The diminished PP trajectory revealed the shank phase angle caused an attenuation of the shank-foot CRPD absolute maximum, thigh-foot CRPD local minimum, and foot PP maximum angular displacement and minimum angular velocity. The significantly delayed and reduced foot minimum angular velocity and maximum angular displacement, occurring just after the foot is oriented horizontally, is predominantly due to the shank's pendular motion because there is a small amount of change in the ankle joint angle during terminal swing. Since there was a general trend of delayed and attenuated swing events during treadmill walking, there was less time to swing

the tibia forward from vertical and the subjects compensated by increasing the phase angle rate of change (e.g. spatial adjustment of the shank to meet temporal constraint of impending foot strike).

Findings from this prospective experiment demonstrate how sagittal plane PPs and CRPDs quantify coordination dynamics and reveal the inherent mechanisms underlying the swing period gait patterns of 20 unimpaired subjects during over-ground and treadmill walking. It was proposed that if the underlying coordination dynamics of healthy subjects could be used to explain how these individuals maintained a normal gait pattern for these two different walking conditions, then PPs and CRPDs may also provide clinically meaningful insights and valuable information for therapeutic modalities that strive to use a treadmill for the rehabilitation of individuals with neurologically based gait impairments.

This prospective experiment demonstrated how PPs and CRPDs complement conventional IGA measures and by describing movement at the level of coordination, these dynamic systems theory (DST) based measures explain the mechanisms underlying temporal-spatial and kinematic differences observed between OG and TM walking. While findings from this study indicate there are different coordination dynamics employed during these two walking tasks, a general decision as to whether or not TM walking is a suitable analogue to OG walking is intentionally left unanswered because the investigator feels such a decision should consider each patient and role of TM usage in rehabilitation before selecting the corresponding level of motion capture data analysis that best characterizes these factors and goals. For example, if TM walking is utilized to address asymmetries and overall gait performance or improve the range of joint angles during the task of gait then temporal-spatial measures or joint angles are appropriate descriptors for these aspects of gait. If inter-segmental coordination, changes in motor control strategies, or motor learning are the goals of TM walking then using PPs and CPRDs to quantify the organization of segments at the level of coordination satisfies this perspective of gait. The alternative perspective of motion capture data offered by these nonlinear tools, provides a means to understand the underlying mechanisms adopted by healthy subjects to maintain a normal gait pattern when presented with the altered temporal and spatial constraints of TM walking. The enhanced perspective of gait offered by PPs and CRPDs may provide valuable clinical insights for patients who struggle with achieving the critical mechanisms of swing limb advancement, contributing to an atypical gait pattern, and help determine how TM walking might be used to address such aberrant coordination dynamics.

6.1.4 Prospective Subjects with Cerebral Palsy: Over-ground vs. Treadmill Walking

Guided treadmill training for individuals with cerebral palsy has been adopted in an effort to improve atypical motor patterns using practice and experience by expanding the range of movement options for the individuals [16,154]. Several researchers have proposed the motor behavior of individuals with CP during treadmill training emerge from the dynamical interaction of the central nervous system, biomechanical elements, psychological factors, and the environment [155-158]. Therefore, the development of measures that capture the motor behavior of this dynamical system is important to improve and optimize the connection between clinical research and clinical treatment. As it has previously been proposed throughout this body of work and by others, the application of dynamic systems theory measures (e.g. PP, CRPD) offer a framework for characterizing segmental interactions and inter-segmental coordination [155-158]. This prospective experiment comparing the over-ground and treadmill walking coordination of individuals with cerebral palsy provides one example application of how scientifically validated findings from these measures may provide such a connection and fill the need for measures of coordination dynamics to help study atypical motor patterns.

Individuals with cerebral palsy (CP) often have difficulty walking on a treadmill when the belt speed is set to the individual's preferred over-ground walking speed. Therefore, many therapeutic interventions on the treadmill try to incrementally increasing the treadmill speed to challenge the individual's motor learning system with the goal of obtaining improved coordination at a walking speed comparable to the individual's over-ground walking speed. This trend was consistent for the treadmill belt speed used for three prospective subjects.

In general, all of the phase portrait orbits were significantly reduced when the prospective subjects with CP walked on the treadmill. Most notable were the shift in posterior pelvic tilt, reduced thigh speed, reduced thigh extension, diminished foot speed, and more circular and reduced foot trajectory. There was not a detectable difference in the pelvis-thigh CRPD during swing and the remaining CRPD curves are attenuated from the subjects' over-ground walking. Conventional gait measures show the subjects had decreased walking speed, shortened step length, reduced step time, It is proposed that the PPs and CRPDs for these two walking conditions reveal the underlying motor control strategies that resulted in these altered kinematics and temporal-spatial measures. Specifically, the subjects increased pelvic tilt to compensate for reducing the amount of thigh extension and instead of modulating the thigh speed throughout swing limb advancement the subjects extended the thigh at a more constant rate. As discussed in Chapter 2, hip hiking and circumduction are two common

compensatory gait adaptations employed by individuals with SKG and C gait patterns to advance and clear the swinging limb. The prospective subjects with CP in this experiment also adopted these compensatory strategies. Specifically, the inter-segmental coordination between the thigh-foot and shank-foot capture these mechanisms in the noticeable attenuation of these CRPDs. Recalling the equation for calculating the relative phase angle and previously discussed curve features, it is proposed that the reduced the involvement of the foot for these compensations manifests in these CRPDs' as 1) attenuated curve indicating less interaction between the segments, and 2) shift toward zero indicating the segments are moving more in-phase with each other. While only three of the four prospective subjects with CP were able to walk on the treadmill, there was a considerable range in their overall functional abilities. Future investigations that examine the treadmill and over-ground gait and coordination strategies for a larger subject size, perhaps organized by functional ability, is warranted. While this experiment is not directly connected to a hypothesis, these findings support the overall proposal that these measures detect changes in segmental spatio-temporal organization and inter-segmental coordination.

6.1.5 Prospective Unimpaired Subjects: Treadmill Walking at Various Speeds

Similar to the other prospective experiments, the main goals of this exploratory prospective experiment was to 1) determine if the unimpaired subjects altered their gait pattern to compensate for the temporal changes of the walking task imposed by increasing the TM belt speed and 2) use the proposed measures of coordination to identify changes in the segmental organization and inter-segmental coordination strategies adopted by this unimpaired cohort. As presented in Chapter 3, coordination in the cyclical task of gait requires the elegant balance between both the spatial and temporal organization of the segments. Therefore, it was proposed that the unimpaired subjects would be able to account for changes in spatial demands of walking on a treadmill at various speeds and adopt a normative gait pattern similar to their treadmill gait pattern.

The unimpaired subjects were able to adapt to the changes in temporal constraints of walking on the treadmill at various speeds by adjusting the spatial and temporal relationship of segments. As the treadmill belt speed increased, the subjects increased the swing period velocity of the thigh, shank, and foot, while maintaining close to the same segment angular displacements at foot off and foot strike. By changing the temporal constraints of the walking task, the subjects responded by changing the timing of the segments' positions by altering the temporal organization (velocity). Interestingly, the CRPD diagrams for these various treadmill walking speeds showed little differences in shape or curve features. As the treadmill belt speed increased, the rate of dissociating the

thigh-foot extension synergy near foot off (thigh-shank, thigh-foot CRPDs) increased reflecting the reduced time the subjects had during swing to initiate swing limb advancement and place the segments in an orientation that resembled the gait pattern during a self-selected walking speed. Additionally, the timing of the local maximum on the shank-foot CRPD shifted sooner toward foot off and also captures this reduced time to clear the foot during swing limb advancement as a result of the decreased swing period time when the treadmill belt speed increased. The results from this experiment not only support the overall proposal that these measures detect changes in segmental spatio-temporal organization and inter-segmental coordination, but they also demonstrate these measures are able to detect changes in only the temporal elements of coordination when subjects are imposed with temporal task constraints.

6.1.6   Changes in Assistive/Resistive Forces Task

The main goals of this exploratory prospective experiment was to 1) determine if the unimpaired subjects altered their gait pattern to compensate for the effects of an assistive force and a resistive force on the advancing limb and 2) use the proposed measures of coordination to identify the segmental organization and inter-segmental coordination strategies adopted to achieve these changes in their gait patterns. In general, it was observed during data capture that in approximately less than 30 seconds the subjects were able to find a motor program that resulted in the (subject perceived) the most efficient (least perceived exerted effort) gait pattern that most closely resembled their preferred treadmill walking pattern. All of the subjects chose to reduce the motion of the thigh, shank, and foot while also increasing trunk involvement (flexion for resistive forces, extension for assistive forces). Additionally, the rate the segments advanced and moved (PP trajectory) became more constant and exhibited less of the finely modulated rates in their regular treadmill and overground walking trials. As reported by the gait and coordination indices in the corresponding results section for this experiment, the subjects were able to maintain a relatively normal gait pattern by modulating the spatio-temporal interaction of their leg segments and draw upon an intact nervous system to find an alternative gait strategy. Perhaps the most important and exciting finding from this particular experiment, in regards to the aims and overall goals of this body of work, is that these subjects adopted a different walking strategy when presented with spatial constraints and these measures of coordination dynamics were able to detect those changes.

6.1.7 Changes in Joint Range of Motion Tasks

It was proposed that these dynamic systems theory based measures are more suitable for characterizing motor control strategies contributing to a gait pattern, quantify organization of individual segments, identify mechanisms of change, and loci of impairment. Since the fundamental organization of the leg segments during gait is linked to gait pathology and guides the rationale for interventions, it was hypothesized that incorporating PPs and CRPDs into instrumented gait analysis will open new avenues for understanding the complexity of coordination and allow clinicians the means to more effectively and efficiently treat patients with neuromuscular gait impairments. The purpose of this set of prospective experiments was to restrict the range of motion for the knee and ankle in subjects free of gait pathology and explored coordination strategies adopted by the unimpaired cohort in relation to the coordination dynamics of individuals with pathological gait patterns. The results from this set of experiments provide a context for the utility of these measures as a complement to conventional IGA measures. The results from these three experiments not only support the overall proposal that these measures detect changes in segmental spatio-temporal organization and inter-segmental coordination, but they also demonstrate these measures are able to detect changes in both the temporal and spatial elements of coordination when subjects are imposed with only spatial task constraints (e.g. restricted joint range of motion).

6.1.7.1 Fixed Knee Extension

The unimpaired subjects made several gait pattern compensations to adapt to the unilateral restricted range of motion about the knee joint imposed by a knee brace. When the knee brace was fixed in full extension, the shape of the pelvis-thigh and thigh-shank CRPDs for the unimpaired subjects is delayed during swing, much like individuals with a stiff knee gait pattern (SKG). Similar to subjects with SKG, the CRPDs for the unimpaired subjects are considerably attenuated. These spatio-temporal changes depicted in the CRPDs capture the cohort's changes in motor control strategies during gait. The unimpaired subjects chose to restrict the dynamic range of motion of the foot and thigh while walking and instead use a combination of hip circumduction and hip hike to clear the advancing swing limb. Individuals with a SKG pattern commonly employ these same compensatory strategies for swing limb advancement. Also the change in hip (e.g. thigh) motion is captured by the thigh phase portrait's shift toward increased extension (thigh angular displacement closer to 90° with respect to global horizontal). It is proposed these limb advancement strategies are partially captured in the sagittal plane curves by the leftward shift of the thigh phase portrait. This

shift indicates the thigh remained slightly more in flexion than when the subjects walking without fixed knee extension. This lateral shift may also reflect the compensatory motions in the coronal plane, but since the focus of this investigation is sagittal plane coordination dynamics it is difficult to distinguish tri-planar compensatory motions and any effect on sagittal plane motion.

Although the ankle was not directly affected by the knee brace, the unimpaired subjects also restricted range of motion at the ankle. This foot compensatory strategy is easily detected on the foot's phase portrait, which has a reduced limit cycle radius and missing local minimum just after foot off on the shank-foot CRPD. The restricted range of motion for the thigh, shank, and foot adopted by the unimpaired cohort is reflected in the reduced circumference of each segment's phase portrait.

Since the phase portraits are normalized to the gait cycle and plotted to show each percentage of swing with a circle, it is also interesting to note the rate of change for the thigh and shank phase angles is fairly constant throughout swing as opposed to varying the rate these two segments advanced in preparation for foot contact. Due to the nature of the experiment, it is difficult to determine if any differences in spatio-temporal curve features are due to walking on a treadmill (unimpaired cohort) verses over-ground walking (subjects with SKG). The differences in pelvis PP magnitudes and center location between the subjects with a SKG and the unimpaired subjects with fixed knee extension may be because the unimpaired subjects did not have any restrictions at the hip joint that often occurs in individuals with cerebral palsy. Overall, it is exciting to note that these proposed measures of coordination dynamics captured changes in motor control strategies, quantified the reorganization of individual segments, and can be used to identify mechanisms of change.

6.1.7.2   Fixed Knee Flexion

The unimpaired subjects made several compensations to their gait pattern to adapt to the restricted range of motion about the knee joint when the knee brace was fixed at 60° of flexion. When the knee brace was fixed in flexion, the shape of the pelvis-thigh CRPD for the unimpaired subjects is almost identical to the subjects with a crouch gait pattern. As with the condition with fixed knee extension, the thigh-shank and shank-foot CRPDs were considerably attenuated and local curve features were attenuated. These changes demonstrate the ability of the CRPD to capture organizational changes of segments (e.g. inter-segmental coordination).

Even though the ankle was not directly affected by the knee brace, the unimpaired subjects chose to restrict the dynamic range of motion while walking with their dominant leg in fixed knee flexion.

156

To compensate for the imposed mechanical constraint at the knee the unimpaired subjects reduced their step length and relied upon increased hip flexion to advance the leg and prolonged dorsiflexion clear the limb during swing. These individual segmental compensations are seen in the thigh and foot PPs' shift right toward more flexion (angular displacement closer to 180° with respect to global horizontal) and reduced limit cycle radius. Also this self imposed restricted range of motion at the ankle is easily detected by the lack of a local minimum just after foot off on the shank-foot CRPD. Overall, it is exciting to note that this experiment demonstrates how the proposed measures of coordination dynamics captured changes in motor control strategies, quantified the reorganization of individual segments, and can be used to identify mechanisms of change.

6.1.7.3 Fixed Ankle Dorsiflexion

Individuals with a transtibial amputation have lost the ability to actively control the motion of joints below the level of amputation and must rely upon the properties of the prosthesis at foot off and during swing limb advancement. By fixing the ankle motion to neutral in the unimpaired prospective subjects, it was proposed there would be compensatory strategies proximal to this fixation that may be similar to the gait pattern of individuals with a transtibial amputation. By using the proposed measures of coordination dynamics to compare the gait pattern of the unimpaired prospective subjects during this condition to the gait pattern of the retrospective subjects with an amputation, the opportunity to examine any differences at the level of coordination would be possible.

Similar to the subjects with a transtibial amputation, the foot PP characteristics of the unimpaired subjects was almost identical and supports the experiment's ability to mimic the "foot" motion of the individuals with an amputation using the ankle brace in the unimpaired subjects. As can be seen in the PPs for these two subject groups, the differences in a segment's position and velocity from the unimpaired retrospective reference increased as the distance of a segment increased from the restricted joint. Additionally, the pelvis and thigh PP reveal the unimpaired subjects relied upon increased anterior pelvic tilt (more horizontal with respect to the global horizontal) and increase thigh extension to advance the swinging limb. This reorganization about the ankle for the more proximal segments was also detected by these measures of coordination dynamics in the pre-doctoral investigation discussed in Chapter 2. The findings from this prospective experiment further support the proposal that individuals with a lower limb amputation who are free of neurological pathology are able to re-organize the spatio-temporal interactions between the residual limb's segments and the prosthesis, as detected by the proposed measures of coordination dynamics. Furthermore, by

analyzing the gait pattern with these coordination measures an alternative perspective into an individual's movement strategies may offer valuable clinical insights that could enhance therapeutic interventions. Since this group of individuals with a lower limb amputation (free of neurological pathology) are able to draw upon the remaining degrees of freedom, account for the inertial properties of their prosthesis, and find another motor solution to gait in order to adopt a relatively normal gait pattern, these strategies and changes may not be detectable with conventional IGA measures thus further supporting the inclusion of PPs and CRPDs when investigating the coordination of a subjects gait pattern. The lower limb amputation case study presented throughout this body of work elaborate this position and provide an additional investigation into the proposal that these IGA measures (PP, CPRD) are detecting different aspects of gait than conventional IGA measures.

6.2 Discussion of Aims and Hypotheses

The following section of this chapter addresses the results from the experiments, models, and analyses corresponding to the four aims and their corresponding hypotheses.

6.2.1 Aim 1

Capabilities of the individual and constraints of the task and environmental all influence the emerging coordination patterns of any movement. Due to the enormous number of variables associated with these three factors, a low dimensional normative reference becomes essential in assisting with the identification of aberrant motor control strategies in subjects with atypical gait patterns resulting from a neuromuscular impairment. The two dynamic systems theory based measures presented in this body of work (e.g. PP, CRPD) complement traditional instrumented gait analysis measures by sharing a common origin of marker trajectories and consolidate the complex relationships and organizational strategies of the leg segments intrinsic to gait. Similar to how normative kinematics and kinetics offers a comparative framework for research and clinical instrumented gait analysis, hopefully by sharing this normative dataset of coordination dynamics will be more readily considered and embraced by both communities. As discussed in Chapter 1, the objective of the first aim was to generate a reference dataset of coordination measures in the sagittal plane coordination for the pelvis, thigh, shank, and foot segments and segment pairings (pelvis-thigh, thigh-shank, shank-foot, thigh-foot) from a large group of individuals free of gait pathology. This reference dataset was then assessed to determine if the proposed measures of coordination dynamics characterize a normal gait pattern.

While PPs and CRPDs are calculated differently than joint kinematics, the coefficients of variation (CVs) for each PP and CRPD are of similar magnitude to the kinematic CVs published by Winter (1983). This finding is logical because the CV describes the extent of variability in these trajectory-based measures that are derived from the same marker set. The sample size, demographic ranges, low CVs, narrow confidence intervals for foot contact conditions, and small CRPD standard deviation bands are evidence that these curves characterize the behavior of normal coordination dynamics in gait. These findings demonstrate the robustness of these coordination patterns across this cohort's considerable demographics and capture the subject-to-subject variability inherent in gait. Elaboration and development of the dynamic systems theory methods used to generate this normative data set provide the next step necessary to make these techniques clinically useful and become integrated with existing instrumented gait analysis measures.

In addition to developing a normative reference for the following aims and hypotheses, the results and unimpaired dataset contribute to the general understanding of healthy gait. While instrumented gait analysis techniques have advanced greatly, there is still a need for more enlightening techniques to improve our understanding of gait strategies and coordination. Healthy gait data is often presented in literature as an afterthought or as a control group for pathological applications. Rarely are there concerted efforts to improve our understanding of the natural variability in gait patterns, so that we may then begin to improve our understanding of pathology. Creating a normative reference of these measures of coordination dynamics during walking is essential for improving our understanding of atypical gait patterns because it provides the means to discover insights into how the nervous system is imposing functional constraints on the limbs. Therefore a normative reference from a large cohort of individuals with unimpaired gait is critical for interpreting coordination findings in individuals with neurological disorders (Aim 2, 4).

It was also proposed that the lack of a unifying and consistent methodology, normative reference, and clinically meaningful demonstrations of the important motor control insights offered by these nonlinear measures have slowed their incorporation into instrumented gait analysis. A normative reference from a large cohort of individuals is critical for understanding normal gait and for interpreting coordination findings in individuals with neurological disorders. Therefore, in an effort to continue advancing the application of dynamic systems theory techniques in locomotion and following the rationale for developing a clinically useful normative reference, as was conducted for conventional instrumented gait analysis measures, this aim provided a normative reference for coordination dynamics constructed from a large cohort of subjects free of gait pathology.

6.2.1.1   PP and CRPD Curve Features

The normative reference set of coordination curves provides the foundation for delineating specific curve features of atypical and typical gait patterns. Extrema of the abscissa and ordinate measures in a PP assist in identifying an individual segment's position and velocity at that instance in the gait cycle and provide insights into how one segment is contributing to the orientation of the entire limb. CRPD extrema indicate the amount and timing of out-of-phase coordination or uncoupling between two segments (Stergiou, 2004). Conversely, the zero crossing on a CRPD indicates the segments are in-phase with each other (Stergiou, 2004). An inflection point demarcates the instant when the relationship between the two segments has reversed and thus the instant when muscle synergies begin changing (e.g. from flexion to extension). Finding the PP and CRPD values corresponding to the percent gait cycle of other common gait evens becomes effortless when these dynamic systems theory measures have been normalized to the gait cycle. The small confidence intervals of the relative phase angles from each CRPD for the four essential footfall conditions of a normal gait cycle show there is great potential for using CRPDs to quantify coordination events. This normative reference can be used in future investigations to elaborate upon findings from this dataset by exploring relationships between PP and CRPD curve features and other conventional instrumented gait analysis measures.

Curve features from CRPDs and PPs can also be used to quantify changes to the neuromuscular system's organization in response to an intervention, identify which segment changed the most post-intervention, and reveal the underlying mechanisms of change. In the example for a subject with a stiff knee gait pattern, the standard surgical treatment for this gait pattern is a rectus femoris transfer, which removes the biomechanical constraint of an extension synergy that promotes the undesirable prolonged coupling of the lower extremity during swing limb advancement (Gage, 1987). Changes in the spatio-temporal organization of segments from this surgical intervention may afford some patients an opportunity to adopt changes in motor control strategies that result in attenuation of this extension synergy and thus achieve more efficient swing limb advancement. Changes in the thigh-foot CRPD minimum quantifies changes in selective motor control strategies between pre and post-intervention and is a means to identify mechanisms of change within a gait pattern. This additional information may aid in the rehabilitation strategies employed to help optimize a patient's benefits from an intervention or treatment.

6.2.2 Aim 2

Since there is presently not a standard method for quantifying coordination dynamics during the cyclical task of gait, the proposed measures of coordination dynamics were compared to three clinical analogues. The purpose of Aim 2 was to then explore the relationship between the proposed measures of coordination dynamics and select clinical performance measures from three clinical analogues that characterize aspects of coordination. Recall from the methods discussion in Chapter 4, that the results from these tests only pertain to the prospective subjects.

6.2.2.1 Hypothesis 2A

It was hypothesized that impairments in the speed and accuracy of voluntary reciprocal movements, as tested by a timed, spatially constrained lower extremity tapping task, would be significantly correlated with task specific coordination deficits characterizing selective motor control. Results presented in Chapter 4 and Appendix G support this hypothesis for the prospective subjects with cerebral palsy. As predicted, the accuracy of target taps increased with target size for all of the prospective subjects with cerebral palsy. Also as expected, the forward swing leg speed increased as target size increased for both subject groups and was significantly slower for the subjects with cerebral palsy than the leg swing speed of the unimpaired subjects. There was also a significant difference in the target accuracy and forward swing leg speed between the unimpaired subjects and the subjects with cerebral palsy. This indicates there was as difference in both the speed and accuracy of these two cohorts for this voluntary reciprocal tapping motor control task.

The timing and magnitude of the maximum instantaneous slope during initial swing of the thigh-shank CRPD was found to be significantly different between the two prospective subject groups. Compared to the unimpaired cohort, the mean ensemble thigh-shank CRPD for subjects with cerebral palsy was attenuated and the occurrence of this coordination event was significantly delayed and shallower. The CRPD's maximum instantaneous slope is a measure of the rate the two segments change dominance. Individuals with a stiff knee or crouch gait pattern are known to have difficult dissociating the thigh and shank segments during initial swing as a result of the impaired motor control due to cerebral palsy. The high correlations between this thigh-shank CRPD maximum instantaneous slope and the forward swing leg velocity for subjects with cerebral palsy indicates this coordination event is capturing these subjects' difficulty with dissociating these two segments at this critical time in swing limb advancement. The low correlation between this coordination event and forward swing limb speed for the unimpaired subjects is consistent with this interpretation and

is expected since this subject group does not have any difficulty with this critical motor task in initial swing. These exciting findings demonstrate certain curve features from CRPDs are capable of characterizing motor control and can detect how varying degrees of motor control impairment affect an individual's gait pattern. Since these proposed measures of coordination dynamics are constructed from marker trajectories, which is the fundamental measurement collected during instrumented gait analysis, they can be used to quantify motor control during gait and do not require additional data collection. Using these measures to quantify an individual's coordination dynamics during gait also alleviates the need to perform additional discrete motor control tasks, none of which are directly analogous to walking, in an effort to indirectly characterize this fundamental element of gait.

It is also interesting to note that the thigh-shank and thigh-foot CRPD minimum near foot off are both highly correlated with the subsequent maximum instantaneous slope and inflection point in the initial to mid swing periods of the gait cycle. These correlations emphasize the importance of the magnitude and timing of this precursor coordination event (e.g. dissociate of thigh-foot extension synergy) and its influence on the coordination dynamics and coordination events for the remainder of swing limb advancement. Although this hypothesis did not exhaustively explore the relationship between the speed-accuracy trade-off during a reciprocal tapping task and the proposed measures of coordination dynamics, these findings support further investigations of these measures and their clinical and research applications.

6.2.2.2 Hypothesis 2B

It was hypothesized that the degree of selective motor control impairments, as tested by the Selective Control Assessment of the Lower Extremity (SCALE), would be significantly correlated with task specific coordination deficits. As presented in Chapter 5, there was a significant difference between the SCALE scores for the unimpaired subjects' and the subjects with cerebral palsy. This indicates there was a difference in these two cohort's ability to perform the selective voluntary motor control tasks.

Since the voluntary selective motor control SCALE tasks of the lower extremity joints are similar to the ability to voluntarily dissociate various synergies during initial swing, it is perhaps of no great surprise that three CRPD coordination events were found to be significantly different between the two subject groups. These three coordination events also quantitatively reveal how the inter-segmental interactions are contributing to a delayed occurrence of critical swing period gait events and offer a mechanistic explanation as to why individuals who struggle with initial swing coordination events are then playing catch up for the remainder of the gait cycle. First, the timing and magnitude

162

of the thigh-shank CPRD minimum near foot off was significantly delayed and attenuated for the subjects with cerebral palsy. This finding indicates that the subjects with cerebral palsy were unable to dissociate the thigh-foot extension synergy at foot off to the same degree and as quickly as the unimpaired subjects and as a result the segment positions were restricted and limited. This finding is consistent with the descriptions of stiff knee and crouch gait patterns in Chapter 2 and demonstrates these proposed measures of coordination dynamics are able to quantify this aberrant motor behavior during the task of gait. The second significant coordination dynamics finding was the rate at which the thigh and shank changed dominance was significantly slower for the subjects with cerebral palsy. The maximum instantaneous slope on the thigh-shank CRPD captures this inter-segmental relationship. The shallower slope for subjects with cerebral palsy captures the difficulty these subjects have with changing segment relationships at the ideal speed. Considering that spasticity is velocity dependent, then it is proposed that the subjects' spasticity is triggered and prevents them from changing segment relationships at a faster speed. The third significant coordination dynamics finding was the timing of the thigh-foot CRPD inflection point in the initial swing period of the gait cycle. This CRPD event corresponds to the instant when two segments begin to change behavior and is again proposed to reflect how the subjects' spasticity delays the timing of when a subject can change segmental relationships. While the relationship between voluntary motor control during gait and the proposed measures of coordination dynamics are not exhaustively discovered, these exciting findings support further investigations of these measures and their clinical and research applications.

6.2.2.3 Hypothesis 2C

It was hypothesized that cerebellar based impairments in spatial accuracy of movement and dynamic balance, tested by lower extremity tasks from the International Cooperative Ataxia Rating Scale (ICARS) and Scale for the Assessment and Rating of Ataxia (SARA), would be significantly correlated with task specific coordination deficits. There was not a significant difference between the ICARS/SARA score for the unimpaired subjects and the subjects with cerebral palsy. However, the small sample size of prospective subjects with cerebral palsy may have contributed to this statistical result. It is also important to note that these two performance tests were originally designed for and validated with individuals diagnosed with cerebellar ataxia, which is a completely different etiology of motor control impairment than that of individuals with cerebral palsy. Two measures were calculated from two of the walking tasks performed by subjects as part of the ICARS/SARA experimental tasks.

The first of these measures was the base of support width during tandem and over-ground walking. Based upon other research studies reported in the literature, it was postulated that a larger base of support would indicate an increased difficulty with dynamic balance during these two walking conditions. There was not a significant difference between the base of support width for the unimpaired prospective subjects and the prospective subjects with cerebral palsy during over-ground walking. Again, this statistical result could be influenced by the fact that only one of the prospective subjects with cerebral palsy who was able to perform the tandem walking task. This one subject was classified at level one of the Gross Motor Function Classification System, indicating little to no impairment with over-ground walking. The base of support width during over-ground walking for all prospective and retrospective subjects was then calculated and revealed statistically significant differences between the two clinical cohorts and the unimpaired cohort. This finding confirms the proposal that the subject groups with impaired or altered motor control adopt a larger base of support in order to ease the dynamic balance requirements of maintaining a bipedal gait pattern and prevent falling.

The second measure derived from these ICARS/SARA tasks was the curvature of the center of mass' trajectory while turning left and right while walking. Based upon other research studies reported in the literature, it was proposed that wider turn radius (e.g. a smaller curvature) during a turn would indicate difficulty in performing the turn and thus impaired coordination and dynamic balance. However, as reported in Chapter 5, there was not a significant difference in the curvature between the two prospective subject cohorts. After reviewing the video and motion capture data of the subjects while they performed this walking task, it was discovered that the subjects with cerebral palsy would slow their walking speed considerably prior to and during the turn and then pivot on the inside leg to change directions. This pivoting technique caused a tighter turn (larger curvature) that was similar to or larger than the turning curvature of the unimpaired subjects. When considering the turn curvature in the context of the adopted movement strategy, the axiom that a smaller curvature is indicative of pathology is too simplistic of a generalization and may be misleading when viewed in isolation. This conclusion about this measure is further supported by the low correlations between the ICARS/SARA score and the maximum curvature for subjects with cerebral palsy.

In regards to the differences in curvature values for the left and right turns of subjects with cerebral palsy, it is proposed that the difference in curvature values is related to the subjects' topographical category. Of the four prospective subjects with cerebral palsy, two were classified as diplegic and two were classified as hemiplegic. Since all four subjects were affected on the right

side and only two were affected on the left side, the curvature of the right turns was larger than the curvature of the left turns because of the number of affected limbs was greater for the right turning tasks. While the relationship between various functional elements of gait (e.g. postural control, dynamic balance) and the proposed measures of coordination dynamics are not exhaustively explored in this hypothesis' tests, these findings support the ability of these measures to characterize varying degrees of coordination ability during gait and warrant further investigation.

6.2.3 Aim 3

The hypotheses of Aim 3 were designed to test the construct validity of the long held analogy that the motion of the legs during swing period is like a passive compound pendulum. Several software simulations using the mathematical pendular model and subject motion capture data were run to compare the motion of a theoretical double pendulum to the sagittal plane motion of the thigh and shank during the swing period of gait for various clinical cohorts.

When examining each cohort's summed residuals (e.g. rankings) for the four different damping conditions, several insights into their underlying coordination dynamics are revealed. The angular displacements of the thigh and shank for the subjects without neurological pathology (e.g. unimpaired subjects, subjects with lower limb amputation) differed more from the theoretical model than the angular velocities of these segments. However, the angular displacement and angular velocity of the thigh and shank segments for the subjects with cerebral palsy differed nearly the same amount from the theoretical model. When considering the velocity dependent nature of spasticity in cerebral palsy, which results in limited range (e.g. angular position) of motion for segments, it makes sense that the gait patterns affected by spasticity would deviate from the theoretical model in descriptors of both position and velocity.

Except for the un-damped condition, the subjects with an above knee amputation were the closest to the theoretical pendulum model. Since individuals with a transfemoral amputation do not have any neurological control at and below the knee joint, they rely upon the inertial properties of their prosthesis to advance the prosthetic limb forward during the swing period of gait. The other subject groups (e.g. unimpaired, stiff knee gait, crouch gait) have some neurological control at the knee, even if it is undesirable, which creates variable damping during swing limb advancement. Considering these differences in the knee joint properties for these different subject categories, it makes sense that those with a lower limb amputation are the closest to the theoretical pendulum model. As mentioned in Chapter 5, future investigations with larger subject sizes could be conducted to determine if the summed residuals for the different damping conditions are clinically meaningful,

what is a clinically trivial interval, and what thresholds are clinically significant.

6.2.3.1 Hypothesis 3A

It was hypothesized that subjects with a lower limb amputation would have coordination dynamics measures with the smallest residual when compared to a passive double pendulum. This was found to be true when subjects were organized by gait pattern. The subjects with a below knee amputation were the closest to the theoretical pendulum. The results from this analysis support the hypothesis that when subjects were organized by general pathology (e.g. unimpaired, cerebral palsy, lower limb amputation) the individuals with a below knee amputation were closest to the theoretical pendulum. The subjects with a lower limb amputation were the closest to the un-damped theoretical pendulum. Based upon these findings, it is proposed that the sagittal plane motion of the thigh and shank during swing for individuals with a lower limb amputation, especially for a transfemoral amputation, is the subject gait pattern that most closely resembles the motion of a passive compound pendulum.

6.2.3.2 Hypothesis 3B

It was hypothesized that subjects with cerebral palsy would have coordination dynamics measures with the smallest residual when compared to an over-damped double pendulum. Results from this analysis did not support this hypothesis when subjects were organized generally by gait pathology (e.g. unimpaired, cerebral palsy, lower limb amputation) and more specifically by gait pattern (e.g. stiff knee gait, crouch gait, amputation level). Of the four damping conditions considered, the subjects with cerebral palsy differed the most from the theoretical pendulum. When the subjects were organized by gait pattern, the subjects with cerebral palsy also differed the most from all damping conditions of the theoretical pendulum. Therefore, it is proposed that based upon these findings, the sagittal plane motion of the thigh and shank during swing for individuals with cerebral palsy is not that of a passive compound pendulum but instead variably damped compound pendulum that is influenced by segment velocity (e.g. spasticity).

6.2.3.3 Hypothesis 3C

It was hypothesized that subjects free of gait pathology would have coordination dynamics measures with the smallest residual when compared to a critically damped double pendulum. Results from this model simulation supported this hypothesis when the subjects were organized generally

by gait pathology. In fact, when organized by gait pathology, the motion of the unimpaired subjects' thigh and shank was the closest of the three subject groups to the theoretical model for the under-damped, critically damped, and over-damped conditions. However, when subjects were organized by gait pattern the results from the model simulation did not support this hypothesis. For the under-damped and critically damped conditions, the unimpaired subjects were ranked second when organized by gait pattern. Although it is difficult to draw conclusions about the rankings, these findings for these damping conditions may indicate the amount of variable damping employed in unimpaired swing limb advancement lies somewhere between these two damping conditions. Future work using more advanced modeling techniques or variable damping functions might reveal the damping profile of the hip and knee joints for unimpaired subjects during swing limb advancement. It is proposed that based upon these findings, the sagittal plane motion of the thigh and shank during swing for individuals free of gait pathology is not that of a passive compound pendulum but instead an elegantly controlled, variably damped compound pendulum.

6.2.4 Aim 4

After establishing a normative reference, comparing these measures of coordination to clinical analogues, and contrasting the pendular motion of the leg during swing to a theoretical pendulum model, the next logical step in developing these coordination measures was to demonstrate they are able to distinguish between different gait patterns of populations with different physiological reasons for impaired swing limb advancement. While this fourth aim is by no means the final step needed before clinical adoption of these measures it is an essential precursor to the dissemination and hopefully adoption of these measures of coordination dynamics by researchers and clinicians in the instrumented gait analysis community.

As discussed in Chapter 1, there is currently not a gold standard for measuring the coordination dynamics of the leg segments during gait. While the proposed model of coordination dynamics uses two low dimensional descriptors (e.g. phase portraits, continuous relative phase diagrams), comparing these measures for large subject cohorts and for each gait cycle time epoch still results in large cumbersome datasets. Therefore in an effort to consolidate these descriptors of coordination into a simple scalar value, two indices of coordination dynamics were created from phase portraits and continuous relative phase diagrams. The first coordination deviation index (CDI) is based upon feature component analysis and was constructed using the entire gait cycle. The second metric, the coordination performance score (CPS), was constructed from significant coordination events occurring during the swing period of gait. After developing these two novel metrics, additional

167

analyses were performed to explore the applicability of these new coordination indices in describing gait pathology for subjects with cerebral palsy or a lower limb amputation. As discussed below, the results from these additional analyses justify the use of these indices to quantify differences in coordination dynamics between various subject groups. These novel indices were then used to quantitatively test this aim's hypothesis and determine whether the proposed model of coordination dynamics is capable of distinguishing between the various pathological gait patterns considered in this body of work.

6.2.4.1 The Coordination Deviation Index

Instrumented gait analysis has become the most commonly used method for quantifying certain aspects of an individual's gait pattern, informing clinical decisions, and assessing treatment outcomes [1,2] in individuals with various motor deficits including cerebral palsy [1,2,3], lower limb amputation [4,5]. In an effort to consolidate the large amount of complex information captured during IGA, several indices have been proposed to quantify gait deviations from a normative reference [6,7,8]. In particular, the gait deviation index (GDI) quantifies changes in an overall kinematic (e.g. joint angle) pattern and its growing popularity in clinical and research applications is a testament to the value and usefulness of such an index. While the GDI has been shown to detect deviations in gait pathology affecting joint angles [7,8,9], this dissertation proposes an index of coordination based on the underlying coordination dynamics as a meaningful and appropriate complement to the GDI when studying the gait pattern of individuals with aberrant coordination. Therefore, a coordination deviation index (CDI) was constructed from sagittal plane PPs and CRPDs. This new coordination index was then compared to the GDI and Gross Motor Function Classification System (GMFCS) level of individuals with varying degrees of motor impairment.

While the manifestation of motor disorders in individuals with cerebral palsy (CP) is complex and uniquely expressed, there are common gait patterns [14] used to describe this group's inability to achieve various spatial and temporal aspects of gait (e.g. gait events and tasks [15,16], decreased step length and walking speed [15,16,17]). Individuals with a lower limb amputation, while from a different etiology than CP, have underlying coordination impairments linked to their gait patterns that limit their ability to perform critical gait events (e.g. decreased walking speed [18], delayed and insufficient peak knee flexion [5], excessive hip flexion [4, 5]).

Molloy et al., 2010 evaluated the relationship of the GDI and gross motor function by using the Gross Motor Function Classification System (GMFCS) and demonstrated the GDI distinguishes between different GMFCS levels in individuals with CP. To evaluate the CDI's ability to stratify gait

pathology related to coordination, we also analyzed the relationship between the GMFCS levels for individuals with CP. Since increasing amputation level for individuals with a LLA has been shown to decrease functional gait abilities [4], the CDI's ability to detect differences in coordination due to amputation level was also examined.

An index constructed from PPs and CRPDs, which describe movement at the level of coordination, provides clinicians and researchers with a metric that may be more meaningful and appropriate in describing the underlying mechanisms of gait pathology. For example, the CRPD measure of inter-segmental coordination describes selective motor control impairments in individuals with CP. Likewise, the CRPD describes coordination strategies and reorganization of segments by individuals with a LLA that result from inertial consequences of amputation and wearing a prosthetic. In conjunction with the normative reference dataset from a large cohort of subjects free of gait pathology constructed in Aim 1, the consolidated metric for indexing the severity or degree of deviation from typical coordination presented in this paper provides an additional application of these coordination measures and hopefully helps ease the incorporation of these techniques into clinical and research applications.

The overall objective of this sub-investigation was to explore the applicability of the CDI in describing gait pathology for two cohorts with different reasons for coordination deficits. The specific aims of this sub-investigation were to 1) generate a coordination deviation index using the GDI methodology for these groups, 2) compare CDI scores of the groups using the GDI as a benchmark to describe varying degrees of gait performance in these distinct groups, and 3) demonstrate that the magnitude of coordination impairment (CDI) corresponds to the magnitude of kinematic impairment (GDI). The results presented in Chapter 5 from these analyses show the CDI is capable of distinguishing between varying levels of gait impairment, the CDI followed similar trends as the GDI for the various clinical groups, and the CDI detected varying levels of motor impairment (e.g. as characterized by GMFCS levels) for individuals with cerebral palsy.

As indicated in Figure 5.3.8A, subjects with gait pathology (e.g. CP, LLA) had significantly reduced CDIs than those free of gait pathology, which is a consistent with trends from other studies using kinematic based indices [6,7,8,9]. Although the patterns of the various cohorts' CDI scores follow the same trend as the GDI scores, the GDI values were significantly different ($p \leq 0.05$) from the CDI values in all subject groups except for those with an above knee amputation. However, if the sample size of this subject group (n=6 legs) was increased there may be a statistically significant difference between the group's GDI and CDI values. Similar to the GDI, decreases in the CDI reflected increases in the diagnosis severity (e.g. topographically, level of amputation). The scatter

plot (Figure 5.3.9A) of the GDI versus CDI shows there is a moderate relationship between the two indices. The significant spread of points suggest these two indices measure different aspects of gait, which further supports the rationale for developing an index based upon coordination dynamics to complement conventional gait analysis measures.

The GMFCS has become the benchmark measure for classifying the functional gait ability of individuals with cerebral palsy [20]. It was hypothesized that as individual's GMFCS levels increased, the CDI would decrease and thus reflect the index's ability to characterize varying levels of coordination impairment affecting gait. As illustrated in Figure 5.3.8B, the CDI value indeed decreased with diminishing gross motor function, as characterized by the GMFCS. Significant differences between the mean CDI and each GMFCS level as well as between GMFCS levels I and III indicate the CDI distinguishes between different levels of coordination impairment. When considering the functional differences between GMFCS levels I and III, it makes sense that the coordination measured in the motion capture environment would more easily differentiate between these two levels than levels I and II. These results further support the theoretical construct of these dynamics systems theory measures and observations from other studies showing that PPs and CRPDs quantify the behavior of coordination [21,22]. Furthermore, the CDI demonstrates these nonlinear measures can be used to distinguish between varying levels of motor function in relation to one's ability to perform the cyclical task of gait.

Six coordination features accounted for 98% of the total variance and were used to reconstruct a subject's coordination dynamics curves (PPs, CRPDs). One disadvantage of using feature analysis is that it requires large normative reference datasets, which many labs may not have. The normative reference dataset used to create the CDI is approximately one third the size of the GDI's reference dataset and is a limitation of this study and this type of feature analysis. It is expected that increasing the number of samples in the normative reference would result in reconstructed subject curves that are closer to the original coordination curves and smooth the reconstructed curves, which presently have sharper extrema due to the sample size and sampling of the gait cycle (2% increments). It is expected that increasing the normative dataset for the CDI would not invalidate the study's findings since the minimum required number of samples (612 samples) for single value decomposition is exceeded with the current normative dataset. Rather it is expected that using a larger normative dataset to create the control features and increasing the number of clinical subjects in each category would result in greater distinction between the cohorts' CDI values, like the subjects' GDI values. In the accompanying electronic addendum, the control features used in this paper are provided along with a clearly defined process for calculating a subject's CDI.

While the CDI was generated from sagittal plane coordination curves, which has been shown to be the plane with significant deviations especially for individuals with CP [14], this index could easily be expanded to incorporate coordination curves from the other two planes of motion. Results from this study's analyses supports further development of the CDI as a complementary measure to the GDI and demonstrate the CDI captures pathology not represented in kinematic based analyses. These findings provide evidence supporting these coordination measures (e.g. PP, CRPD) describe varying degrees of gait performance in subjects with both musculoskeletal and neurological impairments and the use of these measures to characterize subjects with atypical coordination that contributes to an overall aberrant gait pattern. As the GDI is often used to quantify changes in kinematics from an intervention or over time, the CDI may also be a valuable research tool because it provides a deeper level of understanding about the mechanisms associated with changes in joint angles by reflecting the underlying organization of segment oscillations during gait.

Feature analysis was used to create an index of coordination dynamics from PPs and CRPDs and provides a concise metric of the amount an individual's coordination deviates from a normative reference. This investigation demonstrated this new coordination index can distinguish between different gait patterns in two clinical cohorts with different etiologies affecting their coordination and thus ability to produce a typical gait pattern. Comparisons between the GDI and CDI found that while these two indices follow similar trends in various clinical groups, they measure different aspects of gait. Therefore, the CDI may prove to be a valuable research tool for studying populations with impaired motor control because it provides a deeper level of understanding about the mechanisms associated with changes in joint angles by reflecting the underlying organization of segment oscillations during gait.

6.2.4.2 The Coordination Performance Score

Although a variety of gait indices have been presented in the literature (e.g. Gillette Gait Index [1], Gait Deviation Index [2], Gait Performance Score [3]) and are widely accepted measures of gait pathology, all of these indices are constructed exclusively from joint angles and the indices using feature analysis require a large number of normative reference subjects, which may not be available for many labs. Since phase portraits and continuous relative phase diagrams are dynamic systems theory derived nonlinear methods that quantify the timing and position of an individual segment and pairs of segments, these nonlinear techniques were used to quantify the behavior of coordination during the swing period of gait [4,5,6]. An index created from measures more suitable for characterizing motor control mechanisms that contribute to walking, may be more meaningful and

appropriate for studying the gait of individuals with aberrant coordination. Therefore, employing a similar methodology to the gait performance score presented by Baker et al, 2008, statistically significant curve features from PPs and CRPDs were identified and used to create a coordination performance score (CPS). Additionally, these significant coordination events were used to create two nominal regression models capable of distinguishing between unimpaired and impaired gait patterns for individuals with cerebral palsy.

In Chapter 3, coordination was defined as the organization of the timing and position of individual segments and segment pairs during the cyclical task of gait. Successful completion of swing limb advancement is a critical gait achievement because it advances and clears the foot and in anticipation of initial contact, coordinates the timing and sequencing of segments with feed-forward motor control mechanisms. It was assumed that the coordination of limb segments is individual to the mover and influenced by significant coordination events that are required to achieve normal foot contact and constrain the coordination solution. While the methods employed here can be applied to the entire gait cycle, this sub-investigation focused on the critical task of swing limb advancement because it advances the leg, affects footfall for the next cycle, and requires the appropriate coordination and control of body segments [9]. Elucidating the coordination dynamics of this complex task requires a methodology capable of isolating an individual segment's contribution to the system's behavior and identifying the timing and sequencing of adjacent and non-adjacent segment pairs. As discussed in Chapter 3, PPs and CRPDs are low-dimensional measures that satisfy this need because they quantify the pendular like motion of the legs and respective segments during the continuous, cyclical task of gait [4,5,6].

Identifying significant coordination events during the swing period of gait for a cohort of unimpaired subjects provides a means to enhance the understanding of feed-forward motor control strategies employed in swing period gait and offers a reference for subjects with atypical coordination resulting in impaired swing limb advancement. Extracting specific curve features from PPs and CRPDs to identify coordination events demonstrates the clinical utility of these nonlinear measures as a complement to traditional instrumented gait analysis measures. Using significant coordination events from PPs and CPRDs to describe movement at the level of coordination provides clinicians and researchers with a metric that may be more meaningful and appropriate when studying a gait pattern's intrinsic coordination dynamics. Additionally, using techniques derived from these coordination measures to distinguish between different gait patterns demonstrates the value of these measures and their ability to provide a different, yet complementary perspective of instrumented gait analysis data by elucidating underlying individual segment positions and timing that contributes

to a gait pattern. In addition to the methodology and large normative reference provided in Aim 1, the CPS and regression models presented in this body of work provide two additional means to help facilitate the incorporation of these coordination dynamics measures into clinical and research instrumented gait analysis applications.

The overall objective of this sub-investigation was to explore the applicability of curve features from PPs and CRPDs to describe gait patterns with various degrees of coordination impairment. Using stepwise regression models to identify significant swing period coordination events, the CPS was constructed from curve features from sagittal plane PPs for the pelvis, thigh, shank, and foot and CPRDs for the pelvis-thigh, thigh-shank, shank-foot, and thigh-foot segment pairings. The specific aims of this sub-investigation as to 1) determine if significant coordination events existed during the swing period of gait, 2) generate a coordination index from these significant events for three different gait patterns, and 3) determine if these significant events could be used to create regression models capable of distinguishing different gait patterns.

Deciphering the Significant Coordination Events. As presented in Chapter 5, a backward stepwise regression model was used to identify six significant coordination events during the swing period of gait. While more detail is provided in Chapter 3 about various curve features of PPs and CRPDs, a brief review of these curve features is provided here for convenience. Extrema of a PP's abscissa and ordinate measures assist in identifying an individual segment's position and velocity at any instant in the gait cycle and provide insights into how one segment's oscillations are contributing to the orientation of the entire limb. A CRPD zero crossing indicates the two segments are moving in-phase with each other [7], whereas an extremum indicates the instant when the two segments are most out-of-phase with each other [7]. A CPRD inflection point corresponds to when the relationship between the two segments has reversed and thus is the instant when muscle synergies are changing (e.g. flexion to extension). By comparing the timing and potential absence of these significant coordination events from atypical gait patterns to an unimpaired reference, these curve features offer a means for identifying the exact timing during the gait cycle when segment(s) are contributing to an aberrant coordination behavior and specifying which segments are contributing to an impaired gait pattern.

Using the aforementioned curve feature definitions, the following paragraphs offer an interpretation of the six significant coordination events with respect to an unimpaired gait pattern. The thigh-foot CRPD's absolute minimum corresponds to the dissociation of the extension synergy at foot off and the ability to correctly time this essential motor control event is imperative for the initiation of swing period and successful swing limb advancement [16]. The ability to provide suf-

173

ficient forward momentum of the leg segments at foot off and forward pendular motion of the leg is captured in part by the timing of the maximum angular velocity of the thigh's PP. The magnitudes of the maximum and minimum angular displacements of the pelvis PP correspond to the anterior/posterior pelvic range of motion necessary for uninhibited forward rotation of the thigh. The foot's maximum angular displacement, with respect to the global horizontal, indicates the foot's maximum vertical orientation, which corresponds to the timing of foot clearance in swing by active dorsiflexion. The last inflection point of the thigh-foot CRPD corresponds to the instant when the thigh and foot relationship reverses in preparation for foot strike and anticipation of loading response. These significant coordination events also suggest swing period coordination is constrained by the foot's oscillation toward dorsiflexion as it begins to lead the thigh's oscillation. The timing of the six coordination events was compared to the unimpaired cohort's mean timing of Perry's critical gait events [9] and found to not coincide with these other gait events.

The importance of the timing and magnitude of these significant coordination events is demonstrated by the unimpaired cohort's narrow standard deviation and the convergence of events for both individual segments and also nonadjacent segments. By identifying coordination events in the swing period of gait for a cohort of typical subjects, these findings provide a means to enhance the understanding of feed-forward motor control strategies employed in a typical gait pattern and thus offer a reference for subjects with atypical coordination resulting in impaired swing limb advancement. The small standard deviations and narrow confidence intervals of the unimpaired cohort's coordination events also suggest that although each unimpaired individual has unique swing period coordination, an individual's spatio-temporal solution of the available degrees of freedom converges upon shared coordination requirements [1,4,5,17]. Although the existence of these six coordination events indicate there are instances in a normal gait pattern that share common points in the solution of swing limb advancement, an individual's desired variability is preserved as illustrated by the various curve patterns and trajectories between these coordination events. We propose that these underlying, fundamental coordination events describe instances of a preferred state of the motor control system and as a reference, have the potential to illuminate when and how impaired swing limb advancement is manifesting in a gait pattern.

Since individuals with CP are known to have reduced walking speeds [16,26,29,69] and delayed or absent critical gait events during swing period [16,26,29,69], then it is perhaps of no great surprise that the timing and magnitude of these significant coordination events was delayed and attenuated for these subjects (Figure 5.3.10). However, prior to this investigation the underlying mechanisms contributing to the inability to achieve certain swing period gait events, as often characterized by

174

reduced range of motion in joint angles and decreased temporal-spatial variables, had not been identified at the segment level or non-adjacent inter-segmental perspective.

Assessment of the Coordination Performance Score. As shown in Figure 5.3.12, relative to the unimpaired subject group, the CPS values are reduced in the general cohort with CP and the respective subdivisions (stiff knee gait, crouch). There were statistically significant differences between all CP group mean CPS values compared to the unimpaired subjects' mean CPS. These findings support that the CPS is capable of distinguishing between the coordination dynamics of subjects with and without a gait impairment associated with aberrant coordination.

As shown in data presented in Chapter 5, relative to the unimpaired subject group, the CPS values are reduced in the general cohort with CP and the respective subdivisions (stiff knee gait, crouch). There were statistically significant differences between all CP group mean CPS values compared to the unimpaired subjects' mean CPS. These findings support that the CPS is capable of distinguishing between the coordination dynamics of subjects with and without a gait impairment associated with aberrant coordination. Both the CDI and CPS were created from measures more suitable for characterizing motor control mechanisms that contribute to walking and therefore may be more meaningful and appropriate metrics for studying the gait patterns of individuals with aberrant coordination. One advantage of the CPS over the CDI is the techniques used to create this index. By creating an index from significant coordination curve features, the requirement for a large number of normative reference subjects by feature analysis methods is removed. Additionally, this approach to creating a coordination index allows for the easy expansion of significant coordination events during stance and other planes of motion without creating a cumbersome increase in data necessary for calculating the index or generating its normative reference.

Regression Models for Distinguishing Coordination of Different Gait Patterns. While both qualitative [10,15] and quantitative [16,17] classifications for various gait patterns exist using conventional instrumented gait analysis measures, an algorithm created from measures of coordination would provide clinically meaningful information that may assist clinicians and researchers studying the gait of those with impaired motor control. An index and gait classification model constructed from these low-dimensional measures of coordination are free of linear assumptions found in other quantitative gait classification techniques (e.g. principal component analysis, support vector mechanics, cluster analysis), when normalized to the gait cycle are easily related to other gait events, do not require a large reference normative dataset like other techniques, consolidate a segment's spatio-temporal oscillatory behavior, and represent the progression of the limit cycle's trajectory throughout the gait cycle. The high area under the curve (AUC) value for the unim-

paired vs. impaired regression model's receiver operator characteristic (ROC) curve indicates the model's outstanding ability to distinguish between these two general gait pattern categories. The moderate AUC value for the stiff knee gait vs. crouch gait model's ROC curve indicates this model has moderate ability to distinguish between these two gait patterns using only two swing period coordination events. Since the gait pattern of those with cerebral palsy is often a mix of several patterns (e.g. stiff knee gait, crouch), the incorporation of other coordination events occurring in stance period and other planes of motion may increase the AUC value for this regression model and improve its ability to distinguish between these two pathological gait patterns. Another benefit of using regression models to distinguish between gait patterns is that the regression equation and logit can be rearranged to solve for the probability an individual has one of the gait patterns considered.

Example Applications of the CPS. The CPS may be a valuable research tool because it provides a deeper level of understanding about the underlying mechanisms associated with the organization of segment oscillations during swing limb advancement in a concise scalar value. These findings further demonstrate that PPs and CRPDs are capable of characterizing the behavior of coordination in gait, describe varying degrees of gait performance in subjects with neurological impairments, and support the use of these measures for subjects with atypical coordination that contributes to an overall aberrant gait pattern. While examination of a subject's PPs and CPRDs provide rich insights into an individuals' coordination dynamics, calculation of a subject's CPS throughout an intervention may also provide an index for quantitatively tracking the progression of coordination changes resulting from the intervention, as the GDI is often used for describing changes in joint angles.

Since most gait deviations for subjects with cerebral palsy, present in the sagittal plane [10,14], we felt this was an appropriate plane of motion to investigate first. The six coordination events presented are by no means an exhaustive list of significant coordination events and we postulate that different pathological gait patterns may be linked to coordination events in other planes of motion and other segment pairings. Identification of other significant coordination events could then be used to generate new regression models for distinguishing between other gait patterns of interest. For example, pelvis-foot CRPD coordination events in the transverse plane may prove to be more important for distinguishing whether a subject has a true or apparent equinus gait pattern. Further work is needed to determine clinically meaningful thresholds for the probability a subject's gait pattern is one of those considered in the nominal regression model. Hopefully, the versatility of these nonlinear measures and the methods presented here inspire other investigations of different gait patterns, which would simply require different combinations of PPs and CRPDs, portions of

the gait cycle, and planes of motion.

6.2.4.3   Missing Coordination Events by Gait Pattern

The identification of missing coordination events by gait pattern was conducted to demonstrate the utility of the proposed measures of coordination dynamics, their ability to analyze motion capture data at a different level, and identify the specific position, speed, and inter-segmental coordination dynamics that underlie a gait pattern. In addition to addressing Aim 4, by relating these findings to know characteristics of a particular gait pattern the following sections provide clinically meaningful examples of how these measures of coordination dynamics and their curve features elucidate the underlying mechanisms contributing to an overall pattern of gait. Recall Table 5.3.8 provides a list of the missing coordination events, indication of which general subject groups are missing each of these coordination events, and a description of the curve feature. As will be revealed in the discussion below, one coordination event was consistently missing in the two clinical populations considered: first zero-crossing after the swing period maximum on the thigh-shank CRPD. The implications of not achieving this coordination event are discussed below in the context of each subject sub-category. Given the prevalence of this missing coordination event, further investigation into its importance and perhaps weight in relation to other SLA coordination events is warranted and would perhaps reveal an order in which coordination events are removed from a gait pattern as the severity of impairment increases.

Unimpaired Gait Pattern. Of the 140 unimpaired subjects, only 9 of them were missing three coordination events during the swing period of gait. As detailed in Chapter 5, two of these coordination events were zero-crossings. While these few subjects were missing these coordination events, their CRPD curves were the same shape as the others in this cohort. The reason they did not have these two coordination events was because their CRPDs were shifted upward above the zero degree phase angle line; notice the standard deviation bands in Figure 5.2.1. Additionally, the timing of the inflection point on the pelvis-thigh CRPD for these subjects occurred before opposite foot strike. So, while this curve feature does exist, the coordination event occurred earlier in the gait cycle than the definition of this event. By referring to Figure 5.2.1, the standard deviation band on pelvis-thigh CRPD in pre-swing, where this inflection point occurs, is one of the more variable instances in the gait cycle for this CRPD. Even though these curve features may not have occurred (zero-crossing) or occurred outside the defining temporal limits (inflection point), this variability is still within one standard deviation, the curve shapes are the same as the other unimpaired subjects, and this shows that the general inter-segmental relationships exist for all the unimpaired subjects

while maintaining the unique variability of normal gait.

Subjects with Cerebral Palsy. Over seventy-six percent of the subjects with CP were missing at least one coordination event during the swing period of gait. This finding further supports that the proposed measures of coordination in gait are able to distinguish between various gait patterns (Aim 4). Upon a closer look at these missing coordination events, several trends were identified for this general cohort. When organizing the subjects with cerebral palsy by gait pattern (SKG, C) and topographically, over 70% of the subjects were missing at least one coordination event (Figure 5.3.15). This finding provides another example demonstrating how these proposed measures of coordination are able to detect varying degrees of coordination impairment in subjects known to have aberrant coordination as a result of their pathology (Aim 4). Perhaps most interesting of all for this general cohort, is that over 60% of subjects with CP were missing the last zero-crossing on the thigh-shank CRPD. Recalling the description of CRPD curve features and the segmental behavior they capture (Chapter 3), this coordination event captures the instant in the gait cycle when the thigh and shank are moving in-phase with each other (e.g. phase angles change at the same rate), corresponds to the zero-crossing after the maximum in swing, and occurs within the last few percentages of the gait cycle for unimpaired subjects. It is proposed that this coordination event captures the orientation of the segments in anticipation of foot strike and loading response. As discussed in Chapter 2, subjects with CP are often "playing catch up" during swing because spasticity inhibits the ideal segment orientations and delays (or prevents) the occurrence of critical gait and temporal events. The delayed timing of precursor gait events leading up to swing continue to become compounded as these subjects progress through swing limb advancement and into terminal swing, when this coordination event should occur. When recalling these swing limb advancement characteristics for these subjects, it makes sense that this coordination event does not occur in most of the subjects because this cohort is struggling with positioning the thigh and shank in an orientation optimal for foot strike and in the tight temporal constraints at the end of terminal swing.

Hemiplegia. Referring to Figure 5.3.16, it is interesting that none of the subjects with a hemiplegia classification (one side affected) struggled with achieving the first zero-crossing in swing on the pelvis-thigh CRPD, the first zero-crossing after the absolute maximum in swing on the pelvis-thigh CPRD, or the first zero-crossing after foot off on the thigh-shank CRPD. However, a considerable percentage of the subjects with a diplegia classification (both limbs are affected) were unable to achieve this coordination event. While the gait pattern of subjects with a hemiplegia classification may be less impaired than some subjects with a diplegia classification, perhaps this pattern is revealing the coordination implications on both limbs when bilaterally affected and is

characterizing the affects on a contralateral limb's ability to achieve certain coordination events when both limbs are affected by impaired motor control. It is also worth noting that of the subjects with hemiplegic gait who were missing a coordination event, nearly 80% of them were unable to achieve the first zero-crossing after the maximum in swing on the thigh-shank CRPD. As discussed above, this terminal swing coordination event is crucial for proper limb orientation in time for foot strike and loading response. The identification of this trend and specific coordination event demonstrates the valuable insights into the underlying mechanisms that are contributing to and inhibiting subjects with a hemiplegic gait pattern from achieving a normal gait pattern and its compounding affects on the beginning of the next gait cycle.

Diplegia. Of the missing coordination events for the individuals with a diplegic gait pattern, these subjects were able to achieve the last zero-crossing in swing on the shank-foot CRPD. It proposed that this terminal swing zero-crossing captures the positioning (slight dorsiflexion) of the foot with respect to the shank in anticipation of or in an attempt to achieve a heel first initial contact. By achieving this coordination event, these subjects were able to couple the shank and foot and then potentially dorsiflexion, depending upon their final CRPD values (e.g. positive relative phase) after this curve feature. This finding may at first be misleading and seem to indicate that this sub-group had less impaired motor control affecting the ankle joint. However, while this sub-group was able to achieve this coordination event, so where the individuals with a crouch gait pattern. Recalling the description of crouch gait in Chapter 2, these subjects often have increased ankle dorsiflexion in terminal swing as a result of excessive hip and knee flexion. Upon further examination of this sub-group it was found that 92% of the subjects with a diplegic gait pattern also had a crouch gait pattern. Therefore, it is proposed that the achievement of this coordination event is rather a result of the segments orientation due to crouch gait and for the remaining 3 subjects with diplegia it is proposed that these individuals may have a combination of crouch and stiff knee gait and/or their shank and foot are coupled (in-phase) as a result of compensatory mechanisms (e.g. hip hike or circumduction with fixed/excessive dorsiflexion) for limb advancement and foot clearance. Since the segment PPs are created with respect to the global horizontal, such a compensatory gait mechanism could result in a phase angle that captures the foot's global orientation as it is coupled with the shank and cause the relative phase angle from these two segments to be zero. Further examination of this trend for those with a diplegic gait pattern, again demonstrates the ability of these measures to capture the complex and often subtle inter-segmental coordination dynamics and the inherent ease at which these measures quantify such gait behaviors that are more typically clinically qualified.

Stiff Knee Gait Pattern. As previously mentioned, the subjects with cerebral palsy were

organized into four sub-categories: hemiplegia, diplegia, stiff knee gait, and crouch gait. The subjects with a stiff knee gait pattern were the only sub-category of subjects with CP that was missing all ten coordination events (Table 5.3.8). It is proposed that the compensatory mechanisms these subjects used for limb advancement and foot clearance contributes to the inability to achieve these coordination events. It is also important to restate that individuals with a stiff knee gait pattern may also have elements of a crouch gait pattern and therefore struggle with coordination events that fall into both gait patterns. As mentioned above, the affects of the impaired motor control in individuals with a stiff knee gait pattern is compounded throughout the gait cycle, which is especially evident in this sub-group and their inability to achieve the three coordination events of the thigh-foot CRPD in terminal swing. As discussed in Appendix F, the remaining critical gait event in terminal swing is to continue the pendular knee extension from mid-swing in order to prepare the limb for foot contact and weight acceptance during the upcoming initial double support. This ideal terminal swing behavior is captured on the thigh-shank CRPD as the last maximum in swing, followed by an inflection point and zero-crossing and on the thigh-foot CRPD by two local extrema and a zero-crossing. The inability to uncouple and couple the thigh, shank, and foot (often due to compensatory measures) segments at the ideal times throughout swing limb advancement is the hallmark characteristic of a stiff knee gait pattern. These missing CRPD curve features not only quantify these stiff knee gait characteristics in a low dimensional descriptor but also quantify the inter-segmental coordination strategies of adjacent and non-adjacent segment pairings and allow one to examine how individual segment positions and velocities contributes to the overall gait pattern.

Crouch Gait Pattern. The subjects with a crouch gait pattern were unable to achieve nine of the ten coordination events that were missing in subjects with cerebral palsy. As discussed above, this sub-group of subjects were able to achieve last zero-crossing in terminal swing on the shank-foot CRPD. It was proposed that these subjects' CRPDs contained this curve feature as a result of the orientation of their segments (e.g. hip flexion, knee flexion, ankle dorsiflexion), compensatory limb advancement mechanisms, and methods for calculating PPs (e.g. with respect to the global horizontal). It is proposed that instead of this finding indicating the subjects had sufficient degrees of freedom available and the ability to execute this finer degree of motor control, this coordination event is actually capturing the orientation of limb segments as a result of compensatory mechanisms. This finding is an excellent example of understanding how measures of gait are constructed and the element of gait they are designed to quantify. As with any measure of instrumented gait analysis, it is important to consider the method for constructing the measures and the subject's gait pattern, compensatory mechanisms that might provide potentially misleading conclusions, and the subject's

ability to achieve various critical elements of gait.

Subjects with a Lower Limb Amputation. It is worth noting that unlike the subjects with CP, who often had overlapping gait patterns (e.g. SKG and C), none of the subjects with a lower limb amputation had a combination of both amputation levels considered. Therefore, the following trends observed for these two levels of amputation apply exclusively to the respective group unless otherwise indicated. Compared to the subjects with cerebral palsy, less than 40% of subjects with a lower limb amputation that were missing at least one coordination event. This is consistent with the expectation that because the subjects with a lower limb amputation did not have any neurological pathology they have more degrees of freedom, are able to adapt to the inertial properties of the prosthesis and residual limb's remaining levels of neurological control, and opportunities to execute a motor plan that more closely resembles an unimpaired gait pattern. This general cohort trend provides another instance demonstrating these proposed measures of coordination are able to distinguish between varying levels of coordination, as is the case for the two clinical populations studied in this body of work. In general, this cohort was missing three coordination events: 1) the first zero-crossing after the swing period absolute maximum on the pelvis-thigh CRPD, 2) the first zero-crossing after the swing period maximum on the thigh-shank CRPD, and 3) the last zero-crossing in swing period on the shank-foot CRPD. These differences in the ability to achieve the swing period coordination events between the subjects with a LLA and unimpaired subjects is consistent with findings using conventional IGA measures reported in the literature (Chapter 2). Similar to their conventional IGA counterparts, the proposed measures of coordination are able to distinguish between various gait patterns (Aim 4).

Subjects with Unilateral Lower Limb Amputation. As previously mentioned in Chapter 4, the subjects with a lower limb amputation were organized into four sub-categories: below knee amputation (a.k.a. transtibial), above knee (a.k.a. transfemoral) amputation, unilateral amputation, and bilateral amputations. Of the three general missing coordination events for subjects with a LLL, all of the subjects with a unilateral LLA were able to achieve the last zero-crossing in swing period on the shank-foot CRPD. Since the intact limb provides better dynamic stability and balance for these subjects, as opposed to those with a bilateral LLA, it is proposed that they are able to rely upon this dynamic stability to provide a better base of support and require less trunk and other compensatory motions, which allows them to optimize the swing limb advancement of prosthetic and residual limb. While these behavioral characteristics and motions of an individual with a LLA are known clinical qualifications, this is, to the best of the investigator's knowledge, the first investigation using these measures of inter-segmental coordination to quantify these behaviors and pin-point the timing and

magnitude of these relationships in the context of the gait cycle.

Subjects with Bilateral Lower Limb Amputations. Of the subjects with a LLA that were missing a coordination event, all (100%) of the subjects with a bilateral amputation were missing at least one coordination event. Additionally, all of the subjects in this sub-category were unable to achieve the first zero-crossing after the swing period maximum on the thigh-shank CRPD. The interpretation of this curve feature and its relationship and importance to the task of swing limb advancement has been discussed in the previous sections of this investigation. Since both limbs are affected by the amputation in this sub-group, these subjects must rely upon more compensatory motions (e.g. increased trunk involvement) to walk and achieve swing limb advancement compared to those subjects with a unilateral LLA. One reason all of the subjects this sub-group who were missing this coordination is that in addition to the altered swing limb, the contralateral limb's impaired strength, dynamic stability, and postural control may be influencing the swinging limb. This finding warrants further investigation into the potential coordination affects of contralateral limbs and proximal segments (e.g. trunk, arm swing). Also, the passive or dynamic (e.g. C-Leg®) properties of a prosthesis that dictate the motion between the prosthetic thigh and prosthetic shank sections may prevent subjects from achieving the inter-segmental relationship. This finding illustrates how these measures can be combine with conventional IGA measures and offer insights into the coordination dynamics of a gait pattern that could be used to enhance or refine a prosthetic's parameters and joint properties and thus improve the wearer's overall gait.

Transtibial Amputation Gait Pattern. All of the subjects with a transtibial amputation who were missing a coordination event (53.85%) were unable to achieve three coordination events: 1) the first zero-crossing after the swing period absolute maximum on the pelvis-thigh CRPD, 2) the first zero-crossing after the swing period maximum on the thigh-shank CRPD, and 3) the last zero-crossing in swing period on the shank-foot CRPD. In an unimpaired gait pattern, the first zero-crossing after the swing period's absolute maximum on the pelvis-thigh CRPD indicates the phase angles for the pelvis and thigh are changing at the same rate and are thus in-phase with each other. Since subjects with a transtibial amputation no longer have the use of the gastrocnemius-soleus muscles, they rely heavily upon the hip flexors to provide sufficient power generation for SLA (Chapter 2). It is proposed that the inability of to achieve this pelvis-thigh CRPD coordination event reflects the altered hip coordination strategies adopted by these individuals in order to advance the swinging limb. This finding demonstrates how these proposed measures of coordination dynamics identify specific compensatory coordination strategies adopted by these subjects in order to advance the swinging limb. Providing clinicians with this specific and more detailed information about

segment-prosthesis behaviors and interactions has the potential to inform clinical decisions, dynamic prosthetic alignment, and interventions that may correct suboptimal compensatory coordination strategies (refer to transtibial amputation case study). The inability of subjects with a transtibial amputation to achieve the first zero-crossing after the swing period maximum on the thigh-shank CRPD identifies one instance in the gait cycle when the thigh and prosthetic's inter-segmental behavior deviates from an unimpaired gait pattern. In fact, ensuring a prosthesis has an appropriate amount of knee flexion for individuals with a transtibial amputation is one of the most difficult and challenging aspects of the dynamic alignment process. By using these CRPD curve features to identify the spatial and temporal patterns of the residual limb and prosthetic, there is the potential to improve a subject's dynamic alignment process and reduce undesirable compensatory motions and the pain that often accompanies such motions.

Transfemoral Amputation Gait Pattern. The subjects with an amputation at or above the knee joint were able to achieve two of the three coordination events in this general cohort (LLA). A little more than 30% of these subjects were however, unable to achieve the first zero-crossing after the swing period maximum on the thigh-shank CRPD. While one might be inclined to expect that the subjects with a transfemoral amputation may not be able to achieve more coordination events than the subjects with a transtibial amputation, there are numerous other factors that contribute to an individual's functional level and overall gait pattern (e.g. prosthetic type, residual limb proprioception, pain, prosthetic alignment, overall health, strength, etc.). In the context of and limits of this initial sub-investigation, it is difficult to determine how the properties and parameters of different prosthetics (e.g. passive, dynamic, joint mechanisms) influence a subject's coordination dynamics and overall gait pattern. However, it is interesting that this thigh-shank coordination event is so difficult for these subjects to achieve and perhaps after future investigations, this insight could be used inform the prosthetic alignment. Additionally, using such coordination curve features to identify specific instances and segment dynamics that are missing from an individual's gait has the potential to inform prosthetic design, which may be altered in order to reduce the potential influence of the prosthetic on not achieving such coordination events. The inability to achieve this coordination event may also be a characteristic of individuals with a transfemoral amputation. Since only six retrospective subjects were available for this cohort, future investigations with a larger sample size may shed light on this trend and what influences subject characteristics, prosthetic parameters, and functional level may be correlated with the inability to achieve this coordination event.

6.2.4.4 Hypothesis 4A

Using the mean scaled CPS and mean CDI for each subject cohort to characterize the coordination dynamics of subjects with a normal, stiff knee, crouch, and mechanically altered gait patterns, hypothesis 4A was supported by these analyses. Both of these indices quantitatively showed there was a statistically significant difference ($p \leq 0.05$) between these various gait patterns. This is further supported by the qualitative differences that are visually evident in each cohort's set of mean PPs and CRPDs, provided in Chapter 4 and Appendix G.

6.3 Additional Investigations

6.3.1 Exploratory Investigation to Identify Significant Coordination Events

It is worth noting that although two different approaches were taken to identify significant coordination events during the swing period of gait, there was one common coordination event detected by both approaches: the last inflection point on the thigh-foot CRPD. It is proposed that this thigh-foot CRPD inflection point captures the hamstring firing and resulting slight knee flexion that positions the limb segments in anticipation of heel first initial contact and the upcoming task of loading response. Since this thigh-foot CRPD curve feature is a subtle yet critical aspect of swing limb advancement, it is perhaps of no great surprise that these measures of coordination and different investigations flagged this event as an important, salient coordination event. As discussed previously in this chapter and in Chapter 2, the critical and temporal gait events during swing are typically delayed for subjects with cerebral palsy and those with a lower limb amputation. Considering the temporal delay in this coordination event for these subjects it also makes sense that this coordination event was identified as an event for distinguishing between the coordination dynamics of subjects free of gait pathology and those with impaired swing limb advancement. Findings from the pre-doctoral investigation into changes in coordination and functional outcomes after a rectus femoris transfer procedure in children with spastic CP revealed that pre and post-surgery changes in this coordination event were significant. While elaboration upon this pre-doctoral investigation is not within the scope of this document, it is worth noting the continued important of this coordination event from numerous investigations. Future investigations into this coordination event are warranted and may reveal this coordination event as a useful marker for changes in certain gait patterns after a particular intervention. Coordination events identified as significant from the various exploratory investigations conducted in this body of work, especially the thigh-foot CRPD inflection

point, are not definitive. However, it is proposed that the significance of certain coordination events will be different for different gait impairments, so it may be more clinically meaningful to organize and analyze coordination events by gait impairment, as discussed in section 6.2.4.3 above.

6.3.2 Transtibial Amputation Case Study

It was proposed that in an effort to maintain a normative gait pattern, an individual with a lower limb amputation who is free of neurological impairments would adopt distinctly different coordination patterns, as quantified by PPs and CRPDs, depending upon the prosthetic limb's alignment. This case study showed that incorporating measures of coordination dynamics with conventional IGA measures to study the gait pattern of an individual with a transtibial amputation offers clinical insights into the patient's gait pattern that were otherwise undetected by traditional IGA measures.

Although there is not a striking difference between the alignments using conventional instrumented gait analysis measures, there are considerable differences detected by the nonlinear measures, especially for the angular velocity of the shank and the thigh-shank relative phase diagram. The normal reference subject's root mean square error (RMSE) values demonstrate that the patient's larger RMSEs detected by the nonlinear measures is not due an increased sensitivity of these nonlinear measures nor the natural stride-to-stride variability inherent in normal gait. The purpose of using the un-normalized RMSE measure was to examine differences between the subject's alignment conditions and not to quantitatively compare any differences. As explained in Chapter 3, PPs and CRPDs offer an alternative level of analysis of marker trajectory data and these nonlinear methods inherently measure different aspects of gait than such conventional methods as kinematics and kinetics. The application of RMSE values quantitatively support the investigation's proposal that PPs and CRPDs measure a different element of instrumented gait analysis data and thus can offer an alternative means to studying the underlying coordination dynamics that contribute to an individual's gait pattern, as measured by kinematics and kinetics.

Traditional instrumented gait analysis measures did not support changing the alignment of the prosthesis. X-ray measurements support the recommendation to move the prosthetic foot medially to achieve a more optimal mechanical axis in the left leg. Physical therapy was also recommended to help the patient meet the increased strength and endurance demands of the proposed prosthesis alignment change.

Unlike the conventional instrumented gait analysis measures, the RMSEs of nonlinear measures revealed considerable differences between the three prosthetic alignment conditions studied. It is

proposed that these nonlinear measures are detecting the patient's ability to emulate a typical gait pattern, from the perspective of traditional instrumented gait analysis measures, by adopting different coordination strategies for each alignment condition. Specifically, the subject adopted a different coordination strategy by modifying the affected thigh's angular displacement and velocity throughout the gait cycle. This clinical example demonstrates how examining the behavior of an individual segment using PPs provides a means to identify the loci of impairment(s) in a gait pattern and offers insights into the organization of individual segments that may otherwise be undetectable with conventional instrumented gait analysis measures. Further investigation is needed to determine if these coordination strategies may contribute to underlying mechanisms associated with the patient's pain and decreased mobility.

Describing movement at the level of coordination in this population has the potential to enhance the efficacy of a patient's rehabilitation and prosthetic alignment by providing insights into how the nervous system is adapting to and controlling the altered biomechanical properties of the residual limb and prosthetic. Limb amputation leads to major changes in biomechanical and neurophysiological relationships that also influence the physiological quality of the residual limb and contribute to the individual's overall walking ability. Several research studies have found that a major reorganization of both afferent and efferent projections occurs in such patients and that this neurological reorganization contributes to the changes in motor patterns seen in persons with lower limb amputations [8]. This reorganization of the neuromuscular system's many elements demonstrates such individuals are able to consolidate the dynamical system's redundant degrees of freedom while accounting for task and environmental constraints and limb-prosthetic interactions (Bernstein, 1967). These theoretical models suggest the motor control system can re-organize after the reduction or removal of biomechanical constraints and result in coordination changes. For example, compensation for loss of proprioceptive cues, which normally help signal the initiation and terminal of certain gait events, and altered inertial properties can be achieved in individuals with an amputation that are free of neuromuscular pathology.

Determining the optimal prosthesis alignment can be a difficult task, especially in patients who have worn a prosthetic for years and have the ability to adopt a relatively typical gait pattern even with various prosthetic alignments. The alternative perspective of gait provided by these methods provides a means to identify the locus of impairment and offer valuable clinical insights for informing rehabilitation programs and prosthetic alignment.

7 Summary and Conclusions

7.1 Summary of the Proposed Coordination Dynamics Model

Although coordination has been identified as a fundamental element necessary for the successful achievement of walking, this aspect of gait has yet to be embraced into instrumented gait analysis, perhaps in part due to an unfamiliarity or inconsistency of the mathematical methods for generating these coordination curves, the lack of a normative reference, examples of the unique clinical insights offered by these measures, and interpretation of curve features. Therefore, the prospective experiments and four aims of this body work addressed these issues using retrospective and prospective the motion capture data from subjects with an unimpaired gait pattern, subjects with cerebral palsy, and subjects with a lower limb amputation. Specifically, coordination dynamics during the critical gait task of swing limb advancement in the sagittal plane was examined for these subjects with the dynamic systems theory based phase portraits and continuous relative phase diagrams.

Aim 1 created a normative reference dataset for these measures of coordination dynamics from the largest reported cohort of individuals free of gait pathology. This normative dataset provided a context for the utility of these measures as a complement to conventional instrumented gait analysis measures, was a reference for the other three aims and their respective hypotheses, and continued the advancement of the application of dynamic systems theory techniques in locomotion. The detailed explanation and rationale of the techniques used to generate these measures will hopefully provide a more unified methodology and thorough description for constructing these curves for future investigations and researchers.

Currently, there is not a gold standard method or measure for the behavior of coordination that characterizes the timing and position of individual segments and pairs of segments, both adjacent and non-adjacent throughout the cyclical task of gait. Furthermore, only a few other investigations by other researchers have been conducted to explore these measures for individuals with an aberrant gait pattern, demonstrate that these measures characterize coordination, and provide examples of how these techniques can be used to identify the loci of impairment or changes in coordination as result of an intervention. Therefore, the prospective experiments in Aim 2 were designed to expand contribute to this area of gait research by exploring the relationship between the proposed measures of coordination dynamics and select clinical performance measures that characterize aspect of coordination.

Although the theoretical, mathematical pendulum model create in Aim 3 is more simplistic than

other reported models, this model retained the initial conditions and inertial properties of motion capture data from human subjects instead of the approach of other models which unrealistically manipulate parameters (e.g. limb length, center of mass location) to achieve an observed human gait pattern. Originating from a limit cycle, the components of a phase portrait (e.g. angular displacement, angular velocity) were ideally suited to assess the similarity of a theoretical compound pendulum to the motion of the thigh and shank during the swing period of gait. This pendulum model was used to assess the long held construct validity that the sagittal plane motion of the thigh and shank during swing period of gait is analogous to the motion of a passive compound pendulum. While the vast majority of patients with neurological movement disorders primarily struggle with advancing the limb in swing, this critical portion of the gait cycle is rarely addressed in clinical interventions, in part due to the lack of mathematical models and clinically useful techniques for identifying the locus of deviation from the optimal motion.

Lastly, the fourth aim of this body of work examined the coordination dynamics of the unimpaired cohort and the two clinical cohorts, who have different reasons for struggling with the critical gait task of swing limb advancement. Various techniques were used to identify and quantify the different motor control strategies of these subjects and two novel indices of coordination dynamics were created to provide a concise metric for comparing the coordination dynamics between different gait patterns. Using the coordination curves for the cohorts' various gait patterns, numerous examples were provided to illustrate how curve features of PPs and CRPDs provide insights into the motor control strategies of a subject group. Important coordination events and inter-segmental spatio-temporal relationships during swing limb advancement were identified and discussed to demonstrate the unique clinical insights of this alternative level of analysis of tri-planar marker trajectory based data.

The following section provides specific conclusions for each aim and its corresponding hypotheses. Hopefully, this body of work has provided sufficiently compelling evidence to convince the instrumented gait analysis community that these measures offer uniquely valuable clinical insights into the underlying coordination dynamics of a gait pattern and sharing of this work will provide a foundation for the proposed measures of coordination dynamics to be more readily considered and embraced by fellow researchers and clinicians.

7.1.1 General Conclusions for Aim 1

Phase portraits for the pelvis, thigh, shank, and foot and continuous relative phase diagrams for the segment pairs of pelvis-thigh, thigh-shank, shank-foot, and thigh-foot were calculated for the

complete gait cycle. The straightforward description and rationale presented for generating these descriptors of coordination dynamics provides a clearly defined and cohort process for calculating these measures. This normative dataset is the largest reported dataset of sagittal plane coordination measures, including adjacent and non-adjacent segment pairings, for individuals free of gait pathology. The findings from the various analysis of this data support the use of this normative dataset as a reference for coordination dynamics. In addition to providing a normative reference for this body of work, this dataset and methods can be used to improve the general understanding of gait strategies from the level of coordination. Furthermore, by characterizing the natural variability in gait patterns this deliverable offers a means to enhance the general understanding of atypical gait patterns. Various curve features (e.g. coordination events) from these coordination curves for this unimpaired cohort were identified as being significant to the successful completion of swing limb advancement in Chapter 5. Additionally, combination of these coordination events were found to comprise four motor control mechanisms essential to the elegant and efficient achievement of swing limb advancement. Hopefully, disseminating this normative reference and methodology for calculating these coordination measures in a peer reviewed journal will enable other researchers to identify important coordination dynamics in clinical and research populations with musculoskeletal and neurologically based gait pathology and link them to shortcomings in performing critical gait events.

7.1.2 General Conclusions for Aim 2

While there is presently not a gold standard method for quantifying coordination dynamics during the task of gait in the instrumented gait analysis community, the exciting correlations between curve features from coordination curves and select clinical performance tasks from this aim demonstrated that phase portraits and continuous relative phase diagrams quantify essential intersegmental coordination dynamics (e.g. dissociation of synergies) during swing limb advancement. Using these nonlinear measures to quantify coordination from commonly collected instrumented gait analysis data is supported by this aim's findings. The comparison of the various prospectively captured clinical performance measures to discrete coordination events from continuous relative phase diagrams from Aim 2 demonstrated the proposed measures of coordination dynamics can be used to characterize the coordination of segments during the task of gait, detect aberrant coordination, and identify the loci of impairment(s). Findings from this aim support the validity of the theoretical construct that these phase portraits and continuous relative phase diagrams can be used to characterize the behavior of coordination and detect varying degrees of impaired coordination. The

incorporation of these coordination measures into IGA may, in certain cases, alleviate the need for multiple or additional clinical performance measures used to characterize aspects of voluntary motor control in an effort to make correlations between these tasks and the actual coordination dynamics during gait.

7.1.3 General Conclusions for Aim 3

As shown with the theoretical, mathematical pendular software model, swing limb advancement is not a purely passive motion, even for subjects wearing a lower limb prosthetic. While the thigh and shank motion of subjects with a prosthesis was found to differ the least from various constant-damping conditions of a theoretical compound pendulum, the sagittal plane motion of the subject's leg segments/prosthetic still deviated from the theoretical model. The results for this aim's hypotheses further support the general proposal that the task of swing limb advancement is a complex motor control task requiring the elegant timing and organization of segments to successfully and efficiently achieve. Since the leg segments during swing limb advancement are actively controlled (e.g. variable damping), the use of measures (e.g. phase portrait, continuous relative phase diagram) designed to quantify the behavior of coordination is further supported.

7.1.4 General Conclusions for Aim 4

The results from the numerous analyses of this aim demonstrated that the proposed measures of coordination dynamics are able to distinguish between different gait pathologies and patterns associated with altered limb advancement during the swing period of gait. As evident by the PPs and CPRDs generated for this investigation's various subject groups, there are distinct qualitative differences for the different subject cohorts and gait patterns studied. Furthermore, it was found that these visual differences can be quantified by the presence or absence of certain curve features and each of the atypical gait patterns examined (e.g. stiff knee, crouch hemiplegia, diplegia, below knee amputation, above knee amputation) had a unique combination of missing coordination events that corresponded to the cohort's difficulty in successfully achieving swing limb advancement.

Quantification of these different coordination strategies was further explored and characterized by the creation of two novel coordination indices. These indices used different techniques, each with different advantages, to consolidate the large amount of data associated with a subject's coordination curves into a single scalar value. Both indices found statistically significant differences between the different gait patterns and general subject cohorts (e.g. unimpaired, cerebral palsy, and lower limb amputation). Findings from analyses of these indices demonstrated these indices were able to

differentiate between the clinical cohorts and the unimpaired group and decreased significantly as the GMFCS level decreased in subjects with cerebral palsy. Additionally, these coordination indices were significantly different from the subjects' gait deviation index but followed similar trends to the GDI thus reflecting increases in the diagnosis severity of subjects when they were organized topographically and by level of amputation.

Overall, the use of phase portraits and continuous relative phase diagrams to examine and compare different gait patterns for this aim, further demonstrated the additional level of analysis and alternative perspective of marker based trajectory data provided by these measures. The analyses of this aim and its hypothesis further demonstrate the ability of these measures to enhance and expand insights into gait pathology by quantifying the organization of individual segments, identify mechanisms of change, and loci of impairment. Since the fundamental organization of the leg segments during gait is linked to gait pathology and guides the rationale for interventions, incorporating PPs and CRPDs into instrumented gait analysis will open new avenues for understanding the complexity of coordination and allow clinicians the means to more effectively and efficiently treat patients with neuromuscular gait impairments.

7.1.4.1 Coordination Deviation Index

Feature analysis was used to create an index of coordination dynamics from the proposed measures of coordination (e.g. phase portrait, continuous relative phase diagram). This novel index provides a concise metric of the amount an individual's coordination deviates from a normative reference. Investigations into this new index demonstrated the CDI is capable of distinguishing between different gait patterns in two clinical cohorts (e.g. cerebral palsy, lower limb amputation) with different etiologies affecting their coordination and the ability to produce a typical gait pattern. Comparisons between the GDI and CDI found that while these two indices follow similar trends in various clinical groups, they measure different aspects of gait. Therefore, the CDI may prove to be a valuable research tool for studying populations with impaired motor control because it provides a deeper level of understanding about the mechanisms associated with changes in joint angles by reflecting the underlying organization of segment oscillations during gait.

7.1.4.2 Coordination Performance Score

Phase portraits and continuous relative phase diagrams characterize the essential behavior of coordination in gait and offer a quantitative means to elucidate the underlying mechanisms contributing to a gait pattern by analyzing marker trajectory data from a different perspective. The six

significant, sagittal plane coordination events in swing identified by the coordination performance score investigation demonstrates the diverse utility of these measures and the ease of using these measures to deconstruct essential mechanisms of a gait pattern. The proposed coordination performance score for characterizing the deviation of subject's swing period coordination dynamics from a large normative reference provides a clinically useful and concise alternative to examining the PPs and CPRDs. Since coordination measures describe movement at a different level than conventional instrumented gait analysis measures and by nature are low dimensional descriptors, these nonlinear techniques may hold the key to enhancing gait classification algorithms for individuals with impaired coordination (e.g. cerebral palsy).

7.2   Recommendations for Future Work

Even though this body of work provided an initial framework for the methodological generation, clinical interpretation, and applications of sagittal plane coordination dynamics, it is by no means exhaustive. These methods could easily be expanded for the entire gait cycle, incorporate upper body segments, and incorporate coronal and transverse planes of motion. It would be exciting to also apply these methods and measures to other clinical populations who struggle with impaired coordination and other pathological gait patterns. It is proposed that incorporating these measures of coordination to characterize changes in the behavior of segments during other walking tasks while using assistive devices, different prosthetics prosthetic settings/alignments, or after clinical interventions would enhance insights from instrumented gait analysis data. The inclusion of these nonlinear measures into instrumented gait analysis for various walking tasks that are designed to alter or inhibit various aspects of motor control (e.g. obstacle avoidance, treadmill walking with virtual reality) may provide a more meaningful and appropriate measures of an individual's motor control strategies during such tasks. The utility of these measures in clinical and research domains will continue to unfold as the methodology is applied to instrumented gait analysis. While the possibilities for clinical and research applications of these measures are limitless, the following sections provide some additional recommendations for future work to further develop these coordination measures.

7.2.1   Continuous Equations of Coordination Dynamics

This body of work has provided an initial framework with discrete curve values using percentages of the gait cycle as the temporal unit of measure. While instrumented gait analysis data is traditionally viewed discretely, it is proposed that defining these coordination measures with contin-

uous equations would provide additional benefits to analyzing gait data and open the door to new analytical techniques. One means of generating equations for continuous coordination measures is functional data analysis (FDA).

The periodic nature of gait data (e.g. kinematics, phase portraits, continuous relative phase diagrams) implies these cyclical, oscillatory gait curves form a closed curve. The overall shape of these cyclical curves is different for various gait patterns, as addressed in Aim 4, and is often different for the individual when compared to a mean, normative reference. FDA offers a technique that explores the variability in these function data and focuses on the different features of these curves. As detailed by Ramsay (1997), applying FDA to these coordination curves would 1) represent the data in new ways to aid in deeper and additional analysis, 2) highlights various curve characteristics, 3) provide a means to study important sources of pattern and variations among different subjects and cohorts, 4) provide a means to explain the variation in an outcome or dependent variables, and 5) compare two or more sets of data with respect to certain types of variation. By creating functions for these coordination curves, FDA would provide a means to quantitatively determine how two functions depend upon each other and covary with one another. FDA would also provide a means to expand upon the significant coordination events (e.g. curve features) identified in Aims 1 and 4. In particular, FDA could be used to study which modes of variability in two coordination curves are most associated with each other. For example, this methodology could determine how variability in the pelvis-thigh CRPD is related to the variability in the thigh-foot CRPD. This additional perspective into coordination curves might reveal how a physical propagation of errors caused by the inability to achieve one coordination event (e.g. curve feature) at an earlier time in the gait cycle affects coordination dynamics in a later portion of the gait cycle.

To further illustrate the benefits of using continuous measures of coordination, consider the coordination deviation index created in Aim 4. The coordination deviation index (CDI) was created to solve the problem of comparing the magnitude at each discrete time epoch of a subject's the phase portraits and continuous relative phase diagrams to another subject. As with any conventional gait measure or gait index, this metric uses the timing and magnitude of curves but is unable to account for slope. Generating an index that uses continuous equation for each coordination curve would incorporate the three fundamental elements of any curve: timing, magnitude, and slope. From a methodological perspective, this would also alleviate the need for resampling of gait data, remove the effects of temporal normalization on the curves, and drastically reduce the amount of data analyzed and required for normative reference datasets. Latash (2008) stated, "... parameters of equations used within the dynamic systems approach have been selected rather arbitrarily in order to make

sure that the model produces desired coordination patterns." Defining equations for coordination dynamics with a methodology such as functional data analysis offers an elegant solution to this problem.

7.2.2 Incorporation of Electromyographic Data

In chapter 3, current uses of electromyographic data to characterize coordination were discussed. While this approach to quantifying motor control uses a more local perspective, the combination of muscle activation patterns with the more global behavioral perspective afforded by phase portraits and continuous relative phase diagrams has exciting potential. Creating a model of coordination that incorporates the activation of select muscles and the resulting behavior of the entire limb has the potential to provide more specific insights into which muscles are contributing to the motor behavior of an individual's gait pattern. The addition of electromyographic data with the proposed measures of coordination may also provide additional clinical insights that might inform treatment decisions for individuals undergoing an intervention designed to reduce aberrant coordination. The balance between potential and kinetic energy of leg segments can be modeled using phase portraits constructed from a segment's angular displacement and angular acceleration. Including muscle activation patterns with such phase portraits would be another excellent initial investigation into the pendular energetics of a gait pattern.

7.2.3 Incorporation of Forward Modeling Simulations

Creating a multifaceted model of coordination has the potential to significantly expand general knowledge of changes in motor control associated with an intervention, unify different gait analysis methods and descriptors of gait, and provide new, clinically meaningful insights into this constitutive element of gait. As previously mentioned, the incorporation of electromyography data is one way to create an expanded model of coordination dynamics. Another option would be to include these measures of coordination dynamics into some of the advanced forward modeling simulation software programs currently available (e.g. OpenSim), which would also greatly enhance the simple theoretical pendulum model created to address Aim 3. The use of such advanced musculoskeletal models could be used to simulate various clinical interventions and predict different permutations of the resulting gait pattern and thus underlying coordination dynamics. For example, individuals with stiff knee gait often undergo a rectus femoris transfer to surgically remove the muscle's spasticity based inhibitory effects on knee flexion during swing limb advancement. Using a patient's pre-operative instrumented gait analysis data, various forward simulations could be created to assess

how different surgical techniques for this procedure might affect the post-operative gait pattern and potential re-organization of segments (e.g. changes in coordination) about the knee joint in response to this intervention. Additionally, future work using such advanced forward modeling techniques and software programs could expand upon the investigation in Aim 3 into variable damping conditions and potentially generate damping functions for different clinical cohorts.

REFERENCES

1. Bernstein, N 1967, The coordination and regulation of movements, Pergamon Press, New York.

2. Vereijken, B 1992, 'Free(z)ing Degrees of Freedom in Skill Acquisition', Journal of Motor Behavior, vol. 24, no.1, pp. 133-142.

3. Hershler, C 1980, 'Angle–angle diagrams in the assessment of locomotion', American Journal of Physical Medicine, vol. 59, no. 3, pp. 109-125.

4. Kelso, S 1995, Dynamic Patterns: The Self-Organization of Brain and Behavior, The Massachusetts Institute of Technology, Cambridge Massachusetts.

5. Thelen, E 1994, A Dynamic Systems Approach to the Development of Cognition and Action (Cognitive Psychology), The Massachusetts Institute of Technology, Cambridge Massachusetts.

6. Turvey, M 1990, 'Coordination', American Psychologist, vol. 45, no. 8, pp. 938-953.

7. Stergiou, N 2004, Innovative Analysis of Human Movement, Human Kinetics, Illinois, Chapter 4.

8. Popva T. Quoted in Issledovania po biodinamike locomotsii. Chapter 3, col 1: Biodinamika khod'by norma'nogo vzroslogo muzhchiny, edited by N.A. Bernstein. Idat. Vsesoiux. Instit. Eksper. Med., Moscow, 1935.

9. Nordin M, Frankel V. Basic Biomechanics of the Musculoskeletal System. Philadelphia, Lea & Febiger. 1989; pp. 89-111.

10. Lieber RL. Skeletal Muscle Structure, Function, and Plasticity: The Physiological Basis of Rehabilitation. 3rd Ed., 2010, Lippincott Williams & Wilkins, Baltimore MD.

11. Enoka R. Neuromechanics of Human Movement. 4th Ed., 2008, Human Kinetics, Chapaign IL.

12. Henneman, E. (1979). Functional organization of motorneuron pools: the size principle. In H Asanuma & VJ Wilson (Eds.) Integration in the Nervous System. Pp 13-25). Tokyo: Igaku-Shoin.

13. Nashner L, Woollacott M. The organization of rapid postural adjustments of standing humans: an experimental-conceptual model. In: Talbott RE, Humphre DR (Eds.) Posture and movement. New York, Raven. 1979:243-257.

14. Nashner LM. Fixed patterns of rapid postural responses among leg muscles during stance. Exp Brain Res 1977; 30:13-24.

15. Umphred, D 1995, Neurological Rehabilitation, Elsevier Mosby Inc., Missouri.

16. Shumway-Cook, A, Woollacott, M 2012, Motor Control: Translating Research into Clinical Practice, Lippincott Williams & Wilkins, Maryland.

17. Latash, M 2008, Neurophysiological Basis of Movement, Human Kinetics, Illinois, Chapters 33-35.

18. Kandel, E. & Schwartz, J. Principles of Neural Science. 4th edition, Chapter 37.

19. Clark, D. The Brain and Behavior: An Introduction to Behavioral Neuroanatomy, pg 127-129.

20. Bhimani R, Anderson L. Clinical understanding of spasticity: implications for practice. Rehabilitation Research and Practice, 2014, pp.1-10.

21. Purves D, Agustine GJ, Fitpatrick D, et al., editors. Neuroscience. 2nd edition. Sunderland (MA): Sinauer Associates; 2001.

22. Burridge JH, Wood DE, Hermens HJ et al. Theoretical and methodological considerations in the measurement of spasticity. Diability and Rehabilitation, vol 27, no.1-2, pp.69-80, 2005.

23. Kirtley, C 2006, Clinical Gait Analysis: Theory and Practice, Elsevier Churchill Livingstone, Edinburgh.

24. Baker R. The history of gait analysis before the advent of modern computers. Gait & Posture, 2007; 26:331-342.

25. Eberhart HD, Inman VT, Bresler B. The principal elements in human locomotion. In: Klopsteg PE, Wilson PD, editors. Human limbs and their substitutes. New York: McGraw-Hill; 1954. P.437-471.

26. Perry, J 1992, Gait Analysis: Normal and Pathological Function, SLACK Inc., New Jersey.

27. Sutherland DH. Gait disorders in childhood and adolescence. Baltimore: Williams and Wilkins; 1964, p.1-10.

28. Sutherland DH, Hagy JL. Measurement of gait movements from motion picture film. Journal of Bone and Joint Surgery. 1972; 54A:787-797.

29. Gage JR, Schwartz, Koop SE, Novacheck TF. The Identification and Treatment of Gait Problems in Cerebral Palsy. 2nd Ed., Clinics in Developmental Medicine, No. 180-181. London, Mac Keith Press. 2009.

30. Inman VT, Ralston HJ, Todd F. Human Walking. Baltimore, Williams & Wilkins. 1981.

31. Winter DA. (1990). Biomechanics and Motor Control of Human Movement. New York: John Wiley & Sons.

32. Chang FM, Rhodes JT, Flynn KM, Carollo JJ. (2010) The role of gait analysis in treating gait abnormalities in cerebral palsy. Orthop Clin N Am 41:489-506.

33. Alexander MA, Matthew DJ. Pediatric Rehabilitation: Principles and Practice. 4th Edition. Chapter 16, pp. 461-491.

34. Johansson JL, Sherrill DM, Riley PO, Bonato P, Herr A. A clinical comparison of variable damping and mechanically passive prosthetic knee devices. American Journal of Physical Medicine & Rehabilitation 2005; 84:563-575.

35. Segal AD, Orendurff MS, Klute GK, McDowell ML, Pecoraro JA, Shofer J, Czerniecki JM. Kinematic and kinetic comparisons of transfemoral amputee gait using C-Leg® and Mauch SNS® prosthetic knees. Journal of Rehabilitation Research & Development, 2006; vol. 3, no. 7, pp. 857-870.

36. Van der Linde H, Hofstad CJ, Geurts ACH, Postema K, Geertzrn JHB, van Limbeek J. A systematic literature review of the effect of different prosthetic components on human functioning with a lower-limb prosthesis. Journal of Rehabilitation Research & Development, 2004; vol 41, no. 4, pp. 555-570.

37. Hussain S. Xie SQ, Liu G. Robot assisted treadmill training: mechanisms and training strategies. Mechanical Engineering and Physics. 2011; 33:527-533.

38. Sarkodie-Gyan T. Neurorehabilitation Devices: Engineering Design, Measurements, and Control. McGraw-Hill, New York, 2006.

39. Dietz V, Nef T, Rymer WZ. Neurorehabilitation Technology. Springer, London, 2012.

40. Whittle MW. Gait Analysis: An Introduction. 4th Edition, Butterworth Heinemann, Elsevier. 2007.

41. Latash, M. Progress in motor control: volume 1. Illinois: Human Kinetics; 1998.

42. Elftman H. 1996. Biomechanics of muscle. Journal of Bone Joint Surgery. (A) 48:363-377.

43. Rodman PS, McHenry HM. 1980. Bioenergetics and the origin of hominid bipedalism. Am. J. Phys. Anthropol. 52:103-6.

44. Aiello LC, Wells JCK. 2002. Energetics and the evolution of the genus Homo. Annual Review Anthropology. 31: 323-338.

45. Foley RA, Elton S. 1998. Time and energy: the ecological context for the evolution of bipedalism. In Primate Locomotion, ed. E Strasser, J Fleagle, A Rosenberger, H McHenry, pp. 419-33. New York/London: Plenum.

46. Winter DA, (1992). Foot trajectory in human gait: a precise and multifactorial motor control task. Physical Therapy 72: 45-56.

47. Zarrugh MY. (1981). Kinematic prediction of intersegment loads and power at the joints of the leg in walking. Journal of Biomechanics 14: 713-725.

48. Chou LS, Song SM, Draganich LF. (1995). Predicting the kinematics of gait based on the optimum trajectory of the swinging limb. Journal of Biomechanics. 28: 377-385.

49. Saunders JB, Inman VT, Eberhart HD. The major determinants in normal and pathological gait. 1953. The Journal of Bone and Joint Surgery, 35-A, no. 3, 543-558.

50. Mochon S, McMahon TA. 1980. Ballistic walking. Journal of Biomechanics vol 13, pp49-57.

51. McGeer T. 1990a. Passive dynamic walking. International Journal of Robotics Research, 9, 62–82.

52. McGeer T. 1990b. Passive dynamic walking. The International Journal of Robotics Research. 9(2): 1640-1645.

53. McGeer T. 1992. Dynamics and control of bipedal locomotion. Journal of theoretical Biology, 163: 277-314.

54. Gordon, K. E., Ferris, D. P., & Kuo, A. D. (2003). Reducing vertical center of mass movement during human walking doesn't necessarily reduce metabolic cost. In Proc. 27th ann. mtg. Am. Soc. Biomech., Toledo, OH.

55. Ortega, J. D., & Farley, C. T. (2005). Minimizing center of mass vertical movement increases metabolic cost in walking. Journal of Applied Physiology, 99, 2099–2107.

56. Kuo AD. The six determinants of gait and the inverted pendulum analogy: A dynamic walking perspective. Human Movement Science. 2007; 26:617-656.

57. Basmajian JV. 1976. The human bicycle. Biomechanics V-A (P.V. Komi, Ed.), University Park Press, pp. 297-302.

58. Fisher S V, Gullickson G. Energy cost of ambulation in health and disability: a literature review. Arch Phys Med Rebail 1978; 59: 124-133.

59. Odding, E 2006, 'The Epidemiology of cerebral palsy: incidence, impairments and risk factors', Disability and Rehabilitation, vol. 28, no. 4, pp. 183-191.

60. Haak, BS 2009, 'Cerebral palsy and aging'. Developmental Medicine and Child Neurology, vol. 51, no. 4, pp. 16-23.

61. Bradley WC, Daroff RB, Fenichel GM, Marsden CD. Neurology in Clinical Practice: The Neurological Disorders. Volume II, 3rd Edition, Butterworth-Heinemann, Woburn MA, 2000. Chapter 67.

62. Stanley F, Blair E, Alberman E. Cerebral palsies: epidemiology and causal pathways. London United Kingdom: MacKeith Press; 2000.

63. Sanger TD, Chen D, Delgado MR, Gaebler-Spira D, Hallet M, Mink JW, and the Taskforce on Childhood Motor Disorders. Definition and Classification of Negative Motor Signs in Childhood. Pediatrics 2006; 118; 2159.

64. Staudt M, Pavlova M, Bohm S, Grodd W, Krageloh-Mann I. Pyramidal tract damage correlates with motor dysfunction in bilateral periventricular leukomalacia (PVL). Neuropediatrics 2003; 34: 182–88.

65. Bax M, Tydemann C, Flodmark O. Clinical and MRI correlates of cerebral palsy: the European Cerebral Palsy Study. JAMA 2006; 296: 1602-1608.

66. Lance JW. 1980. Symposium synopsis. In: Feldman RG, Young RR, Koella WP, editors. Spasticity: Disordered control. Chicago: Yearbook Medical. p 485-494.

67. Olsson MC, Kruger M, Meyer LH, Ahnlund L, Gransberg L, Linke WA, Larsson L. 2006. Fibre type-specific increase in passive muscle tension in spinal-cord injured subjects with spasticity. Journal of Physiology 577:339-52.

68. Leonard CT, Hirschfeld H, Fossberg H. (1991). The development of independent walking in children with cerebral palsy. Dev Med Child Neurol 33: 567-577.

69. Sutherland DH, Davids JR. (1993) Common gait abnormalities of the knee in cerebral palsy. Clinical Orthopaedics and Related Research. 288:139-147.

70. Goldberg SR, Ounpuu S, Delp SL. The importance of swing-phase initial conditions in stiff-knee gait. J Biomech 2003;36(8):1111-6.

71. Gage WH, Winter DA, Frank JS, et al. Kinematic and kinetic validity of the inverted pendulum model in quiet standing. Gait & Posture 2004; 19(2):124-32.

72. Novacheck TF, Gage JR. Orthopedic management of spasticity in cerebral palsy. Childs Nerv Syst 2007; 23(9):1015-31.

73. Ziegler-Graham K, MacKenzi E, Ephraim P, Travison G, Brookmeyer R. (2008) Estimating the prevalence of limb loss in the United States: 2005 to 2050. Arch Phys Med Rehabil vol 89: 422-429.

74. Dillingham TR, Pezzin LE, Shore AD. Reamputation, mortality, and health care costs among persons with dysvascular lower-limb amputations. Arch Phys Med Rehab, 2005; vol 86: 480-486.

75. Burke MJ, Roman V, Wright V. Bone and joint changes in lowerlimb amputees. Ann Rheum Dis 1978;37(3):252-4.

76. Kulkarni J, Adams J, Thomas E, Silman A. Association between amputation, arthritis and osteopenia in British male war veterans with major lower limb amputations. Clin Rehabil 1998;12(4):348-53.

77. Deans S, McFadyen AK, Rowe PJ. Physical activity and quality of life: a study of a lower-limb amputee population. Prosthetics and Orthotics International 2008; 32:186-195.

78. Smith D, Michael JW, Bowker JH. Atlas of Amputations and Limb Deficiencies: Surgical, Prosthetic, and Rehabilitation Principles. 3rd ed. Illinois; 2004.Chapters 29-32.

79. Day HJB (1991). The ISO/ISPO classification of congenital limb deficiency. Prosthetics and Orthotics International, 15: 67-69.

80. Eberhart, H.D, Elftman H, Inman VT. (1954). The locomotor mechanism of the amputee. Human Limbs and their Substitutes. McGraw-Hill, New York.

81. Radcliffe CW. Functional considerations in the fitting of above-knee prostheses. Selected Articles From Artificial Limbs, Huntington, NY, Kreiger Publishing Co, Inc, 1970, pp. 5-30.

82. Prinsen EC, Nederhand MJ, Rietman JS. Adaptation strategies of the lower extremities of patients with a transtibial or transfemoral amputation during level walking: a systematic review. Arch Phys Med Rehabil 2011; 92:1311-1325.

83. Breakey J. Gait of unilateral trans-tibial amputees. Orthot Prosthet 1976;30:17-24.

84. Murray M, Mollinger L, Sepic SB, Gardner GM. Gait patterns in trans-femoral amputee patients: hydraulic swing control versus constant-friction knee components. Arch Phys Med Rehabil 1983;64:339-45.

85. Engsberg JR, Lee AG, Tedford KG, Harder JA. Normative ground reaction force data for able-bodied and transtibial amputee children during walking. J Pediatr Orthop 1993;13:169-73.

86. Suzuki K. Force plate study on the artificial limb gait. J Jpn Orthop Assoc 1972;46:43-55.

87. Engsberg JR, Lee AG, Patterson JL, Harder JA. External loading comparisons between able-bodied and transtibial amputee children during walking. Arch Phys Med Rehabil 1991;72:657-61.

88. Nolan L, Wit A, Dudzinski K, Lees A, Lake M, Wychowanski M. Adjustments in gait symmetry with walking speed in trans-femoral and trans-tibial amputees. Gait & Posutre 17 (2003): 142-151.

89. Hurwitz DE, Sumner DR, Block JA. Bone density, dynamic joint loading and joint degeneration. Cells Tissues Organs 2001;169(3):201-9.

90. Waters R L, Perry J, Antonelli D, Hisplop H. Energy cost of walking of amputees: the influence of amputation level. J Bone Jt Surg 1976; 58-A:42-46.

91. Waters R L, Yakura JS. The energy expenditure of normal and pathological gait. Crit Rev Phys Rehabil Med 1989; 1:183-209.

92. Traballesi M, Porcacchia P, Averna T, Brunelli S. Energy cost of walking measurements in subjects with lower limb amputations: A comparison study between floor and treadmill test. Gait & Posture 27 (2008): 70-75.

93. Torburn L, Powers CM, Guiterrez R, Perry J. Energy expenditure during ambulation in dysvascualar and traumatic below-knee amputees: a comparison of five prosthetic feet. J Rehabil Res Dev 1995;32:111–9.

94. Donker SF, Beek PJ. Interlimb coordination in prosthetic walking: effects of asymmetry and walking velocity. Acta Psychologica, 2002; 110:265-288.

95. Schmalz T, Blumentritt S, Jarasch R. Energy expenditure and biomechanical characteristics of lower limb amputee gait: The influence of prosthetic alignment and different prosthetic components. Gait & Posture 2002, 16: 255-263.

96. Latash, M. Neurophysiological Basis of Movement. 2nd edition, Chapter 21, 33-35.

97. Sanders CT. Lower-Limb Amputations: A Guide to Rehabilitation. Philadelphia, Pa: FA Davis Co; 1986:13-33.

98. Munin MC, Espejo-De Guzman MC, Boninger ML, Fitzgerald SG, Penrod LE, Signh J. Predictive factors for successful early prosthetic ambulation among lower-limb amputees. J Rehabil Res Dev 2001; 38:379-384.

99. Torburn L, Perry J, Ayyappa E, Shanfield SL. Below-knee amputee gait with dynamic elastic response prosthetic feet: A pilot study. Journal of Rehabilitation Res. Dev. 1990; 27:369-384.

100. Powers CM, Boyd LA, Fontaine CA, Perry J: The influence of lower-extremity muscle force on gait characteristics in individuals with below-knee amputations secondary to vascular disease. Phys Ther 1996, 76: 369-385.

101. Powers CM, Rao S, Perry J. Knee kinetics in transtibial amputee gait. Gait & Posture 8 (1998): 1-7.

102. Dziuba AK, Tylkowska, Jaroszczuk S. Index of mechanical work in gait of children with cerebral palsy. Acta of Bioenginering and Biomechanics, 2014; vol 16, no. 3, 77-87.

103. Schwartz M, Rozumalski A. The gait deviation index: a new comprehensive index of gait pathology. Gait & Posture 2008; 28:351-357.

104. Fowler EG, Staudt LA, Greenberg MB, Oppenheim WL. Selective control assessment of lower extremity (SCALE): development, validation, and interrater reliability of a clinical tool for patients with cerebral palsy. Developmental Medicine and Child Neurology. 2009; 51:607-614.

105. Fowler EG, Goldberg EJ. The effect of lower extremity selective voluntary motor control on interjoint coordination during gait in children with spastic diplegic cerebral palsy. Gait & Posture 2009; 29:102-107.

106. Weyer A, Abele M, Schmitz-Hubsch T, Schoch B, Frings M, Timmann D, Klockgether T. Reliability and Validity of the Scale for the Assessment and Rating of Ataxia: A study in 64 ataxia patients. Movement Disorders, vol 22, no.11, 2007; p.1633-1637.

107. Trouillas P, Takayanagi T, Hallet M, Currier RD, Subramony SH, Wessel K, Bryer A, Diener HC, Massaqui S, Gomez CM, Coutinho P, Hamida MB, Campanella G, Filla A, Schut L, Timann D, Honnorat J, Nighoghossian N, Manyam B. International Cooperative Ataxia Rating Scale for pharmacological assessment of the cerebellar syndrome. Journal of the Neurological Sciences. 1997; 145:205-211.

108. Tison F, Yekhel F, Balestre E, Chrysostome V, Quinn N, Wenning G, Poewe W. Application of the international cooperative ataxia scale rating in multiple system atrophy. Movement Disorders, 2002; vol 17, no. 6, pp. 1248-1254.

109. Newell, K.M. (1986). Constraints on the development of coordination. In M.G. Wade & H.T.A. Whiting (Eds.), Motor development in children: Aspects of coordination and control (pp. 341-360). Dordrecht, Netherlands: Martinus Nijhoff.

110. Schmidt RA, Lee TD. Motor Control and Learning: A Behavioral Emphasis. 4th Ed., Human Kinetics, 2005, Champaign, IL.

111. Fitts PM. The information capacity of the human motor system in controlling the amplitude of movement. Journal of Experimental Psychology. 1954; 47:381-391.

112. Wren TA, Rethlefsen S, Kay RM. Prevalence of specific gait abnormalities in children with cerebral palsy: influence of cerebral palsy subtype, age, and previous surgery. J Pediatr Othrop 2005;25(1):79-83.

113. Sutherland DH, Santi M, Abel MF. Treatment of stiff-knee gait in cerebral palsy: a comparison by gait analysis of distal rectus femoris transfer verses proximal rectus release. Journal of Pediatric Orthop. 1990; 10:433-441.

114. Alexander MA, Matthews DJ. Pediatric Rehabilitation: Principles and Practice. 4th Ed. 2010, Demos Medical Publishing, New York NY. Chapter 16.

115. DeBruin, H., Russell, D.J., Latter, J.E., Sadler, JT., 1982. Angle-angle diagrams in monitoring and quantification of gait patterns for children with cerebral palsy. American Journal of Physical Medicine; vol. 61, no. 4, pp. 176–92.

116. Clark, J., Phillips, S., 1993. A longitudinal study of intralimb coordination in first year of independent walking: a dynamical systems analysis. Child Development, 64, 1143-1157.

117. Winstein, C., Garfinkel, A., 1989. Qualitative dynamics of disordered human locomotion: a preliminary investigation. Journal of Motor Behavior, vol 21, no 4, 373-391.

118. Farmer, S., Pearce, G., Stewart, C., 2006. Developing a technique to measure intra-limb coordination in gait: applicable to children with cerebral palsy. Gait & Posture, 28, 217-221.

119. Barela, J., Whitall, J., Black, P., Clark, J., 2000. An examination of constraints affecting the intralimb coordination of hemiparetic gait. Human Movement Science, 19, 251-273.

120. Scholz JP, Kelso JAS. 1989. A quantitative approach to understanding the formation and changes of coordination movement patterns. Journal of Motor Behavior, 21(2):122-144.

121. Schmidt RC, Treffner PJ, Turvey MT. 1992. Dynamical aspects of learning an interlimb rhythmic movement pattern. Journal of Motor Behavior 24:67-83.

122. Byrne JE, Stergiou N, Blanke D, Houser JJ, Kurz M. 2002, Comparison of gait patterns between young and elderly women: An examination of coordination. Perceptual and Motor Skills 94:265-280.

123. Strogatz SH. Nonlinear Dynamics and Chaos: With Applications to Physics, Biology, Chemistry, and Engineering. 1994. Perseus Books Publishing, Cambridge MA.

124. Kabada MP, Ramakrishnan K, Wooten ME. Measurement of lower extremity kinematics during level walking. J Orthop Res. 1990; 8: 338-392.

125. Hagio S, Kouzaki M. The flexible recruitment of muscle synergies depends on the required force-generating capability. J Neurophysiol 112: 316–327, 2014.

126. Clark DJ, Ting LH, Zajac FE, Neptune RR, Kautz SA. Merging of healthy motor modules predicts reduced locomotor performance and muscle coordination complexity post-stroke. J Neurophysiol 103: 844 – 857, 2010.

127. Steele KM, Tresch MC, Perreault EJ. The number and choice of muscles impact the results of muscle synergy analyses. Frontiers in Computational Neuroscience. 2013; 7, article 105: 1-9.

128. Zajac, FE. Muscle and tendon: properties, models, scaling, and application to biomechanics and motor control. Crit Rev Biomed Eng 14: 359–411, 1989.

129. Kurz, M, 2002. Effect of normalization and phase angle calculations on continuous relative phase. Journal of Biomechanics, 35, pp. 369-374.

130. Stergiou N, Jensen JL, Bates BT, Scholten SD, Tzetzis, G., 2001. "A dynamical systems investigation of lower extremity coordination during running over obstacles". Clinical biomechanics, 16 (3), p. 213.

131. Kugler PN, Kelso JAS, Turvey MT. On the concept of coordinative structures as dissipative structure. I. Theoretical lines of convergence. In G.E. Stelmach & J. Requin (Eds.), Tutorials in motor behavior. Amsterdam: North Holland, 1980.

132. Hamill J, Van Emmerik RE, Heiderscheit BC, Li L. 1999. A dynamical systems approach to lower extremity running injuries. Clinical Biomechanics, 14:297-308.

133. Van Emmerik RE, McDermott WJ, Haddad JM, Van Wegen EEH. 2004. Age-related changes in upper body adaptation to walking speed in human locomotion. Gait & Posture, 22:233-239.

134. Haddad JM, Van Emmerik RE, Whittlesey SN, Hamill J. 2006. Adaptations in interlimb and intralimb coordination to asymmetrical loading in human walking. Gait & Posture, 23:429-434.

135. Stergiou N, Decker LM. 2011. Human movement variability, nonlinear dynamics, and pathology: Is there a connection? Human Movement Science. P.1-20.

136. Kadabba, M., Ramakrishnan H., Wootten M., 1990. Measurement of lower extremity kinematics during level walking. Journal of Orthopaedic Research, 8, 383-392.

137. Carollo, J., Matthews, D., 2002. Strategies for clinical motion analysis based on functional decomposition of the gait cycle. PMR Clinics of North America, 13:949-977.

138. Baker, R., McGinley J.L., Schwartz, M., Beynon, S., Rozumalski, A., Graham, H.K., Tirosh, O., 2008. The gait profile score and movement analysis profile. Gait & Posture, 30:265-269.

139. Bleck, EE., 1987. Orthopaedic Management in Cerebral Palsy. Clinics in Developmental Medicine No. 99/100. London: Mac Keith Press. p 50–52.

140. Marks, M.C., Alexander, J., Sutherland, D.H., Chambers, H.G., 2003. Clinical utility of the Duncan-Ely test for rectus femoris dysfunction during the swing phase of gait. Developmental Medicine & Child Neurology, 45: 763-768.

141. Dutton, M. Orthopaedic Examination, Evaluation, and Intervention. 2nd Ed., pg. 880-881.

142. Molloy M, McDowell BC, Kerr C, Cosgrove AP. Further evidence of validity of the Gait Deviation Index. Gait & Posture. 2010;31:479–82.

143. Carollo, J., Matthews, D. Pediatric Rehabilitation: Principles and Practice. 4th Edition. Chp16 Assessment of human gait, motion, and motor function. 2009

144. Ramsay, J.O., Silverman, B.W., Functional Data Analysis. 1997, Springer-Verlag, New York.

145. Alton F, Baldey L, Caplan S, Morrissey MC. A kinematic comparison of overground and treadmill walking. Clinical Biomechanics 1998: 13: 434-440.

146. Murray MP, Spurr GB, Sepic SB, Gardner GM, Mollinger LA. Treadmill vs. floor walking: kinematics, electromyogram, and heart rate. Journal of Applied Physiology 1985: 59(1): 87–91.

147. Riley PO, Paolini G, Della Croce U, Paylo KW, Kerrigan DC. A kinematic and kinetic comparison of overground and treadmill walking in healthy subjects. Gait & Posture 2007: 26: 17-24.

148. Nymark JR, Balmer SJ, Melis EH, Lemaire ED, Millar S. Electromyographic and kinematic nondisabled gait differences at extremely slow overground and treadmill walking speeds.

149. White SC, Yack HJ, Tucker CA, et al. Comparison of vertical ground reaction forces during overground and treadmill walking. Med Sci Sports Exer 1998; 30(10): 1537–1542.

150. Lee SJ, Hidler J. Biomechanics of overground vs. treadmill walking in healthy individuals. Journal of Applied Physiology 2007: 104: 747-755.

151. Regnaux JP, Robertson J, Smail DB, Daniel O, Bussel B. Human treadmill walking needs attention. Journal of Neuroengineering Rehabilitation 2006,3:19.

152. Finley J, Statton M, Bastian A. A novel optic flow pattern speeds split-belt locomotor adaptation. Journal of Neurophysiology 2014: 111: 969-976.

153. Strathy, G.M., E.Y. Chao, and R.K. Laughman. Changes in knee function associated with treadmill ambulation. Journal of Biomechanics 16: 517-522, 1983.

154. Begnoche, D., Pitettie, K. Effects of traditional treatment and partial body weight treadmill training on the motor skills of children with spastic cerebral palsy: a pilot study. Pediatric Physical Therapy, 2007, 19(1):11-19.

155. Thelen, E. Motor development: a new synthesis. Am Psychol. 1995;50: 79 –95.

156. Kamm, K., Thelen, E., Jensen, J.L. A dynamic systems approach to motor development. Phys Ther. 1990;70:763–775.

157. Scholz, JP. Dynamic pattern theory: some implications for therapeutics. Phys Ther. 1990;70:827–843.

158. Kelso, J.A.S. Anticipatory dynamic systems, intrinsic pattern dynamics and skill learning. Human Movement Sci. 1991;10:93–111.

Appendix A   Internal Review Board Documents

A.1   Prospective Subject Pre-screening Script and Form

PI: "Hello, my name is Kate Worster and I am a doctoral student at the University of Colorado in Denver. Thank you for your interest in my research project. Can you tell me to which flyer you are responding or in which group of subjects you might participate?

My research project will use motion capture technology at the Center for Gait and Movement Analysis Lab at the Children's Hospital Colorado to learn more about the coordination of walking. A study subject will walk over-ground and on a treadmill while I collect video and motion capture data. The total data collection session at the lab would last 1 to 2 hours at most, with the opportunities for resting breaks in between walking. A subject who participates in this study will wear clothing he/she owns such as a tank top and shorts or a bathing suit, whichever feels most comfortable, during the data collection. Are you still interested in participating?"

Interested subject/parent: "No." PI: "Thank you for your time and I hope you have a wonderful day."

Interested subject/parent: "Yes." PI: Thank you for your interest in this study. Before you come to the Center for Gait and Movement Analysis Laboratory to learn more about the study, it would be helpful to see if you are likely to qualify to be in the study. In order to do this, I would like to ask you a couple of eligibility questions. It should take about 5 minutes to go through these questions. You do not have to answer any question that might make you uncomfortable or you simply would not like to answer, but without answers to these questions you will not be eligible to participate in this study. I will not record your name or any other information that would identify you on the form I use to record your answers until I know you have qualified for this study. If you do not qualify for this study, I will immediately destroy any information I have collected. Before I begin asking you questions, I am required to give you the number of COMIRB, the Ethics Board that oversees our research. The number is (303) 724-1055. If you have any questions or concerns please contact them at this number.

Do you have any questions about the pre-screening questions I will ask you or about the study?

Do I have your permission to begin the questions?

1.) Do you speak and understand English?

_Yes _No _No answer

2.) Are you between the ages of 7-100?

_Yes _No _No answer

3.) Can you walk continuously unassisted, without a device such as a walker or cane, for 3 minutes?

_Yes _No _No answer

4.) Do you have a diagnosis of one of the following: spastic cerebral palsy or have a lower limb amputation?

_Yes _No _No answer

a. If yes to spastic cerebral palsy:

i. Do you take any medications or use medical devices that affect how you walk?

_Yes _No _No answer

ii. Have you been diagnosed with any additional neuromuscular or cardiovascular conditions?

_Yes _No _No answer

b. If yes to lower limb amputation:

i. Have you been using the prosthetic limb for at least 6 months for independent walking?

_Yes _No _No answer

ii. Do you have a below knee or above knee amputation?

_Yes _No _No answer

iii. Have you been diagnosed with any neuromuscular or cardiovascular conditions?

_Yes _No _No answer

5.) Have you had surgery at your hip, knee, or ankle within the last 2 years?

_Yes _No _No answer

6.) Have you been diagnosed or are aware of having a leg length discrepancy of greater than 2 cm or 1?

_Yes _No _No answer

7.) Do you have pain in a hip, knee, and/or ankle joint?

_Yes _No _No answer

8.) Do you have reliable transportation to Children's Hospital Colorado?

_Yes _No _No answer

9.) Would you be willing to consent to motion capture trials and video of you walking?

_Yes _No _No answer

If interested subject meets all inclusion criteria and none of the exclusion criteria:

PI: "Based upon your answers, you are likely to qualify to be in this study. Would you like to schedule a time to visit the Center for Gait and Movement Analysis?"

Study Code for Interested Participant: _____

A.2   Prospective Subject Combined Consent and HIPPA Authorization Form

You are being asked to be in a research study. This form provides you with information about the study. A member of the research team will describe this study to you and answer all of your questions. Please read the information below and ask questions about anything you don't understand before deciding whether or not to take part.

Why is this study being done?

Adults or children ages 13-18 without gait pathology & typically developing children.

This study plans to learn more about how individuals without pathological gait walk in response to varying conditions. We will study how you walk in the various conditions:

- At your preferred speed over ground and on a treadmill

- Over ground at faster and slower speeds

- On a treadmill at your preferred speed with small weights added to your legs

- When you are supported by a harness that partially lifts your weight (lower gravity) and will prevent falling on the treadmill if needed

- Walking on a treadmill at your preferred speed with resistance and assistance to your legs by using cables attached to your ankles

- Turning a corner

- With one foot in front of the other (tandem)

You are being asked to be in this research study because you are either an adult or child between the ages of 13-18 years without gait pathology or a typically developing child. Data from how you walk will be used to help us understand individuals who have difficulty walking and potentially develop new ways to help those individuals walk more like you.

Subjects with a diagnosis of lower limb amputation, cerebellar ataxia, or spastic cerebral palsy.

This study plans to learn more about how an individual with your diagnosis walks in response to varying conditions. We will study how you walk in the various conditions:

- At your preferred speed over ground and on a treadmill

- When you are supported by a harness that partially lifts your weight (lower gravity) and will prevent falling on the treadmill if needed

- Turning a corner

- With one foot in front of the other (tandem)

You are being asked to be in this research study because you have a diagnosis of either a lower limb amputation, cerebellar ataxia, or spastic cerebral palsy. Data from how you walk will be used to help us understand other individuals with a similar diagnosis.

Other people in this study

Up to 80 people from your area (Colorado) will participate in the study as subjects whose motion capture data will be captured prospectively. Additionally, motion capture data previously collected at the Center for Gait and Movement Analysis Laboratory will be reviewed and included in this study. Of this previously recorded data, there will be a maximum of 280 typically developing subjects, a maximum of 280 subjects with cerebral palsy, and a maximum of 10 subjects with a lower limb amputation. Combining the number of all subjects in this study, there will be a maximum total of 650 subjects, consisting of at most 300 typically developing subjects, 300 subjects with cerebral palsy, 20 subjects with cerebellar ataxia, and 20 subjects with a lower limb amputation.

What happens if I join this study?

If you join the study, you will wear comfortable athletic clothing (e.g. shorts, t-shirt, tennis shoes) while walking in our two motion capture environments. Before you walk in the motion

capture environments, measurements of your legs, arms, weight, and height will be taken for the computer models. As part of a noninvasive movement evaluation, you will also be asked to move your legs through various motions (e.g. extend your knee, flex your hip, etc.). 35 passive retro-reflective markers will be placed on your legs, torso, arms, and head to capture your movement. Two video cameras will record video of you (from the shoulders down) walking and performing the study's motion capture tasks. All of the study's tasks are for research purposes only. After you've completed your study and if you'd like, we will give you a compact disk with your motion capture data and computer model for your own use/record. The motion capture session for a typically developing subject will last 2-3 hours. The motion capture session for an atypical subject will last 1-2 hours.

What are the possible discomforts or risks?

Discomforts you may experience while in this study include slight discomfort while in the body weight support harness worn during the treadmill walking tasks. For your safety, all treadmill walking tasks will be performed while wearing a harness to prevent injury. Other possible risks include the possibility of falling during the over-ground walking tasks. There is a risk that people outside of the research team will see your research information. We will do all that we can to protect your information, but it cannot be guaranteed.

What are the possible benefits of the study?

This study is designed for the researcher to learn more about how normal adults or typically developing children walk in response to various conditions and how an individual with the diagnosis of a lower limb amputation, cerebellar ataxia, or spastic cerebral palsy walk. There is no direct benefit for your participation in the study. This study is not designed to treat any illness or to improve your health. Also, there may be risks, as discussed in the section describing the discomforts or risks.

Will I be paid for being in the study?

You will not be paid to be in the study.

Will I have to pay for anything?

It will not cost you anything to be in the study.

Is my participation voluntary?

Taking part in this study is voluntary. You have the right to choose not to take part in this study. If you choose to take part, you have the right to stop at any time. If you refuse or decide to withdraw later, you will not lose any benefits or rights to which you are entitled.

Can I be removed from this study?

The study investigator may decide to stop your participation without your permission if the study investigator thinks that being in the study may cause you harm, or for any other reason.

Who do I call if I have questions?

The researcher carrying out this study is Kate Worster. You may ask any questions you have now. If you have questions, concerns, or complaints later, you may call Kate Worster at 720-777-8216 or email at kate.worster@childrenscolorado.org. You will be given a copy of this form to keep.

You may have questions about your rights as someone in this study. You can call Kate Worster with questions. You can also call the responsible Institutional Review Board (COMIRB). You can call them at 303-724-1055.

Who will see my research information?

The University of Colorado Denver and the hospital(s) it works with have rules to protect information about you. Federal and state laws including the Health Insurance Portability and Accountability Act (HIPAA) also protect your privacy. This part of the consent form tells you what information about you may be collected in this study and who might see or use it. The institutions involved in this study include:

- University of Colorado Denver

- Children's Hospital Colorado

We cannot do this study without your permission to see, use and give out your information. You do not have to give us this permission. If you do not, then you may not join this study. We will

see, use and disclose your information only as described in this form and in our Notice of Privacy Practices; however, people outside the University of Colorado Denver and its affiliate hospitals may not be covered by this promise. We will do everything we can to keep your records a secret. It cannot be guaranteed.

The use and disclosure of your information has no time limit. You can cancel your permission to use and disclose your information at any time by writing to the study's Primary Investigator, at the name and address listed below. If you do cancel your permission to use and disclose your information, your part in this study will end and no further information about you will be collected. Your cancellation would not affect information already collected in this study.

Kate Worster
Children's Hospital Colorado
Center for Gait and Movement Analysis
13123 East 16th Avenue B476 Aurora CO 80045

Both the research records that identify you and the consent form signed by you may be looked at by others who have a legal right to see that information.

- Federal offices such as the Food and Drug Administration (FDA) that protect research subjects like you.

- People at the Colorado Multiple Institutional Review Board (COMIRB).

- The study investigator and the rest of the study team.

- Officials at the institution where the research is being conducted and officials at other institutions involved in this study who are in charge of making sure that we follow all of the rules for research.

We might talk about this research study at meetings. We might also print the results of this research study in relevant journals. But we will always keep the names of the research subjects, like you, private. You have the right to request access to your personal health information from the Investigator.

Information about you that will be seen, collected, used and disclosed in this study:

- Demographic Information (age, sex)

- Portions of my previous and current Medical Records that are relevant to this study: Diagnosis(es)

- All motion capture data (markers and de-identified video)

What happens to Datathat are collected in this study?

Scientists at the University of Colorado Denver and the hospitals involved in this study work to find the causes and cures of disease. The data collected from you during this study are important to this study and to future research. If you join this study:

- The data are given by you to the investigators for this research and so no longer belong to you.

- Both the investigators and any sponsor of this research may study your data collected from you.

- If data are in a form that identifies you, UCD or the hospitals involved in this study may use them for future research only with your consent or IRB approval.

- Any product or idea created by the researchers working on this study will not belong to you.

- There is no plan for you to receive any financial benefit from the creation, use or sale of such a product or idea.

Agreement to be in this study and use my data I have read this paper about the study or it was read to me. I understand the possible risks and benefits of this study. I understand and authorize the access, use and disclosure of my information as stated in this form. I know that being in this study is voluntary. I choose to be in this study. I will get a signed and dated copy of this consent form.

Signature: _____
Date: _____
Print Name: _____
Consent form explained by: _____
Date: _____
Print Name: _____
Investigator: _____
Date: _____ Investigator must sign within 30 days
Date:_____
Witness of Signature: _____
Witness of consent process: _____
Date:_____
Child
Consent form explained by: _____
Print Name: _____
Date:_____
Investigator: _____
Date: _____

A.3   Informed Assent Form

Informed Assent for ages: 7-12

What is this study about?

I am being asked if I want to be in this study. The goal of this study is to learn more about how people walk.

Why are you asking me?

(For subject with cerebral palsy only) I am being asked to be in the study because I have what doctors call cerebral palsy and this changes how I walk.

(For subject with a lower limb amputation only) I am being asked to be in the study because I have what doctors call a lower limb amputation and this changes how I walk.

(For subject without gait impairment only) I am being asked to be in the study because I walk normally.

What Do I Have to Do or What Will Happen to Me?

If I am in the study, I will:

- The Researcher will do a short physical exam.

- Walk on the ground and on a treadmill.

- Spend 1 to 2 hours at the motion capture lab.

Will this Hurt?

When I walk on the treadmill, I will wear a harness for my safety that may feel uncomfortable but it will not hurt me. I will wear markers on my legs, arms, head, and trunk that are like stickers and will not hurt me.

Do I get anything for being in the study?

If I am in the study, I will get a compact disc containing all my data and the computer model of me if I would like one.

Can I ask Questions?

I asked any questions I have now about the study. All my questions were answered. I know that if I have a question later, I can ask and get an answer. If I want to, I can call Kate Worster at 720-777-8216.

Do I Have to Do This?

I know that I do not have to be in this study. No one will be mad at me if I say no.

I want to be in the study at this time. _Yes _No

I will get a copy of this form to keep.

Child's Printed Name: _____

Child's Signature: _____

Date: _____

Witness or Mediator:_____

Date:_____

I have explained the research at a level that is understandable by the child and believe that the child understands what is expected during this study.

Signature of Person Obtaining Assent:_____ Date:_____

Initials:_____

A.4 Prospective Subject Data Collection Form

DATA COLLECTION SHEET FOR PROSPECTIVE SUBJECTS

Subject Study ID: _____ Age: _____

Height (cm): _____ Weight (kg): _____

Dominant Leg (L/R): _____

ANTHROPOMETRICS (cm): L R

Leg Length: _____ _____

Knee Width: _____ _____

Ankle Width: _____ _____

Elbow Width: _____ _____

Wrist Thickness: _____ _____

Hand Thickness: _____ _____

MODIFIED ICARS TASKS

Knee-Tibia Test: L_____ R_____

Tandem Walking: _____

Turning & Walking: _____

Grade			Left			Right		
			Hip	Knee	Ankle	Hip	Knee	Ankle
Normal (2pt)				▓	▓		▓	▓
Impaired (1pt)			▓		▓	▓		▓
Unable (0pt)			▓	▓		▓	▓	
Total Limb Score	Left=	Right=						

Resisted Synergy	Left			Right		
	Hip	Knee	Ankle	Hip	Knee	Ankle
Knee ext w/resisted limb ext	▓		▓	▓		▓
Dorsiflex w/resisted limb flex	▓	▓		▓	▓	

Descriptors	Left			Right		
	Hip	Knee	Ankle	Hip	Knee	Ankle
Hip Flexion Contracture		▓	▓		▓	▓
Hamstring Tightness		▓	▓		▓	▓
Mirrors motion on opposite limb						
Motion slower than 3 sec verbal count						
Moves one direction only (note motion achieved)						
Movement of other joints						
Motion <= 50% of available range of motion						

Figure A.4.1: SCALE data capture and scoring sheet.

Appendix B   Procedural Fidelity of Performance Measures
B.1   SCALE Tasks

The following sections provide the methodology, instructions, procedures and scoring criteria for the Selective Control Assessment of the Lower Extremity (SCALE) exam administered to each prosective subject.

Before asking the subject to perform each joint test, the examiner passively moved the joint to assess the subject's range of motion. To assure the subject understood the task, the examiner first demonstrated the movement sequence while supporting the limb. The language used to instruct subject is provided for each joint's task. To guide subjects at the desired speed of movement, the examiner provided a verbal three-second count during each task. Multiple attempts were allowed and feedback to improve performance was used when necessary. The following general instructions were given to each subject prior to the beginning of the exam: "I am going to ask you to move in a certain way. Move the way I ask you to move. Try not to move any other part of your body. If you have any questions or you don't understand what I am asking you to do, please tell me."

The five factors used as grading criteria for each subject were: 1) ability to selectively move each joint; 2) involuntary movement at other joints including the contralateral limb; 3) ability to reciprocate movement; 4) speed each movement was performed; and 5) generation of force as demonstrated by excursion within the subject's available range of motion. In addition to the specific joint task scoring descriptions provided above, the following general criteria for designating a movement task as 'normal', 'impaired', or 'unable' is consistent with the original definitions of the SCALE performance tasks. The designation of a 'normal' performance is defined as when the subject completes the desired movement sequence in time with the examiner's three-second verbal count and without movement of untested ipsilateral or contralateral leg joints. The designation of 'impaired' is defined as when the subject is able to isolate joint motion during part of the task, but also is only able to move the joint in one direction, subject's movement is less than 50% of the approximate available passive range of motion found during the passive demonstration, movement occurs at a non-tested joint (e.g. mirror movements), or the subject performs the task slower than the examiner's three-second verbal cadence. The task is designated 'unable' if the subject does not initiate the movement or performs the motion using a synergistic mass flexor or extensor pattern (e.g. simultaneous, obligatory flexor or extensor pattern at two or more joints). A SCALE score for each limb (left, right) is obtained by summing the points assigned to each joint. Since only the hip, knee, and ankle, joints are being measured for this research project, a maximum limb score of 6 points is possible.

B.1.1   Hip Flexion/Extension

- **Purpose:** Test subject's voluntary ability to use selectively control hip flexion/extension.

- **Subject Position:** Subject lies on one side with bottom leg flexed for stability and top leg extended. The task is performed for each hip.

- **Instruction to Subject:** Subject was asked to flex, extend then flex the hip while keeping the knee extended. For example: "Move your leg forward, back, then forward again while keeping your knee straight. I will take you through the motion first, and then I'd like you to do it yourself."

- **Passively Guided Motion:** While supporting weight of limb, the examiner moves each leg through flexion, extension, and flexion in time with a verbal three-second count. Examiner also stabilizes pelvis and/or has subject use hands to keep pelvis erect and trunk in neutral alignment.

- **Active Motion by Subject:** Subject flexes, extends, and flexes hip while maintaining knee in extension and with examiner supporting weight of limb.

- **Scoring:** The list below provides the criteria and corresponding score for this aspect of the SCALE procedure.

◇ 2 = Normal performance of task. Completes isolated movement within 3 second verbal count.

◇ 1 = Impaired performance of task. Less than 50% of available motion; slower than 3 second count; mirror movements of contralateral limb; motion at other joints; and/or movement occurs only in one direction.

◇ 0 = Unable to perform task. Cannot flex or flexes with simultaneous knee flexion.

B.1.2   Knee Extension/Flexion

- **Purpose:** Test subject's voluntary ability to use selectively control knee flexion/extension.

- **Subject Position:** Subject sits on the edge of the exam table with hip and knee flexed. If needed, can use arms for trunk support, to maintain an upright sitting posture, and vertical pelvis position. The task is performed for each knee.

- **Instruction to Subject:** Subject was asked to flex, extend then flex the knee. For example: "Bend your knee, extend your knee, and then bend your knee. Try to do this without leaning further back or moving your other leg. I will take you through the motion first, and then I'd like you to do it yourself."

- **Passively Guided Motion:** Examiner stabilizes the thigh while moving the subject's shank through the knee flexion, extension, and flexion motion in time with a three-second verbal count.

- **Active Motion by Subject:** Subject flexes, extends, and flexes knee while maintaining trunk support and with examiner providing a verbal cadence for the speed of movement.

- **Scoring:** The list below provides the criteria and corresponding score for this aspect of the SCALE procedure.

    ◇ 2 = Normal performance of task. Completes isolated movement within 3 second verbal count.

    ◇ 1 = Impaired performance of task. Less than 50% of available motion; slower than 3 second count; mirror movements of contralateral limb; motion at other joints; and/or movement occurs only in one direction.

    ◇ 0 = Unable to perform task. Cannot extend or extends knee only with simultaneous hip extension (extensor synergy).

B.1.3   Ankle Dorsiflexion/Plantarflexion

- **Purpose:** Test subject's voluntary ability to use selectively control ankle dorsi/plantarflexion.

- **Subject Position:** Subject sits on exam table with hip and knee flexed. If needed, can use arms for trunk support, to maintain an upright sitting posture, and vertical pelvis position. The task is performed for each ankle.

- **Instruction to Subject:** Subject was asked to flex, extend, and then flex the ankle while the examiner supports the leg with the knee extended. For example: "Keep your knee straight and while I support the weight of your leg, move your foot up, then down, then up again. I will take you through the motion first, and then I'd like you to do it yourself."

- **Passively Guided Motion:** Examiner supports limb under distal portion of shank and with care to touch only the lateral sides of the foot, examiner moves the ankle through plantarflexion, dorsiflexion, and plantarflexion in time with a verbal three-second count.

- **Active Motion by Subject:** Subject plantarflexes, dorsiflexes, and plantarflexes ankle while examiner supports weight of limb as knee is extended and in time with examiner's verbal cadence.

- **Scoring:** The list below provides the criteria and corresponding score for this aspect of the SCALE procedure.

    - ◇ 2 = Normal performance of task. Completes isolated movement within 3 second verbal count. Must observe at least 15° arc of dorsiflexion motion.
    - ◇ 1 = Impaired performance of task. Less than 50% of available motion; slower than 3 second count; mirror movements of contralateral limb; motion at other joints; movement occurs only in one direction; simultaneous inversion or primarily moves toes.
    - ◇ 0 = Unable to perform task. Cannot dorsiflex or dorsiflexes with simultaneous hip and knee flexion (flexor synergy).

B.1.4 SCALE Resisted Synergies

B.1.4.1 Knee Extension with Resisted Limb Extension

- **Purpose:** Test for presence of extension synergy.

- **Subject Position:** Subject sits at the edge of the exam table hip and knee flexed. If needed, can use arms for trunk support, to maintain an upright sitting posture, and vertical pelvis position. The task is performed for each leg.

- **Instructions to Subject:** Subject is asked to push his/her thigh upward against the examiner's hand, which is placed at the distal end of the subject's thigh, and resist the examiner from pushing the thigh downward.

- **Active Motion by Subject:** Examiner provides resistance to hip flexion at the distal thigh as subject flexes hip. Examiner watches for simultaneous dorsiflexion of the ankle.

- **Score:** The table below provides the score criteria for this aspect of the SCALE procedure.

Table B.1.1: SCALE scoring for knee extension with rested limb extension task.

Score	Criteria
Absent	No perceptible dorsiflexion.
Present	Perceptible dorsiflexion at ankle with resistance to hip flexion.

B.1.4.2 Plantarflexion Contracture Test

- **Purpose:** This task tests for the presence of a contracture at the ankle during plantarflexion.

- **Subject Position:** Subject sits at the edge of the exam table hip and knee flexed. If needed, can use arms for trunk support, to maintain an upright sitting posture, and vertical pelvis position. The task is performed for each leg.

- **Instructions to Subject:** Subject is asked to push his/her foot downward against the examiner's hand, which grips the subject's foot at the medial side of the first metatarsal and lateral side of the fifth metatarsal, and resist the examiner from pushing the foot upward. The subject is instructed to try to maintain a neutral position of the ankle.

- **Active Motion by Subject:** Examiner provides resistance to hip flexion at the distal thigh as subject flexes hip. Examiner watches for simultaneous dorsiflexion of the ankle.

- **Score:** The table below provides the score criteria for this aspect of the SCALE procedure.

Table B.1.2: SCALE scoring for plantarflexion contracture task.

Score	Criteria
2	Range of motion beyond $\approx 90°$.
1	Passive range of motion at $\approx 90°$.
0	Passive range of motion does not achieve ($\approx 90°$).

B.1.4.3   Hip Flexion Synergy Test

- **Purpose:** This task tests for the presence of a synergy during hip flexion.

- **Subject Position:** Subject sits at the edge of the exam table hip and knee flexed. If needed, can use arms for trunk support, to maintain an upright sitting posture, and vertical pelvis position. The task is performed for each leg.

- **Instructions to Subject:** Subject is asked to push his/her thigh upward against the examiner's hand, which is placed at the distal end of the subject's thigh, and resist the examiner from pushing the thigh downward.

- **Active Motion by Subject:** Examiner provides resistance to hip flexion at the distal thigh as subject flexes hip. Examiner watches for simultaneous dorsiflexion of the ankle.

- **Score:** The table below provides the score criteria for this aspect of the SCALE procedure.

Table B.1.3: SCALE scoring for hip flexion synergy task.

Score	Criteria
2	No perceptible dorsiflexion.
1	Mild to invariant dorsiflexion at ankle with resistance to hip flexion.
0	Perceptible dorsiflexion at ankle with resistance to hip flexion.

B.1.5   SCALE Desriptors

The following SCALE descriptors were performed and serve as general descriptors for the subject. The scores for these SCALE descriptors were not included in the SCALE limb score.

B.1.5.1   Hip Adduction Contracture

- **Purpose:** This task is to test for the presence of a contracture at the hip during adduction.

- **Subject Position:** Subject lies on side with bottom leg flexed for stability. The task is performed for each leg.

- **Instructions to Subject:** Subject was asked to relax his/her leg as examiner supports the weight of the leg and moves it away from his/her side until resistance from joint's range of motion is met.

- **Passively Guided Motion:** While supporting weight of limb, the examiner moves leg to max abduction in coronal plane.

- **Score:** The table below provides the score criteria for this aspect of the SCALE procedure.

Table B.1.4: SCALE scoring for hip adduction contracture task.

Score	Criteria
2	Normal performance of task. Hip abducts beyond horizontal.
1	Impaired performance of task. Hip abducts to horizontal.
0	Unable to perform task. Hip does not abduct to horizontal.

B.1.5.2 Hamstring Tightness

- **Purpose:** This task is performed to assess the amount, if any, of hamstring tightness.

- **Subject Position:** Subject lies in a supine position on the exam table. The task is performed for each leg.

- **Passively Guided Motion:** Subject is asked to relax his/her leg as examiner supports the weight of the leg at the ankle and moves it away from the table as far as comfortably possible or until motion is felt at the opposite anterior superior iliac spine. The examiner's other hand is placed on the subject's opposite anterior superior iliac spine to provide pelvic stability. If hamstring muscles provide resistance or there is a catch, the leg is lowered slightly and then raised again at a slower rate to determine range of motion.

- **Score:** The table below provides the score criteria for this aspect of the SCALE procedure.

Table B.1.5: SCALE scoring for hamstring tightness task.

Score	Criteria
2	Normal performance of task. Leg flexes from starting position to $\approx 90°$.
1	Impaired performance of task. Leg is flexed between $\approx 45°$-$90°$.
0	Unable to perform task. Hamstring tightness limits hip flexion to $\lesssim 45°$.

B.1.5.3 Thomas Test

- **Purpose:** For subjects with a reduced hip flexion/extension range of motion, this test was used to assess the tightness of the muscles involved in or effecting hip flexion (e.g. rectus femoris, illiopsoas).

- **Subject Position:** Subject lies in a supine position on the exam table and brings one knee in toward the chest, thus flexing the hip, while the other leg remains extended on the table.

- **Passively Guided Motion:** Examiner assist's subject if unable to perform this motion independently. Examiner watches for extended leg's orientation, hip motion, and pelvis orientation. A positive test indicates the subject has decreased hip flexibility due to tightness of the rectus femoris and/or iliopsoas muscles.

- **Score:** The table below provides the score criteria for the Thomas test [141].

Table B.1.6: SCALE scoring for Thomas test.

Score	Criteria
2	Test is negative. Contralateral hip does not flex, leg remains extended horizontally, and no rotation of pelvis occurs.
1	Test is positive. Leg is flexed up to $\approx 45°$ from horizontal.
0	Test is positive. Leg is flexed $\gtrsim 45°$ from horizontal.

B.1.5.4   Duncan Ely Test

- **Purpose:** For subjects with cerebral palsy, this test was used to assess spasticity of the rectus femoris muscle.

- **Subject Position:** Subject lies in a prone position on the exam table with one leg extended.

- **Passively Guided Motion:** Examiner flexes the subject's knee rapidly while the patient lies prone in a relaxed state with the other leg extended. If resistance or a catch is felt by the examiner and/or simultaneous hip flexion occurs, then spasticity is present in the rectus femoris muscle.

- **Score:** The table below provides the score criteria for the Duncan Ely test [139,141].

Table B.1.7: SCALE scoring for Duncan Ely test.

Score	Criteria
2	Normal performance of task. Knee flexes from extended position to $\gtrapprox 90°$.
1	Impaired performance of task. Knee is flexed greater than $\approx 45°$ but $< 90°$.
0	Unable to perform task. Knee is flexed to less than $\approx 45°$.

B.2   Select ICARS and SARA Tasks

The following sections provide the scoring criteria for the prospective subjects who performed select walking tasks from the International Cooperative Ataxia Rating Scale (ICARS) and Scale for the Assessment and Rating of Ataxia (SARA) exams. Prior to performing the tasks, subjects were given a verbal description of the task and the examiner demonstrated each task. Subjects were then asked to perform the task at a self-selected speed. Each task for a subject was scored using the following criteria. The score for each ICARS/SARA task was then summed and used as the subject's final ICARS/SARA score. A score of 40 points is the maximum possible score and indicates no impairment or difficult performing the tasks. A subject score that is less than 40 points indicates varying levels of difficulty in performing the tasks.

B.2.1   Forward Walking Capacities

The following descriptions were used to score each prospective subject's forward walking ability.

- 8 = Normal, no difficulties in walking

    - ◇ 7 = Almost normal naturally
    - ◇ 6 = Walking without support, but clearly abnormal and irregular
    - ◇ 5 = Walking without support but with considerable staggering
    - ◇ 4 = Walking with autonomous support no longer possible; patient requires intermittent support of the wall
    - ◇ 3 = Walking only possible with light support by one arm required (e.g. one stick/person), severe staggering
    - ◇ 2 = Walking >10m only possible with strong support (e.g. two special sticks, stroller, or accompanying person)
    - ◇ 1 = Walking <10m only possible with strong support (e.g. two special sticks, stroller, or accompanying person) 0 = Unable to walk, even with support

B.2.2 90° Turning Task

The following descriptions were used to score each prospective subject's ability to execute left and right 90 degree turns.

- 8 = Normal, no difficulties in turning

- 7 = Almost normal naturally

- 6 = Walking without support, but clearly abnormal and irregular

- 5 = Walking without support but with considerable staggering; difficulties in half turn but without support

- 4 = Walking with autonomous support no longer possible; patient requires intermittent support

- 3 = Walking only possible with light support by one arm required (e.g. one stick/person), severe staggering

- 2 = Walking >10m only possible with strong support (e.g. two special sticks, stroller, or accompanying person)

- 1 = Walking <10m only possible with strong support (e.g. two special sticks, stroller, or accompanying person)

- 0 = Unable to walk, even with support

B.2.3 Tandem Walking Task

The following descriptions were used to score each prospective subject's ability to execute tandem walking.

- 8 = Normal, no difficulties in tandem walking

- 7 = Almost normal naturally, but unable to walk with feet in tandem position

- 6 = Walking clearly abnormal and irregular, tandem walking >10 steps not possible

- 5 = Walking without support but with considerable staggering

- 4 = Walking with autonomous support no longer possible; patient requires intermittent support

- 3 = Walking only possible with light support by one arm required (e.g. one stick/person), severe staggering

- 2 = Walking >10m only possible with strong support (e.g. two special sticks, stroller, or accompanying person)

- 1 = Walking <10m only possible with strong support (e.g. two special sticks, stroller, or accompanying person)

- 0 = Unable to walk, even with support

B.2.4   Knee-Tibia Slide Task

The following descriptions were used to score each prospective subject's ability to touch the heel on the opposing limb's knee and slide the heel down the tibial crest, pick up the heel, and repeat this motion for a total of three times per limb.

4 = Normal

3 = Lowering of heel in continuous axis, but movement is decomposed in several phases, without real jerks, or abnormally slow. Slightly abnormal, contact to shin maintained

2 = Lowering jerkily in the axis, clearly abnormal, goes off shin up to 3 times during 3 cycles

1 = Lowering jerkily with lateral movements, severely abnormal, goes off shin 4 or more times during 3 cycles

0 = Lowering jerkily with extremely strong lateral movements or unable to perform task

B.2.5   Action Tremor in Heel-to-Knee test

The following descriptions were used to score the amount of action tremor present for each prospective subject's during the knee-tibia slide task.

- 4 = No trouble

- 3 = Tremor stopping immediately when heel reaches knee

- 2 = Tremor stopping in less than 10 seconds after reaching the knee

- 1 = Tremor continuing for more than 10 seconds after reaching the knee

- 0 = Uninterrupted tremor or unable to perform task

Appendix C   Pendulum Equations of Motion
C.1   Equations of Motion

The Lagrangian approach was used to solve for the equations of motion of a simple, two dimensional compound pendulum. First, the equations of motion were solved without damping or inertia terms. Second, the equations were solved to account for these two terms. This second set of equations was then re-organized to ease its formatting and translation into the custom Matlab function that was used to compare the motion of the theoretical pendulum to the sagittal plane motion of the thigh and shank from subject motion capture data during the task of swing limb advancement (Aim 3). The following figures provide the derivation and final equations of motion for two different compound pendulum models.

Figure C.1.1: Part 1 of Lagrangian approach to solving the equations of motion for a double pendulum without damping or inertia terms.

THEN THE <u>LAGRANGIAN</u> IS

$$L = T - V$$

$$= \left[\tfrac{1}{2}m_1 \ell_1^2 \dot{\theta}_1^2 + \tfrac{1}{2}m_2\left(\ell_1^2\dot{\theta}_1^2 + \ell_2^2\dot{\theta}_2^2 + 2\ell_1\ell_2\dot{\theta}_1\dot{\theta}_2\cos(\theta_1-\theta_2)\right)\right] - \left[-(m_1+m_2)g\ell_1\cos\theta_1 - m_2 g\ell_2\cos\theta_2\right]$$

$$\boxed{L = \left[\tfrac{1}{2}(m_1+m_2)\ell_1^2\dot{\theta}_1^2 + \tfrac{1}{2}m_2\ell_2^2\dot{\theta}_2^2 + m_2\ell_1\ell_2\dot{\theta}_1\dot{\theta}_2\cos(\theta_1-\theta_2)\right] + \left[(m_1+m_2)g\ell_1\cos\theta_1 + m_2 g\ell_2\cos\theta_2\right]}$$

• FOR θ_1, FIRST FIND THE PARTIAL OF L W.R.T. PARTIAL OF $\dot{\theta}_1$.

$$\frac{\partial L}{\partial\dot{\theta}_1} = m_1\ell_1^2\dot{\theta}_1 + m_2\ell_1^2\dot{\theta}_1 + m_2\ell_1\ell_2\cos(\theta_1-\theta_2)\dot{\theta}_2$$

WHOSE DERIVATIVE IS

$$\frac{d}{dt}\left(\frac{\partial L}{\partial\dot{\theta}_1}\right) = (m_1+m_2)\ell_1^2\ddot{\theta}_1 + m_2\ell_1\ell_2\ddot{\theta}_2\cos(\theta_1-\theta_2) - m_2\ell_1\ell_2\sin(\theta_1-\theta_2)(\dot{\theta}_1-\dot{\theta}_2)\dot{\theta}_2$$

SO THEN

$$\frac{\partial L}{\partial\theta_1} = -\ell_1 g(m_1+m_2)\sin\theta_1 - m_2\ell_1\ell_2\dot{\theta}_1\dot{\theta}_2\sin(\theta_1-\theta_2)$$

• FOR θ_2, FIND PARTIAL OF L W.R.T. $\dot{\theta}_2$

$$\frac{\partial L}{\partial\dot{\theta}_2} = m_2\ell_2^2\dot{\theta}_2 + m_2\ell_1\ell_2\cos(\theta_1-\theta_2)$$

WHOSE DERIVATIVE IS

$$\frac{d}{dt}\left(\frac{\partial L}{\partial\dot{\theta}_2}\right) = m_2\ell_2^2\ddot{\theta}_2 + m_2\ell_1\ell_2\ddot{\theta}_1\cos(\theta_1-\theta_2) - m_2\ell_1\ell_2\dot{\theta}_1\sin(\theta_1-\theta_2)(\dot{\theta}_1-\dot{\theta}_2)$$

SO THEN

$$\frac{\partial L}{\partial\theta_2} = m_2\ell_1\ell_2\dot{\theta}_1\dot{\theta}_2\sin(\theta_1-\theta_2) - \ell_2 m_2 g\sin\theta_2$$

LAGRANGE'S EQN: $\dfrac{d}{dt}\left(\dfrac{\partial L}{\partial\dot{\theta}_1}\right) - \dfrac{\partial L}{\partial\theta_1} = 0$

OBTAIN A SYS w/2 EQNS, THEN...

$$\frac{d}{dt}\left(\frac{\partial L}{\partial\dot{\theta}_2}\right) - \frac{\partial L}{\partial\theta_2} = 0$$

$$\frac{d}{dt}\left(\frac{\partial L}{\partial\dot{\theta}_1}\right) - \frac{\partial L}{\partial\theta_1} = 0$$

Figure C.1.2: Part 2 of Lagrangian approach to solving the equations of motion for a double pendulum without damping or inertia terms.

$\underline{\text{INCLUDING DAMPING}}$

$\left(\begin{array}{l} L_i \text{ is} \\ \text{DISTANCE FROM} \\ \text{PIVOT TO CoM} \end{array}\right)$

$$T = \tfrac{1}{2}(m_1 + m_2)L_1^2\dot{\theta}_1^2 + \tfrac{1}{2}m_2 L_2^2\dot{\theta}_2^2 + m_2 L_1 L_2 \dot{\theta}_1\dot{\theta}_2\cos(\theta_1 - \theta_2) + \tfrac{1}{2}I_1\dot{\theta}_1^2 + \tfrac{1}{2}I_2\dot{\theta}_2^2$$

$$V = -(m_1 + m_2)gL_1\cos\theta_1 - m_2 gL_2\cos\theta_2$$

$$R = \tfrac{1}{2}\xi_1\dot{\theta}_1^2 + \tfrac{1}{2}\xi_2(\dot{\theta}_2 - \dot{\theta}_1)$$

$$\delta W = f_1\delta x_1 + f_2\delta y_2$$

$$\frac{\partial R}{\partial \theta_1} = \xi_1\dot{\theta}_1 - \tfrac{1}{2}\xi_2\dot{\theta}_1$$

$$\frac{d}{dt}\left(\frac{\partial L}{\partial\dot{\theta}_i}\right) - \frac{\partial L}{\partial\theta_i} + \frac{\partial R}{\partial\theta_i} = \frac{\partial(\delta W)}{\partial(\delta\theta_i)}$$

$$\frac{\partial R}{\partial\theta_2} = \tfrac{1}{2}\xi_2\dot{\theta}_2$$

1.) $\dfrac{\partial(\delta W)}{\partial(\delta\theta_1)} = (m_1 + m_2)L_1\ddot{\theta}_1 + m_2 L_2\ddot{\theta}_2\cos(\theta_1 - \theta_2) + m_2 L_2\dot{\theta}_2^2\sin(\theta_1 - \theta_2) + (m_1 + m_2)g\sin\theta_1$
$\qquad\qquad + \xi_1\ddot{\theta}_1 - \tfrac{1}{2}\xi_2\ddot{\theta}_2 + I_1\ddot{\theta}_1$

2.) $\dfrac{\partial(\delta W)}{\partial(\delta\theta_2)} = m_2 L_2\ddot{\theta}_2 + m_2 L_1\ddot{\theta}_1\cos(\theta_1 - \theta_2) - m_2 L_1\dot{\theta}_1^2\sin(\theta_1 - \theta_2) + m_2 g\sin\theta_2 + \tfrac{1}{2}\xi_2\ddot{\theta}_2$
$\qquad\qquad + I_2\ddot{\theta}_2$

Figure C.1.3: Part 1 of Lagrangian approach to solving the equations of motion for a double pendulum with damping and inertia terms. This set of equations were used for the software model and all analyses.

224

1) EoM $$\ddot{\theta}_1 = \frac{-m_2 L_2 \ddot{\theta}_2 \cos(\theta_1-\theta_2) - m_2 L_2 \dot{\theta}_2^2 \sin(\theta_1-\theta_2) - (m_1+m_2)g\sin\theta_1}{(m_1+m_2)L_1}$$

2) $$\ddot{\theta}_2 = \frac{-m_2 L_1 \ddot{\theta}_1 \cos(\theta_1-\theta_2) + m_2 L_1 \dot{\theta}_1^2 \sin(\theta_1-\theta_2) - m_2 g\sin\theta_2}{m_2 L_2}$$

SOLVE FOR $\ddot{\theta}_1$, 1ST SUB IN $\ddot{\theta}_2$ VALUE

$$\ddot{\theta}_1 = \frac{-m_2 L_2 \left[\dfrac{-m_2 L_1 \ddot{\theta}_1 \cos(\theta_1-\theta_2) + m_2 L_1 \dot{\theta}_1^2 \sin(\theta_1-\theta_2) - m_2 g\sin\theta_2}{m_2 L_2}\right]\cos(\theta_1-\theta_2) + m_2 L_1 \dot{\theta}_1^2 \sin(\theta_1-\theta_2) - m_2 g\sin\theta_2}{(m_1+m_2)L_1}$$

DISTRIBUTE $-m_2 L_2$ AND $\cos(\theta_1-\theta_2)$ THROUGH ...

$$\ddot{\theta}_1 = \left[\frac{+m_2 L_2\, m_2 L_1 \ddot{\theta}_1 \cos(\theta_1-\theta_2)\cos(\theta_1-\theta_2)}{m_2 L_2} + \frac{m_2 L_2 \cos(\theta_1-\theta_2)m_2 L_1 \dot{\theta}_1^2 \sin(\theta_1-\theta_2)}{m_2 L_2} - \frac{m_2 L_2\, m_2 g\sin\theta_2 \cos(\theta_1-\theta_2)}{m_2 L_2}\right.$$
$$\left. + m_2 L_1 \dot{\theta}_1^2 \sin(\theta_1-\theta_2) - m_2 g\sin\theta_2\right]/(m_1+m_2)L_1$$

MOVE BOTH $\ddot{\theta}_1$ TERMS TO SAME SIDE AFTER MULTIPLYING ALL BY $(m_1+m_2)L_1$

$$(m_1+m_2)L_1 \ddot{\theta}_1 - \frac{m_2 L_2 \cos(\theta_1-\theta_2)m_2 L_1 \ddot{\theta}_1 \cos(\theta_1-\theta_2)}{m_2 L_2} = \frac{-m_2 L_2 \cos(\theta_1-\theta_2)m_2 L_1 \dot{\theta}_1^2 \sin(\theta_1-\theta_2)}{m_2 L_2}$$
$$+ \frac{m_2 L_2\, m_2 g\sin\theta_2 \cos(\theta_1-\theta_2)}{m_2 L_2} - m_2 L_2 \dot{\theta}_2^2 \sin(\theta_1-\theta_2) - (m_1+m_2)g\sin\theta_1$$

MULTIPLY ALL BY $m_2 L_2$

$$m_2 L_2 (m_1+m_2)L_1 \ddot{\theta}_1 - m_2 L_2 \cos(\theta_1-\theta_2)m_2 L_1 \ddot{\theta}_1 \cos(\theta_1-\theta_2) = -m_2 L_2 \cos(\theta_1-\theta_2)m_2 L_1 \dot{\theta}_1^2 \sin(\theta_1-\theta_2)$$
$$+ m_2 L_2\, m_2 g\sin\theta_2 \cos(\theta_1-\theta_2) + \left(-m_2 L_2 \dot{\theta}_2^2 \sin(\theta_1-\theta_2) - (m_1+m_2)g\sin\theta_1\right)m_2 L_2$$

ISOLATE $\ddot{\theta}_1$

$$\ddot{\theta}_1 \left[(m_1+m_2)m_2 L_2 L_1 - \left[m_2 L_1 \cos(\theta_1-\theta_2)m_2 L_2 \cos(\theta_1-\theta_2)\right]\right] = \;...$$

$\ast$ $$\ddot{\theta}_1 = \frac{\left(-m_2 L_2 \dot{\theta}_2^2 \sin(\theta_1-\theta_2) - g(m_1+m_2)\sin\theta_1\right)m_2 L_2 - m_2 L_2 \cos(\theta_1-\theta_2)\left(m_2 L_1 \dot{\theta}_1 \sin(\theta_1-\theta_2) - m_2 g\sin\theta_2\right)}{(m_1+m_2)m_2 L_1 L_2 - (m_2 L_1 \cos(\theta_1-\theta_2)m_2 L_2 \cos(\theta_1-\theta_2))}$$
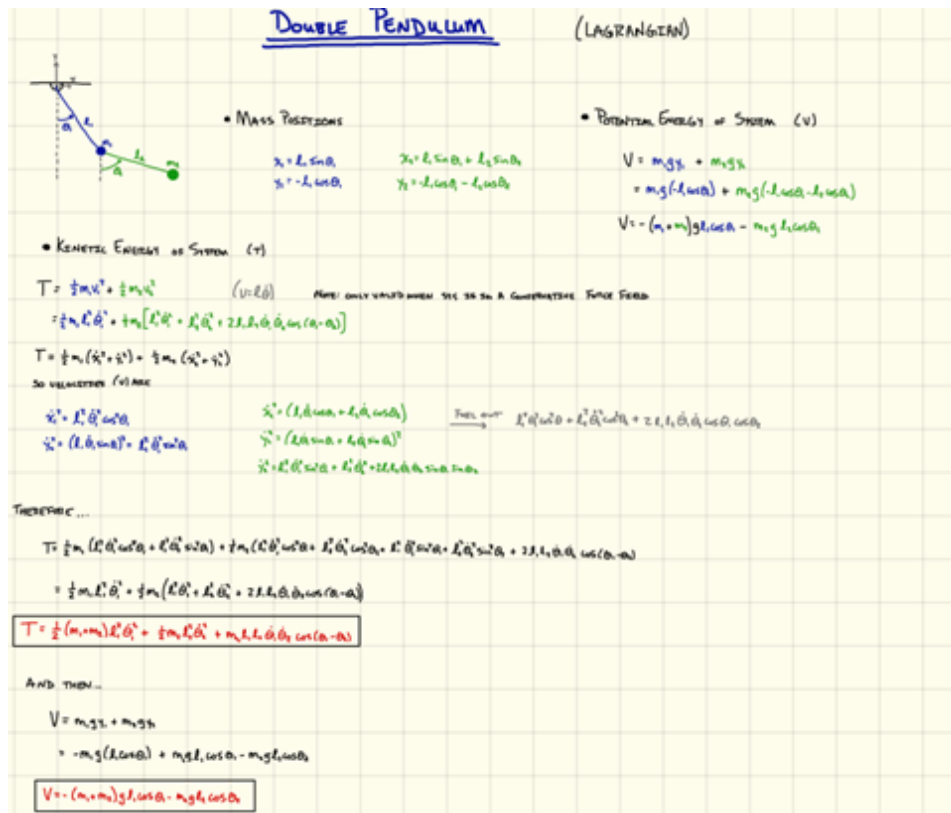
Figure C.1.4: Part 2 of Lagrangian approach to solving the equations of motion for a double pendulum with damping and inertia terms. This set of equations were used for the software model and all analyses.

Double Pend. w/ Damp. & Inertia

#1 $(m_1+m_2)L_1\ddot{\theta}_1 + \xi_1\dot{\theta}_1 + I_1\ddot{\theta}_1 = -m_2L_2\ddot{\theta}_2\cos(\theta_1-\theta_2) - m_2L_2\dot{\theta}_2^2\sin(\theta_1-\theta_2) - (m_1+m_2)g\sin\theta_1 + \frac{1}{2}\xi_2\dot{\theta}_2$

#2 $\ddot{\theta}_2 = \dfrac{-m_2L_1\ddot{\theta}_1\cos(\theta_1-\theta_2) + m_2L_1\dot{\theta}_1^2\sin(\theta_1-\theta_2) - m_2g\sin\theta_2}{(m_2L_2 + \frac{1}{2}\xi_2 + I_2)}$

Solve for $\ddot{\theta}_1$ Sub In $\ddot{\theta}_2$ Terms

$(m_1+m_2)L_1\ddot{\theta}_1 + \xi_1\dot{\theta}_1 + I_1\ddot{\theta}_1 = -m_2L_2\cos(\theta_1-\theta_2)\left[\dfrac{-m_2L_1\ddot{\theta}_1\cos(\theta_1-\theta_2) + m_2L_1\dot{\theta}_1^2\sin(\theta_1-\theta_2) - m_2g\sin\theta_2}{(m_2L_2 + \frac{1}{2}\xi_2 + I_2)}\right]$

$\quad -m_2L_2\dot{\theta}_2^2\sin(\theta_1-\theta_2) - (m_1+m_2)g\sin(\theta_1) + \frac{1}{2}\xi_2\left[\dfrac{-m_2L_1\ddot{\theta}_1\cos(\theta_1-\theta_2) + m_2L_1\dot{\theta}_1^2\sin(\theta_1-\theta_2) - m_2g\sin\theta_2}{(m_2L_2 + \frac{1}{2}\xi_2 + I_2)}\right]$

Group all $\ddot{\theta}_1$ Terms on Left after Factoring

$(m_1+m_2)L_1\ddot{\theta}_1 + \xi_1\ddot{\theta}_1 + I_1\ddot{\theta}_1 \dfrac{-m_2L_2\cos(\theta_1-\theta_2)m_2L_1\cos(\theta_1-\theta_2)\ddot{\theta}_1}{(m_2L_2+\frac{1}{2}\xi_2+I_2)} + \dfrac{\frac{1}{2}\xi_2 m_2 L_1\cos(\theta_1-\theta_2)\ddot{\theta}_1}{(m_2L_2+\frac{1}{2}\xi_2+I_2)} =$

$\dfrac{m_2L_1\dot{\theta}_1^2\sin(\theta_1-\theta_2)}{(m_2L_2+\frac{1}{2}\xi_2+I_2)} - \dfrac{m_2g\sin\theta_2}{(m_2L_2+\frac{1}{2}\xi_2+I_2)} - m_2L_2\dot{\theta}_2^2\sin(\theta_1-\theta_2) - (m_1+m_2)g\sin\theta_1 + \dfrac{\frac{1}{2}\xi_2 m_2 L_1\dot{\theta}_1^2\sin(\theta_1-\theta_2)}{(m_2L_2+\frac{1}{2}\xi_2+I_2)} -$

$\cdots \quad - \dfrac{\frac{1}{2}\xi_2 m_2 g\sin\theta_2}{(m_2L_2+\frac{1}{2}\xi_2+I_2)}$

Multiply all by $(m_2L_2 + \frac{1}{2}\xi_2 + I_2)$

LHS $\ddot{\theta}_1\left[(m_1+m_2)L_1(m_2L_2+\frac{1}{2}\xi_2+I_2) + \xi_1(m_2L_2+\frac{1}{2}\xi_2+I_2) + I_1(m_2L_1+\frac{1}{2}\xi_2+I_2) - m_2L_2\cos(\theta_1-\theta_2)m_2L_1\cos(\theta_1-\theta_2) + \frac{1}{2}\xi_2 m_2L_1\cos(\theta_1-\theta_2)\right] =$

RHS $-m_2L_1\dot{\theta}_1^2\sin(\theta_1-\theta_2) - m_2g\sin\theta_2 - \left[m_2L_2\dot{\theta}_2^2\sin(\theta_1-\theta_2) - (m_1+m_2)g\sin\theta_1\right](m_2L_2+\frac{1}{2}\xi_2+I_2)$

$\quad + \frac{1}{2}\xi_2 m_2L_1\dot{\theta}_1^2\sin(\theta_1-\theta_2) - \frac{1}{2}\xi_2 m_2 g\sin\theta_2$

Simplify

LHS $\ddot{\theta}_1\left[(m_2L_2+\frac{1}{2}\xi_2+I_2)((m_1+m_2)L_1+\xi_1+I_1) - m_2^2L_1L_2\cos^2(\theta_1-\theta_2) + \frac{1}{2}\xi_2 m_2L_1\cos(\theta_1-\theta_2)\right] =$

RHS $-m_2L_1\dot{\theta}_1^2\sin(\theta_1-\theta_2) - m_2g\sin\theta_2 - \left[m_2L_2\dot{\theta}_2^2\sin(\theta_1-\theta_2) - (m_1+m_2)g\sin\theta_1\right](m_2L_2+\frac{1}{2}\xi_2+I_2)$

$\quad + \frac{1}{2}\xi_2 m_2(L_1\dot{\theta}_1^2\sin(\theta_1-\theta_2) - g\sin\theta_2)$

Isolate $\ddot{\theta}_1$

$\ddot{\theta}_1 = \dfrac{-m_2L_1\dot{\theta}_1^2\sin(\theta_1-\theta_2) - m_2g\sin\theta_2 - \left[m_2L_2\dot{\theta}_2^2\sin(\theta_1-\theta_2) - (m_1+m_2)g\sin\theta_1\right](m_2L_2+\frac{1}{2}\xi_2+I_2) + \frac{1}{2}\xi_2 m_2(L_1\dot{\theta}_1^2\sin(\theta_1-\theta_2) - g\sin\theta_2)}{\left[(m_2L_2+\frac{1}{2}\xi_2+I_2)((m_1+m_2)L_1+\xi_1+I_1) - m_2^2L_1L_2\cos^2(\theta_1-\theta_2) + \frac{1}{2}\xi_2 m_2L_1\cos(\theta_1-\theta_2)\right]}$

Figure C.1.5: Part 3 of Lagrangian approach to solving the equations of motion for a double pendulum with damping and inertia terms. This set of equations were used for the software model and all analyses.

226

C.2   Matlab Code

The following code was called by Matlab's built-in function ode45 to solve the double pendulum's equations of motion. All angles are in radians. Characters or lines with % at the beginning are commented out.

```
% Parameters (derived from a subject/cohort) passed through Matlab function statement
% linkage mass (kg)
m1 = params(1); m2 = params(2);
% linkage length (m)
L1 = params(3); L2 = params(4);
% proximal (1) & distal (2) pivots' damping coefficients
z1 = params(5); z2 = params(6);
% Set up variables
% y(1) = angular displacement of proximal linkage
% y(2) = angular velocity of proximal linkage
% y(3) = angular displacement of distal linkage
% y(4) = angular velocity of distal linkage
g = -9.81; % constant, acceleration due to gravity (m/s2)
I1 = m1*(L1^2)*y(2); % Inertia of proximal linkage kg*( m/s2)*(radians/sec)
I2 = m2*(L2^2)*y(4);
% Inertia of distal linkage kg*( m/s2)*(radians/sec)
% Simplify and group differential equations' terms
A = (m2*L2 + 0.5*z2 + I2);
B = m1 + m2;
C = g*sin(y(1));
D = -m2*L1*(y(2)^2)*sin(y(1)-y(3));
E = m2*L2*(y(4)^2)*sin(y(1)-y(3));
F = L1*(y(2)^2)*sin(y(1)-y(3));
G = (m2^2)*L1*L2*(cos(y(1)-y(3))*cos(y(1)-y(3)));
H = 0.5*z2*m2*L1*cos(y(1)-y(3));
J = (B*L1 + z1 + I1);
K = m2*L1*cos(y(1)-y(3));
N = (y(4)^2)*sin(y(1)-y(3));
% Differential Equations
dy(1) = y(2); % Angular velocity of proximal linkage
% Angular acceleration of proximal linkage
% dy(2) = (e*d-b*f)/(a*d-c*b); % equation without damping or inertia
dy(2) = ( D - m2*C - (E-B*g*sin(y(1)))*A + 0.5*z2*m2*(F-C) ) / ( (J*A) - G + H ); % proximal
linkage's equation with damping and inertial terms
dy(3) = y(4); % Angular velocity of distal linkage
% Angular acceleration of distal linkage
% dy(4) = (a*f-c*e)/(a*d-c*b); % equation without damping or inertia
dy(4) = ( G*N + K*B*g*sin(y(1)) + (-D - C)*J ) / ( (J*A) + G + H ); % distal linkage's
equation with damping and inertia terms
```

Appendix D   Phase Angle Investigation

This appendix provides the methods and results for the investigation into normalization of phase angle calculation. The phase angle (ϑ) is calculated by taking the inverse tangent (a.k.a. arctangent) of the x and y values.

Algorithm D.1 Phase angle equations.

$$tan(\vartheta) = {}^{sin(y)}\!/_{cos(x)}$$

Alternatively stated, the phase angle is the inverse of the slope of the line with end points of (0,0) and (x, y).

Algorithm D.2 Alternative phase angle equations.

$$\vartheta = atan\big({}^{sin(y)}\!/_{cos(x)}\big) = tan^{-1}\big({}^{sin(y)}\!/_{cos(x)}\big)$$

In this particular application, the phase portrait plane is a 2D plane formed by the x axis, consisting of angular displacement angles, and the y axis, consisting of angular velocity angles. The tangent function is a trigonometric ratio and is undefined when $\cos(x)=0$. Therefore the tangent function has a vertical asymptote whenever $\cos(x)=0$. Similarly, the tangent and sine functions have zeros at integer multiples of π because $\tan(\vartheta)=0$ when $\sin(y)=0$. The arctangent is simply the inverse of the tangent function. The one argument arctangent function (atan) can not distinguish between diametrically opposite directions. For example, the angle between the x-axis and the vector (1, 1) is calculated with the following equation.

Algorithm D.3 Equation to calculate the angle between the x-axis and phase angle vector.

$$atan(\vartheta) = \big({}^{sin(1)}\!/_{cos(1)}\big) = 45°$$

However, the angle between the x-axis and the vector (-1, -1), yields the same answer as above even though the actual angle is -135°. The atan2 function takes into account the signs of both vector components and places the angle in either quadrant I, II, III, or IV depending upon the sign of x and y.
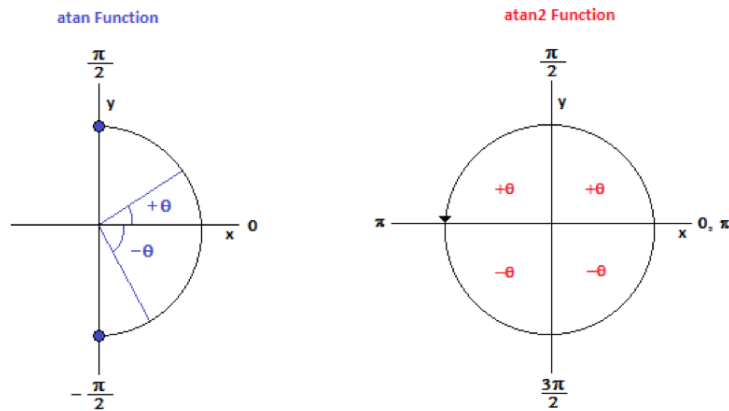
Figure D.0.1: Quadrants for atan (left) and atan2 (right) functions

228

Table D.0.1: Properties of the tangent and arc tangent functions.

Property	Tangent	atan	atan2
Domain	$-\infty < \tan(\vartheta) < +\infty$	$-\infty < \tan(\vartheta) < +\infty$	$-\infty < \tan(\vartheta) < +\infty$
Range	$\theta \exists \mathbb{R}$ (all real numbers)	$-\pi/2 < \vartheta < \pi/2$	$-\pi < \vartheta < \pi$
Y-intercept	(0,0)	(0,0)	(0,0)
Quadrant	I,II,III,IV	I,IV	I,II,III, IV

To demonstrate the noise induced by using the atan2 Matlab function instead of the atan Matlab function, the following phase angles and resulting relative phase angles from a subject with cerebral palsy are provided. This comparison of Matlab tangent functions was conducted for the majority of the subjects with cerebral palsy and those free of gait pathology, all of which demonstrated differences in the resulting phase angle and relative phase angle values.
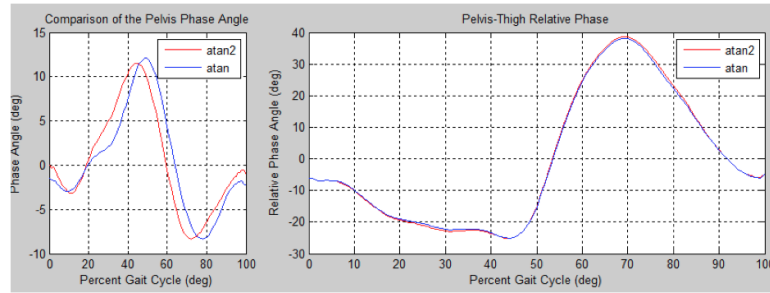
Figure D.0.2: Calculation of pelvis-thigh relative phase angles using Matlab's atan function (blue) and atan2 function (red).
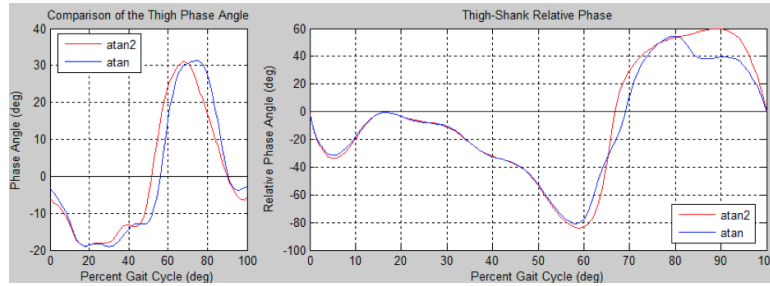
Figure D.0.3: Calculation of thigh-shank relative phase angles using Matlab's atan function (blue) and atan2 function (red).
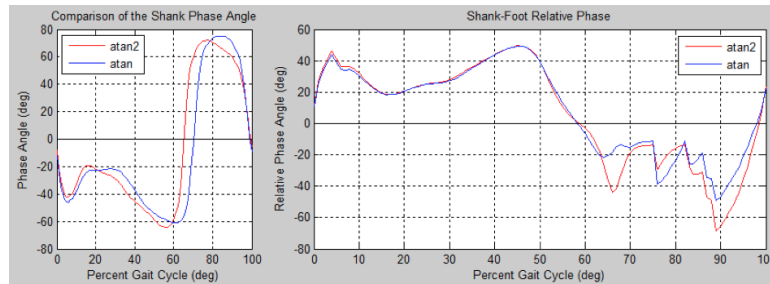
Figure D.0.4: Calculation of shank-foot relative phase angles using Matlab's atan function (blue) and atan2 function (red).
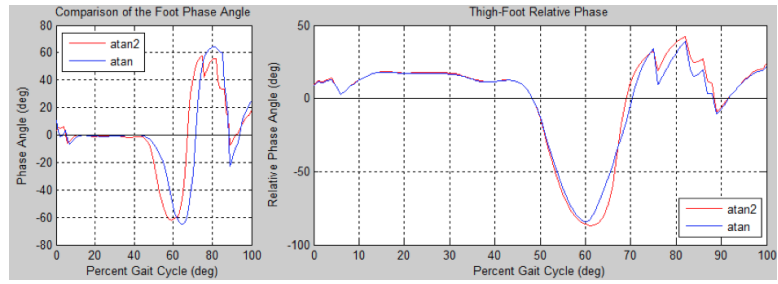
Figure D.0.5: Calculation of thigh-foot relative phase angles using Matlab's atan function (blue) and atan2 function (red).

Appendix E   Additional Methods

E.1   Representative Trial Selection

The following algorithm was implemented into a custom Matlab program and used to identify the representative motion capture trial for each subject and each motion capture condition.
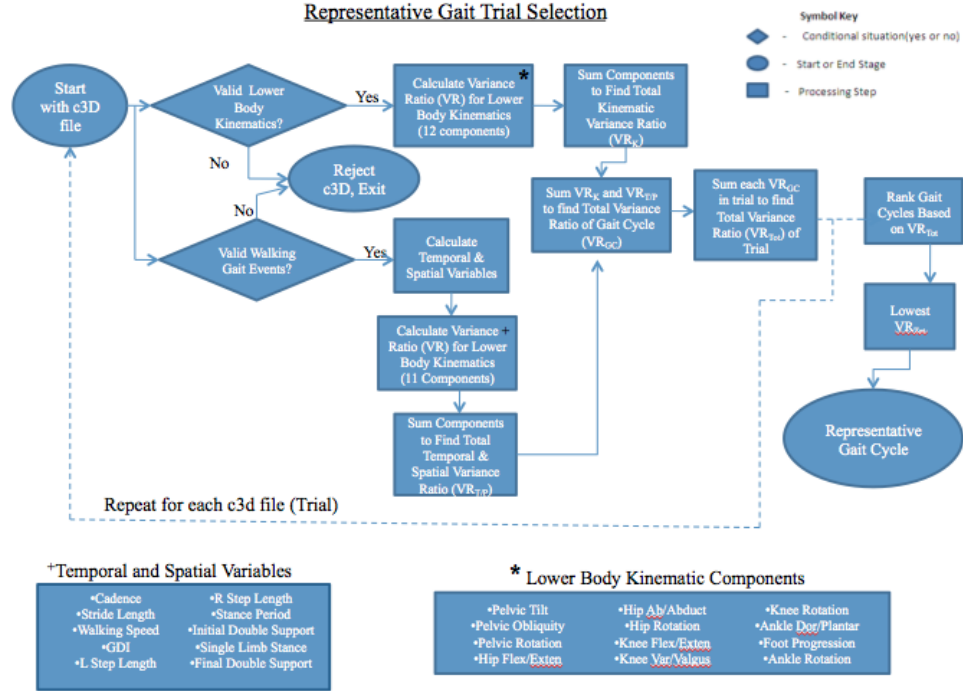
Figure E.1.1: Algorithm used by custom Matlab function to select a subject's representative motion capture trial.

E.2   Coordination Deviation Index Calculation

The following section contains the equations and methodology for calculating the coordination deviation index (CDI). Sagittal plane PPs (pelvis, thigh, shank, foot) and CRPD (pelvis-thigh, thigh-shank, shank-foot, thigh-foot) were calculated in 2% increments throughout the entire gait cycle and form the coordination dynamics vector (cd) for each subject.

$$\bar{cd} = [Pelvis_{ang.displ.}, Pelvis_{ang.velocity}, \ldots, ThighFoot_{CRPD}]^T$$

$$\bar{cd} = [cd_{1-51.}, cd_{52-102.}, \ldots, cd_{561-612.}]^T$$

In order to create a normative reference for each subject's final CDI score, control features for single value decomposition analysis must be generated. The size of the control features must have the same length as a coordination vector and be greater than or equal to that same length. The top five gait trials from each retrospective subject were concatenated together to form one long trial for each subject. Then the coordination vectors were calculated for 120 unimpaired retrospective subject's concatenated gait trial and combined together to form a coordination dynamics matrix CD with dimensions of 612x1941, where 1941 is the total number of gait cycles.

$$[CD] = \begin{bmatrix} cd_1^1 & cd_1^2 & ... & cd_1^{630} \\ cd_2^1 & cd_2^2 & ... & cd_2^{630} \\ ... & ... & ... & ... \\ cd_{51}^1 & cd_{102}^2 & ... & cd_{612}^{630} \end{bmatrix}$$

The singular value decomposition of CD was then calculated using Matlab's build in function svd. The unit length singular vectors $\{\hat{f}_1, \hat{f}_2, \hat{f}_3, ..., \hat{f}_{612}\}$ and singular values $\{\lambda_1, \lambda_2, \lambda_3, ..., \lambda_{612}\}$ were stored as separate variables in the Matlab code. The singular vectors or coordination features were then used to form an optimal orthonormal basis (f-basis) for reconstruction of the coordination curves. This basis is considered optimal because it maximizes variance accounted for (VAF) by using the minimum number of features necessary to reconstruct the original coordination curves.

Using the f-basis, an mth order approximation of any coordination dynamics vector is calculated using the following equation, where the feature components cd_k are defined as $cd_k = g \bullet \hat{f}_k$.

$$\bar{cd}^m = \sum_{k=1}^{m} (cd_k \hat{f}_k)$$

These feature components can be arranged as a vector $\bar{cd} = (cd_1, cd_2, cd_3, ..., cd_m\}$ and thought of as the coordination dynamics vector projected into the kth feature directions.

Two different criteria were used to determine the appropriate order of reconstruction $(m=m_{crit})$ that will produce a reconstructed cd^m vector that is "sufficiently" close to $\bar{cd}$. The first criterion is an evaluation of the portion of overall variation accounted for by the first m features (VAF_m), which was calculated with the following equation.

$$VAF_m = \frac{\sum_{i=1}^{m} \lambda_i^2}{\sum_{j=1}^{612} \lambda_j^2}$$

The fidelity of the reconstructed coordination dynamics vector $\bar{cd}_m$ compared to the original coordination dynamics vector $\bar{cd}$ was measured and used as the second criterion. This fidelity of reconstruction (ψ) was calculated as the projection of the reconstructed coordination dynamics vector onto the original coordination dynamics vector and normalized by the magnitude of the original coordination dynamics vector.

$$\psi = \frac{cd \bullet cd_m}{||cd||^2}$$

A perfect reconstruction of the coordination dynamics vector $(\bar{cd} = \bar{cd}_m)$ corresponds to $\psi=1$ and decreases toward zero as $\bar{cd}_m$ deviates from $(\bar{cd})$.

Now that a control feature basis has been constructed, a CDI can be calculated for any subject. Let $\bar{cd}^N$ be the average of the feature components for the all the subjects in the unimpaired control group. The feature components $\bar{cd}^N$ then describe the average normative coordination dynamics. The Euclidean distance between the coordination dynamics vector of any subject (c^s) and $\bar{cd}^N$ can be calculated using the following equation.

$$d^{s,N} = ||c^s - \bar{c}^N||$$

This distance is then used to calculate a raw CDI score for the subject using the following equation.

$$CDI_{raw}^s = ln(d^{s,N})$$

While the raw CDI can be used in it current form as a measure of gait pathology related to coordination, the following scaling steps are implemented to help improve its interpretability. The sample mean and standard deviation of CDI_{raw}^s are used to calculate the subject's z-score with respect to the average normative feature components. This scaling results in a CDI value that is measured (scaled) a distance away from the average feature components from the unimpaired cohort.

$$zCDI_{raw}^s = \frac{CDI_{raw}^s - mean(CDI_{raw}^N)}{stdev(CDI_{raw}^N)}$$

Lastly, by multiplying the z-scores by 10 and subtracting them from 100 the final CDI for the subject is computed.

$$CDI^s = 100 - 10(zCDI_{raw}^s)$$

Theoretically, an individual without any deviations from the normative reference would have a perfect CDI score of 100. Every 10-point increment below the theoretical perfect score corresponds to an increasing number standard deviations away from the normative reference. Therefore, a subject's CDI value can be interpreted as follows. A CDI score greater than or equal to 100 indicates the subject's (sagittal plane) coordination dynamics is at least as close to the unimpaired average as that of a randomly selected unimpaired subject. A CDI greater than or equal to 100 indicates the absence of (sagittal) coordination pathology. Every 10 points the CDI falls below 100 corresponds to one standard deviation away from the unimpaired mean. For example, a subject with a CDI of 75 indicates the coordination dynamics of that subject(s) is 2.5 standard deviations away from the unimpaired mean.

E.3   Legend of Swing Period Coordination Events

The following table provides a list of the thirty-seven coordination events, identified from three curve features (e.g. zero-crossing, inflection point, extremum), in the swing period of gait.

Table E.3.1: Legend of swing period coordination events.

CRPD CE	Description	PP CE	Description
PelvThi 1	AbsoluteMax in Swing	Pelv 1	Min Ang Displacement
PelvThi 2	1st zero-crossing in Swing	Pelv 2	Max Ang Displacement
PelvThi 3	1st zero-crossing after Abs Max in Swing	Pelv 3	Min Ang Velocity
PelvThi 4	Inflection point between OFOn and Max in Swing	Pelv 4	Max Ang Velocity
PelvThi 5	1st Inflection point after Max in Swing	Thi 1	Min Ang Displacement
ThiSha 1	AbsoluteMin in Swing	Thi 2	Max Ang Displacement
ThiSha 2	AbsoluteMax in Swing	Thi 3	Min Ang Velocity
ThiSha 3	1st zero-crossing after FO	Thi 4	Max Ang Velocity
Thisha 4	1st zero-crossing after Swing Max	Sha 1	Min Ang Displacement
ThiSha 5	Inflection point after FO	Sha 2	Max Ang Displacement
ShaFoot 1	1st Max after FO	Sha 3	Min Ang Velocity
ShaFoot 2	AbsoluteMin in Swing	Sha 4	Max Ang Velocity
ShaFoot 3	Inflection point after Swing Abs Min	Foot 1	Min Ang Displacement
ShaFoot 4	Last zero-crossing in Swing	Foot 2	Max Ang Displacement
ThiFoot 1	Absolute Min in Swing	Foot 3	Min Ang Velocity
ThiFoot 2	1st zero-crossing before 1st max after FO/Abs Min	Foot 4	Max Ang Velocity
ThiFoot 3	2nd zero-crossing after FO (MidSw)		
ThiFoot 4	Abs Max between 1st & 2nd zero-crossing after FO		
ThiFoot 5	Last min in Swing (occurs after 2nd zero-crossing, after FO)		
ThiFoot 6	Last zero-crossing in Swing		
ThiFoot 7	Last inflection point in Swing		

E.4 Transtibial Amputation Case Study Methods

The motion capture data from one of the retrospective subjects with a lower limb amputation was investigated with the measures of coordination dynamics to determine if clinically meaningful insights could be gained from these measures that were otherwise undetected with conventional instrumented gait analysis measures. This 35-year old female with a left transtibial amputation underwent an instrumented gait analysis to determine if her recent, diminishing ability to walk was due to generalized pain in her right knee and right ankle or if it was due the current prosthetic

fitting. In spite of a relatively successful recovery, in the last few years the patient's independent ambulation has reduced to 30-60 minutes of walking and she now uses a manual wheelchair as her primary means of mobility.

Conventional IGA measures were generated from three-dimensional motion tracking and an array of ten force plates to compare the right leg and three different prosthesis alignments while the subject walked at a self-selected speed on level ground. The first alignment condition was the standard prosthesis setting (0.1875 inches out, lateral side), the foot was moved 0.125 inches medially for the second alignment, and the foot was moved 0.25 inches laterally for the third alignment. These different alignments are demonstrated in the following figure.
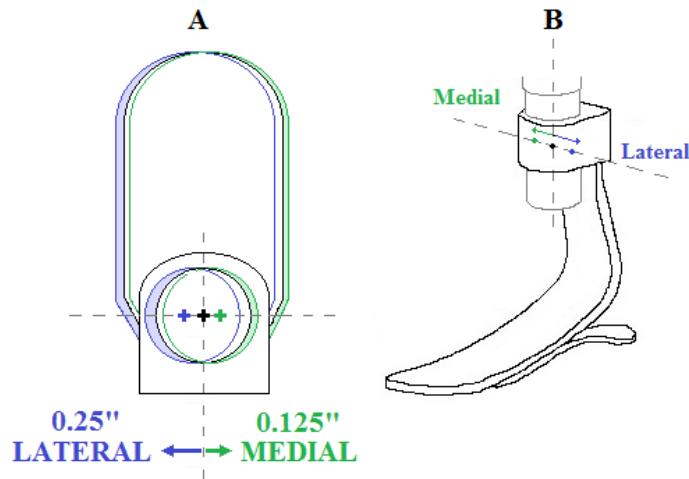
Figure E.4.1: Diagram of the three prosthetic alignments tested, where black indicates standard prosthesis alignment, blue indicates lateral alignment, and green indicates medial alignment. Transverse view of prosthetic (A) and isometric view of prosthetic (B).

Foot floor contact events were manually identified, a Woltring filter with mean square error of 17 was applied to all marker trajectories, and the Vicon Plug-in-Gait model was applied to every trial in the Vicon Nexus software. The GAMS custom Matlab program calculated the variance ratio for each trial's kinematics and temporal-spatial measures. The representative trial, from each alignment condition's set of 5 trials, was identified, using the GAMS Matlab program, as the trial with the lowest variance ration and used for the remainder of the analyses. The kinematic, kinetic, and temporal-spatial measures for the three fittings and the patient's right leg were calculated. Additionally, sagittal and coronal phase portraits and continuous relative phase diagrams for the pelvis, thigh, and shank were generated. To quantify and differences between each fitting and the right leg, the root mean square error (RMSE) was calculated for the traditional instrumented gait analysis and nonlinear measures. As a reference to these RMSE values for conventional and nonlinear measures, the corresponding variables were calculated from motion capture data of a 32-year old unimpaired female subject's representative over-ground walking trial.

Appendix F Normal Coordination Dynamics
F.1 Coordination Mechanisms of Unimpaired Swing Limb Advancement

This section of the appendix demonstrates the proposed measures of coordination dynamics (e.g. sagittal plane PPs and CRPDs) explain the inherent mechanisms underlying the swing period gait patterns of 20 healthy subjects during OG and TM walking. Changes in the subjects' gait patterns described by conventional IGA measures are proposed to be accomplished by altering the timing and organization of the following four mechanisms, elucidated by coordination dynamics, that are essential for successful completion of swing limb advancement. The following figure is the mean PPs and CRPDs for the over-ground and treadmill walking conditions of the twenty unimpaired propsective subjects. Several coordination events (e.g. curve features) were studies and with the use of pendular models of the subjects' leg motion and these nonlinear measures, four essential mechanisms of the coordination dynamics during swing limb advancement are proposed. The following figure identifies the coordination events associated with each of the four mechanisms and the table below provides the mean, standard deviation, and associated mechanism for each coordination event.
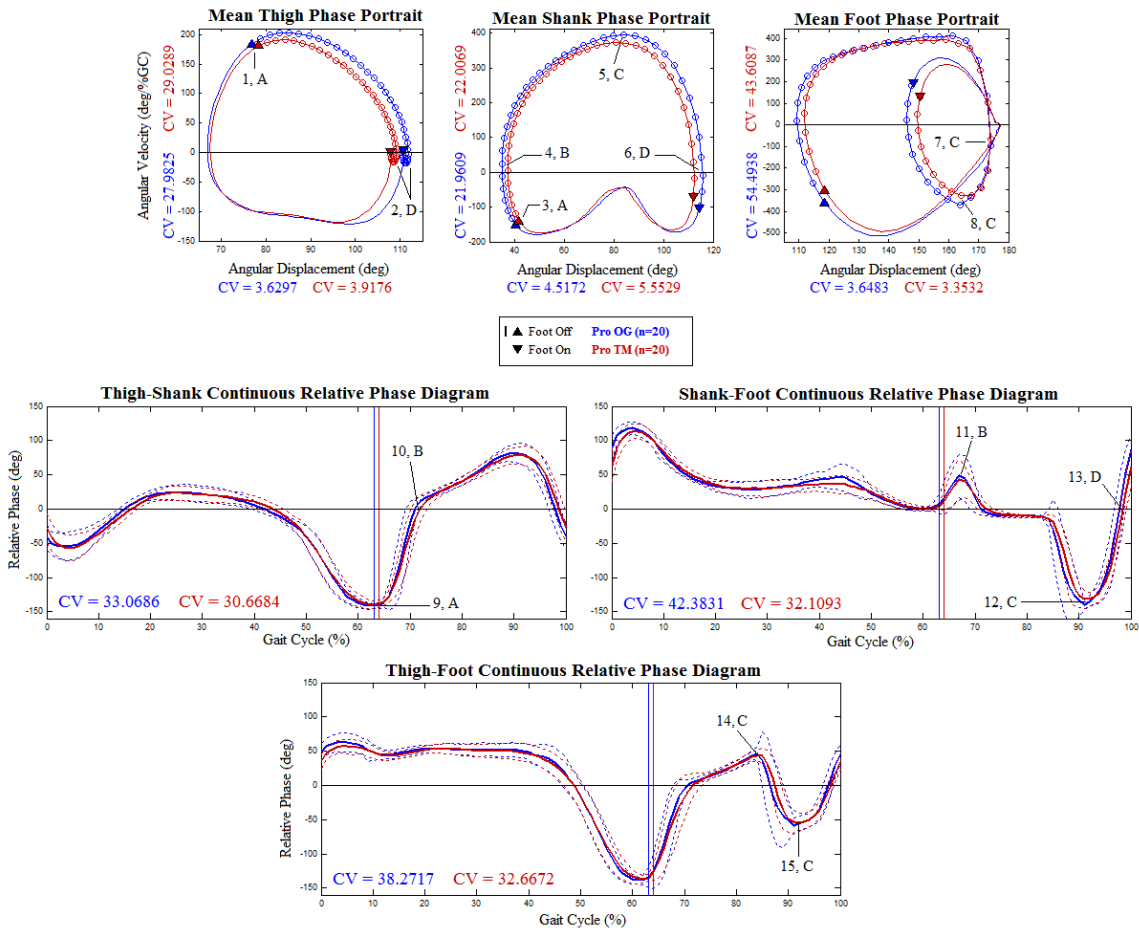
Figure F.1.1: Coordination events associated with the proposed swing limb advancement mechanism are show on the mean sagittal PPs (read clockwise) and ensemble CRPDs for the right thigh, shank, and foot from the unimpaired prospective cohort's OG and TM walking trials.

236

Table F.1.1: The mean and standard deviation for the magnitude and/or timing (percent gait cycle = %GC) of swing period coordination events (CE) for the unimpaired prospective cohort's over-ground and treadmill walking conditions. Each CE is also associated with a mechanism category.

Coordination Event	OG	TM	Mechanism
1. Thigh min AD (%GC)	64 (1.65)	65 (1.45)	A
2. Shank min AV (°/%GC)	-155.97 (23.10)	-138.29 (20.72)	A
3. Thigh-Shank abs. swing min (°)	-141.28 (4.44)	-137.74 (7.02)	A
4. Shank min AD (°)	34.73 (2.57)	37.27 (3.92)	B
5. Thigh-Shank zero-crossing post FO (%GC)	71 (1.57)	72 (1.61)	B
6. Shank-Foot local max post FO(°)	74.81 (25.39)	50.91 (25.17)	B
7. Shank max AV (°/%GC)	399.89 (37.47)	373.68 (35.46)	C
8. Foot max AD (°)	178.45 (0.54)	175.15 (1.44)	C
9. Foot min AV (%GC)	88 (1.79)	91 (1.10)	C
Foot min AV (°/%GC)	-444.18 (58.93)	-375.59 (61.26)	C
10. Thigh-Foot local max (°)	58.58 (9.68)	48.85 (7.09)	C
11. Shank-Foot abs. swing min (%GC)	88 (1.77)	91 (1.17)	C
Shank-Foot abs. swing min (°)	-146.94 (5.15)	-136.74 (5.91)	C
12. Thigh-Foot min terminal swing (%GC)	89 (2.86)	91 (1.32)	C
Thigh-Foot min terminal swing (°)	-67.65 (9.57)	-57.46 (11.57)	C
13. Thigh max AD (°)	112.35 (3.27)	109.62 (3.47)	D
14. Shank max AD (%GC)	98 (0.97)	99 (0.88)	D
Shank max AD (°)	116.10 (2.53)	112.71 (3.84)	D
15. Shank-Foot last zero-crossing (%GC)	98 (1.06)	99 (0.83)	D

By identifying coordination events in the swing period of gait for a cohort of typical subjects, these findings provide a means to enhance the understanding of feed-forward motor control strategies employed in a typical gait pattern and thus offer a reference for subjects with atypical coordination resulting impaired swing limb advancement. It is suggested that although each typically developing individual has unique swing period coordination, an individual's solution converges upon shared critical coordination requirements. Although the existence of these fundamental coordination events indicate there are instances in a normal gait pattern that share common points in the solution of swing limb advancement, an individual's desired variability is preserved as illustrated by the various curve patterns and trajectories between these coordination events. These underlying, fundamental coordination events (CE) describe instances of a preferred state of the motor control system and as a reference, have the potential to illuminate when and how impaired swing limb advancement is manifesting in a gait pattern.

F.1.1 Uncoupling of Thigh-Foot Trajectories

Mechanism A is the uncoupling of the thigh-foot trajectories at foot off. Three CEs, occurring at foot off, quantify the simultaneous uncoupling of ankle plantarflexion and hip extension. First, the delayed timing of the thigh's minimum angular displacement during TM walking occurred while the thigh was in a trailing limb posture. Second, the magnitude of the minimum angular velocity of the shank was significantly less negative during TM walking and directly affects the shank phase angle, which in turn influences the thigh-shank relative phase angle's magnitude. Third, the absolute minimum of the thigh-shank CRPD during TM walking was significantly less negative. This CRPD minimum corresponds to a reversal in the relationship between the thigh and shank and indicates when these two segments are most out-of-phase with each other. A negative relative phase angle indicates the thigh segment's contribution to this value is dominant and the positive slope after this minimum means the shank is becoming the leading segment in the relative phase

angle calculation. The delayed timing of knee flexion to 40° and reduced hip range of motion during TM walking is further expanded upon by these CEs, which reveal the reduced range is due to a delayed timing of foot off that causes the thigh PP trajectory to advance closer to vertical (e.g. decreasing, divergent TM PP trajectory). These three CEs reveal the speed at which segments are dissociating from this extension synergy is being reduced and contributing to the overall gait pattern at foot off. As a result of the reduced shank angular velocity and because the thigh is closer to vertical at foot off during TM walking, the absolute minimum of the thigh-shank CPRD is attenuated.

F.1.2   Knee-Ankle Functional Paradox

Mechanism B captures the coordination dynamics of the thigh, shank, and foot during initial swing. The following diagram highlights the segments orientation and corresponding thigh, shank, and foot phase portrait features.
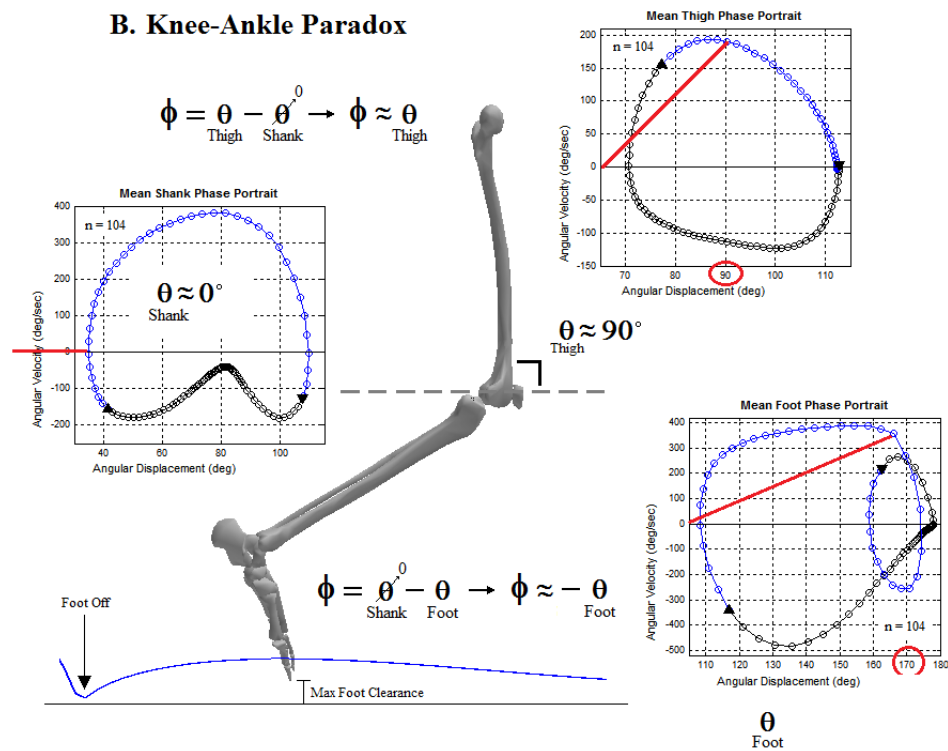
Figure F.1.2: Diagram of knee-ankle functional paradox and corresponding thigh, shank, and foot phase portraits.

Achieving sufficient knee flexion for uninhibited foot clearance and leg swing is an important function of the leg during swing limb advancement. Adequate knee flexion, sufficient forward limb momentum from rapid hip flexion, and activation of the biceps femoris muscle to reach maximum knee flexion are three mechanisms, whose precise timing and magnitude must be accomplished in order to lift the foot enough for unobstructed ground clearance and limb advancement [17]. In addition to identifying these critical functions in initial swing, Perry presented the paradoxical relationship between the knee and ankle joints while lifting the foot. Three CEs capture this paradoxical knee-ankle relationship: thigh-shank CRPD zero-crossing after foot off, shank-foot CRPD local maximum, and shank minimum angular displacement. During TM walking, attenuation of the shank minimum angular displacement and resulting reduction in angular velocity not only expounds upon how the peak knee flexion and stride length are reduced but also

corresponds to a shank PP phase angle near zero. Therefore the relative phase angle magnitude of the shank-foot CRPD's reflects changes in the foot PP trajectory, resulting in a local maximum that captures when the foot is at its most vertical orientation with respect to the floor. The thigh-shank CRPD zero-crossing indicates these two segments are in-phase with each other because the PP trajectories for these two segments are changing at the same rate, the thigh PP phase angle is decreasing, and the increasing shank PP phase angle begins dominating the relative phase angle as it swings forward about the knee. These three CEs elucidate the precise temporal and spatial organization of these segments necessary for the optimal segment organization critical for sufficient foot clearance and reveal the paradoxical knee-ankle relationship between during limb clearance.

F.1.3   Passive Knee Extension

This third mechanism (C) describes the pendular segmental relationships during passive extension of the knee. As the thigh PP trajectory rate of change decreases and approaches an abscissa zero-crossing (e.g. maximum angular displacement), the foot PP trajectory is accelerating as the foot approaches a horizontal orientation with respect to the floor and transitions from plantarflexion to dorsiflexion (e.g. near ankle kinematic zero-crossing). This change in relationship between these two segments manifests as a local maximum on the thigh-foot CRPD, which is predominantly influenced by the foot PP phase angle because the thigh PP phase angle is approximately zero. The attenuation of this extremum during TM walking means the subjects increased the rate of change in the foot PP trajectory (e.g. position and velocity) in order to sufficiently advance the foot in time for the up-coming foot strike and compensate for an overall reduced swing period duration.

Once the foot is located ahead of the hip joint center, the pendular motion of the leg segments and momentum from hip flexion contributes to completion of swing limb advancement (e.g. passive knee extension). A significant reduction in the magnitude of the shank's maximum angular velocity during TM walking coincides with the PP trajectory beginning to noticeably diverge to a smaller orbit from the OG trajectory causing a reduced pendular velocity and displacement of the shank for the remainder of swing period. Other studies reporting shorter swing period duration have also observed increased cadence and shorter step length, all of which can be attributed to decreased hip and knee extension, in part as a result of the altered pendular motion of the contralateral support limb as moves backward by the tread and rotates about the hip instead of the inverted pendular motion about the ankle during OG walking. Considering these altered pendular mechanics of the legs, the temporal-spatial and kinematics of the leg segments during terminal swing can be further expounded upon by the abated shank PP trajectory during TM walking. The diminished PP trajectory revealed the shank phase angle caused an attenuation of the shank-foot CRPD absolute maximum, thigh-foot CRPD local minimum, and foot PP maximum angular displacement and minimum angular velocity. The significantly delayed and reduced foot minimum angular velocity and maximum angular displacement, occurring just after the foot is oriented horizontally, is predominantly due to the shank's pendular motion because there is a small amount of change in the ankle joint angle during terminal swing. Since there was a general trend of delayed and attenuated swing events during TM walking, there was less time to swing the tibia forward from vertical and the subjects compensated by increasing the phase angle rate of change (e.g. spatial adjustment of the shank to meet temporal constraint of impending foot strike).

F.1.4   Anticipation of Heel First Initial Contact

The fourth mechanism (D), captures the elegant organization of the lower limb segments in anticipation of a heel first initial contact and the impending task of loading response. In order to position the leg segments in the ideal locations under the temporal constraint of a reduced swing period and spatial constraint of a shorter stride length during TM walking, the segments must be coupled and uncoupled at the appropriate instances in the gait cycle. Preparation of the limb segments for a heel first initial contact and weight acceptance during loading response is associated with the thigh PP maximum angular displacement, shank PP maximum angular displacement, and

shank-foot CRPD zero-crossing, after which antagonistic action of the hamstrings decelerate the hip and prevent excessive knee extension. As previously mentioned, during TM walking the thigh and shank PP trajectories noticeably diverge from the OG trajectories as a compensation for the decreased swing period duration and shorter stride length. The delayed occurrence of the final zero-crossing on the shank-foot CRPD reveals the subjects postponed when the relationship between these two segments switched from knee extension to slight flexion. The maximum angular displacement of the shank corresponds to the preparatory positioning of the lower leg and the ability to achieve full knee extension with slight knee flexion in anticipation of heel strike and weight acceptance. The subjects' intact nervous systems were capable of maintaining a normal kinematic pattern by using small adjustments in coordination dynamics to reorganize and appropriately position the segments for heel first initial contact and loading response within the last few percentages of the gait cycle.

F.2 Sagittal Thigh-Shank Coordination Dynamics

The remaining sections of this appendix provide additional observations about sagittal phase portrait and continuous relative phase diagram curve features during the task of swing limb advancement. The contents in the following sections of the appendix are meant to serve as a general primer that relates these curve features to the segmental and inter-segmental behavior in Euclidean space. While the observations and interpretations were made from a large cohort of unimpaired subjects, the mean phase portraits and mean ensemble continuous relative phase diagrams were constructed from an exemplar unimpaired retrospective subject while walking over-ground at a self-selected speed. All plot magnitudes and timings reported are approximate values and are used as a general guide.

F.2.1 Pre-Swing 50-60%
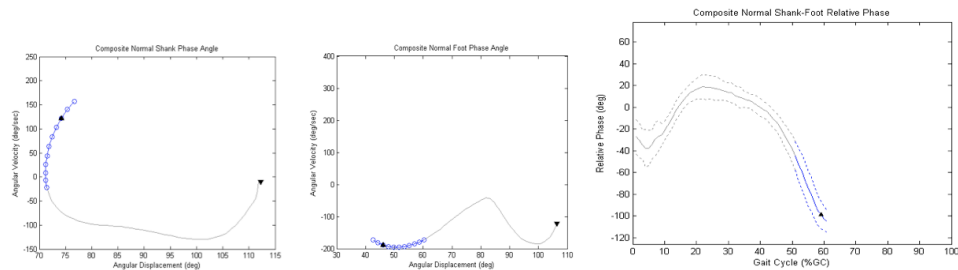
Figure F.2.1: Thigh and shank phase portraits & continuous relative phase diagram from 50-60% of gait cycle.

Similar to the terminal stance phase, the pre-swing phase has three important mechanisms that must occur in order to gain sufficient knee flexion and prepare the limb for swing. First, the center of pressure (CoP) must transition to the distal side of the (MP) joints so as to remove any stabilizing forces on the foot and shank (see previous section about these forces). Secondly, the gastrocnemius muscle must fire so as to cause a direct flexor action on the knee joint, which prepares the foot for sufficient ground clearance. Thirdly, in order for the stance limb to sufficiently unload, the body weight must be rapidly transferred from the stance limb to the opposite limb.

F.2.1.1 Thigh Phase Portrait

As the stance limb is unloaded and stabilizing forces that were present in terminal stance are removed, the thigh begins to increase its angular velocity toward flexion. All three of the

previously mentioned critical pre-swing mechanisms result in approximately 40° of passive knee flexion. This is displayed on the thigh phase portrait as an increase in angular displacement and on the shank phase portrait as a decrease in angular displacement, therefore causing both phase portrait trajectories to continue in a clockwise circular direction.
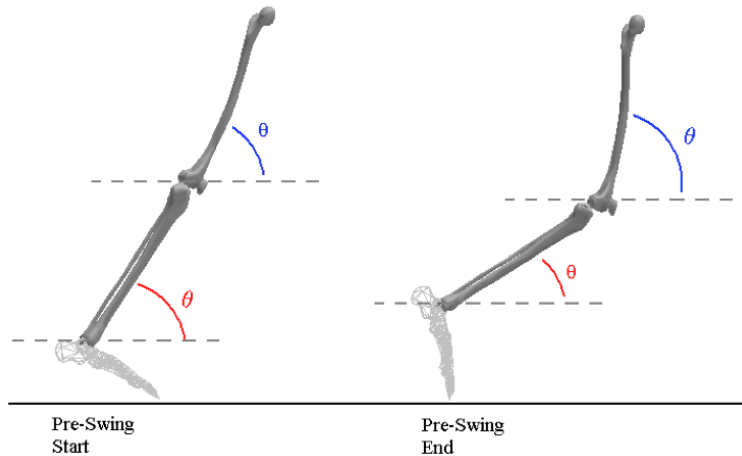
Figure F.2.2: Thigh and shank angular displacement changes at the start and end of pre-swing.

During the beginning of this phase, the thigh phase portrait has the absolute minimum angular displacement between approximately 70° and 75° for the entire gait cycle. This corresponds to the zero crossing discussed in the terminal stance section and trailing limb posture.

F.2.1.2 Shank Phase Portrait

In conjunction with the residual tension in the plantarflexion muscles, the removal of tibial stability allows for acceleration of heel rise and tibial advancement. This mechanism manifests in phase space as a decrease in the rate of change of the shank's angular displacement and a local minimum. This second local minimum of stance corresponds to an approximate angular displacement of 50° and an angular velocity of -200°/s. After this local minimum, the shank's phase trajectory begins to prepare for foot off by moving toward flexion (decreasing extension angular velocity and decreasing angular displacement), as a result of the knee flexion caused by the firing of the gastrocnemius muscle and previously mentioned critical pre-swing mechanisms. Foot off will occur at or within a few percents of the gait cycle of this local minimum; variations in this gait event are attributed to the individual variations of each person's gait.

F.2.1.3 Continuous Relative Phase Diagram

The relative phase diagram's negative slope increases in magnitude, which corresponds to the increased angular velocity of the thigh, indicating the thigh is moving faster than the shank in phase space. If the efficient biomechanics of gait are to occur this trend cannot continue past foot off, therefore at approximately foot off the curve reaches the absolute minimum relative phase angle for the entire gait cycle.
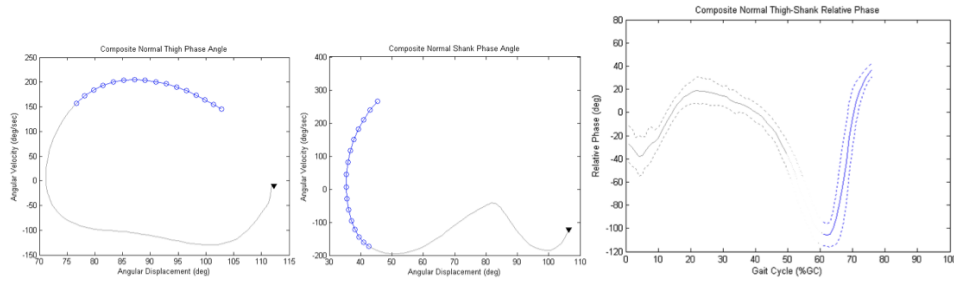
Figure F.2.3: Thigh and shank phase portraits & continuous relative phase diagram from 60-75% of gait cycle.

The most important function of the leg during this gait cycle is to achieve sufficient knee flexion (60°) for uninhibited foot clearance and swing. Again, there are three mechanisms, whose precise timing and magnitude, must be accomplished in order to lift the foot enough for unobstructed ground clearance and limb advancement. The first of these critical mechanisms, adequate knee flexion of (40°) occurs at the end of the pre-swing phase. Secondly, rapid flexion of the hip is required to instigate ample limb momentum. Lastly, active flexion of the knee by the biceps femoris muscle ensures the knee reaches the required 60° of flexion.

In addition to identifying the critical events of the knee in initial swing, Perry also presents the paradoxical relationship between the knee and ankle joints during this phase while lifting the foot. Knee flexion as opposed to ankle dorsiflexion allows for sufficient foot clearance. However, in order to obtain this essential knee flexion, other distal mechanisms are more influential in achieving this flexion value than the knee joint itself. This paradoxical relationship is an exemplar case in gait that shows how individual segment movement behavior and inter-segmental coordination, derived from nonlinear techniques, provides clinical insights into the complex and dynamic relationships of segments during gait.

F.2.2.1 Thigh Phase Portrait

During this phase of gait, the thigh is moving at its highest flexion angular velocities (200°/s) and is therefore advancing the thigh toward the cycle's maximum angular displacement. When considering the analogy of a pendulum, it is logical that at the thigh's maximum angular velocity or maximum kinetic energy, the thigh is approximately vertical. Physiologically, this maximum (flexion) angular velocity and the segment's momentum can be attributed to the rapid contraction of the iliacus muscle and is one of the three critical initial swing mechanisms previously mentioned. Once the thigh has reached its peak angular velocity and vertical orientation, at approximately 65% of the gait cycle, it stays true to its pendular motion and begins to decelerate while continuing to advance forward in swing.

F.2.2.2 Shank Phase Portrait

When the thigh is vertical and at its maximum angular velocity, the shank is at its smallest angular displacement for the entire gait cycle (35°). This minimum angular displacement of the shank corresponds to a zero crossing of the angular velocity axis. For the shank, this zero crossing represents the transition from extension to flexion of the shank. Additionally, the smallest angular displacement angle of the shank corresponds to flexion of the knee and the ankle's ability to transition from passive plantarflexion to active dorsiflexion (refer to shank-foot initial swing

section for more details). When the thigh is vertical and the knee is approaching its peak knee flexion, the ankle begins to actively dorsiflex to assist in foot clearance. These three crucial mechanical events are easily identified on the phase portraits below, as local extrema and illustrate the paradox between the knee and ankle during limb clearance.
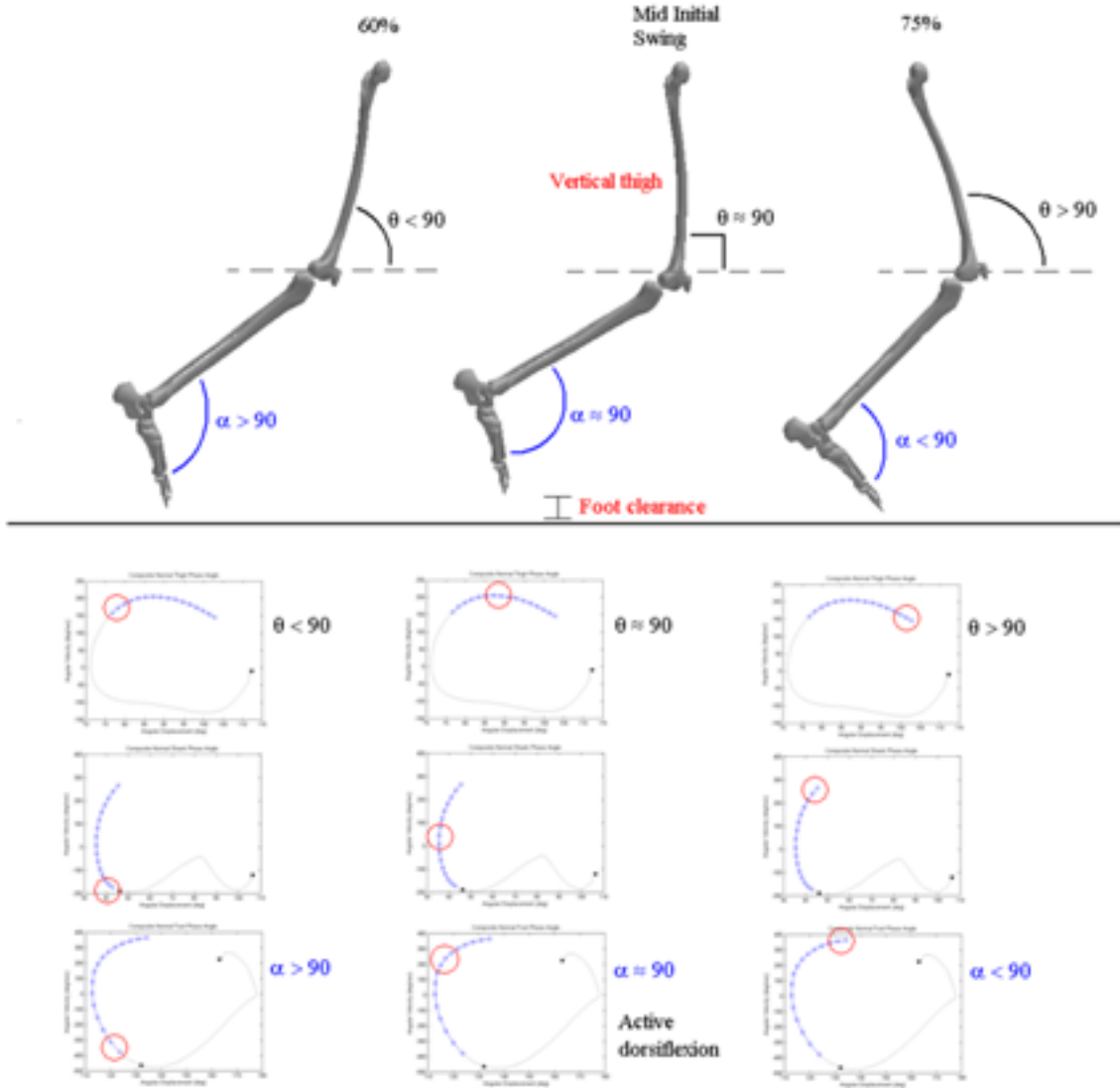
Figure F.2.4: Dynamic connection between knee and ankle movement critical for foot clearance.

Deviation of the occurrence of any of these events will impair the limb's ability to effectively continue its swing momentum, achieve the required swing knee flexion, and clear the foot.

F.2.2.3   Continuous Relative Phase Diagram

The paradox of foot clearance and inter-dependence of critical events at the knee and ankle are also clearly illustrated with the thigh-shank and shank-foot relative phase diagrams. When the shank's angular velocity is approximately zero, its phase angle is also zero. At this same time in

the gait cycle the thigh is vertically oriented so its phase angle is approximately 45°, as shown in the figure below.
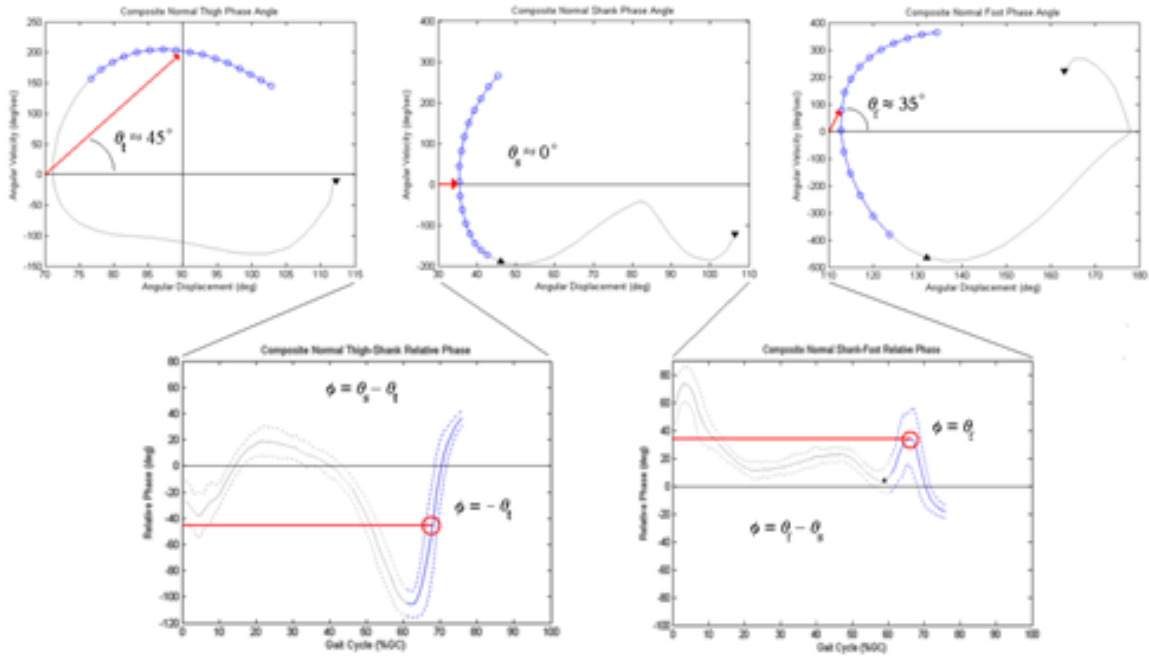
Figure F.2.5: Moment of optimal foot clearance demonstrated on the thigh-shank & shank-foot continuous relative phase diagrams.

Therefore the thigh-shank relative phase angle is approximately -45° and corresponds to the previously mentioned critical events at the knee and ankle that are necessary for foot clearance. This inflection point on the thigh-shank relative phase curve also corresponds to the maximum instantaneous slope during swing and is also a critical value to achieve during the swing phase in order to sufficiently prepare the limb for terminal stance and the impending foot contact of the next gait cycle. Similarly, the shank-foot relative phase curve illustrates the dynamic and complex relationships between the lower limb segments. Once the ankle begins to actively dorsiflex, the corresponding foot phase angle is approximately 35°. At this same time in the gait cycle, the shank's phase angle is zero; therefore a local maximum of approximately 35° can be seen on the shank-foot relative phase diagram. The low dimensionality of the relative phase diagram allows for effortless identification of these critical and complex gait mechanisms and requires the examination of only two curves, compared to using multiple kinematic curves.

F.2.3 Mid-Swing 75-87%
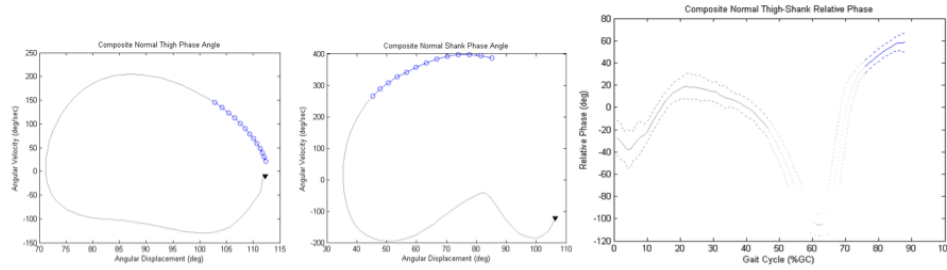
Figure F.2.6: Thigh and shank phase portraits & continuous relative phase diagram from 75-87% of gait cycle.

Once the foot has cleared the ground, knee extension is a necessary motion in order to continue limb advancement so as to prepare the swing limb for the up-coming heel strike and beginning of a new stance phase. The transition from knee flexion to extension is passively achieved by hip flexion and the compound pendular motion of the thigh and shank.

F.2.3.1 Thigh Phase Portrait

The thigh segment is continuing to advance toward its absolute maximum angular displacement value for the entire gait cycle. During this portion of thigh advancement, the angular velocity begins to decrease in anticipation of reaching the maximum necessary hip flexion and so as not to overshoot and cause hyper-flexion of the hip or hyper-extension of the knee.

F.2.3.2 Shank Phase Portrait

Once the foot has sufficiently cleared the ground and becomes anterior to the hip joint center, the knee begins to extend. At this phase in the gait cycle the shank's position in Euclidean space is trailing the thigh's position. Passive knee flexion is achieved as a result of the combined influence of hip flexion and the force of gravity acting on the shank. Returning to the analogy of a compound pendulum, the momentum caused by hip flexion pulls the shank forward in conjunction with gravity's pull on the shank, as illustrated in the following figure. When the shank reaches a vertical orientation, these two forces balance each other out.
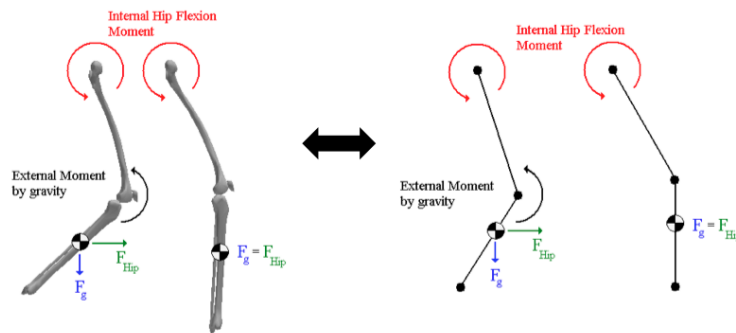
Figure F.2.7: Compound thigh-shank pendulum free body diagram, with force of hip flexion on shank (green arrow) and force of gravity on shank (blue arrow).

The shank phase portrait continues advancing toward its maximum angular displacement during the swing phase, which is traditionally known as the achievement of tibia vertical. When the shank reaches a vertical orientation, the corresponding angular velocity (400°/s) is the maximum for the entire gait cycle.

F.2.3.3   Continuous Relative Phase Diagram

The thigh-shank relative phase diagram continues to approach its absolute maximum (60°) at the end of this gait cycle phase. Additionally, there is a noticeable change in the slope's steepness during this phase when compared to the slope during initial swing. This decrease in the steepness of the slope can be attributed to the decreasing angular velocity of the thigh. Depending upon the individual's particular gait pattern, there may be a distinguishable double bump at this phase in the gait cycle.

F.2.4   Terminal Swing 87-100%
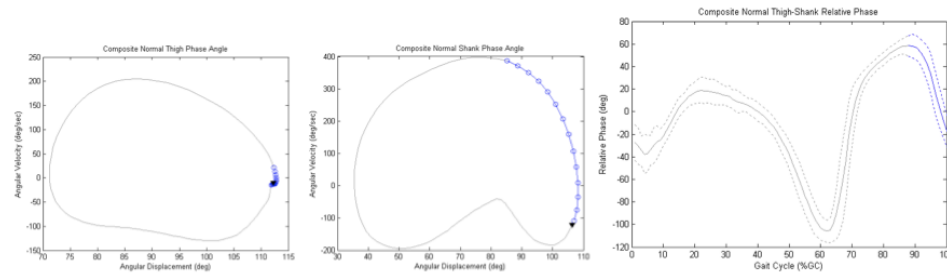
Figure F.2.8: Thigh and shank phase portraits & continuous relative phase diagram from 87-100% of gait cycle.

At this final phase in the gait cycle, the remaining critical event is to continue the knee extension from mid swing in order to prepare the limb for foot contact and weight acceptance during initial double support.

F.2.4.1   Thigh Phase Portrait

The thigh continues to decelerate now that optimal hip flexion has been achieved (30°). In phase space this optimal hip flexion can be correlated with an angular displacement between 110° and 115° and an angular velocity of zero, as shown in the figure below.
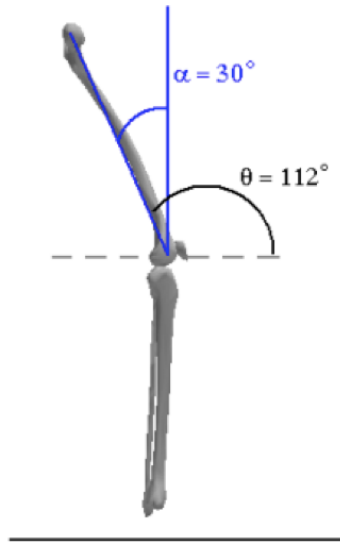
Figure F.2.9: Angle of the thigh with respect to global horizontal and global vertical at maximum hip extension in terminal stance phase.

Additionally, at the end of terminal swing, the hamstrings muscle fires in order to prevent excessive knee extension and contribute to the deceleration of the hip. The following figure depicts this subtle muscle activation, which is easily distinguishable on the thigh phase portrait as a sudden decrease in the angular displacement away from the absolute maximum.
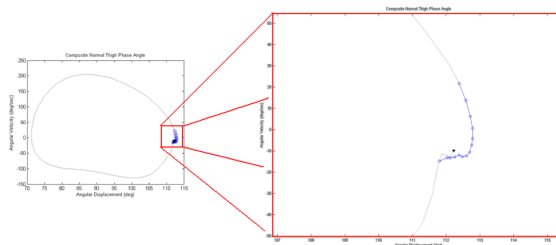
Figure F.2.10: Hamstrings activation preventing excessive knee extension on thigh phase portrait.

At the completion of this phase, the thigh's phase portrait values should correspond to the initial contact angular displacement of 110° and an angular velocity of -20°/s.

F.2.4.2 Shank Phase Portrait

The shank continues to increase its angular displacement as the knee is extended in preparation for stance. The shank reaches its absolute maximum angular displacement for the entire gait cycle at approximately 97% of the gait cycle. This maximum angular displacement (108°) corresponds to zero angular velocity. The quadriceps muscles are activated to lift the combined weight of the shank and foot during this phase. As the shank and foot are lifted by the quadriceps, the force of gravity pulls on the shank and causes a slight decrease in the segment's angular displacement. This action should result in a final angular displacement of 106° and an angular velocity of -120°/s.

F.2.4.3   Continuous Relative Phase Diagram

During the beginning of this phase, the absolute maximum relative phase angle (60°) demarcates a change in the coordination relationship between the thigh and shank. After this maximum, the slope becomes negative and indicates the thigh is now moving faster in phase space than the shank. This negative slope will continue for the remainder of the gait cycle and result in a zero crossing. At approximately 97% of the gait cycle, corresponding to the shank phase portrait's zero crossing; the relative phase angle will be zero. This zero crossing on the relative phase diagram indicates the transition from the shank leading the thigh to the thigh now leading the shank in phase space. At the completion of this phase, the relative phase diagram will have a value of approximately -25° which is ideally equivalent to the starting initial contact value.

F.3   Sagittal Shank-Foot Coordination Dynamics

F.3.1   Pre-Swing 50-60%
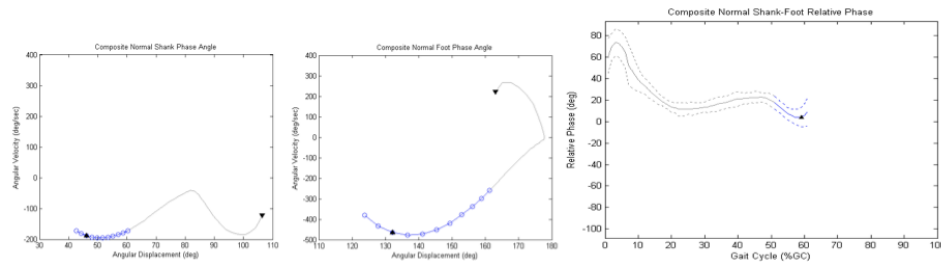
Figure F.3.1: Shank and foot phase portraits & continuous relative phase diagram from 50-60% of gait cycle.

Pre-swing begins with opposite foot contact on the walking surface and ends with foot off. Prior to foot off, the ankle rapidly plantarflexes so as to create the ballistic forward forces necessary to sufficiently propel the lower leg into the initial phases of swing.

F.3.1.1   Shank Phase Portrait

The trajectory of the shank's (and foot) phase portrait begins to approach a local minimum that corresponds approximately to the maximum plantarflexion of the gait cycle, as shown by the vertical line in the sagittal plane ankle kinematic curve below.
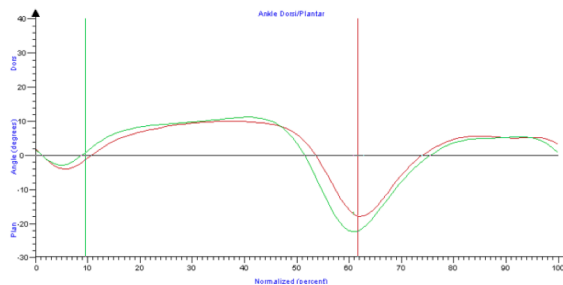
Figure F.3.2: Minimum sagittal ankle (kinematic) plantarflexion corresponding to local minimum on shank & foot phase portraits.

This local minimum (≈50°) on the shank phase portrait corresponds to the largest negative angular velocity (-200°/s) for the entire gait cycle. After this minimum and in anticipation of foot off, the shank phase portrait begins to approach flexion (positive angular velocity) and its smallest angular displacement as a precursor to trailing limb posture.

F.3.1.2 Foot Phase Portrait

At the end of terminal stance, there is no stabilizing force within the foot, so the unrestricted foot plantarflexes as a result of the firing of the gastrocnemius muscle. The foot phase portrait continues toward the largest negative angular velocity or local minimum, which corresponds to the maximum plantarflexion in the entire gait cycle. After this local minimum (135°), the trajectory of the foot phase portrait's angular velocity begins to approach zero.

F.3.1.3 Continuous Relative Phase Diagram

The local minima of the phase portraits described above also correspond to a local minimum in the relative phase diagram, which has a relative phase angle of approximately zero. This local extrema indicates a change in the coordination pattern between the shank and foot, which can be physiologically attributed to the lack of a stabilizing force on the foot causing unrestricted plantarflexion. Furthermore, this precursor event is crucial for preparation of foot off and efficient biomechanics for unimpaired swing limb advancement. Foot off will occur within a few percentages of the gait cycle of this local minimum and might be slightly before foot off as a result of the individual's trailing limb posture. This local minimum is followed by a positive relative phase slope, which corresponds to the expected increasing and passive plantarflexion movement of the foot and is not the predominantly contributing segment of the relative phase angle.

F.3.2 Initial Swing 60-75%
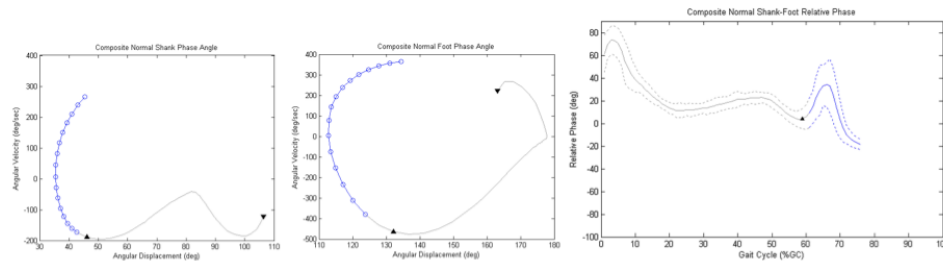
Figure F.3.3: Shank and foot phase portraits & continuous relative phase diagram from 60-75% of gait cycle.

This phase begins with foot off and ends with feet being adjacent, which in order to occur requires the ability to transition from passive plantarflexion to active dorsiflexion for sufficient limb clearance. Other critical inter-segmental coordination strategies must occur for sufficient limb clearance but those are created by other more proximal segments.

F.3.2.1 Shank Phase Portrait

Slightly after the foot's transition from passive plantarflexion to active dorsiflexion, the shank phase portrait crosses the angular velocity axis' zero point denoting a transition from extension to flexion. Additionally, this zero crossing is correlated with the smallest angular displacement (≈35°) of the shank for the entire gait cycle.

F.3.2.2 Foot Phase Portrait

The absolute minimum angular displacement of the foot for the entire gait cycle occurs in this phase and corresponds to a zero crossing at the angular velocity axis. The zero angular velocity and the minimum angular displacement (≈115°) distinguish the transition from passive plantarflexion to the beginning of active dorsiflexion. This is a critical event in the gait cycle because it signifies the ability (at the ankle) to sufficiently prepare for limb clearance during swing. At the end of the gait phase, the foot begins to plateau and maintains a constant rate of angular velocity while it continues to dorsiflex. Additionally, this clearance of the toes at the end of initial swing results in the foot being in a near neutral position at approximately the same time the swing foot is opposite the stance limb.

F.3.2.3 Continuous Relative Phase Diagram

The local minimum (≈50°) at or just prior to foot off is followed by a positive relative phase slope and as previously mentioned corresponds to the expected increasing and passive plantarflexion movement of the foot (which is not the predominantly contributing segment). However, if effective ankle function is to be achieved in swing (i.e. limb clearance) the foot cannot remain passively in plantarflexion and therefore it must begin to actively dorsiflex (≈35°). This motor control schema change is indicated on the relative phase diagram as a local maximum that is approximately half of the maximum in the loading response phase. This change in motor schema is a critical mechanism that not only allows for sufficient limb clearance at the ankle but also at the knee.

F.3.3 Mid-Swing 75-87%
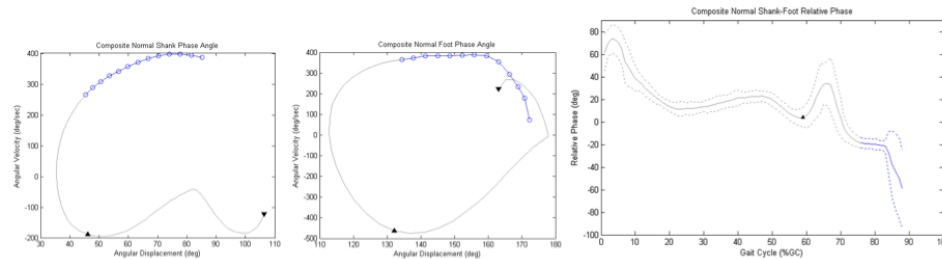
Figure F.3.4: Shank and foot phase portraits & continuous relative phase diagram from 75-87% of gait cycle.

Mid-stance is initiated when the swing foot is adjacent to the stance foot. As the swing leg continues to advance, the tibia will become vertical and in preparation for terminal stance the ankle must continue dorsiflexion until it reaches a neutral position.

F.3.3.1 Shank Phase Portrait

At the occurrence of feet being adjacent to each other, the shank has an angular displacement of approximately 40° and continues throughout this phase to flex toward a vertical (90°) angular displacement. When the tibia reaches vertical, this corresponds to the absolute maximum angular velocity (400°/s) for the entire gait cycle. Additionally, when the angular displacement is equal to 90°, the ankle has reached a neutral position. Throughout this gait phase the shank continues to increase its rate of forward swing advancement, due to the passive pendular momentum of the segment, and begins to approach its fastest rates of movement which occur in terminal stance.

F.3.3.2 Foot Phase Portrait

As the lower limb continues to advance forward during this phase and the tibia becomes vertical, the downward torque on the ankle increases. Therefore in order to achieve sufficient foot clearance and preparation for terminal stance and initial contact the ankle must increase the internal dorsiflexion moment to adequately counter this external plantarflexion moment. For typically developing ankles this will result in a near neutral foot position, as shown on the phase diagram's downward turn (160°, 350°/s) toward a negative angular velocity and deviation from the preceding nearly horizontal slope and approximate angular velocity of 380°/s.
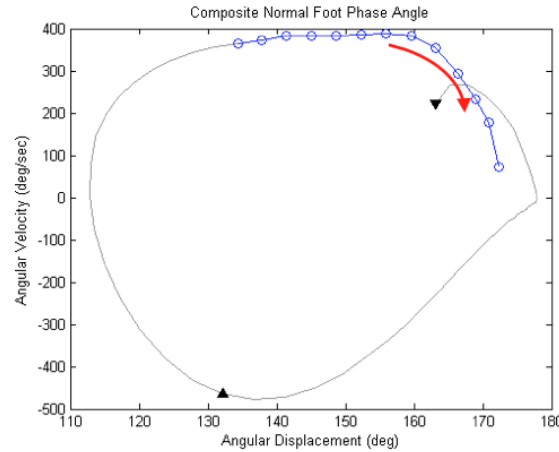
Figure F.3.5: Initiation of increased internal dorsiflexion moment and ankle approaches neutral position.

When the foot is neutral, the angular displacement should be nearly 180° and coincides with the tibia being vertical.

F.3.3.3 Continuous Relative Phase Diagram

The shank is now the leading segment in phase space and therefore the relative phase angle is negative. Since the two segments are moving at approximately the same speed in phase space the slope of the relative phase diagram is nearly horizontal ($\varphi \approx$ -20°), with perhaps a slight negative trend as the shank begins to approach its fastest rates of forward advancement. As the tibia reaches a vertical position and the ankle achieves a neutral position, the relative phase curve makes a significant and rapid direction change downward to the maximum negative phase angle for the entire gait cycle (Figure F3.6).
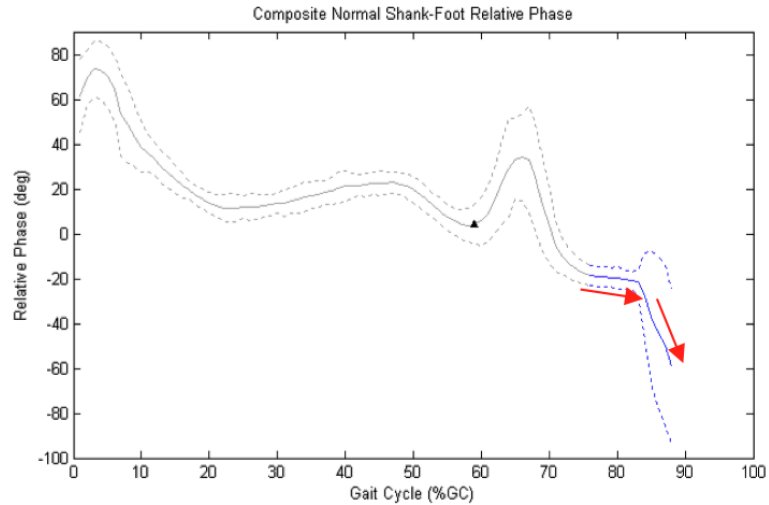
Figure F.3.6: The first arrow indicates nearly horizontal slope and the second arrow demarcates the rapid change toward the local maximum at ankle neutral/tibia vertical.

F.3.4   Terminal Swing 87-100%
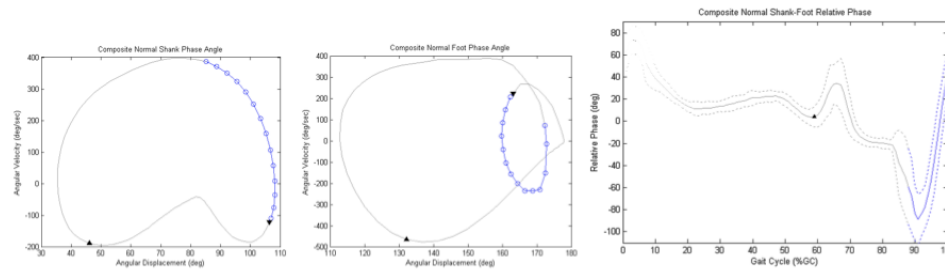
Figure F.3.7: Shank and foot phase portraits & continuous relative phase diagram from 87-100% of gait cycle.

Upon achieving a tibia vertical position the swing limb is in its final stages and makes significant changes in the motor control schema so as to adequately prepare for initial contact and loading response. The quadriceps muscles contract to support the shank and foot as the thigh is extended in preparation for heel first initial contact.

F.3.4.1   Shank Phase Portrait

At the initiation of this phase, the shank is vertical but as a result of the passive pendular momentum created at foot off continues to propel the shank forward beyond vertical but at a decreasing angular velocity. At the last few percents of gait cycle, the hamstrings eccentrically contract just enough to reduce the angular velocity to zero. This zero crossing also corresponds to the maximum angular displacement ($\approx 110°$) of the shank for the entire gait cycle. At this second zero crossing of the shank phase portrait, the firing of the hamstrings causes the shank to move ever so subtly into extension. This anticipatory firing of the hamstrings and resulting extension of the shank optimally positions the segment for initial contact and the upcoming demand of weight

acceptance. Therefore the shank's angular displacement will be slightly less than the maximum value at zero angular velocity.

F.3.4.2 Foot Phase Portrait

In preparation for initial contact, the pretibial muscles continue to contract and ensure the ankle maintains a neutral or slightly dorsiflexed position. During the first portions of this phase in the gait cycle the foot's angular displacement changes are predominately a result of the shank's continued forward advancement beyond vertical and not the result of independent foot movement. However, at this time in the gait cycle the foot is now leading the shank in Euclidean space and has an angular displacement ranging from 160° to 170°. An effectively functioning ankle will be slightly dorsiflexed and have an angular displacement in the range listed above so as to achieve heel contact. During the last portions of this phase, the ankle actively dorsiflexes the foot in anticipation of optimal heel contact. The following figure illustrates this dynamic movement of the foot, which is shown as a loop that is now moving toward a positive angular velocity and final dorsiflexed position. In the last percentages of this phase the foot phase portrait should return to the initial phase values of an angular displacement of ≈165° and an angular velocity of ≈210°/s.
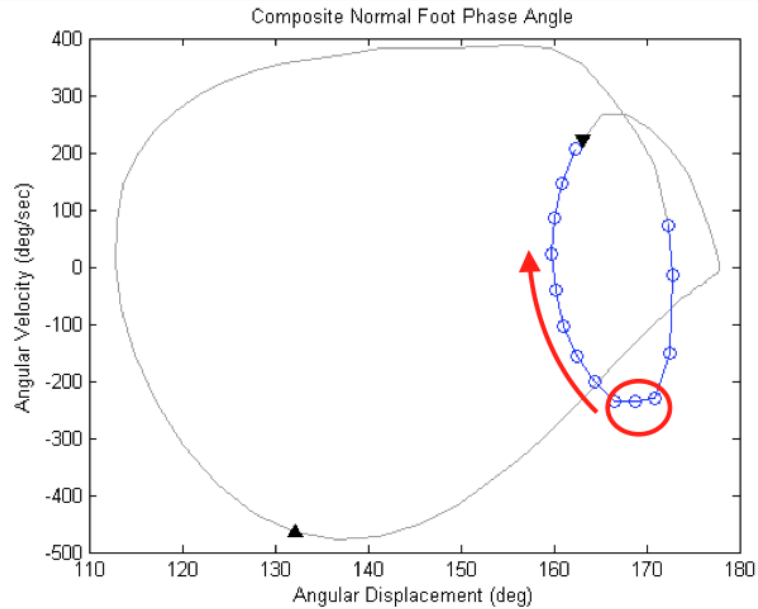
Figure F.3.8: Ankle neutral and tibia vertical (circled). Dorsiflexion trend in preparation for heel contact (arrow).

F.3.4.3 Continuous Relative Phase Diagram

When the shank reaches a vertical position and the ankle achieves a neutral position, the relative phase curve equals the maximum negative phase angle for the entire gait cycle. This maximum will occur at a relative phase angle of approximately 110° and signifies a change in the coordination strategies of the shank and foot. After this maximum the foot must maintain it's near neutral position as the shank continues swinging forward toward maximum flexion. As the shank continues to increase its angular displacement, the relative phase curve will rapidly change its slope to a positive trend. At approximately, 97% of the gait cycle the firing of the hamstring muscles is correlated with a zero crossing of the relative phase diagram, for at this point in the gait cycle the

shank will be retracted slightly from its maximum flexion position toward extension in preparation for initial contact. For the remaining percentages of the gait cycle, the foot assumes the role of the leading segment in phase space (indicated by a positive relative phase value). Terminal swing on the relative phase diagram should correspond to the same relative phase value at initial contact of this gait cycle, which is approximately 65°.

Appendix G   Additional Results

G.1   Additional Results for Prospective Experiments

The following table provides the various cohorts' mean values for the timing of critical and temporal gait events.

Table G.1.1: Mean values for the timing of critical and temporal gait events.

Cohort	FO (%GC)	FA (%GC)	TV (%GC)
N Pro (n=20)	65 (1.65)	79 (1.35)	87 (1.50)
N Retro (n=120)	60 (2.14)	77 (1.08)	85 (1.49)
CP Pro (n=4)	68 (4.93)	83 (3.15)	94 (2.74)
CP Retro (n=55)	62 (5.44)	79 (3.12)	93 (3.78)
LLA Retro (n=15)	62 (3.16)	79 (1.85)	87 (1.22)

Cohort	Knee 0° (%GC)	Max Knee Flex (%GC)	Max Hip Flex (%GC)	Knee 40° (%GC)
N Pro (n=20)	96 (2.24)	74 (1.43)	93 (5.66)	65.9 (1.33)
N Retro (n=120)	93 (1.43)	73 (1.47)	94 (4.95)	64 (2.19)
CP Pro (n=4)	67 (20.79)	85 (8.28)	98 (3.27)	65 (1.41)
CP Retro (n=55)	98 (8.39)	80 (6.05)	96 (3.56)	62 (7.00)
LLA Retro (n=15)	92 (19.28)	75 (4.67)	96 (4.78)	59 (19.81)

Mean (standard deviation) timing (%GC) of each cohort's temporal and critical gait events of gait for over-ground walking, where FO = foot off, FA = feet adjacent, and TV = tibia vertical.

The following table provides the various cohorts' mean values for common temporal-spatial descriptors of gait and the timing of critical and temporal gait events during over-ground walking.

Table G.1.2: Cohorts' common temporal-spatial descriptors of gait.

Cohort	Rapid Ankle Dorsiflexion (°/%GC)	Ankle 0° (%GC)	Walking Speed (m/min)	Cadence (steps/min)
N Pro (n=20)	-2.10 (0.39)	85 (5.81)	81.18 (11.42)	110.60 (7.19)
N Retro (n=120)	-2.24 (0.58)	74 (7.40)	77.00 (9.60)	118.93 (13.48)
CP Pro (n=4)	-1.01 (0.46)	84 (11.17)	62.00 (7.93)	113.63 (9.65)
CP Retro (n=55)	-1.19 (0.58)	77 (12.63)	55.53 (15.48)	128.29 (21.66)
LLA Retro (n=15)	-0.62 (0.46)	79 (17.60)	66.66 (10.76)	108.62 (11.16)

Cohort	Stride Length (m)	Stride Time (sec)	Step Time (sec)
N Pro (n=20)	1.47 (0.17)	1.09 (0.07)	0.54 (0.04)
N Retro (n=120)	1.30 (0.15)	1.02 (0.11)	0.51 (0.06)
CP Pro (n=4)	1.12 (0.18)	1.07 (0.09)	0.54 (0.04)
CP Retro (n=55)	0.87 (0.19)	0.96 (0.16)	0.49 (0.09)
LLA Retro (n=15)	1.23 (0.18)	1.11 (0.11)	0.57 (0.06)

Mean (standard deviation) of each cohort's critical gait events and common temporal-spatial measures of gait.

The following table was generated from the unimpaired prospective cohort's over-ground walking task.

Table G.1.3: Relative phase angles for common temporal gait events for unimpaired prospective subjects.

CRPD	Foot Strike 0% (±0.00%)		Opposite Foot Off 13% (±1.40%)	
Pelvis-Thigh	2.49 (±11.99)	-2.96 to 0.96	-38.93 (±5.84)	-35.16 to -32.84
Thigh-Shank	-41.88 (±18.27)	-52.30 to -45.70	-12.31 (±8.43)	-22.54 to -19.46
Shank-Foot	90.57 (±18.54)	96.93 to 103.07	57.20 (±6.70)	51.06 to 54.94
Thigh-Foot	48.69 (±13.04)	49.12 to 52.88	44.89 (±6.35)	29.89 to 34.11

CRPD	Opposite Foot On 50% (±0.80%)		Foot Off 65% (±1.70%)	
Pelvis-Thigh	-25.46 (±12.36)	-28.50 to -23.50	67.22 (±2.87)	58.65 to 61.35
Thigh-Shank	-40.04 (±14.95)	-46.06 to -39.94	-136.87 (±7.37)	-137.54 to -134.46
Shank-Foot	22.52 (±7.92)	15.83 to 18.17	27.31 (±30.54)	1.87 to 4.13
Thigh-Foot	-17.53 (±19.59	-29.82 to -22.18	-109.55 (±36.20)	-137.30 to -128.70

Mean, 1 standard deviation, and 95% confidence intervals for the relative phase angles (degrees) at common temporal gait events for unimpaired prospective subjects. The prospective cohort's mean and 1 standard deviation for the percent gait cycle for each temporal gait event is also reported.

The following table indicates if the continuous relative phase angle values for the unimpaired prospective subjects are within the 95% confidence intervals of the continuous relative phase angle values for unimpaired retrospective subjects.

Table G.1.4: Comparison of the unimpaired prospective and retrospective subjects' relative phase angles.

CRPD	Foot On	Opposite Foot Off	Opposite Foot On	Foot Off
Pelvis-Thigh	Y	N	Y	N
Thigh-Shank	Y	N	Y	Y
Shank-Foot	N	N	N	N
Thigh-Foot	N	N	N	N

Comparison of the unimpaired prospective and retrospective subject's groups. Y indicates the unimpaired prospective groups' CRPD values fall within the 95% confidence intervals of the unimpaired prospective subjects and N indicates the prospective groups CRPD values are outside of the retrospective group's 95% confidence intervals.

The following figure provides a closer view of the continuous relative phase diagrams during swing period for the prospective unimpaired subjects' various treadmill speeds walking task.
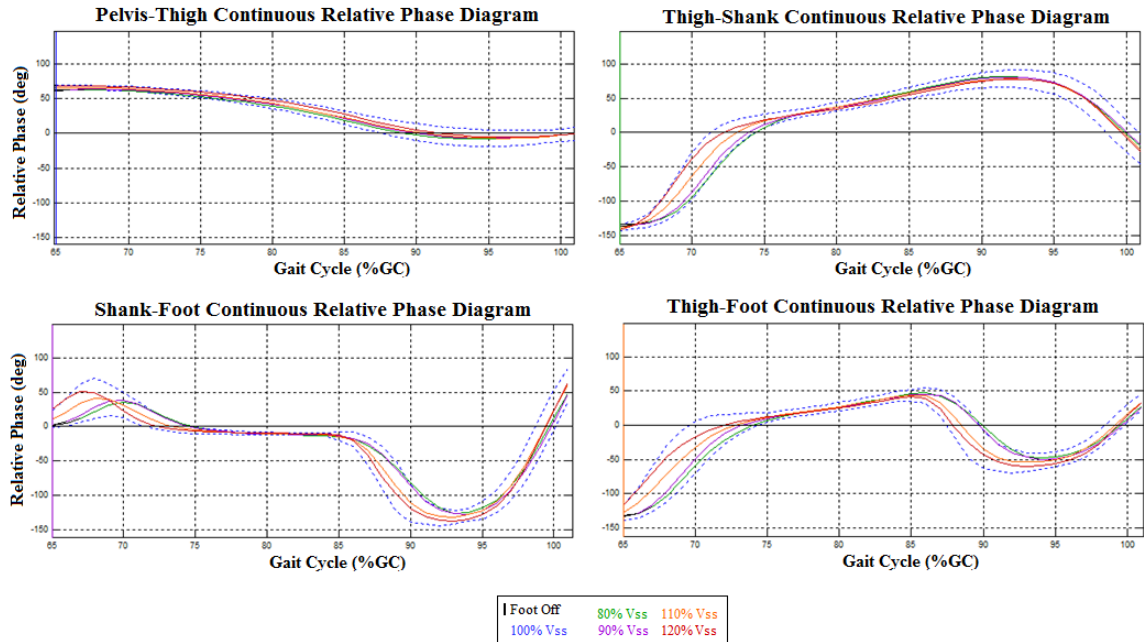
Figure G.1.1: Continuous relative phase diagrams for treadmill walking conditions of unimpaired prospective subjects.

Zoomed in view of swing period, ensemble continuous relative phase diagrams for treadmill walking conditions of unimpaired prospective subjects (green=80%Vss, purple=90%Vss, blue=100%Vss, orange=110%Vss, red=120%Vss).

The figure below contains the mean ensemble sagittal plane kinematic curves for the prospective subjects' over-ground and treadmill walking tasks.
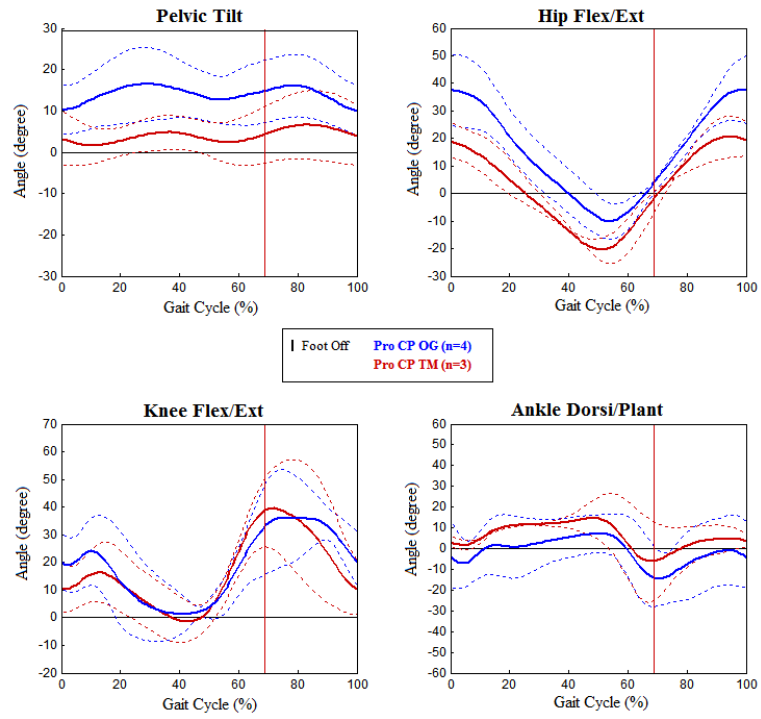
Figure G.1.2: Kinematic curves for unimpaired prospective subjects.
Mean ensemble sagittal plane kinematic curves for the unimpaired prospective subjects'
over-ground (blue) and treadmill (red) walking tasks.

The following table presents the results for the investigation into the invariance and independence of select coordination events for the different unimpaired subjects.

Table G.1.5: r^2 and Pearson (P) values for four critical coordination events.

Demographic	Thigh-Foot CRPD Local Min		Thigh-Foot CRPD Inflection Point	
	r^2	P	r^2	P
Age (n=140)	0.0522%	0.0228	0.6154%	0.0784
Age (n=120)	0.7573%	0.0870	2.4363%	0.1561
Age(n=20)	4.4938%	0.2120	15.4845%	0.3935
Leg Length (n=140)	0.0093%	0.0096	0.2711%	0.0521
Leg Length (n=120)	0.4798%	0.0693	0.6455%	0.0803
Leg Length (n=20)	17.7090%	0.4208	4.9186%	0.2218
Weight (n=140)	0.0435%	0.0208	0.0004%	0.0020
Weight (n=120)	0.1616%	0.0402	0.2766%	0.0526
Weight (n=20)	12.8970%	0.3591	9.0148%	0.3002

Demographic	Shank PP Max AD		Foot PP Max AV	
	r^2	P	r^2	P
Age (n=140)	0.0580%	0.0241	0.7480%	0.0865
Age (n=120)	1.6828%	0.1297	2.6548%	0.1629
Age(n=20)	1.9005%	0.1379	0.3544%	0.0595
Leg Length (n=140)	0.2454%	0.0495	1.1511%	0.1073
Leg Length (n=120)	0.3060%	0.0553	1.9602%	0.1400
Leg Length (n=20)	9.5086%	0.3084	0.4989%	0.0706
Weight (n=140)	0.0116%	0.0108	0.3325%	0.0577
Weight (n=120)	0.1280%	0.0358	1.7335%	0.1317
Weight (n=20)	3.4638%	0.1861	0.7726%	0.0879

r^2 and Pearson (P) values for the four critical coordination events identified with the independent and invariant methodology for the unimpaired subjects, where AD is angular displacement, and AV is angular velocity.

Descriptive statistics for the four critical coordination events identified using criteria of independence and invariance for the unimpaired prospective subjects.

Table G.1.6: Timing of four critical coordination events for all subjects.

Coordination Event	Thigh-Foot CRPD Local Min		Thigh-Foot CRPD IP	
	Mean (SD)	95% CI	Mean (SD)	95% CI
All (n=140)	89.91 (±2.13)	85.74 to 94.08	97.74 (±1.25)	95.29 to 100.19
Retro (n=120)	89.98 (±2.16)	85.75 to 94.22	97.80 (±1.24)	95.38 to 100.22
Pro (n=20)	89.95 (±2.86)	84.35 to 95.55	98.50 (±1.43)	95.69 to 101.00

Coordination Event	Shank PP Max AD		Foot PP Max AV	
	Mean (SD)	95% CI	Mean (SD)	95% CI
All (n=140)	98.35 (±1.23)	95.93 to 100.77	82.94 (±3.65)	75.77 to 90.10
Retro (n=120)	98.46 (±1.15)	96.20 to 100.71	83.03 (±3.61)	75.96 to 90.10
Pro (n=20)	99.1 (±0.97)	97.20 to 101.00	84.35 (±2.70)	79.06 to 89.64

Mean, standard deviation (SD), and 95% confidence intervals (CI) of the timing of the four critical coordination events identified with the independent and invariant methodology for unimpaired prospective subjects, where IP is an inflection point, AD is angular displacement, and AV is angular velocity. The gait cycle was indexed from 1 to 101% for this analysis.

Table G.1.7: Timing of four critical coordination events identified with the independent and invariant methodology.

# Subjects	Age (yr)	Thigh-Foot CRPD Min (%GC)	Thigh-Foot CRPD IP	Shank PP Max AD	Foot PP Max AV
75	7 to 18	90 (2.16)	98 (1.31)	98 (1.23)	83 (3.89)
44	20 to 28	90 (2.00)	98 (1.18)	99 (1.04)	83 (3.37)
10	30 to 38	91 (3.06)	98 (0.99)	99 (1.14)	84 (3.00)
6	40 to 46	91 (1.22)	97 (0.89)	98 (0.71)	83 (2.86)
5	50 to 66	89 (1.15)	98 (1.53)	99 (1.53)	80 (2.52)

Means and standard deviations of the timing of the four critical coordination events identified with the independent and invariant methodology for all unimpaired subjects sorted by age, where IP is an inflection point, AD is angular displacement, and AV is angular velocity. The gait cycle was indexed from 1 to 101% for this analysis.

The third sub-investigation into the four critical coordination events identified by the invariance and independence criteria examine the timing of these events in relation to the timing of other swing period gait events and tasks. The following figure depicts the conventional critical and temporal gait events and the timing of the critical coordination events for the unimpaired retrospective cohort.

Figure G.1.3: Diagram of the timing of the four critical coordination events identified by the invariant and independent criteria with the timing of temporal and critical gait events during the swing period of the gait cycle. The mean and standard deviation of event timings were calculated from the unimpaired retrospective subjects (n=120) and the gait cycle was index from 0 to 100%.

G.2   Additional Results for Aim 2

The following table provides the prospective subjects' mean accuracy of target taps, for the three target sizes, for the reciprocal tapping task.

Table G.2.1: Average accuracy of foot taps hitting the target for the three target sizes (80%, 100%, 120%) used in Hypothesis 2A for the prospective

Cohort Subject ID	Accuracy for Target Size 80%	100%	120%	Cohort Subject ID	Accuracy for Target Size 80%	100%	120%
N1000	45.98	66.57	66.1	N1011	63.61	69.25	63.57
N1001	31.12	42.34	44.88	N1012	89.09	89.03	85.58
N1002	47.05	89.03	94.86	N1013	89.13	89.26	84.5
N1003	46.79	50.9	46.53	N1014	72.72	79.09	68.41
N1004	86.23	81.94	77.93	N1015	94.46	90.24	76.54
N1005	87.92	84.75	84.35	N1016	87.92	84.75	84.35
N1006	90.9	92.45	73.22	N1017	90.9	92.45	73.22
N1007	79.99	63.03	49.62	N1018	79.99	63.03	49.62
N1008	91.47	85.04	67.68	N1019	91.47	85.04	67.68
N1009	85.19	86.69	91.21	C1000	85.19	86.69	91.21
N1010	66.26	81.5	90.82	C1001	66.26	81.5	79.93
N1011	63.61	69.25	63.57	C1002	63.61	69.25	77.33
N1012	89.09	89.03	85.58	C1003	89.09	89.03	35.29
N1013	89.13	89.26	84.5				

The following table provides the p-values from t-tests comparing the timing and magnitude of thigh-shank CRPD coordination events in initial swing that were significantly different between the prospective subjects with cerebral palsy (CP) and the unimpaired prospective subjects (N).

Table G.2.2: T-test results between the mean timing (%GC) and magnitude for initial swing thigh-shank continuous relative phase diagram (CRPD) coordination events for the prospective unimpaired subjects and subjects with CP. The coordination events were a minimum (min), maximum instantaneous slope (MiS), inflection point (IP), and a zero crossing (0x).

Comparison	Thigh-Shank CRPDMin (%) (%GC)	(°)	Thigh-Shank CRPD MiS (%GC)	(°)
N vs CP	0.246	0.173	0.309	0.025

Comparison	Thigh-Shank CRPD IP (%GC)	(°)	Thigh-Shank CRPD 0x (%GC)	(°)
N vs CP	0.335	0.653	0.314	0.201

The following table provides the p-values from t-tests comparing the timing and magnitude of thigh-foot CRPD coordination events in initial swing that were significantly different between the prospective subjects with cerebral palsy (CP) and the unimpaired prospective subjects (N).

Table G.2.3: T-test results between the mean timing (%GC) and magnitude for initial swing thigh-foot continuous relative phase diagram (CRPD) coordination events for the prospective unimpaired subjects and subjects with CP. The coordination events were a minimum (min), maximum instantaneous slope (MiS), inflection point (IP), and a zero crossing (0x).

Comparison	Thigh-Foot CRPD Min (%GC)	(°)	Thigh-Foot CRPD MiS (%GC)	(°)
N vs CP	0.415	0.305	0.476	0.837

Comparison	Thigh-Foot CRPD IP (%GC)	(°)	Thigh-Foot CRPD 0x (%GC)	(°)
N vs CP	0.197	0.692	0.649	0.613

The following table provides the SCALE and ICARS/SARA task scores for the prospective subjects with cerebral palsy.

Table G.2.4: SCALE and ICARS values for prospective subjects with cerebral palsy.

| Prospective Subject | SCALE | | ICARS/SARA |
	Left Limb	Right Limb	Score
C1000	5	4	34
C1001	6	6	35
C1002	4	4	24
C1003	2	2	7

Scores for the Selective Control Assessment of the Lower Extremity (SCALE) and International Cooperative Ataxia Rating Scale (ICARS)/Scale for the Assessment and Rating of Ataxia (SARA) exams for the prospective subjects with cerebral palsy.

The following table provides a conditionally formatted correlation matrix for forward swing limb velocity (FSLC) and target accuracy for the three target sizes of the prospective reciprocal tapping task and over-ground (OG) walking for the thigh-shank CRPD.

Table G.2.5: Correlation matrix for forward swing limb velocity and target accuracy.

	Unimpaired (n=20)		Cerebral Palsy (n=4)	
	Thigh-Shank MiS (%GC)	Thigh-Shank MiS (°/%GC)	Thigh-Shank MiS (%GC)	Thigh-Shank MiS (°/%GC)
OG Walking FSLV (mm/s)	-0.4660	0.2746	-0.0389	0.3881
80% FSLV (mm/s)	-0.1957	-0.1916	-0.7882	0.9386
100% FSLV (mm/s)	-0.1466	-0.1109	-0.7672	0.9452
120% FSLV (mm/s)	-0.1265	-0.0698	-0.7428	0.9602
80% Accuracy	-0.3045	-0.0325	-0.0064	0.3862
100% Accuracy	-0.0215	-0.2043	0.6025	-0.1809
120% Accuracy	0.0344	-0.0366	0.6162	-0.2383

Correlation matrix, with conditional formatting, for forward swing limb velocity (FSLC) and target accuracy for the three target sizes of the reciprocal tapping task and over-ground (OG) walking, with the magnitude and timing of the maximum instantaneous slope (MiS) in initial swing for the thigh-shank CRPD.

The following table is the correlation matrix, with conditional formatting, for the magnitude and timing of coordination events during initial swing for the thigh-shank and thigh-foot CRPDs of the prospective subjects with CP.

Table G.2.6: Correlation matrix for coordination events for subjects with cerebral palsy.

CP	Thigh-Shank Min (%GC)	Thigh-Shank Min (deg)	Thigh-Shank MiS (%GC)	Thigh-Shank MiS (deg)	Thigh-Shank IP (%GC)	Thigh-Shank IP (deg)	Thigh-Shank 0x (%GC)	Thigh-Shank 0x (deg)	Thigh-Foot Min (%GC)	Thigh-Foot Min (deg)	Thigh-Foot MiS (%GC)	Thigh-Foot MiS (deg)	Thigh-Foot IP (%GC)	Thigh-Foot IP (deg)	Thigh-Foot 0x (%GC)	Thigh-Foot 0x (deg)
Thigh-Shank Min (%GC)	1.0000															
Thigh-Shank Min (deg)	0.9243	1.0000														
Thigh-Shank MiS (%GC)	0.8725	0.6329	1.0000													
Thigh-Shank MiS (deg)	-0.8034	-0.7442	-0.8050	1.0000												
Thigh-Shank IP (%GC)	0.9646	0.9805	0.7138	-0.7025	1.0000											
Thigh-Shank IP (deg)	0.7942	0.9569	0.3973	-0.5402	0.9229	1.0000										
Thigh-Shank 0x (%GC)	0.8826	0.6401	0.9966	-0.7644	0.7323	0.4160	1.0000									
Thigh-Shank 0x (deg)	-0.4401	-0.7477	0.0384	0.3043	-0.6436	-0.8862	0.0314	1.0000								
Thigh-Foot Min (%GC)	0.8787	0.9938	0.5434	-0.6850	0.9632	0.9821	0.5528	-0.8152	1.0000							
Thigh-Foot Min (deg)	0.9186	0.7017	0.9921	-0.7862	0.7858	0.4899	0.9965	-0.0516	0.6202	1.0000						
Thigh-Foot MiS (%GC)	0.5998	0.8443	0.1330	-0.3355	0.7865	0.9622	0.1555	-0.9652	0.8982	0.2364	1.0000					
Thigh-Foot MiS (deg)	0.8730	0.6214	0.9761	-0.6766	0.7336	0.4159	0.9906	0.0468	0.5373	0.9865	0.1638	1.0000				
Thigh-Foot IP (%GC)	0.8447	0.9809	0.4794	-0.6168	0.9503	0.9951	0.4939	-0.8498	0.9959	0.5644	0.9320	0.4867	1.0000			
Thigh-Foot IP (deg)	0.8471	0.8106	0.6125	-0.3673	0.8989	0.8037	0.6636	-0.4843	0.7991	0.7061	0.6953	0.7245	0.8101	1.0000		
Thigh-Foot 0x (%GC)	-0.1776	0.2100	-0.5860	0.0882	0.0467	0.4172	-0.5998	-0.7905	0.3072	-0.5348	0.6172	-0.6349	0.3550	-0.1239	1.0000	
Thigh-Foot 0x (deg)	0.6527	0.3219	0.8743	-0.4183	0.4792	0.1169	0.8989	0.3564	0.2293	0.8700	-0.1254	0.9351	0.1833	0.5906	-0.8537	1.0000

Correlation matrix, with conditional formatting, for the magnitude and timing (%GC) of coordination events during initial swing for the thigh-shank and thigh-foot CRPDs of the prospective subjects with cerebral palsy (CP), with the maximum instantaneous slope (MiS), inflection point (IP), and zero-crossing (0x).

The next table is a correlation matrix, with conditional formatting, for the magnitude and timing of coordination events during initial swing for the thigh-shank and thigh-foot CRPDs of the unimpaired prospective subjects.

Table G.2.7: Correlation matrix for coordination events for unimpaired subjects.

Typ Dev	Thigh-Shank Min (%GC)	Thigh-Shank Min (deg)	Thigh-Shank MiS (%GC)	Thigh-Shank MiS (deg)	Thigh-Shank IP (%GC)	Thigh-Shank IP (deg)	Thigh-Shank 0x (%GC)	Thigh-Shank 0x (deg)	Thigh-Foot Min (%GC)	Thigh-Foot Min (deg)	Thigh-Foot MiS (%GC)	Thigh-Foot MiS (deg)	Thigh-Foot IP (%GC)	Thigh-Foot IP (deg)	Thigh-Foot 0x (%GC)	Thigh-Foot 0x (deg)
Thigh-Shank Min (%GC)	1.0000															
Thigh-Shank Min (deg)	0.4702	1.0000														
Thigh-Shank MiS (%GC)	0.9128	0.4330	1.0000													
Thigh-Shank MiS (deg)	-0.1503	-0.6841	-0.1856	1.0000												
Thigh-Shank IP (%GC)	0.7158	0.4216	0.7594	-0.1053	1.0000											
Thigh-Shank IP (deg)	0.2965	0.4343	0.2416	-0.3459	0.3958	1.0000										
Thigh-Shank 0x (%GC)	0.8519	0.4899	0.9326	-0.2320	0.8979	0.3932	1.0000									
Thigh-Shank 0x (deg)	0.4290	0.4494	0.4654	-0.0704	0.4350	0.5033	0.5536	1.0000								
Thigh-Foot Min (%GC)	0.8642	0.3082	0.8433	-0.0880	0.6503	0.3504	0.7659	0.3515	1.0000							
Thigh-Foot Min (deg)	0.3664	0.8938	0.3415	-0.6778	0.2855	0.3616	0.3462	0.3760	0.2224	1.0000						
Thigh-Foot MiS (%GC)	0.7714	0.2638	0.7995	-0.0662	0.7625	0.3656	0.7957	0.3499	0.9141	0.1560	1.0000					
Thigh-Foot MiS (deg)	-0.2345	-0.1092	-0.2453	0.0462	0.0118	0.0347	-0.2244	-0.4373	-0.1346	-0.0471	0.0872	1.0000				
Thigh-Foot IP (%GC)	0.8283	0.3339	0.8535	-0.1447	0.7364	0.3232	0.8414	0.4280	0.9313	0.2208	0.9524	-0.1792	1.0000			
Thigh-Foot IP (deg)	0.1769	-0.1145	0.1133	0.1229	-0.1461	-0.3973	0.0192	-0.0626	0.1686	-0.2697	0.0485	-0.3703	0.2292	1.0000		
Thigh-Foot 0x (%GC)	0.5916	0.4180	0.7111	-0.3653	0.8007	0.5261	0.7964	0.2698	0.6454	0.4243	0.7481	0.0763	0.7325	-0.2721	1.0000	
Thigh-Foot 0x (deg)	-0.2705	-0.0773	-0.1530	-0.2154	-0.1662	0.0810	-0.1307	-0.1134	-0.1357	-0.1941	-0.0451	0.2184	-0.0402	0.3012	-0.0137	1.0000

Correlation matrix, with conditional formatting, for the magnitude and timing (%GC) of coordination events during initial swing for the thigh-shank and thigh-foot CRPDs of the unimpaired prospective subjects, with the maximum instantaneous slope (MiS), inflection point (IP), and zero-crossing (0x).

The table below is a conditionally formatted correlation matrix for the SCALE score and significant thigh-shank CRPD initial swing coordination events for all prospective subjects with cerebral palsy.

Table G.2.8: Correlation matrix for prospective subjects with cerebral palsy.

CP (n=4)	SCALE	Thigh-Shank CRPD Min (%GC)	Thigh-Shank CRPD Min (°)	Thigh-Shank CRPD MiS (°/%GC)	Thigh-Foot CRPD IP (%GC)
SCALE	1.0000				
Thigh-Shank CRPD Min (%GC)	-0.5833	1.0000			
Thigh-Shank CRPD Min (°)	-0.5408	0.9174	1.0000		
Thigh-Shank CRPD MiS (°/%GC)	0.7044	-0.8257	-0.7483	1.0000	
Thigh-Shank CRPD IP (%GC)	-0.6431	0.7993	0.9273	-0.5838	1.0000

Correlation matrix, with conditional formatting, for all prospective subjects with cerebral palsy, where MiS is the maximum instantaneous slope and IP is the inflection point.

The following conditionally formatted table is a correlation matrix for all unimpaired prospective subjects and the significant initial swing coordination events from the thigh-shank CRPD.

Table G.2.9: Correlation matrix for unimpaired prospective subjects.

Unimpaired (n=20)	Thigh-Shank CRPD Min (%GC)	Thigh-Shank CRPD Min (°)	Thigh-Shank CRPD MiS (°/%GC)	Thigh-Foot CRPD IP (%GC)
Thigh-Shank CRPD Min (%GC)	1.0000			
Thigh-Shank CRPD Min (°)	0.4702	1.0000		
Thigh-Shank CRPD MiS (°/%GC)	-0.1503	-0.6841	1.0000	
Thigh-Shank CRPD IP (%GC)	0.8283	0.3339	-0.1447	1.0000

Correlation matrix, with conditional formatting, for all unimpaired prospective subjects, where MiS is the maximum instantaneous slope and IP is the inflection point.

The conditionally formatted correlation matrix below examines the relationship between the 90°turn curvature (κ) and common temporal-spatial gait measures for all unimpaired prospective subjects.

Table G.2.10: Correlation matrix for unimpaired prospective subjects for 90° turning task.

Unimpaired (n=20)	OG Vss (m/min)	Cadence (steps/min)	Stride Length (m)	Left Max κ	Right Max κ
OG Vss (m/min)	1.0000				
Cadence (steps/min)	0.4270	1.0000			
Stride Length (m)	0.8888	0.1706	1.0000		
Left Max κ	-0.5672	-0.3640	-0.5386	1.0000	
Right Max κ	-0.3053	0.4452	-0.2013	0.1708	1.0000

Correlation matrix, with conditional formatting, for all unimpaired prospective subjects, where κ is the turn curvature and OG Vss is the self-selected over-ground walking speed.

The conditionally formatted correlation matrix below examines the relationship between the 90°turn curvature (κ), ICARS/SARA scores, and common temporal-spatial gait measures for all prospective subjects with cerebral palsy.

Table G.2.11: Correlation matrix for prospective subjects with cerebral palsy for 90° turning task.

CP (n=4)	OG Vss (m/min)	Cadence (steps/min)	Stride Length (m)	Left Max κ	Right Max κ	ICARS/SARA
OG Vss (m/min)	1.0000					
Cadence (steps/min)	-0.3772	1.0000				
Stride Length (m)	0.8980	-0.7461	1.0000			
Left Max κ	-0.4444	-0.0893	-0.2759	1.0000		
Right Max κ	-0.4087	-0.0840	-0.2527	0.9989	1.0000	
ICARS/SARA	0.1912	0.8005	-0.2424	-0.1120	-0.0795	1.0000

Correlation matrix, with conditional formatting, for all prospective subjects with cerebral palsy (CP), where K is the turn curvature and OG Vss is the self-selected over-ground walking speed.

The following table provides descriptive statistics for the base of support width for the various subject cohorts for over-ground walking.

Table G.2.12: Base of support values for subjects.

Statistic	N (n=140)	CP (n=59)	LLA (n=15)
Mean	43.94	88.45	60.21
Standard Deviation	30.34	42.38	49.04
Variance	920.77	1795.65	2404.68

Mean, standard deviation, and variance for base of support during representative over-ground walking trial for unimpaired subjects (N), subjects with cerebral palsy (CP), and subjects with a lower limb amputation (LLA).

G.3   Additional Results for Aim 3

The following table contains the normalized root mean square error values between the unimpaired cohort and theoretical pendulum model for the proximal and distal linkages/segments for the four damping conditions.

Table G.3.1: Unimpaired cohort's rankings for 4 pendulum model damping conditions.

Unimpaired Subjects (n=120 legs)					
Damping	**Rank**	**NRMSE** θ_{Prox}	**NRMSE** $\dot{\theta}_{Prox}$	**NRMSE** θ_{Dist}	**NRMSE** θ_{Dist}	**$\sum$NRMSE**
$\zeta = 0$	1	7.7889	3.5904	9.5761	2.3629	23.31834
$\zeta = 0.5$	2	7.7903	3.0455	9.5609	5.1828	25.57953
$\zeta = 1.0$	4	7.7915	2.4586	9.5553	6.4973	26.30241
$\zeta = 1.5$	3	7.7926	1.8609	9.5527	6.9674	26.17355

Unimpaired cohort's rankings for 4 different pendulum model damping conditions with the normalized root mean square error (NRMSE) for the angular displacement (θ) and angular velocity ($\dot{\theta}$) between the proximal (Prox) and distal (Dist) linkages/leg segments.

The following table contains the normalized root mean square error values between the cohort with a stiff knee gait and theoretical pendulum model for the proximal and distal linkages/segments for the four damping conditions.

Table G.3.2: Rankings of subjects with a stiff knee gait pattern for 4 pendulum model damping conditions.

Subjects with Stiff Knee Gait Pattern (n=60 legs)					
Damping	**Rank**	**NRMSE** θ_{Prox}	**NRMSE** $\dot{\theta}_{Prox}$	**NRMSE** θ_{Dist}	**NRMSE** θ_{Dist}	**$\sum$NRMSE**
$\zeta = 0$	1	7.7889	3.5904	9.5761	2.3629	23.31834
$\zeta = 0.5$	2	7.7903	3.0455	9.5609	5.1828	25.57953
$\zeta = 1.0$	4	7.7915	2.4586	9.5553	6.4973	26.30241
$\zeta = 1.5$	3	7.7926	1.8609	9.5527	6.9674	26.17355

Rankings of subjects with a stiff knee gait pattern for 4 different pendulum model damping conditions with the normalized root mean square error (NRMSE) for the angular displacement (θ) and angular velocity ($\dot{\theta}$) between the proximal (Prox) and distal (Dist) linkages/leg segments.

The following table contains the normalized root mean square error values between the cohort with a crouch gait pattern and theoretical pendulum model for the proximal and distal linkages/segments for the four damping conditions.

Table G.3.3: Rankings of subjects with a crouch gait pattern for 4 pendulum model damping conditions.

| Subjects with Crouch Gait Pattern (n=46 legs) | | | | | |
Damping	Rank	NRMSE θ_{Prox}	NRMSE $\dot{\theta}_{Prox}$	NRMSE θ_{Dist}	NRMSE $\dot{\theta}_{Dist}$	$\sum$NRMSE
$\zeta = 0$	1	7.7889	3.5904	9.5761	2.3629	23.31834
$\zeta = 0.5$	2	7.7903	3.0455	9.5609	5.1828	25.57953
$\zeta = 1.0$	4	7.7915	2.4586	9.5553	6.4973	26.30241
$\zeta = 1.5$	3	7.7926	1.8609	9.5527	6.9674	26.17355

Rankings of subjects with a crouch gait pattern for 4 different pendulum model damping conditions with the normalized root mean square error (NRMSE) for the angular displacement (θ) and angular velocity ($\dot{\theta}$) between the proximal (Prox) and distal (Dist) linkages/leg segments.

The table below contains the normalized root mean square error values between the cohort a below knee amputation and theoretical pendulum model for the proximal and distal linkages/segments for the four damping conditions.

Table G.3.4: Rankings of subjects with a below knee amputation for 4 pendulum model damping conditions.

| Subjects with Below Knee amputation (n=13 legs) | | | | | |
Damping	Rank	NRMSE θ_{Prox}	NRMSE $\dot{\theta}_{Prox}$	NRMSE θ_{Dist}	NRMSE $\dot{\theta}_{Dist}$	$\sum$NRMSE
$\zeta = 0$	1	7.6708	1.9320	9.5298	1.3166	20.4492
$\zeta = 0.5$	4	7.6703	2.2121	9.5135	6.9797	26.3756
$\zeta = 1.0$	3	7.6712	1.6234	9.5094	7.5373	26.3413
$\zeta = 1.5$	2	7.6723	0.8886	9.5079	7.7061	25.7749

Rankings of subjects with a below knee amputation for 4 different pendulum model damping conditions with the normalized root mean square error (NRMSE) for the angular displacement (θ) and angular velocity ($\dot{\theta}$) between the proximal (Prox) and distal (Dist) linkages/leg segments.

The table below contains the normalized root mean square error values between the cohort an above knee amputation and theoretical pendulum model for the proximal and distal linkages/segments for the four damping conditions.

Table G.3.5: Rankings of subjects with an above knee amputation for 4 pendulum model damping conditions.

| Subjects with Above Knee amputation (n=6 legs) | | | | | |
Damping	Rank	NRMSE θ_{Prox}	NRMSE $\dot{\theta}_{Prox}$	NRMSE θ_{Dist}	NRMSE $\dot{\theta}_{Dist}$	$\sum$NRMSE
$\zeta = 0$	1	7.6434	3.1021	9.5982	2.0961	22.4398
$\zeta = 0.5$	2	7.6446	2.7131	9.5814	4.5142	24.4533
$\zeta = 1.0$	3	7.6455	2.2694	9.5748	5.8505	25.3401
$\zeta = 1.5$	4	7.6463	1.7987	9.5716	6.3408	25.3574

Rankings of subjects with an above knee amputation for 4 different pendulum model damping conditions with the normalized root mean square error (NRMSE) for the angular displacement (θ) and angular velocity ($\dot{\theta}$) between the proximal (Prox) and distal (Dist) linkages/leg segments.

G.4   Additional Results for Aim 4

G.4.1   Additional Results for Coordination Deviation Index (CDI)

The following figure shows the result for determining the number of control features required for a 98% reconstruction quality of an individual's sagittal plane phase portraits and continuous relative phase diagrams.
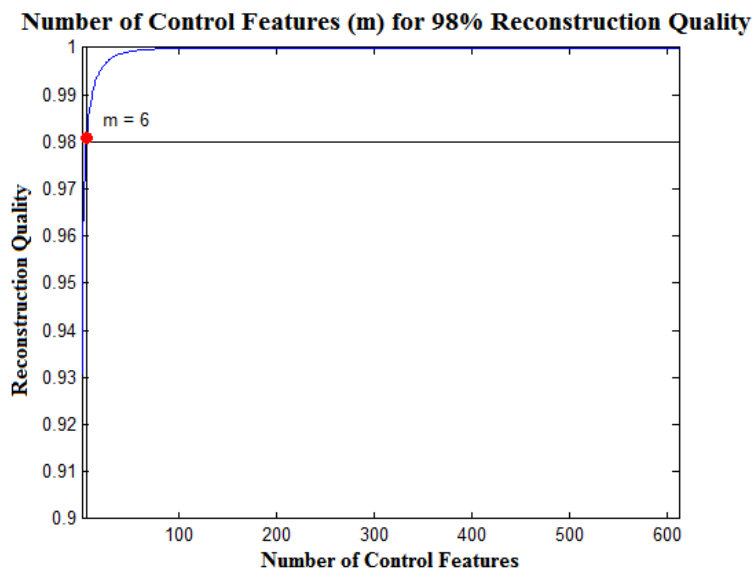

Figure G.4.1: Number of control features for CDI.
Number of control features required for a 98% reconstruction quality of the coordination curves used to calculate a subject's coordination deviation index (CDI).

The next figure provides the original and reconstructed (using the 98% reconstruction quality from above) coordination curves for a randomly selected unimpaired subject.
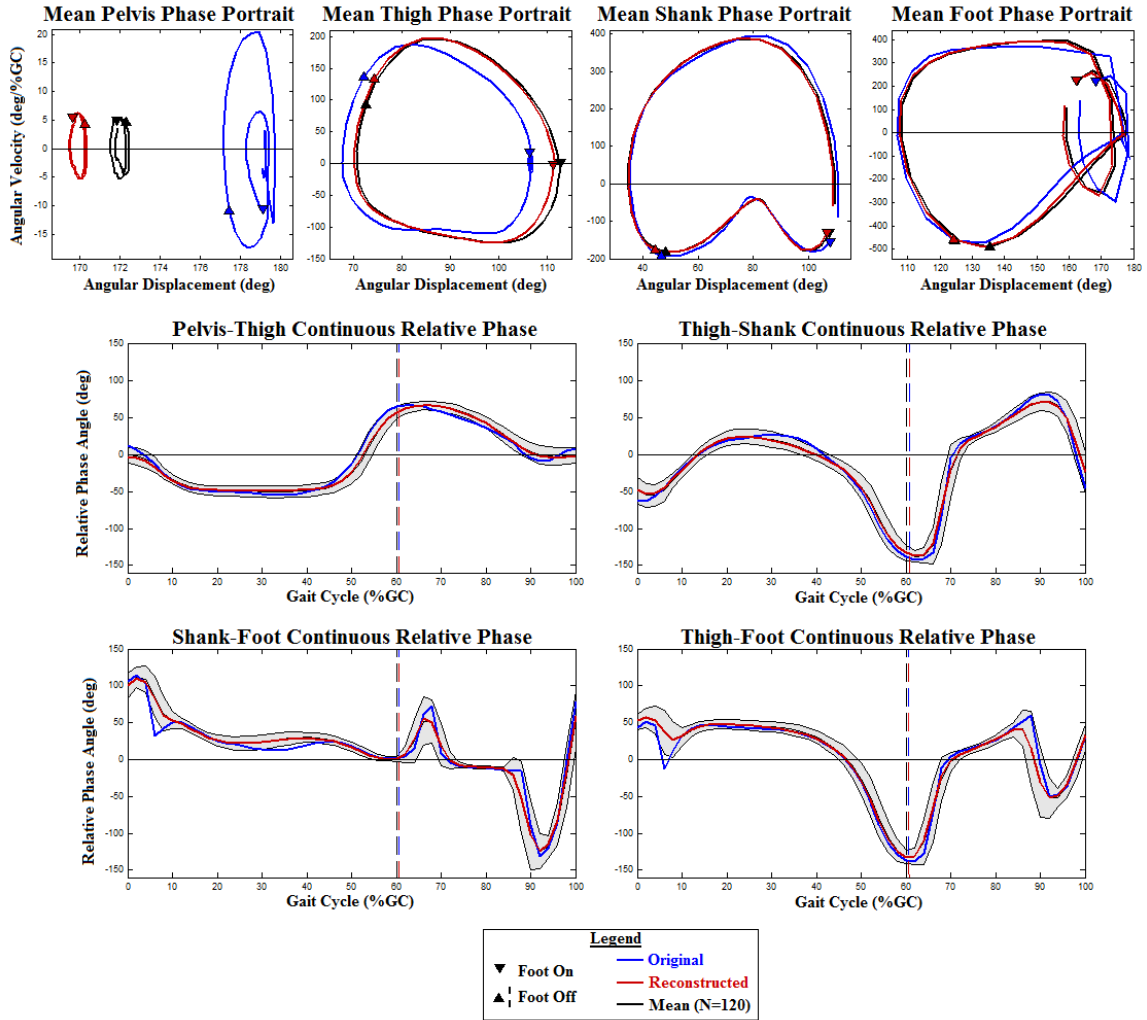
Figure G.4.2: Reconstruction of coordination curves.
The original (blue) and reconstructed (red) phase portraits and continuous relative phase diagrams for an unimpaired subject with the mean ensemble curves (black/grey) of retrospective unimpaired subjects (n=120).

Lastly, the table below provides the demographic characteristics, gait deviation index, and coordination deviation index for the unimpaired subjects, subjects with cerebral palsy (CP), and subjects with a lower limb amputation (LLA)

Table G.4.1: Demographic characteristics and indices values for subjects.

Group	Legs (#)	Age (yr)	Leg Length (mm)	Weight (kg)	GDI	CDI
Unimpaired	120	19.3 ±11.5	845.5 ±97.0	58.2 ±19.5	101.9 ±8.4	98.2 ±8.5
CP	100	11.9 ±4.9	716.3 ±96.3	33.2 ±12.7	70.4 ±8.6	84.8 ±8.6
Stiff Knee	54	10.6 ±3.6	700.0 ±96.5	32.2 ±14.1	72.1 ±9.0	85.0 ±6.0
Crouch	46	13.5 ±5.8	735.4 ±93.4	34.4 ±11.0	68.5 ±7.7	84.5 ±7.3
Hemiplegia	10	11.2 ±4.1	719.8 ±88.5	31.4 ±13.6	71.4 ±9.3	84.7 ±4.6
Diplegia	90	12.0 ±5.0	715.9 ±97.5	33.4 ±12.7	70.3 ±8.5	84.8 ±6.8
GMFCS I	39	12.3 ±6.1	721.2 ±112.1	33.3 ±13.9	71.1 ±8.1	85.8 ±6.2
GMFCS II	57	11.0 ±3.1	707.0 ±84.9	32.0 ±11.5	70.9 ±8.4	84.7 ±6.4
GMFCS III	4	21.5 ±4.0	801.3 ±20.6	50.1 ±4.3	57.0 ±3.6	75.5 ±6.9
LLA	15	17.0 ±7.6	832.4 ±147.7	53.6 ±24.3	78.7 ±11.8	84.8 ±7.2
Below Knee	9	16.2 ±7.2	821.2 ±171.8	49.1 ±23.5	76.3 ±13.1	85.2 ±7.8
Above Knee	6	18.8 ±9.0	856.7 ±82.1	63.3 ±25.3	83.7 ±6.78	83.9 ±6.1

Mean and standard deviation (SD) of demographic characteristics, GDI, and CDI for unimpaired subjects, subjects with cerebral palsy (CP), and subjects with a lower limb amputation (LLA). Subjects with CP were sorted by gait pattern, affected side, and Gross Motor Function Classification System (GMFCS) level. Subjects with a LLA were also sorted by level of amputation.

G.4.2 Additional Results for Coordination Performance Score Statistical Analysis

A logistic regression analysis was used to examine the robustness of a model that predicts a CP type gait pattern from a normal gait pattern based on select swing period coordination events. Cross-validation was used to compare predicted probabilities based on the complete dataset versus the cross-validated predicted probabilities. Of the six significant coordination events identified, three swing period coordination events were used for this regression model. The magnitude of the thigh-foot CRPD minimum near foot off (TF1), the magnitude of the pelvis PP's minimum angular displacement (P1), and the percent gait cycle of the foot PP's maximum angular displacement (pF2).

Table G.4.2: Response profile for the atypical vs. typical gait pattern regression model, where probability modeled is CP=1.

Ordered Value	CP	Total Frequency
1	0	140
2	1	106

Table G.4.3: Model fit statistics for the atypical vs. typical gait pattern regression model.

Criterion	Intercept Only	Intercept and Covariates
AIC	338.314	64.500
SC	341.819	78.522
-2 Log L	336.314	56.500

Table G.4.4: Results of maximum likelihood estimates analysis for the atypical vs. typical gait pattern regression model.

Parameter	DF	Estimate	Standard Error	Wald Chi-Square	Pr > ChiSq
Intercept	1	62.7352	13.7467	20.8270	<.0001
P1	1	-0.3092	0.0682	20.5490	<.0001
TF1	1	0.2138	0.0489	19.1173	<.0001
pF2	1	0.1707	0.0642	7.0649	0.0079

Table G.4.5: Odds ratio estimates for the atypical vs. typical gait pattern regression model coordination events, where P1 is the magnitude of the minimum angular displacement of the pelvis in swing, TF1 is the magnitude of the thigh-foot CRPD minimum near foot off, and pF2 is the percent gait cycle of the foot PP's maximum angular displacement.

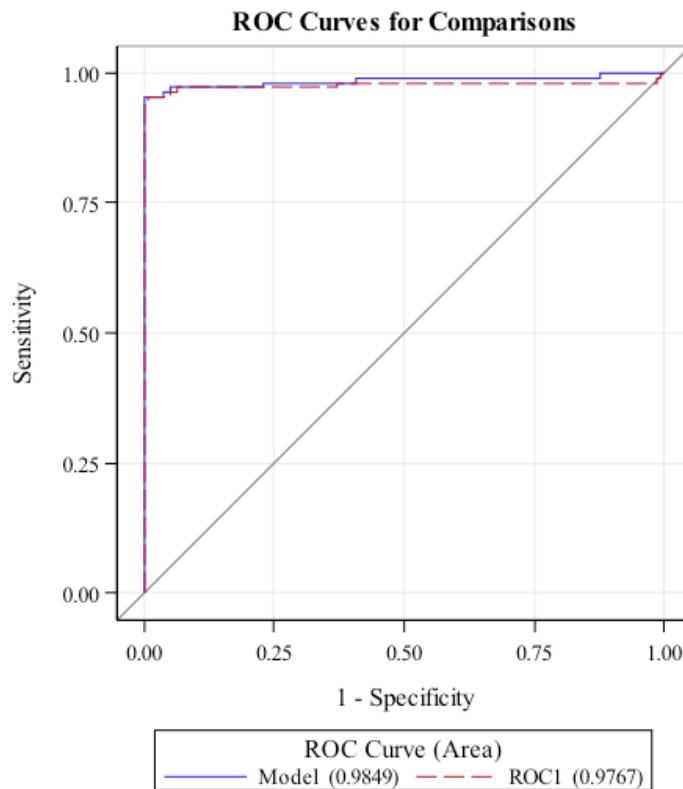| Effect	Point Estimate	95% Wald Confidence Limits	
P1	0.734	0.642	0.839
TF1	1.238	1.125	1.363
pF2	1.186	1.046	1.345

Figure G.4.3: Receiver operator curve (ROC) comparison between the regression model and ROC1.

Table G.4.6: Receiver operator curve association statistics for the atypical vs. typical gait pattern regression model.

ROC Model	Area	Standard Error	95% Confidence Limits	
Model	0.9849	0.00938	0.9665	1.0000
ROC1	0.9767	0.0136	0.9501	1.0000

Table G.4.7: Receiver operator curve contrast test results for the atypical vs. typical gait pattern regression model, with degrees of freedom (DF), Chi-square value, and corresponding probability (Pr) of the Chi-square.

Contrast	DF	Chi-Square	Pr > ChiSq
Reference = Model	1	2.0299	0.1542

Table G.4.8: Analysis of variance for the atypical vs. typical gait pattern regression model, with degrees of freedom (DF), sum of squares, mean square, and F test statistic and probability from the F test.

Source	DF	Sum of Squares	Mean Square	F value	Pr > F
Model	3	0.83464	0.27821	72.12	< 0.0001
Error	242	0.93350	0.00386		
Corrected Total	245	1.76814			

Table G.4.9: Parameter estimates for the coordination events of the atypical vs. typical gait pattern, with standard error of each estimate, t value, probability from t-test, tolerance (TOL), and variance inflation factor (VIF).

Variable	DF	Parameter Estimate	Standard Error	t Value	TOL	VIF
Intercept	1	8.74246	0.85378	10.24	.	0
P1	1	-0.04577	0.00424	-10.80	0.82985	1.20504
TF1	1	0.03298	0.00304	10.86	0.91249	1.09590
pF2	1	0.03815	0.00399	9.57	0.88654	1.12797

The second logistic regression analysis was used to examine the robustness of a model that predicts a stiff knee gait pattern from a crouch type gait pattern based on select swing period coordination events. Cross-validation was used to compare predicted probabilities based on the complete dataset versus the cross-validated predicted probabilities. Of the six significant coordination events identified, two swing period coordination events were used for this regression model. The magnitude of the thigh-foot CRPD minimum near foot off (TF1), and the magnitude of the pelvis PP's minimum angular displacement (P1).

Table G.4.10: Response profile for the stiff knee vs. crouch gait pattern regression model, where probability modeled is stiff knee gait=1.

Ordered Value	SKG	Total Frequency
1	0	46
2	1	60

Table G.4.11: Model fit statistics for the stiff knee vs. crouch gait pattern regression model.

Criterion	Intercept Only	Intercept and Covariates
AIC	147.093	141.931
SC	149.756	149.922
-2 Log L	145.093	135.931

Table G.4.12: Testing global null hypothesis (β=0) for the stiff knee vs. crouch gait pattern regression model.

Test	Chi-Square	DF	Pr > ChiSq
Likelihood Ratio	9.1615	2	0.0102
Score	8.7291	2	0.0127
Wald	7.8151	2	0.0201

Table G.4.13: Results of maximum likelihood estimates analysis for the stiff knee vs. crouch gait pattern regression model.

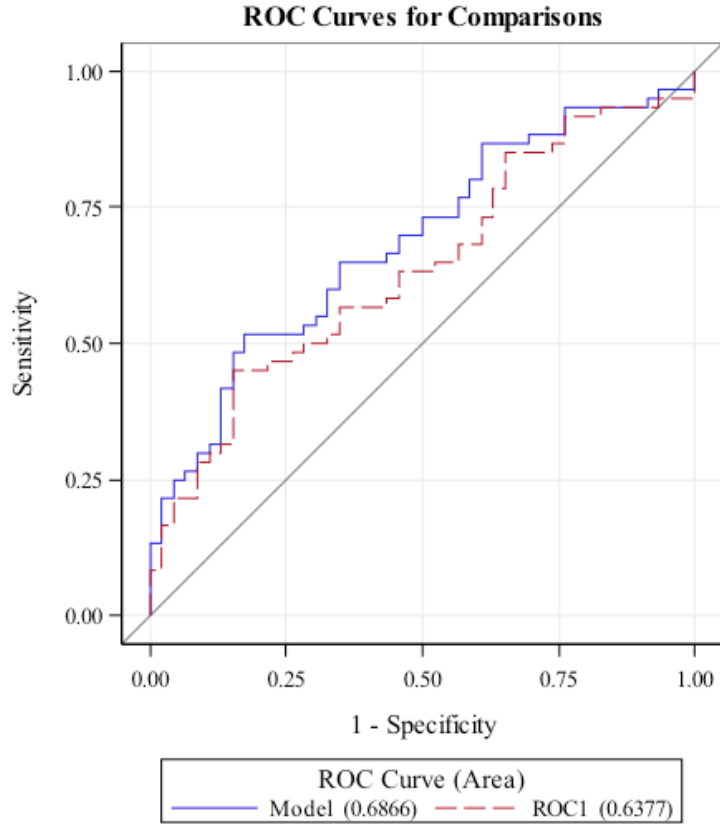| Parameter	DF	Estimate	Standard Error	Wald Chi-Square	Pr > ChiSq
Intercept	1	7.8164	4.0629	3.7013	0.0544
P1	1	-0.0564	0.0258	4.7657	0.0290
TF1	1	-0.0147	0.00717	4.1792	0.0409

Figure G.4.4: Receiver operator curve (ROC) comparison between the regression model and ROC1.

Table G.4.14: Receiver operator curve association statistics for the stiff knee vs. crouch gait pattern regression model.

ROC Model	Area	Standard Error	95% Confidence Limits	
Model	0.9849	0.00938	0.9665	1.0000
ROC1	0.9767	0.0136	0.9501	1.0000

Table G.4.15: Receiver operator curve contrast test results for the stiff knee vs. crouch gait pattern regression model, with degrees of freedom (DF), Chi-square value, and corresponding probability (Pr) of the Chi-square.

Contrast	DF	Chi-Square	Pr > ChiSq
Reference = Model	1	28.7487	< 0.0001

Table G.4.16: Analysis of variance for the stiff knee vs. crouch gait pattern regression model, with degrees of freedom (DF), sum of squares, mean square, and F test statistic and probability from the F test.

Source	DF	Sum of Squares	Mean Square	F value	Pr > F
Model	2	0.49201	0.24601	4.67	0.0114
Error	103	5.42525	0.05267		
Corrected Total	105	5.91727			

Table G.4.17: Parameter estimates for the coordination events of the stiff knee vs. crouch gait pattern, with standard error of each estimate, t value, probability from t-test, tolerance (TOL), and variance inflation factor (VIF).

Variable	DF	Parameter Estimate	Standard Error	t Value	TOL	VIF
Intercept	1	2.23955	0.93245	2.40	.	0
TF1	1	-0.00398	0.00165	-2.42	0.97898	1.02147
P1	1	-0.01305	0.00593	-2.20	0.97898	1.02147

G.4.3   Additional Results for Hypothesis 4A

The following figures contain the PPs and CRPDs for the various gait pattern comparisons conducted to address Hypothesis 4A of Aim 4.
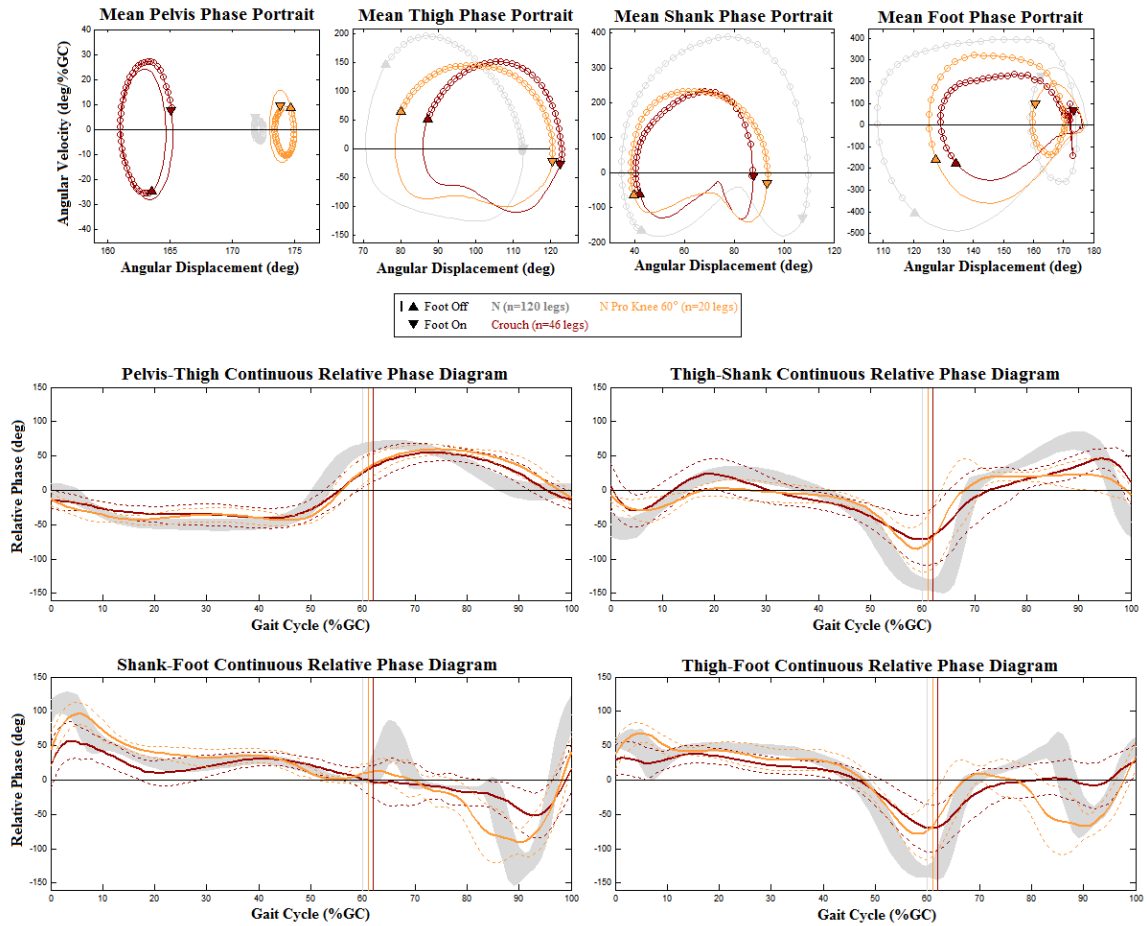

Figure G.4.5: Phase portraits and continuous relative phase diagrams for over-ground walking for all subjects with a crouch gait pattern (orange), all subjects with a stiff knee gait pattern (red), and all retrospective unimpaired subjects (grey).
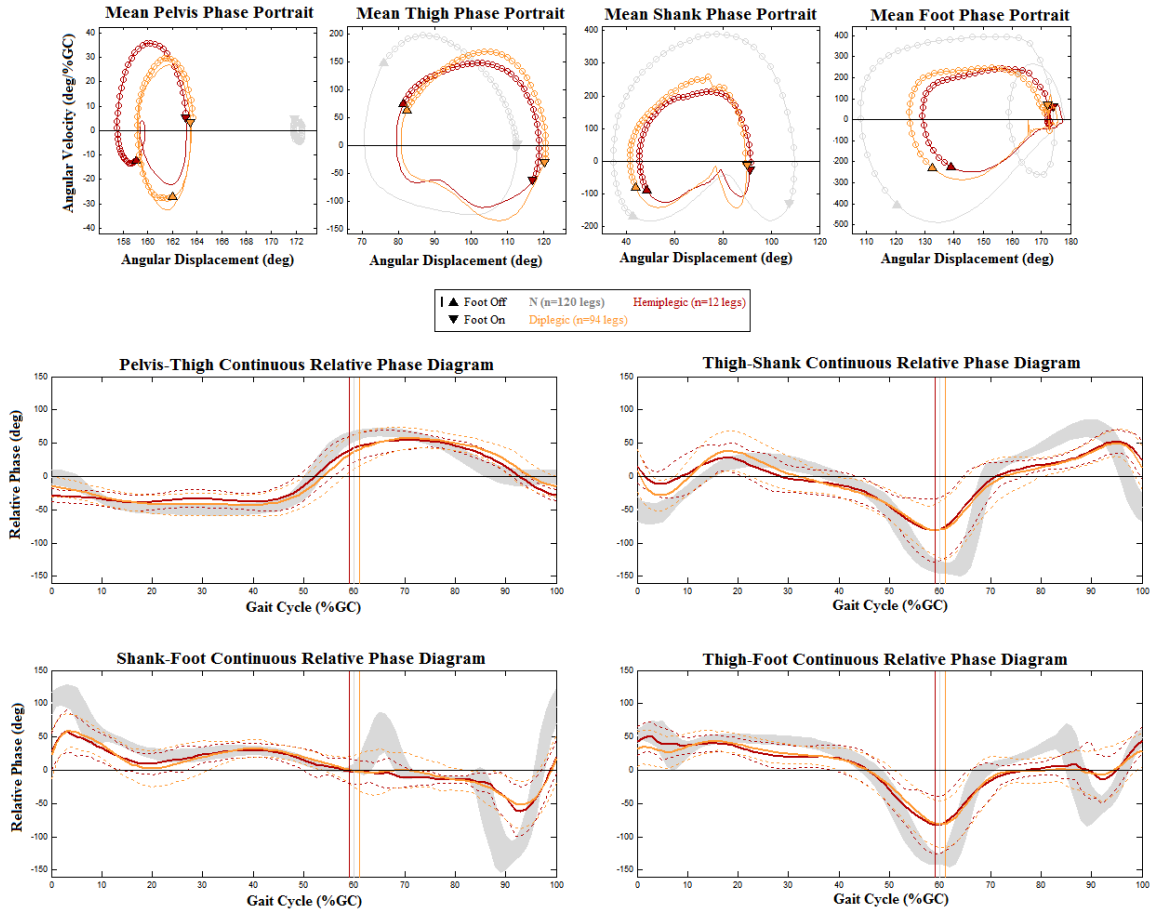
Figure G.4.6: Phase portraits and continuous relative phase diagrams for over-ground walking for all subjects with CP classified as hemiplegic (red), all subjects with CP classified as diplegic (orange), and all retrospective unimpaired subjects (grey).
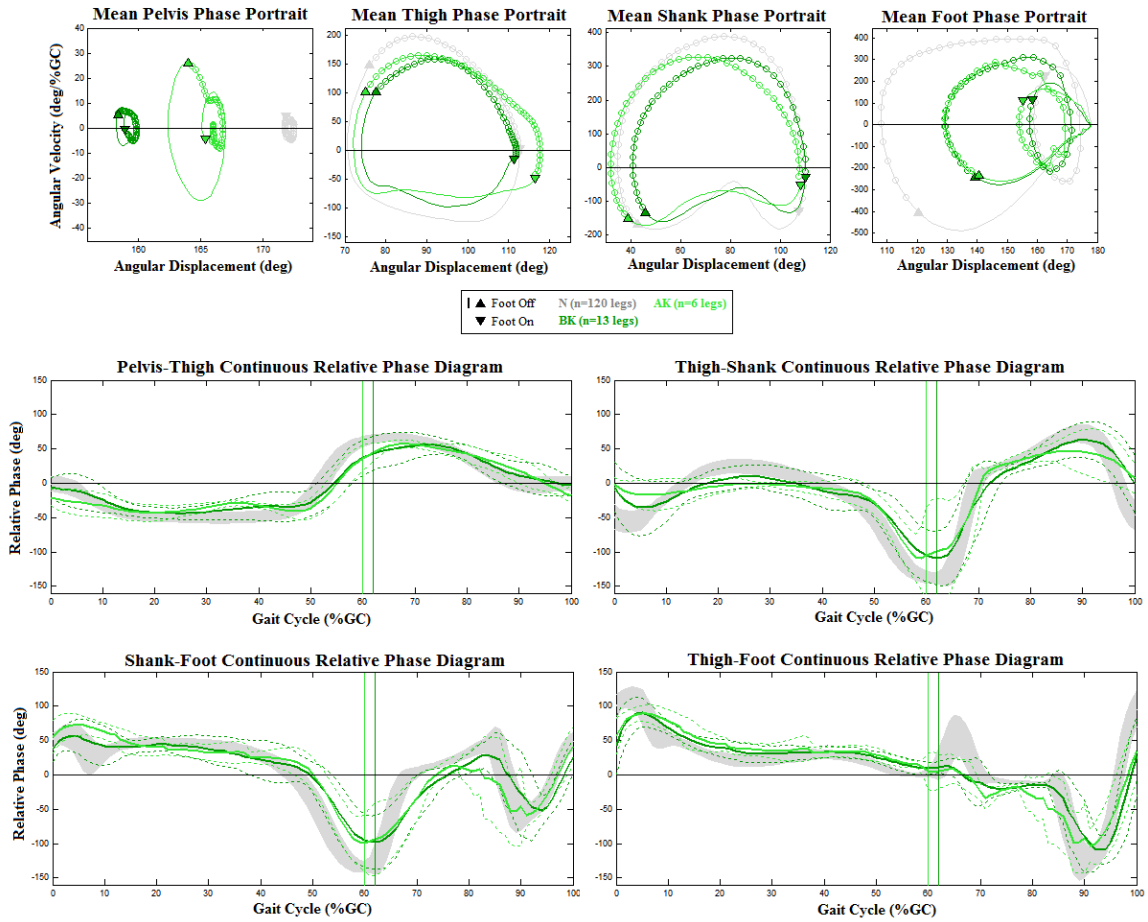
Figure G.4.7: Phase portraits and continuous relative phase diagrams for over-ground walking for all subjects with a below knee LLA (dark green), all subjects with an above knee LLA (light green), and all retrospective unimpaired subjects (grey).
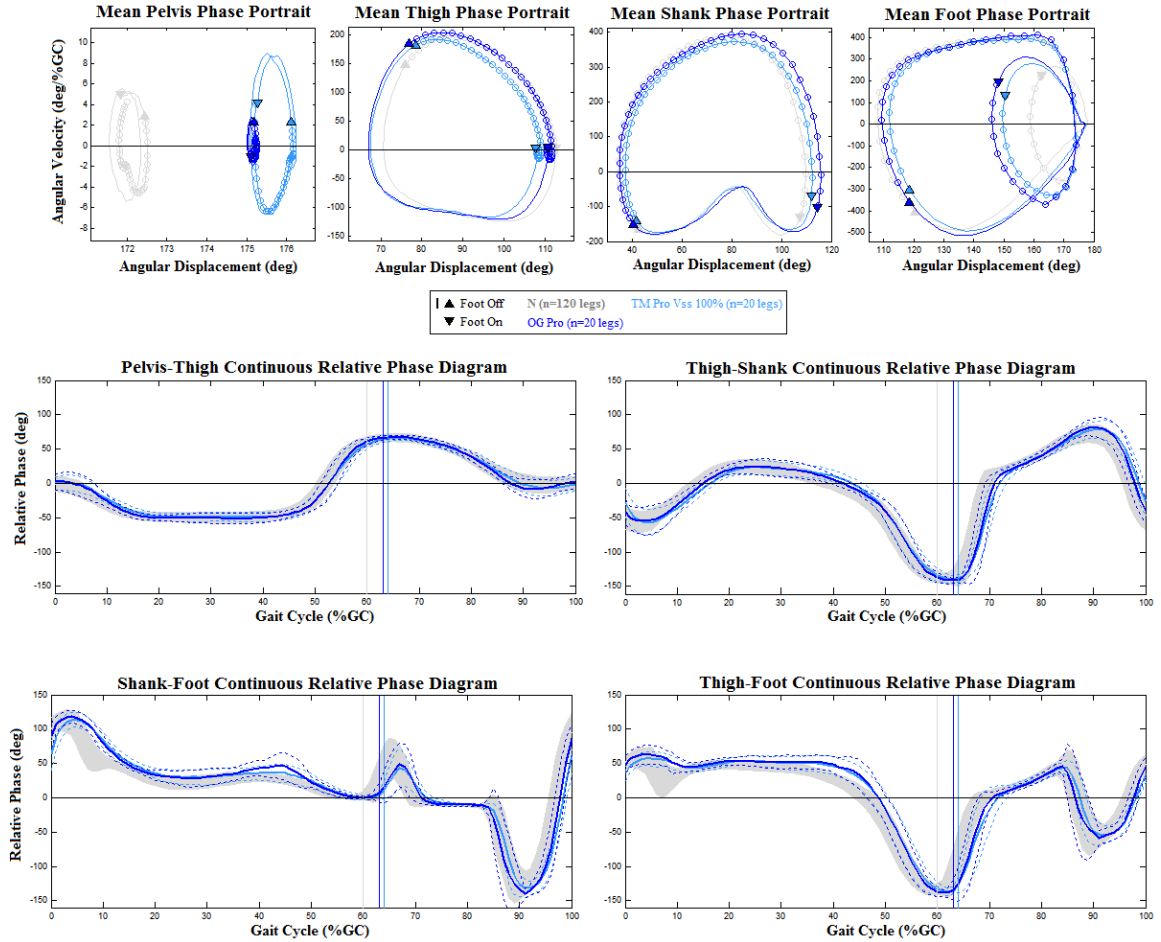
Figure G.4.8: Phase portraits and continuous relative phase diagrams for unimpaired prospective subjects (dark blue) for over-ground (OG) walking at a self-selected speed (Vss), unimpaired prospective (light blue) for treadmill walking (TM) at the same Vss, and retrospective unimpaired cohort's mean coordination curves (grey) for over-ground walking at Vss.

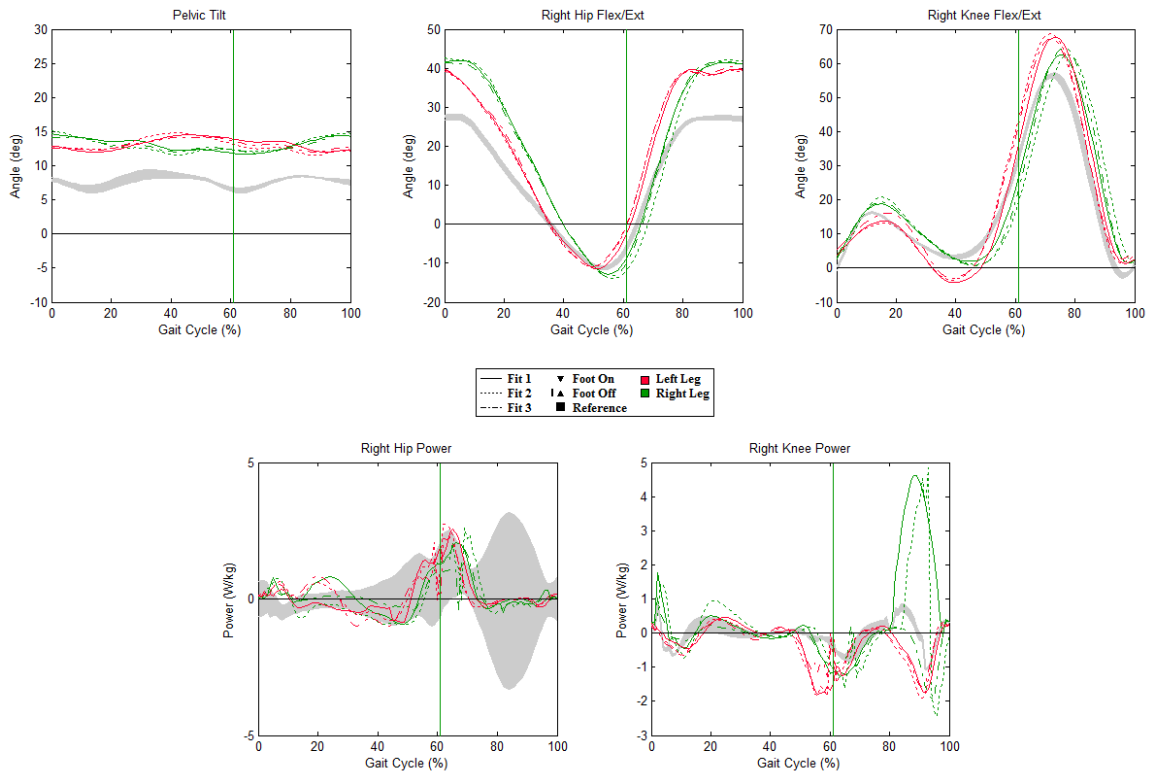## G.5   Additional Results for Transtibial Amputation Case Study

Figure G.5.1: Sagittal plane kinematic and kinetic curves for the left (red) and right (green) legs for the three prosthetic alignment conditions.
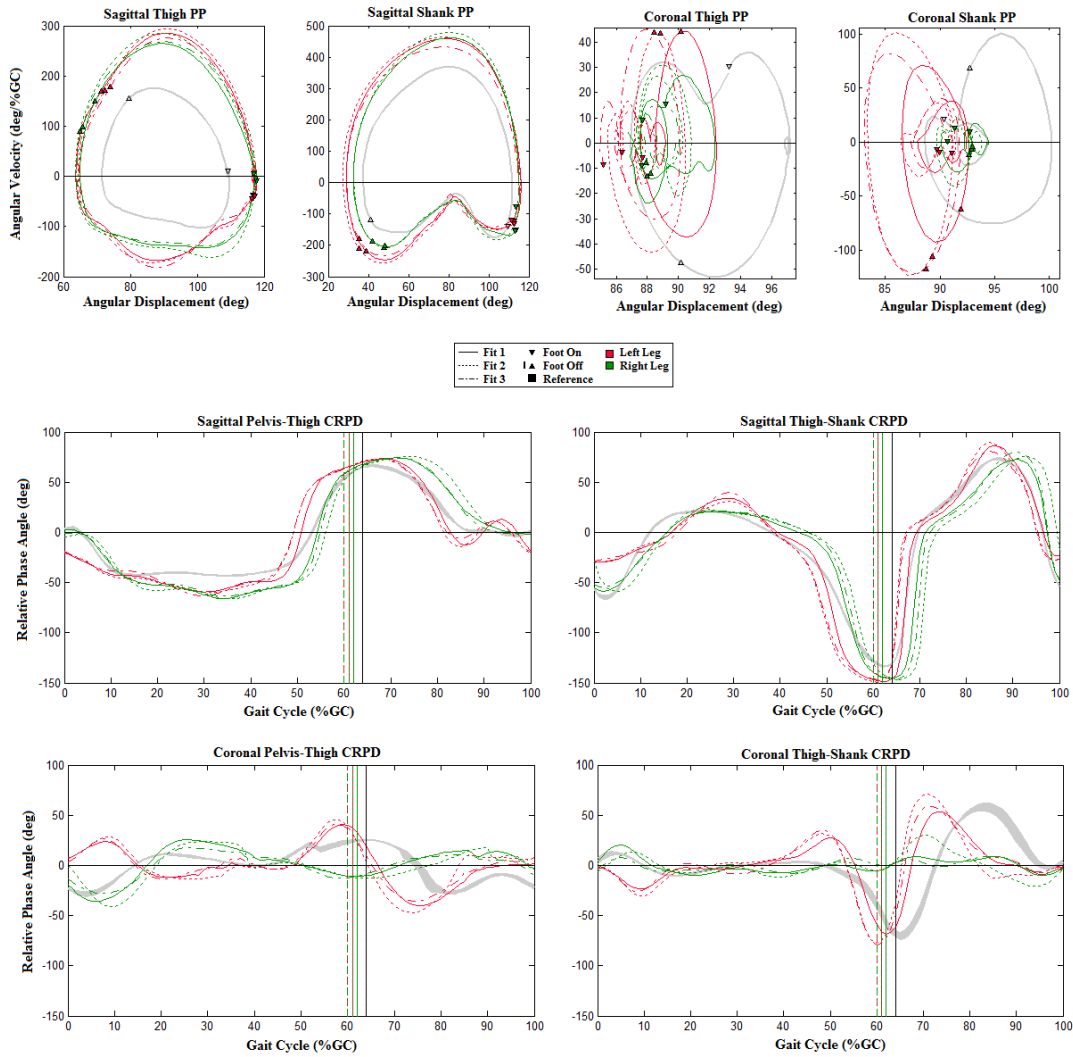
Figure G.5.2: Sagittal and coronal plane phase portraits and continuous relative phase diagrams for the left (red) and right (green) legs for the three prosthetic alignment conditions.

G.6 Additional Results for Exploratory Investigation to Identify Significant Coordination Events

Table G.6.1: Comparison of unimpaired prospective (shoes) subjects' critical coordination events and unimpaired retrospective (barefoot) subjects' critical events using the independence and invariance criteria.

| Demographic	Foot PP		Thigh-Foot CRPD Local Min		Thigh-Foot CRPD Zero-crossing		Shank PP	
	r^2	P	r^2	P	r^2	P	r^2	P
Age(n=120)	0.20%	0.0447	0.10%	0.0316	0.10%	0.0316	0.10%	0.0316
Age(n=20)	0.75%	0.0865	0.05%	0.0228	0.62%	0.0784	0.06%	0.0241
LegLength(n=120)	1.90%	0.1378	0.30%	0.0548	0.30%	0.0548	0.60%	0.0775
LegLength(n=20)	1.15%	0.1073	0.01%	0.0096	0.27%	0.0521	0.25%	0.0495
Weight(n=120)	0.90%	0.0949	0.00%	0.0000	0.20%	0.0447	0.20%	0.0447
Weight(n=20)	0.33%	0.0577	0.04%	0.0208	0.00%	0.0020	0.01%	0.0108
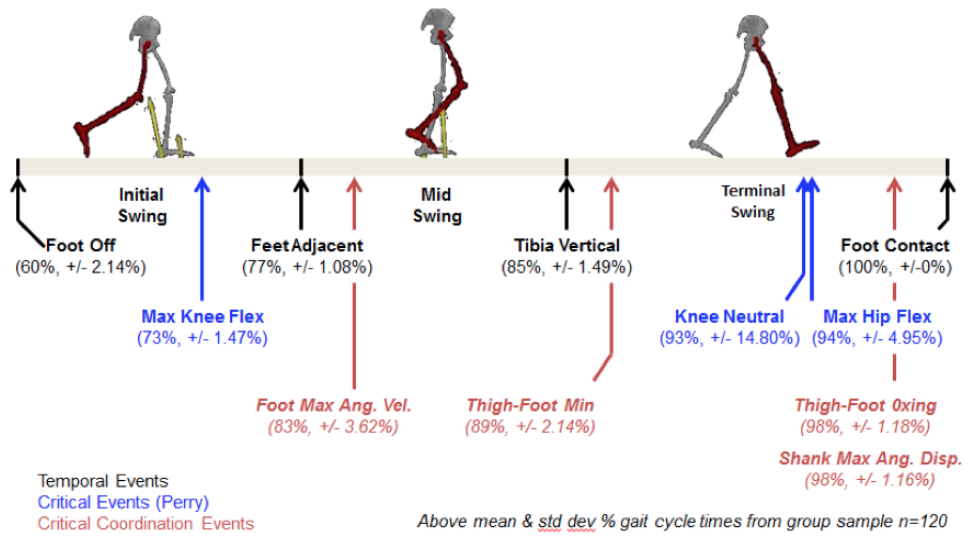
Figure G.6.1: Timing of critical coordination events with respect to the critical and temporal events of gait during swing period.